Polyamidoamine epichlorohydrin-based papers : mechanisms of wet strength development and paper repulping

Eder José Siqueira

UNIVERSITÉ DE GRENOBLE

THÈSE

Pour obtenir le grade de

DOCTEUR DE L'UNIVERSITÉ DE GRENOBLE

Spécialité : **Mécanique des Fluides, Energétique, Procédés**

Arrêté ministériel : 7 août 2006

Présentée par

Eder José SIQUEIRA

Thèse dirigée par **Evelyne MAURET** et
codirigée par **Mohamed Naceur BELGACEM**

préparée au sein du **LGP2 – Laboratoire de Génie des Procédés Papetiers**
dans **l'École Doctorale IMEP2**

POLYAMIDEAMINE EPICHLOROHYDRIN-BASED PAPERS: MECHANISMS OF WET STRENGTH DEVELOPMENT AND PAPER REPULPING

Thèse soutenue publiquement le **05 juin 2012**,
devant le jury composé de :

Madame Ana Paula COSTA
Professeur - Universidade da Beira Interior. Covilhã - PORTUGAL, Rapporteur

Madame Marie-Pierre LABORIE (Présidente du jury)
Professeur - Institute of Forest Utilization and Works Science - Albert-Ludwigs University of Freiburg. Freiburg - ALLEMAGNE, Rapporteur

Monsieur Jean-Pierre JOLY
Chargé de Recherche CNRS, Université Henri Poincaré Nancy I. Vandoeuvre - FRANCE, Examinateur

Madame Séverine SCHOTT
Docteur Ingénieur - Ahlstrom LabelPack. Pont-Evêque - FRANCE, Examinateur

Madame Evelyne MAURET
Professeur – Institut National Polytechnique de Grenoble (PAGORA). FRANCE, Directeur de Thèse

Monsieur Mohamed Naceur BELGACEM
Professeur – Institut National Polytechnique de Grenoble (PAGORA). FRANCE, Directeur de Thèse

ABSTRACT

Polyamideamine epichlorohydrin (PAE) resin is a water soluble and the most used permanent wet strength additive in alkaline conditions for preparing wet strengthened papers. In this thesis, we studied some properties of PAE resins and wet strengthened papers prepared from them. In order to elucidate PAE structure, liquid state, ^{1}H and ^{13}C NMR was carried out and permitted signals assignment of PAE structure. PAE films were prepared to study cross-linking reactions and then thermal and ageing treatments were performed. According to our results, the main PAE cross-linking reaction occurs by a nucleophilic attack of N atoms in the PAE and/or polyamideamine structures forming 2-propanol bridges between PAE macromolecules. A secondary contribution of ester linkages to the PAE cross-linking was also observed. However, this reaction, which is thermally induced, only occurs under anhydrous conditions. The mechanism related to wet strength development of PAE-based papers was studied by using CMC as a model compound for cellulosic fibres and PAE-CMC interactions as a model for PAE-fibres interactions. Based on results from NMR and FTIR, we clearly showed that PAE react with CMC that is when carboxylic groups are present in great amounts. Consequently, as the number of carboxylic groups present in lignocellulosic fibres is considerably less important and the resulting formed ester bonds are hydrolysable, we postulate that ester bond formation has a negligible impact on the wet strength of PAE-based papers. In the second part of this work, a 100% *Eucalyptus* pulp suspension was used to prepare PAE-based papers. PAE was added at different dosages (0.4, 0.6 and 1%) into the pulp suspension and its adsorption was indirectly followed by measuring the zeta potential. Results indicate that the adsorption, reconformation and/or penetration phenomena reach an apparent equilibrium at around 10 min. Moreover, we showed that the paper dry strength was not significantly affected by the conductivity level (from 100 to 3000 µS/cm) of the pulp suspension. However, the conductivity has an impact on the wet strength and this effect seems to be enhanced for the highest PAE dosage (1%). We also demonstrated that storing the treated paper under controlled conditions or boosting the PAE cross-linking with a thermal post-treatment does not necessarily lead to the same wet strength. Degrading studies of cross-linked PAE films showed that PAE degradation in a persulfate solution at alkaline medium was more effective. A preliminary study of coated and uncoated industrial PAE-based papers was also performed. For uncoated paper, persulfate treatment was the most efficient. For coated papers, all treatments were inefficient in the used conditions, although a decrease of the wet tensile force of degraded samples was observed. The main responsible of the decrease of persulfate efficiency for coated papers was probably related to side reactions of free radicals with the coating constituents.

Key-words: polyamideamine epichlorohydrin resin, PAE cross-linking reactions, carboxymethylcellulose, wet strength mechanism, PAE-based papers, polyelectrolytes adsorption, paper recycling.

RÉSUMÉ EN FRANÇAIS

1. Introduction

Le travail présenté dans ce manuscrit s'intéresse au mode d'action des résines thermodurcissables utilisées pour conférer au matériau papier des propriétés spécifiques. En effet, certains papiers sont destinés, au cours de leur usage, à être en contact avec des liquides et en particulier de l'eau. C'est le cas, par exemple, des papiers absorbants, de certains papiers filtres, mais aussi de papiers pour étiquettes ou pour billets de banque. En présence d'eau, les papiers perdent rapidement leur résistance mécanique, essentiellement due à la présence en grand nombre de liaisons hydrogène, d'où la nécessité d'un traitement : l'objectif est de maintenir un certain niveau de résistance des papiers saturés en eau. Ces traitements consistent à introduire dans la suspension fibreuse, en cours d'élaboration, des pré-polymères cationiques s'adsorbant à la surface des fibres. Après la formation de la feuille de papier, la feuille humide est séchée et c'est au cours de cette étape que s'amorce la réticulation de ces polymères. Elle conduit à la formation d'un réseau tridimensionnel de polymère dans le matelas fibreux. Ce réseau permet au papier de conserver ses propriétés mécaniques lorsqu'il est en contact avec de l'eau. Il présente ce que l'on appelle communément une résistance à l'état humide (REH).

Un des inconvénients de ce type de traitement est lié aux difficultés de recyclage des papiers obtenus. Il nécessite un traitement particulièrement intensif et coûteux qui couple une action mécanique (désintégration, dépastillage) à une action chimique (utilisation d'hydroxyde de sodium, par exemple). Même si ces produits sont largement utilisés, les mécanismes mis en jeu que ce soit pour le développement des propriétés de REH ou pour le recyclage ne sont pas totalement compris. Dans ce contexte, ce travail a pour objectif d'étudier le mode d'action de pré-polymères de polyamideamine épichlorhydrine (PAE), couramment utilisés en papeterie pour conférer au matériau papier une résistance à l'état humide (REH). Il s'intéresse à la caractérisation de solutions commerciales de PAE et à l'étude des mécanismes réactionnels de ces pré-polymères. Il traite également de l'effet de certains paramètres de production du papier sur l'efficacité des traitements. Enfin, il apporte de éléments nouveaux sur la compréhension de l'étape de recyclage.

Le manuscrit est divisé en deux parties :

(i.) Caractérisation des résines PAE pour une meilleure compréhension des phénomènes de réticulation,

(ii.) Utilisation des résines PAE en papeterie : préparation et recyclage de papiers traités.

1.1. Caractérisation des résines PAE pour une meilleure compréhension des phénomènes de réticulation

Dans cette partie, nous nous sommes intéressés à la caractérisation de solutions commerciales de PAE : des analyses spectroscopique en RMN du liquide ont été menées et des titrations colloïdales ont été réalisées en fonction du pH et de la force ionique du milieu.

Dans un second temps, un travail approfondi a été conduit pour comprendre les phénomènes de réticulation se produisant dans des films de PAE. Pour ce faire, nous avons effectué :

(i.) un travail de recherche bibliographique approfondie du sujet,

(ii.) la mise au point de protocoles de formation de films,

(iii.) la mise au point d'un protocole de traitement thermique des films pour provoquer de façon reproductible la réticulation de la PAE (polymères thermodurcissables) et ceci en testant différentes températures et durées,

(iv.) la caractérisation de ces films : recherche de solvants, comportement dans l'eau, caractérisation par FTIR en transmission principalement, par analyse mécanique dynamique (DMA), par analyse calorimétrique différentielle (DSC), en RMN du solide, étude en microscopie électronique à balayage.

La même approche expérimentale a ensuite été appliquée à la caractérisation de films composés de PAE et de carboxy-méthylcellulose (CMC) dans différentes proportions en masse (75%/25% ; 50%/50% ; 25%/75%) avant et après traitement thermique. Dans ce cas particulier, la CMC est utilisée comme composé modèle des fibres cellulosiques papetières. La CMC permet donc de mettre en évidence des

réactions susceptibles de se produire notamment avec les groupements carboxyliques des hémicelluloses des fibres. Là encore, des essais de caractérisation par spectrométrie infra-rouge, RMN du solide, par analyse mécanique dynamique (DMA), par analyse calorimétrique différentielle (DSC) ont été menés. Les films ont également été observés en microscopies optique et électronique à balayage et ces essais ont été complétés par de la micro-analyse X.

Cette première partie de l'étude a montré l'importance des conditions de préparation des films de PAE sur leurs propriétés. Ces résultats nous ont permis de proposer une méthode de formation dans une enceinte climatique à 50% d'humidité relative et à 23°C.

Nous avons par ailleurs pu mettre au point les conditions expérimentales en analyse mécanique dynamique (DMA) pour ce type de produit. Les traitements thermiques des films ont été effectués à 105°C pendant des durées variables (10 et 30 min et 1, 2, 4, 6, 12, 24h) et les résultats obtenus sont parfaitement cohérents. Les essais en analyse calorimétrique différentielle (DSC) ont nécessité un protocole spécifique de formation de film « in situ » dans les coupelles destinées à l'analyse. Là encore, les conditions opératoires ont été optimisées. Les caractérisations en FT-IR ont permis de mettre en évidence des pics endotermiques et exothermiques caractéristiques des produits testés avant et après traitement thermique. Enfin, un travail très important a été réalisé en RMN du liquide et du solide. Les résultats obtenus en RMN du liquide sur de la PAE en solution ont conclu à la faisabilité de la technique sur des produits industriels où la présence en grande quantité de sous-produits des réactions peut rendre difficile l'interprétation des résultats. En RMN du solide, la réalisation d'essais sur des films ayant subi ou non des traitements thermiques a été concluante.

L'analyse des essais obtenus en FTIR, RMN, DMA et DSC a permis de mettre en relation les résultats obtenus pour ces différentes techniques et nous a conduit à une description des mécanismes réactionnels de réticulation de la PAE. Ils montrent notamment que certains mécanismes décrits dans la littérature doivent être remis en cause. Notons qu'il n'existe pas à ce jour de travaux publiés sur une caractérisation aussi complète de tels matériaux.

La Figure 1.1 montre, par exemple, l'évolution de la charge de la PAE en solution en fonction du pH.

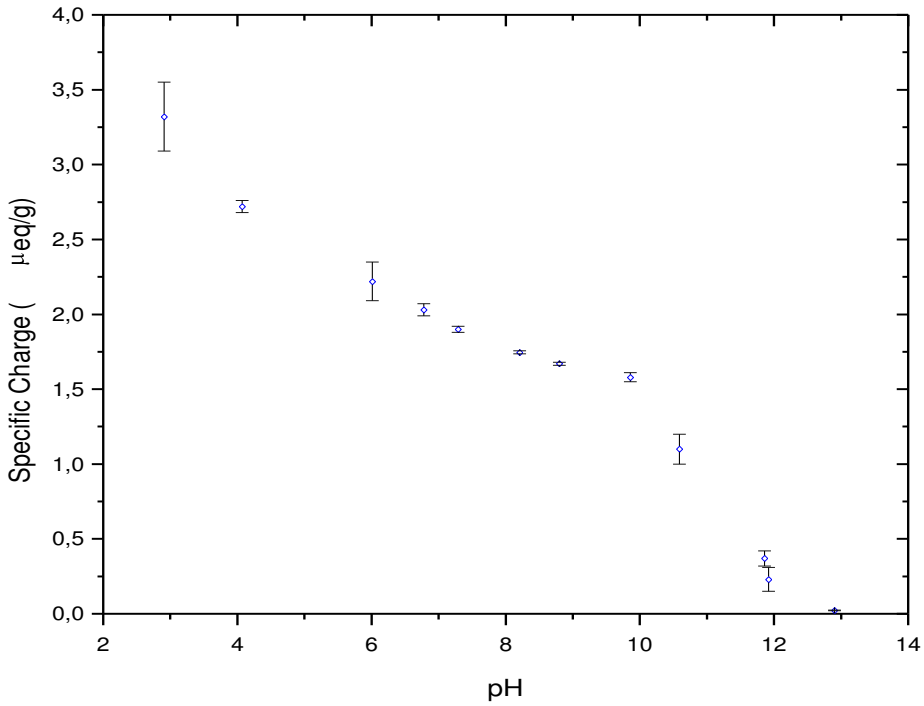

Figure 1.1 : *Titration colloïdale de la solution industrielle de PAE pour la détermination de la charge en fonction du pH.*

La diminution de la charge avec l'augmentation du pH traduit la déprotonation des fonctions amine et, aux plus forts pH, l'ouverture éventuelle du cycle azétidinium. Les essais menés en RMN ont permis de confirmer la structure chimique de la PAE (voir Figures 1.2 et 1.3). Les lettres repérant les différents pics font référence à la structure de la PAE donnée en Figure 1.2.

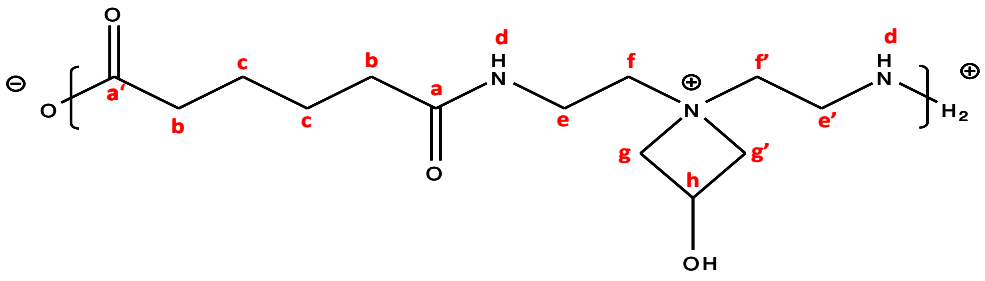

Figure 1.2 : *Structure de la PAE obtenue à partir des essais en RMN du liquide.*

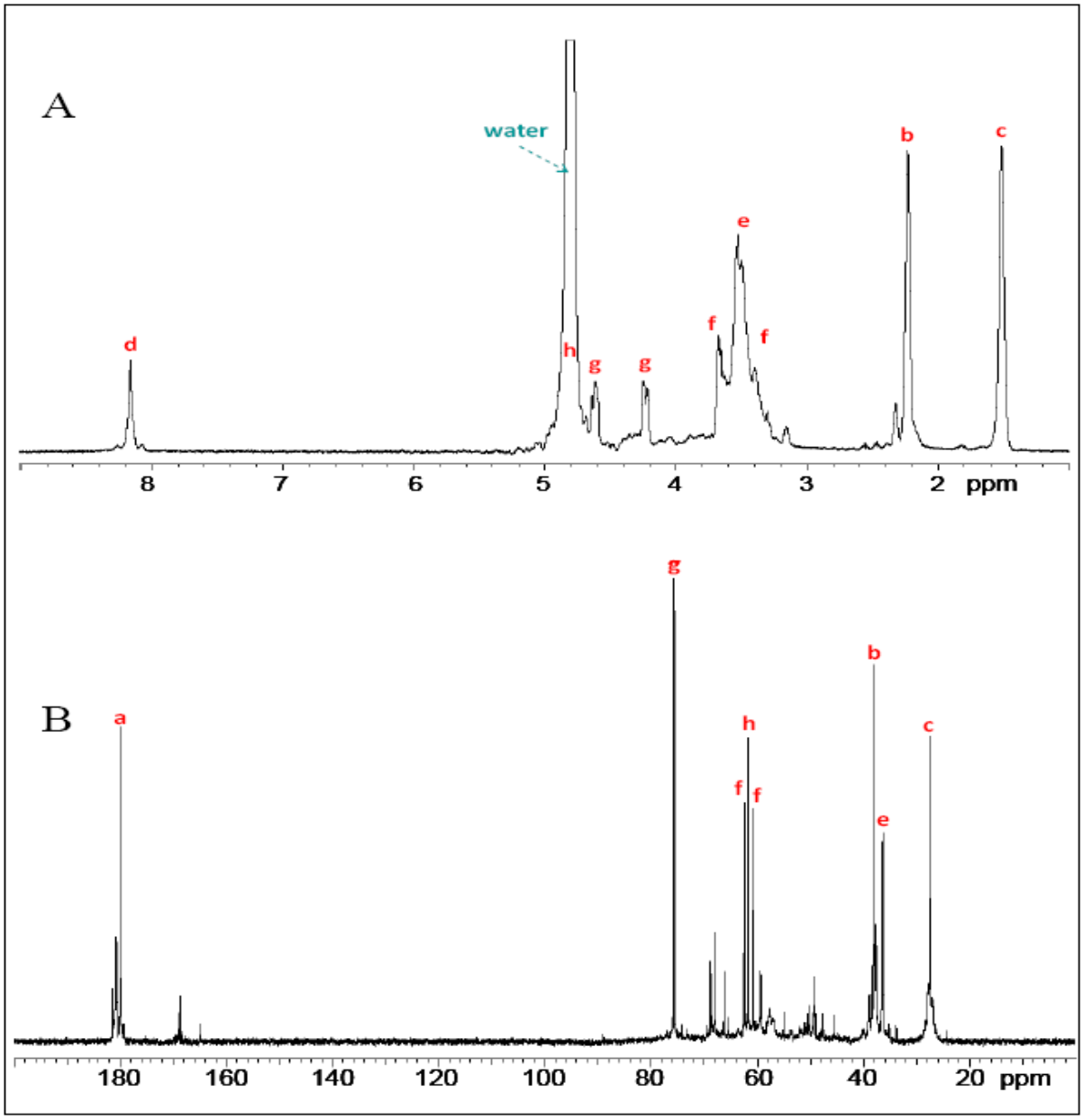

Figure 1.3 : *Spectres RMN de la solution commerciale de PAE dans D_2O/DCl à 25°C* ***A)*** *^{1}H and* ***B)*** *^{13}C.*

Cette affectation a été rendue possible par l'utilisation de plusieurs techniques de RMN comme le montre le Tableau I.1.

Tableau I.1 : *Résultats obtenus en RMN du liquide – techniques mises en oeuvre.*

a (NHCO)	**h**	**g**	**f**	**i**	**e**	**b**	**c**	**d**	
180	61.7	75.65	62.35 60.8		36.25	38.1	27.4		δ ^{13}C
	CH	**CH_2**	**CH_2**		**CH_2**	**CH_2**	**CH_2**		**DEPT 135**
1	0.5	1	2x0.5		1	1	1		Integrals (^{13}C)
	4.8	4.6 4.2	3.7 3.4		3.5	2.2	1.51	8.16	δ ^{1}H **$^{1}J_{CH}$** HMQC **correlations**
3.5 2.2 1.5	4.6 4.2	4.8 3.7 3.4	4.8 3.5 4.6 4.2		8.16 3.7 3.4	1.5	2.2		^{1}H **$^{n}J_{CH}$** HMBC **correlations**
	75.7 62 60	61.7 62.3 60.8	75.7 61.7 36.3		180 60.8	180 27.4	180 38.1	36.25	^{13}C
	4.6 4.2	4.8 4.2 4.6	3.5		8.16 3.7 3.4	1.51	2.2	3.5	^{1}H **$^{n}J_{HH}$** COSY **correlations**

La caractérisation des films par FTIR, avant et après traitement thermique, montre des différences entre les spectres (Figure 1.4).

La mise en relation de ces résultats avec la RMN du solide et les analyses en DMA (voir Figure 1.5) et en DSC permettent d'arriver aux conclusions suivantes :

(i.) la réaction principale de réticulation est une attaque nucléophile des atomes d'azote par le cycle azétidinium avec la formation d'amines tertiaires et de liaisons 2-propanol entre les chaînes de PAE (Figure 1.6),

(ii.) cette réaction peut être accélérée par un traitement thermique à une température supérieure à la Tg du polymère déterminée par DMA. On peut cependant

avoir une réticulation complète sans traitement thermique à condition de stocker le film à température ambiante pendant une durée voisine de 3 mois,

(iii.) il existe une réaction secondaire entre les cycles azétidinium et les groupements terminaux (carboxyliques) de la PAE (Figure 1.7). Cependant, cette réaction ne se produit qu'après un traitement thermique et les liaisons formées sont facilement hydrolysables (notamment au cours d'un stockage à l'air ambiant). Les films montrent des comportements différents si ces liaisons existent (films rigides) ou sont hydrolysées (films souples). Ces liaisons ont été mises en évidence à la fois par FTIR et RMN (voir par exemple la Figure 1.8).

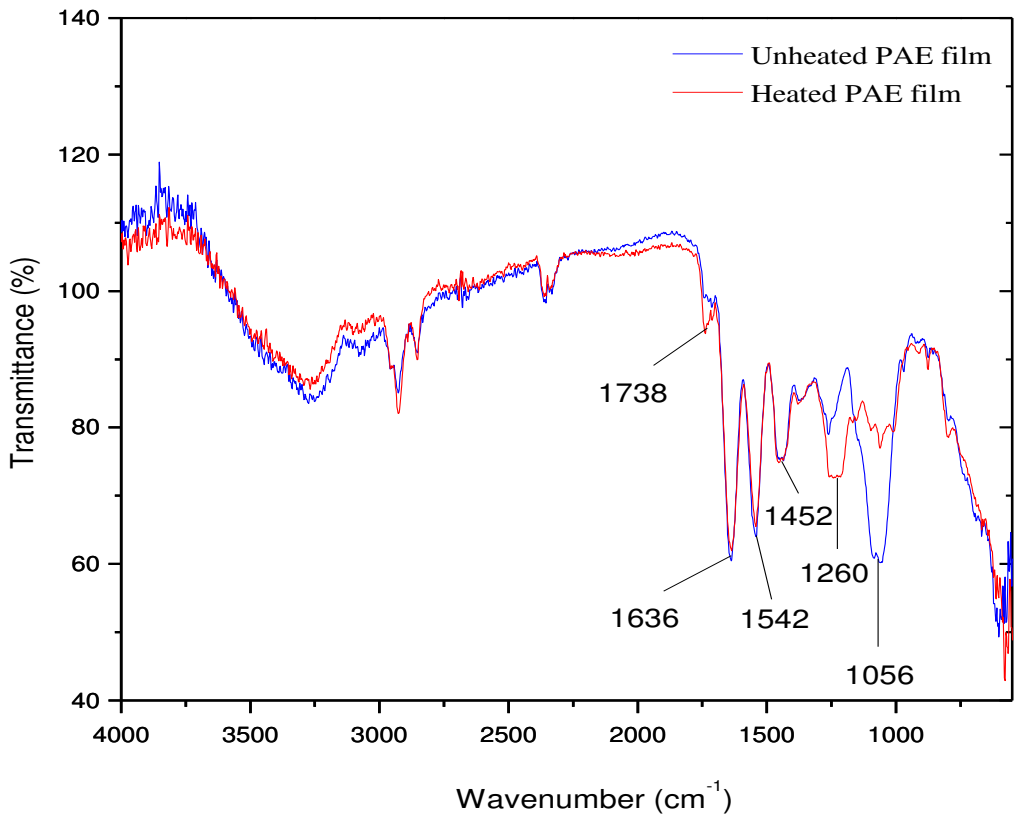

Figure 1.4 : *Analyse FTIR de films de PAE avant et après un traitement thermique à 105°C pendant 24h.*

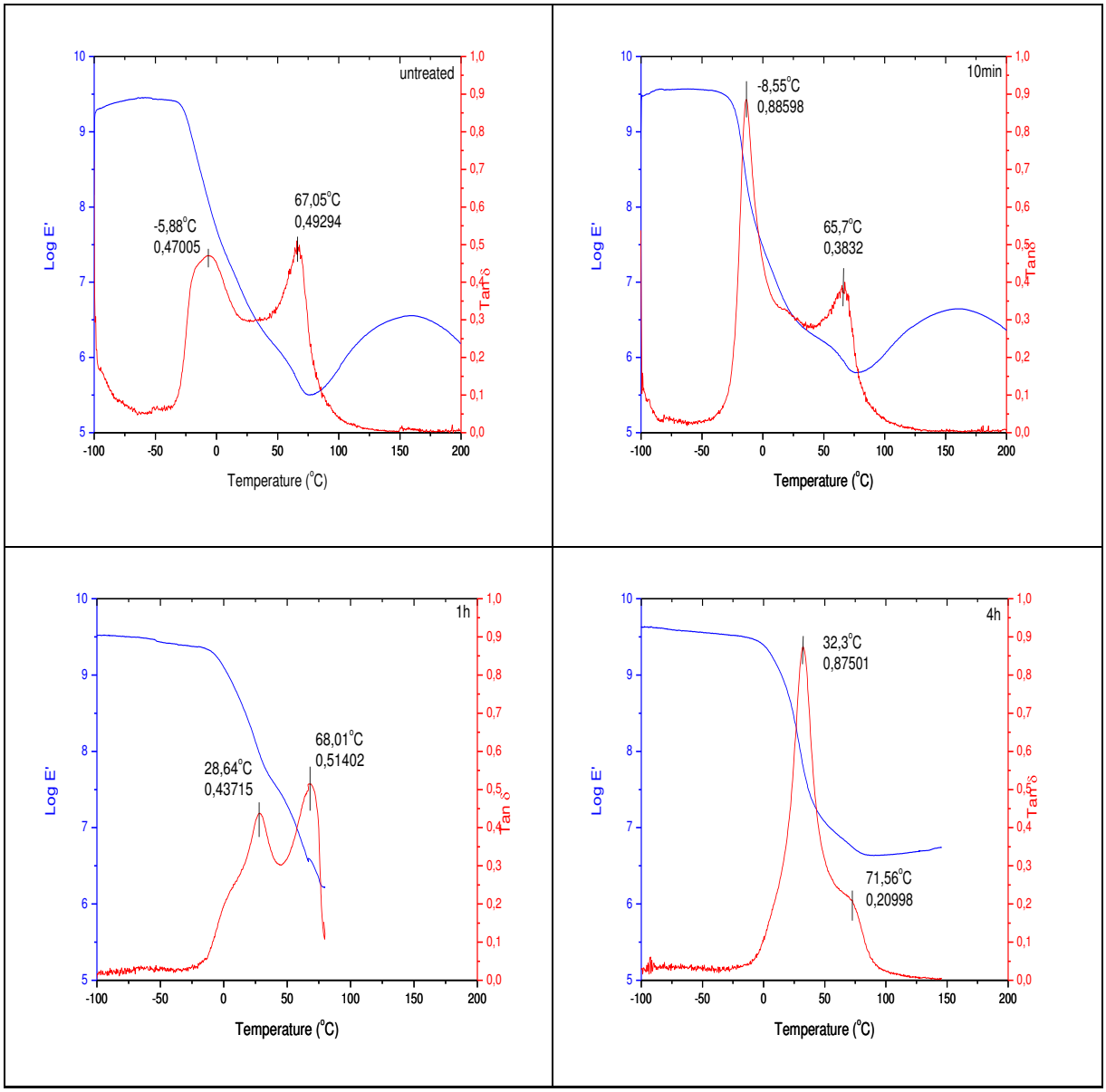

Figure 1.5 : *Courbes Log E'et tan δ obtenues en DMA pour des films de PAE n'ayant subi aucun traitement thermique et avec un traitement thermique à 105°C pendant 10 min et 1 et 4h.*

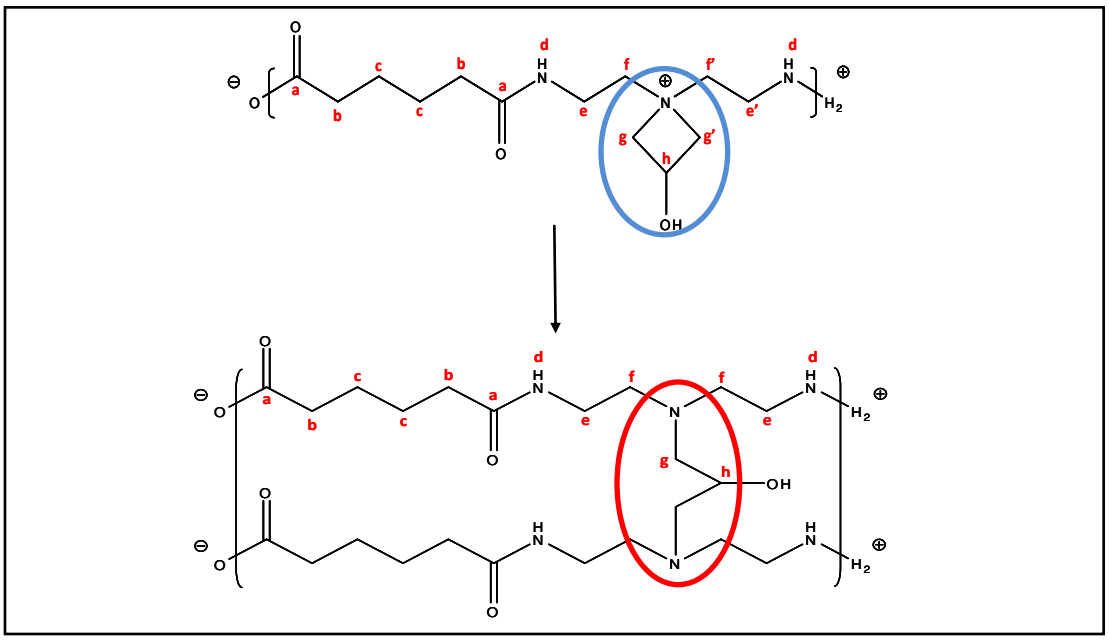

Figure 1.6 : *Réaction prépondérante de réticulation de la PAE.*

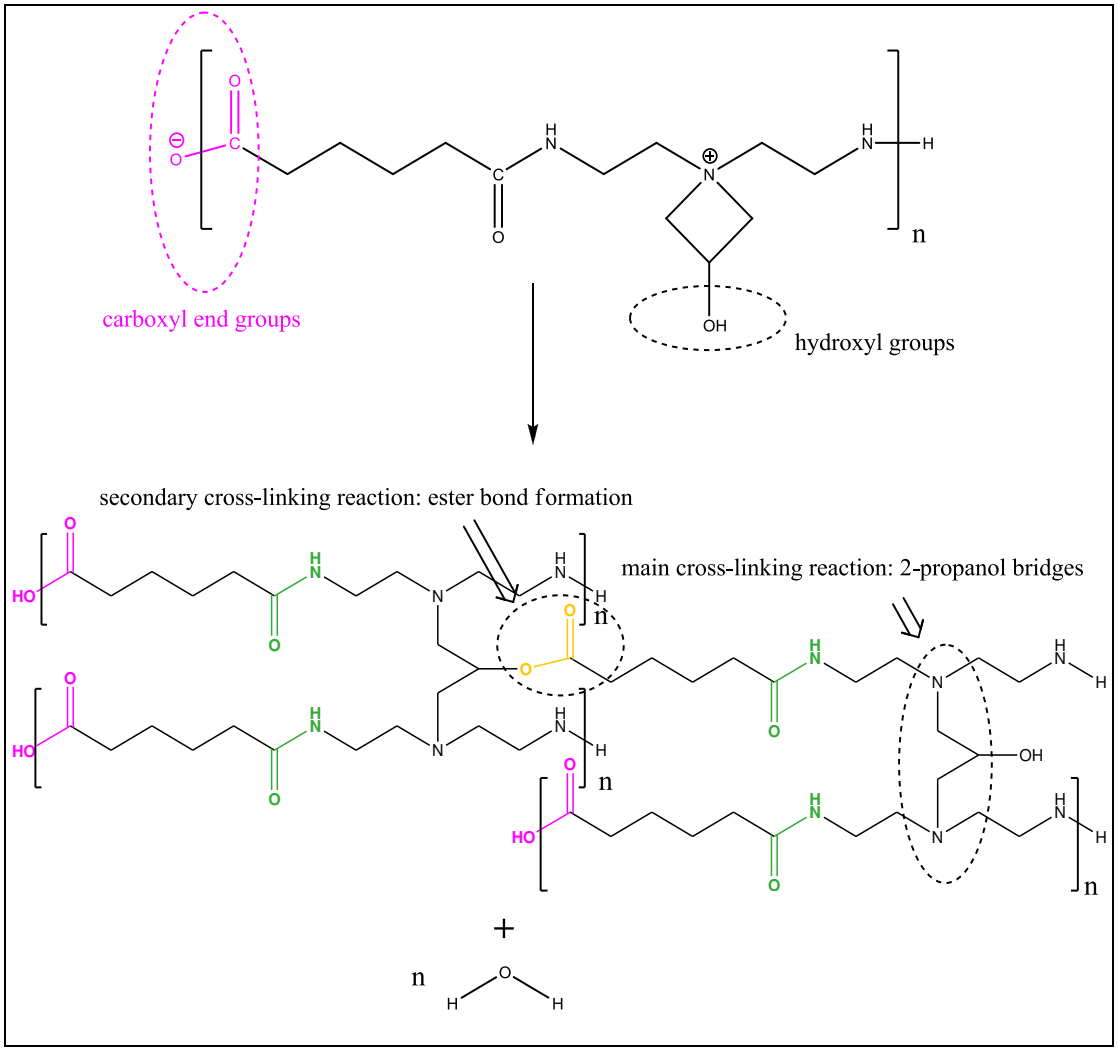

Figure 1.7 : *Réaction secondaire de réticulation de la PAE.*

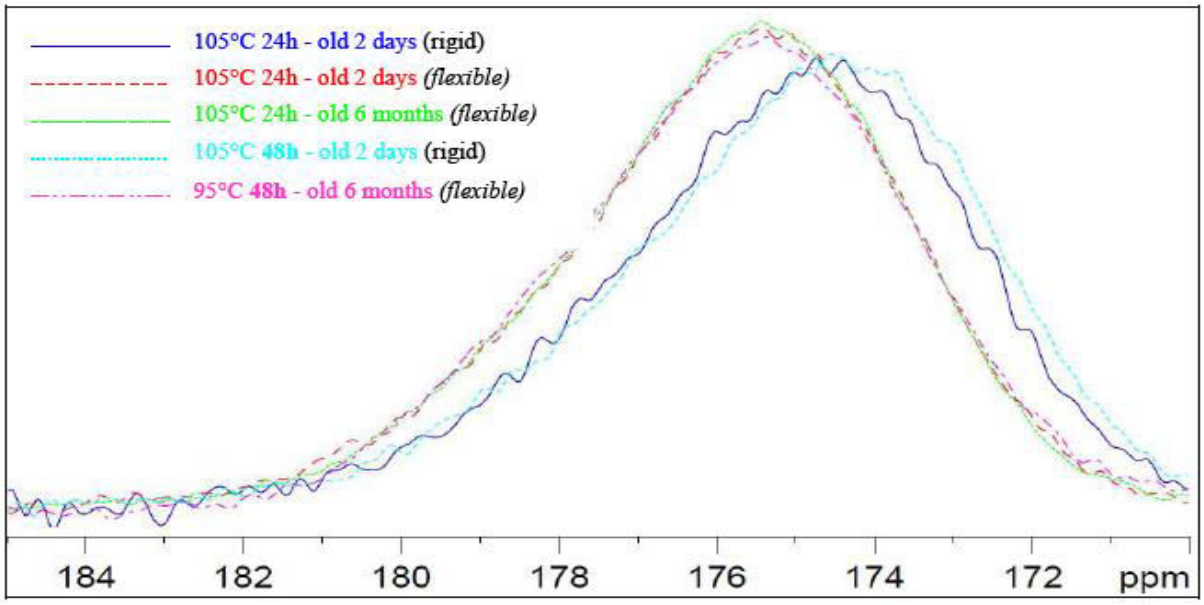

Figure 1.8 : *RMN du solide (spectre du ^{13}C) pour des films de PAE traités thermiquement (région des carbonyles et carboxyles : 170-182 ppm). Films conservés à l'air ambiant (souples) et en atmosphère anhydre (rigides).*

Des études ont été menées en adoptant la même démarche pour des films produits à partir de CMC et de mélange de CMC et de PAE. Les résultats obtenus sont novateurs. Il n'existe pas de travaux publiés à ce jour sur la caractérisation de tels matériaux. Les films composés de CMC seule ont montré des comportements différents selon que le produit utilisé était riche en sels (NaCl : cas du produit industriel) ou purifié. En présence de PAE, la formation de liaisons ester après un traitement thermique a pu être très facilement mise en évidence du fait de la présence en grande quantité de groupements carboxyliques associés à la CMC (Figure 1.9).

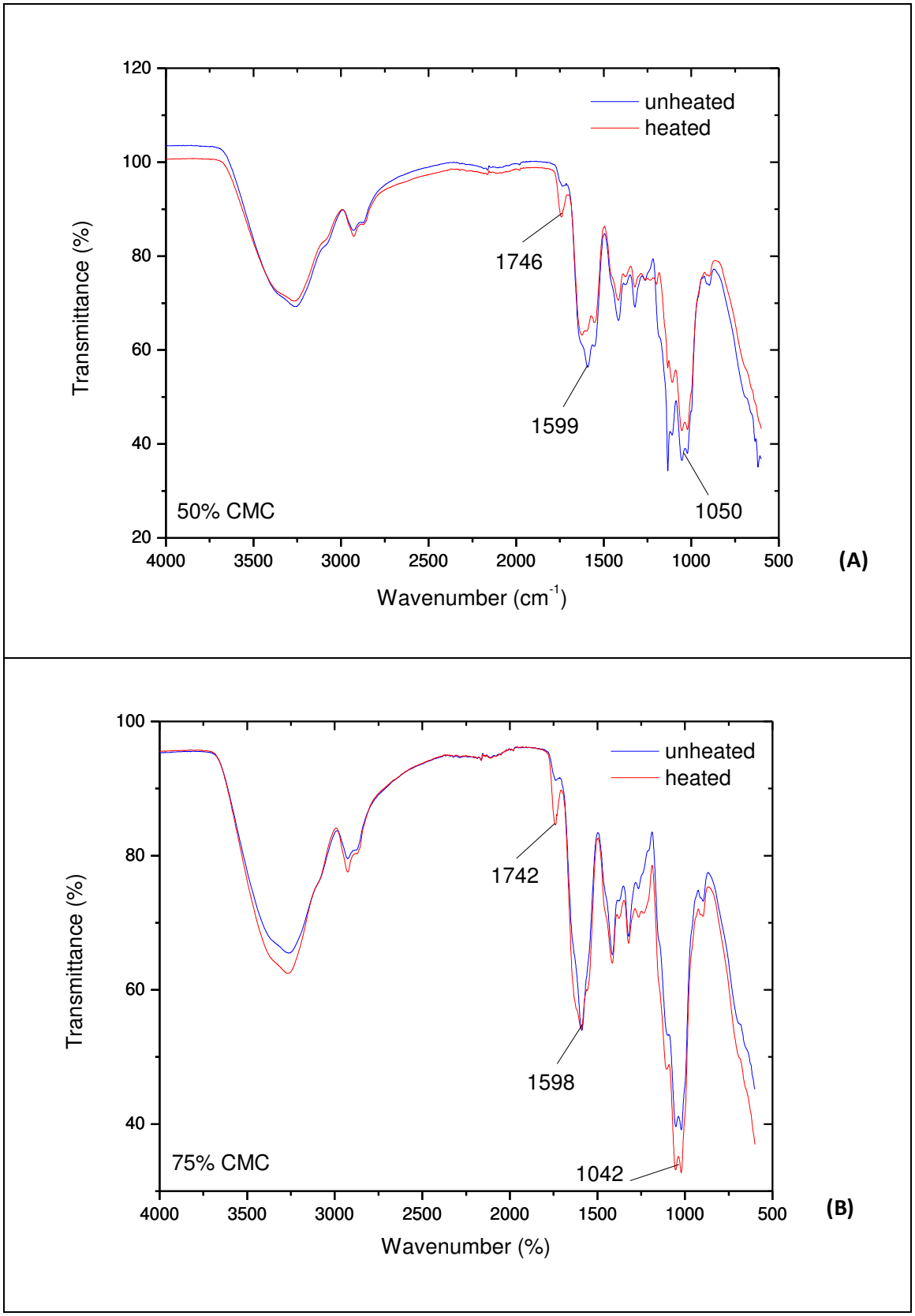

Figure 1.9 : *Spectres FTIR de films de CMC/PAE non traités et traités thermiquement (A) 50 et (B) 75 % de CMC.*

2. Utilisation des résines PAE en papeterie : préparation et recyclage de papiers traités REH.

Dans un premier temps, une campagne de caractérisation des propriétés REH de papiers de laboratoire (formettes) obtenus dans différentes conditions a été menée. Se basant sur des méthodologies relativement classiques pour nos domaines, cette étude a été réalisée avec plusieurs objectifs :

(i.) vérifier un certains nombre de travaux de la littérature présentant des résultats soient contradictoires, soient perçus comme assez peu fiables,

(ii.) apporter des réponses sur l'effet de certains paramètres de production des papiers pour lesquels il n'existe pas de données quantitatives dans la littérature,

(iii.) répondre à des interrogations du partenaire industriel sur l'efficacité des traitements REH.

Les principales étapes de cette étude ont été les suivantes : préparation des suspensions fibreuses (désintégration, raffinage), traitement des suspensions (introduction des additifs), caractérisation des suspensions (morphologique, physico-chimique), préparation des feuilles de laboratoire et caractérisation physique des papiers obtenus. Les paramètres suivants ont été fixés : composition fibreuse (100% fibres d'eucalyptus), raffinage (30 degrés Schopper Riegler), pH de travail (entre 7 et 8), concentration des suspensions fibreuses (10 g/L), conditions de mélange des additifs et mode de préparation des papiers de laboratoire (séchage de 10 min à 80°C). Les paramètres de fabrication plus spécifiquement étudiés ont également été choisis : réalisation ou non d'un traitement thermique des papiers (10 min à 130°C), temps de contact entre la suspension fibreuse et les additifs, force ionique du milieu, concentration des additifs de REH ajoutée, durée de stockage des papiers en atmosphère normalisée. Cette étude a permis de :

(i.) caractériser les suspensions fibreuses : analyse morphologique, titrations colloïdales pour la détermination des charges de surface (utilisation du polyDADMAC

ou de la PAE comme agent titrant), titrations conductimétriques et potentiométriques pour la détermination des charges totales,

(ii.) caractériser la cinétique d'adsorption de la PAE par les fibres lignocellulosiques de façon indirecte et directe : suivi du potentiel zêta des éléments de la suspension fibreuse au cours de l'adsorption de PAE, mesure de la quantité de PAE adsorbée par analyse élémentaire,

(iii.) caractériser l'effet sur la résistance à l'état humide des papiers :

- de la quantité de PAE ajoutée,
- de la conductivité de la suspension fibreuse (100 à 3000 µS/cm),
- d'un traitement thermique des papiers à 130°C,
- du temps de stockage des papiers (entre 1 jour et 6 mois).

Pour mieux comprendre les mécanismes d'amélioration de la REH des papiers après un traitement à la PAE, des observations en microscopie électronique à balayage de sections de bandes de papier après une rupture en traction ont été réalisées. En parallèle de cette étude, des essais de dégradation ont été effectués sur des films de PAE pure dans le but d'évaluer l'efficacité des traitements chimiques réalisés habituellement sur des papiers traités REH. L'objectif de cette étude était de faire le point sur l'effet des additifs non chlorés utilisés pour la remise en suspension des papiers traités REH. Nous avons donc travaillé plus particulièrement avec les réactifs suivants : soude, acide sulfurique, peroxyde d'hydrogène et persulfate de potassium. Industriellement, les papiers REH sont remis en suspension en présence de soude et/ou de persulfate de potassium mais il existe très peu d'études sur cette opération unitaire et aucune publication ne s'intéresse à l'effet des réactifs sur des films. Les mêmes réactifs ont été utilisés sur des papiers industriels traités REH prélevés sur une machine à papier avant et après une étape d'enduction (papiers couché et non couché pour étiquettes, fabriqués en milieu neutre et traités à la PAE). L'objectif était de comparer l'efficacité des traitements des papiers à celle obtenue pour de la PAE pure. Nous nous sommes également intéressés à l'effet de l'opération d'enduction. Pour ces essais de dégradation, des méthodes expérimentales fiables et reproductibles ont dû être mises au point.

Pour les films réticulés, ce protocole consiste à mettre en contact dans des conditions d'agitation rigoureusement contrôlées un film de PAE traité thermiquement et un réactif dans différentes conditions de pH, de temps et de température. Au terme de cette étape, le mélange réactif + film est filtré sur une toile Nylon (1µm), rincé à l'eau distillée et la partie gel du film traité est conservée, séchée et pesée. Dans certains cas, le produit est caractérisé en FTIR dans le but de mettre en évidence les modifications chimiques subies par le film réticulé à l'issue de cette étape de dégradation. Pour les papiers, des bandelettes ont été découpées et mises en contact avec la solution aqueuse contenant le réactifs pendant un temps donné et à température contrôlée. Après cette première étape, les bandelettes sont rincées et soumises à un essai de traction. La force à la rupture est comparée à celle obtenue pour des papiers humides n'ayant subi aucun traitement.

Dans le but d'étudier l'effet des conditions de fabrication de papiers de laboratoire sur la REH, différentes suspensions fibreuses ont été caractérisées en l'état et après un traitement mécanique de raffinage : propriétés morphologiques des pâtes et propriétés physico-chimiques. Le choix a été fait de s'intéresser principalement à une pâte d'Eucalyptus. De nombreux essais ont été réalisés : titration colloïdale par la PAE et le polyDADMAC (Tableau II.1), propriétés électrocinétiques des pâtes, charge totale (Tableau II.2).

Tableau II.1 : *Charge de surface des fibres d'Eucalyptus raffinées à 30°SR déterminée par titration colloïdale.*

Surface charge (µeq/g)	***Titrant***	***Sodra Blue***	***Suzano***
Streaming potential	***Polydadmac***	**7.52**	**11.7**
	PAE	**11.0**	**13.7**
Electrophoretic mobility	***Polydadmac***	**4.42**	**4.94**
	PAE	**6.23**	**8.40**

Une deuxième campagne d'essais a été réalisée sur l'effet des conditions opératoires sur le niveau de REH de papiers de laboratoire. Les travaux ont permis de suivre le potentiel zêta de la surface des fibres papetières en fonction du temps d'agitation et du temps de contact dans des conditions expérimentales rigoureusement

définies. Ils ont permis de confirmer que pour des temps de contact testés et conformes à ceux pratiqués industriellement, un équilibre apparent en terme d'adsorption était atteint.

Tableau II.2 : *Charge totale des fibres d'Eucalyptus raffinées à 30°SR déterminée par titration conductimétrique et potentiométrique*

Total charge (µeq/g)		***Sodra Blue***	***Suzano***
Potentiometric	***NaOH***	25.5 ± 4.8	44.0 ± 7.6
Conductometric	***NaOH***	30.2 ± 1.2	39.8 ± 1.7
	$NaHCO_3$	10.2 ± 1.8	14.9 ± 2.7

L'effet du temps de stockage des papiers de laboratoire a été également analysé sur une période de 6 mois. Les résultats ont montré que la REH se stabilise après environ 5 semaines de stockage et que cette stabilisation est atteinte plus rapidement si un post-traitement thermique est appliqué au papier après séchage. En revanche, le niveau de REH reste le même à partir environ d'un mois de stockage avec ou sans post-traitement thermique. Les essais ont permis également de montrer que la conductivité était un paramètre important et ceci d'autant plus que le dosage de PAE est élevé bien. Malgré tout, il est apparu que son effet restait réduit par rapport à ce qui est annoncé classiquement dans la littérature (Figure 2.1).

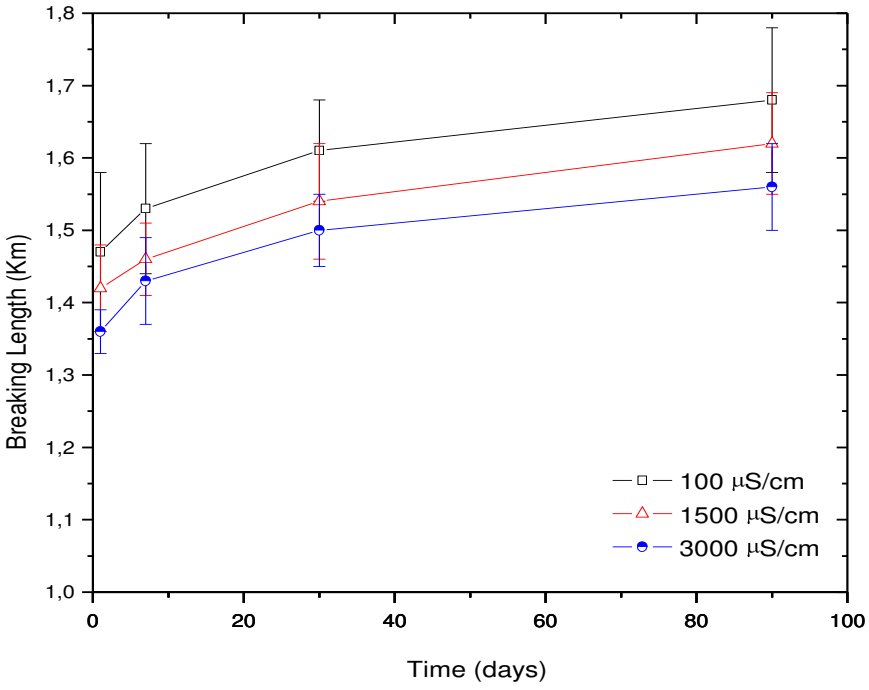

Figure 2.1 : *Évolution de la longueur de rupture à l'état humide de papiers traités avec 1% de PAE en fonction du temps de stockage et pour différents niveaux de conductivité.*

En ce qui concerne les essais de dégradation des films de PAE, les résultats montrent que les deux réactifs les plus efficaces sont le peroxyde d'hydrogène et le persulfate de potassium. Dans les conditions expérimentales les plus efficaces (c'est-à-dire couplés à l'utilisation de soude), ces réactifs provoquent une perte en masse du film de PAE supérieure à 30%. En conclusion, cette étude montre qu'il est possible d'optimiser l'utilisation d'agents chimiques pour intensifier l'opération de désintégration des papiers REH traités à la PAE.

Tableau II.3 : *Essais de dégradation des films de PAE dans l'eau ou dans des solutions aqueuses en présence de réactifs (temps de réaction 3h ; température : 80°C). Δm est la perte relative de masse du film après traitement. Les indices i et f correspondent à des mesures réalisées respectivement en début et en fin d'essai. Masse de film traité : environ 8 g dans 100 mL de solution.*

	(mmol)	pH_i	***Conductivity*** $(\mu S/cm)_f$	pH_f	***Conductivity*** $(\mu S/cm)_f$	Δm ***(%)***
H_2O	100mL	5.9	1.64	3.2	12980	7.48
NaOH	20	11	7800	10	44400	17.4
H_2SO_4	1.04	2.8	921	3	13200	7.31
$K_2S_2O_8$	1.04	3.9	2162	3	8160	17.8
H_2O_2	1	5.4	6.4	2.6	5990	20.7
H_2O_2 + ***NaOH***	1 + 30	12	7564	11.5	16450	22.3

* avant ajout du peroxyde d'hydrogène

Comme discuté plus haut, l'étude de la dégradation des films a été complétée par celle de papiers industriels. Nous avons dans un premier temps montré que les papiers testés présentaient tous des propriétés physiques très proches et une REH voisine comprise entre 20 et 25 % (voir Tableau II.4). La résistance à l'état humide était stable au bout de 10 min dans l'eau. Les essais de dégradation ont montré que cette résistance pouvait être significativement diminuée par l'utilisation de certains additifs. A titre d'exemple, les Tableaux II.5 et II.6 montrent des résultats obtenus pour le papier fabriqué en milieu neutre (couché et non couché).

Tableau II.4 : *Propriétés de résistance mécanique en traction en état sec et humide des papiers industriels couchés (NC) et non couchés (NU).*

	Force (N)	**Breaking length (Km)**	**Stretch (mm)**	**Specific energy (mJ/g)**	**Young modulus (GPa)**
NC dry	61.7 ± 2.9	6.42 ± 0.32	1.51 ± 0.11	592 ± 63	8.90 ± 0.32
NU dry	46.3 ± 3.5	6.51 ± 0.53	1.72 ± 0.12	724 ± 9	6.11 ± 0.41
NC wet	19.6 ± 1.3	2.02 ± 0.13	3.38 ± 0.20	424 ± 64	0.444 ± 0.385
NU wet	13.0 ± 1.8	1.84 ± 0.25	3.78 ± 1.58	397 ± 77	1.06 ± 0.35

Tableau II.5: *Effet des traitements de dégradation des papiers non couchés sur les propriétés de résistance mécanique en traction. Certains essais ont été doublés pour s'assurer de la reproductibilité de la méthode.*

	pH_f	**Force (N)**	**Stretch (mm)**	**TEA index (mJ/g)**	**Young modulus (GPa)**
NaOH (1.5%)	12	7.00 ± 0.32	2.36 ± 0.15	42.8 ± 4.9	0.200 ± 0.007
H_2O_2 (2.75%)	6.4	6.80 ± 0.63	1.80 ± 0.23	100 ± 23	0.69 ± 0.07
	6.4	7.20 ± 0.27	1.81 ± 0.09	111.3 ± 8.7	0.91 ± 0.09
H_2O_2 (2.75%) + **NaOH** (1.5%)	11.3	4.40 ± 0.23	1.50 ± 0.09	56.4 ± 6.4	0.61 ± 0.04
	11.5	4.60 ± 0.20	1.59 ± 0.13	62.8 ± 9.3	0.63 ± 0.05
$K_2S_2O_8$ (2.75%)	2.7	nm*	nm*	nm*	nm*
$K_2S_2O_8$ (2.75%) + **NaOH** (1.5%)	11.4	nm*	nm*	nm*	nm*
H_2SO_4 (1.5%)	7.1	9.90 ± 0.63	2.56 ± 0.10	63.9 ± 5.0	0.26 ± 0.02

* nm : non mesurable

Tableau II.6 : *Effet des traitements de dégradation des papiers couché sur les propriétés de résistance mécanique en traction.*

	pH_f	**Force (N)**	**Stretch (mm)**	**TEA index (mJ/g)**	**Young modulus (GPa)**
NaOH (1.5%)	12	11.4 ± 0.5	2.70 ± 0.20	59.6 ± 7.0	0.298 ± 0.010
H_2O_2 (2.75%)	6.4	12.3 ± 0.6	2.52 ± 0.12	198 ± 17	1.17 ± 0.09
	6.4	12.0 ± 0.5	2.52 ± 0.21	186 ± 21	0.950 ± 0.130
H_2O_2 (2.75%) + **NaOH** (1.5%)	11.3	7.40 ± 0.78	1.84 ± 0.25	88.9 ± 22.4	0.92 ± 0.11
	11.2	7.60 ± 0.21	1.95 ± 0.13	93.7 ± 10.2	0.83 ± 0.08
$K_2S_2O_8$ (2.75%)	2.4	6.00 ± 0.11	1.78 ± 0.19	74.2 ± 9.9	0.97 ± 0.08
$K_2S_2O_8$ (2.75%) + **NaOH** (1.5%)	11.6	7.60 ± 0.40	1.90 ± 0.11	90.7 ± 11.3	0.88 ± 0.09
H_2SO_4 (1.5%)	7.0	14.2 ± 2.6	2.59 ± 0.81	73.3 ± 26.6	0.383 ± 0.01

Dans ces Tableaux, les quantités de réactifs sont exprimées en fraction massique par rapport à la masse sèche de papier traité. Ces fractions massiques sont représentatives de ce qui est classiquement fait industriellement. Les essais ont été réalisés à 80°C pendant 40 min. Après le traitement, les bandelettes de papier sont immédiatement rincées et testées en traction. Ces résultats montrent que :

(i.) l'efficacité des réactifs n'est pas forcément identique quand on compare les résultats obtenus avec les films et ceux obtenus pour les papiers,

(ii.) c'est le persulfate de potassium, réactif assez classiquement mis en œuvre industriellement, qui est le plus efficace dans les conditions expérimentales testées en laboratoire : ce produit agit probablement selon un mécanisme de réaction radicalaire,

(iii.) la couche présente sur les papiers enduits modifie sensiblement les résultats obtenus et diminue l'efficacité des réactifs dont on suppose qu'ils sont partiellement consommés par les constituants de la couche (latex, charges minérales, additifs).

En conclusion, cette étude a permis d'optimiser les conditions de recyclage des papiers grâce à :

- une meilleure compréhension de l'effet des paramètres de production des papiers sur la valeur de la résistance à l'état humide,
- une étude de la dégradation de films de PAE,
- une étude de la dégradation de papiers industriels,
- la proposition de mécanismes réactionnels (réaction radicalaire) pour le persulfate de potassium.

Du point de vue du fonctionnement de l'opération unitaire de désintégration des papiers, elle a permis de montrer le fort impact de la couche des papiers enduits sur l'efficacité des traitements.

3. CONCLUSION

Les résines PAE sont largement utilisées depuis les années 1960 du fait de leur efficacité et de leur coût relativement modéré. Les mécanismes à l'origine de la résistance à l'état humide des papiers traités ne sont cependant pas parfaitement connus. De même, la maîtrise des conditions de recyclage des papiers traités REH n'est pas parfaite. Dans ce contexte, les objectifs de ce travail étaient d'acquérir des connaissances pour mieux comprendre et/ou optimiser :

- le mode d'action de ces produits par la caractérisation des résines PAE et des mécanismes de réticulation,
- l'effet des paramètres de fabrication des papiers sur la résistance à l'état humide des papiers traités,
- le recyclage des papiers.

Nous avons pu ainsi mettre en évidence les réactions intervenant au cours de la réticulation de la résine PAE étudiée. L'utilisation de CMC en tant que composé modèle des fibres cellulosiques papetières a permis de confirmer qu'une réaction des cycles azétidinium avec les groupements carboxyliques de la CMC était possible. Néanmoins, compte tenu des résultats obtenus, il apparaît peu probable que ce type de réaction joue un rôle important pour la résistance à l'état humide du papier et sa contribution peut donc être considérée comme négligeable.

Dans une deuxième partie, nous nous sommes intéressés aux conditions de production de papiers REH de laboratoire. Comme attendu, la force ionique de la suspension fibreuse modifie l'efficacité des traitements REH mais de façon très réduite et presque négligeable aux faibles dosages en PAE. Les effets du temps de stockage des papiers et d'un traitement thermique ont également été étudiés.

Enfin, dans une dernière étape, nous avons évalué l'effet de certains réactifs sur le recyclage de films de PAE et de papiers REH. Même si les résultats ne sont pas entièrement transposables d'un cas à l'autre, le réactif le plus efficace à la fois pour les films et le papier est le persulfate de potassium qui agit très probablement selon un mécanisme de réaction radicalaire. Cette étude a également permis de montrer que l'enduction du papier contribuait à faire chuter de façon très significative l'efficacité des traitements de dégradation.

SUMMARY

PART II - USE OF PAE RESIN IN PAPERMAKING: IMPROVEMENT OF THE PREPARATION AND REPULPING OF PAE-BASED PAPERS

FIGURES

PART I - CHARACTERIZATION OF PAE RESIN: TOWARD A BETTER UNDERSTANDING OF CROSS-LINKING MECHANISMS

PART II – USE OF PAE RESIN IN PAPERMAKING: IMPROVEMENT OF THE PREPARATION AND REPULPING OF PAE-BASED PAPERS

TABLES

PART I - CHARACTERIZATION OF PAE RESIN: TOWARD A BETTER UNDERSTANDING OF CROSS-LINKING MECHANISMS

PART II - USE OF PAE RESIN IN PAPERMAKING: IMPROVEMENT OF THE PREPARATION AND REPULPING OF PAE-BASED PAPERS

GENERAL INTRODUCTION

During World War II, the need for wet strengthened papers initiated a development of wet strength resins. The literature in this subject is extensive, and several reviews are available (Chan, 1994; Espy, 1995 and 1992; Dunlop-Jones, 1991; Britt, 1981; Westfeldt, 1979; Bates et al., 1969; Stannett, 1967). The wet strength treatment of papers consists in introducing the additive into the fibrous suspension (virgin and/or recycled) before the formation of the fibrous mat. These cationic resins are generally adsorbed by the fibres through oppositely attractive electrostatic interactions. During the drying of the paper sheets, the polymer cross-links under heating and a three-dimensional network is formed providing for the papers their wet strength. However, the action mode of these chemicals is not perfectly known. Typically, papers treated with wet strength resins retain at least 15% of their paper dry tensile force after complete wetting with water. These cross-linked polymers make the paper resistant for re-pulping unless they are attacked with the right combination of chemicals and mechanical energy.

Polyamideamine epichlorohydrin (PAE) resin is a water soluble additive which has been developed and commercialized from the end of the 1950s. It is still the most used permanent wet strength additive in alkaline conditions for preparing wet strengthened papers because of its good performance and relatively low costs. Nevertheless, there is a lack of data concerning this chemical in the literature.

In papermaking, carboxymethylcellulose (CMC) helps improving the paper dry strength and is also used in combination with PAE resins during preparation of PAE-based wet strengthened papers. In the later case, CMC is usually introduced before the addition of the PAE solution into the fibre pulp suspension. A complex is supposed to be formed between the two oppositely charged polyelectrolytes. This complex exhibits a positive net charge that is lower than that associated to PAE macromolecules. The combined addition of CMC and PAE is then a way to adsorb more PAE onto the fibres before reaching the neutralization or saturation of the fibre surface.

Besides considering the mechanisms of wet strength development, the recycling of the PAE treated papers and broke present many problems. The re-pulping is normally realized at high temperature and in high concentration of additives. Here again, the involved reactions are not well known and the effectiveness of these treatments is too low.

From these considerations, the main objectives of this thesis are:

(i.) the characterization of PAE resin and wet strength development mechanisms;

(ii.) the preparation and characterization of PAE-based wet strengthened papers;

(iii.) the comparison of the efficiency of additives used for the repulping of PAE-based papers.

Thus, this manuscript has been organized following two main parts:

- Part I - Characterization of PAE resin: toward a better understanding of cross-linking mechanisms.
- Part II - Use of PAE resin in papermaking: improvement of the preparation and repulping of PAE-based papers.

In the Part I, Chapter I presents a literature review focusing first on the main properties and characteristics of polyelectrolytes. A brief resume of the main wet strength resins is presented and a special attention is given for PAE resin. The utilization of PAE-CMC polyelectrolytes complexes for preparing PAE-based wet strengthened papers is also briefly discussed. Chapter II describes the techniques used for characterizing PAE solutions and PAE, CMC and PAE-CMC complexes films. In Chapter III, the obtained results are discussed. In order to study the cross-linking reaction of PAE macromolecules, ageing studies of PAE films were carried out. Chapter IV presents a study of CMC salts which is a chemical normally used in combination with PAE resin to prepare PAE-based papers. Finally, Chapter V consists in an innovative study aiming to elucidate the mechanism related to PAE resin when used to prepare PAE-based wet strengthened papers. In this case, CMC is viewed as a model compound for cellulosic fibres and CMC-PAE interactions as a model for fibres-PAE interactions. Thus, new insights and evidences of the reaction mechanism for PAE in wet strengthened papers will be proposed.

In the Part II, Chapter I is dedicated to a literature review of the papermaking process and the main properties and characteristics of fibrous and non fibrous materials used in the production of paper and board. This chapter ends with a discussion about articles available in the literature concerning both the use of PAE in papermaking and

the recycling of PAE-based papers. Chapter II focus on the preparation and characterization of *Eucalyptus* pulp suspension. Total and surface charges of the pulp, as well as a morphological characterization of the fibres before and after refining are presented and discussed. Experimental results concerning adsorption of PAE resin by *Eucalyptus* pulp suspension are also presented. Chapter III describes the preparation and characterization of PAE-based wet strengthened papers. Effects of the conductivity of the pulp suspension, concentration of PAE in the pulp, thermal post-treatment and storage time of the handsheets on wet and dry tensile strengths of PAE-based papers were investigated. In the same chapter, the degradation of PAE films and of industrial PAE-based wet strengthened papers by various reagents was studied in order to improve the efficiency of the repulping step. Finally, a general conclusion highlights the main results and perspectives of this work.

PART I

CHARACTERIZATION OF PAE RESIN: TOWARD A BETTER UNDERSTANDING OF CROSS-LINKING MECHANISMS

INTRODUCTION

Wet strength additives are used to develop or to conserve the mechanical strength of papers when wetted. They are added in some products such as: tissue paper, paper towels, milk cartons, photographic base paper, hamburger wrappers, bank notes, waterproof liner boards/corrugated medium, and others (Obokata *et al.*, 2005; Häggkvist, 1998). According to their chemical composition, they can act as: protection agents by preventing fibre swelling and protecting bonds already existing and/or they form new water resistant bonds through reinforcement mechanisms (Espy, 1995).

The first wet strength agent used in papermaking was discovered in 1930, the polyethyleneimine (PEI), but its wet strength mechanism was not well understood. Some years later, cheaper and more efficient resins based on formaldehyde were developed. Nonetheless, formaldehyde resins (UF) are toxic and their performance limited to acidic conditions. Thus, the search for new wet strength additives with good performance in neutral and alkaline conditions continued. In 1960, wet strength resins based on polyamideamine epichlorohydrin (PAE) partially replaced the formaldehyde resins (Obokata and Isogai, 2004a,b; Devore *et al.*, 1993). Nowadays, they are still the most used wet strength chemicals due to their good performance and relative low costs, but they present some drawbacks. PAE resins induce paper stiffening and may slightly decrease the water absorption capacity which is useful in packaging products but not in tissue papers. Other drawbacks of PAE-based papers are their bad re-pulpability and toxic by-products from PAE synthesis.

For most resins, the wet strength treatment of papers generally consists in introducing the additive into the fibrous suspension before the formation of the fibrous mat. These resins are adsorbed by the fibres through attractive electrostatic interactions taking place between the positively charged functional groups in the structure of the resin and the negative charge borne by the carboxylic groups of the lignocellulosic fibres. During the drying of the paper sheet, the polymer cross-links under heating and a three-dimensional network is formed providing to the paper its wet strength. Depending on the product used, we can obtain a permanent wet strength, i.e. relatively non affected when the contact time of the paper with water increases, or a temporary wet strength

which decreases until disappearing when contact time of the paper with water is increased.

Many wet strength additives are used at levels less than 1% (w/w) based on dry fibre weight. The migration of these additives from the fibre surface to its interior over prolonged exposure times can diminish their effectiveness. Though wet strength resins are usually added to impart wet strength, the mechanical strength of the cross-linked network often contributes directly to dry strength too.

The wet strength resins may impart wet strength to the paper by two mechanisms acting or not together: cross-linking of cellulose or hemicelluloses by the formation of resin-fibres chemical bonds and the protection of fibre-fibre contacts by a network of cross-linked resin molecules that does not necessary react with functional groups of the fibres (Lindstrom *et al.*, 2005). Among the acid wet strength resins normally used, urea-formaldehyde resins appear to impart wet strength only by self-cross-linking, while melamine-formaldehyde resins also seem to cross-link the carboxylic groups directly. On the other hand among neutral/alkaline curing resins, azetidinium resins (comprising most polyamideamine epichlorohydrin resins), seem to react with carboxyl groups of the lignocellulosic fibres together with a self-cross-linking of the resin. Epoxy resins react by self-cross-linking, and also with carboxylic and hydroxyl groups of the lignocellulosic fibres (Espy, 1995). Aldehyde resins cross-link cellulose fibres reversibly by forming hemiacetal bonds, and with self-cross-linking through the amide groups, as likely possibility, at least among polyacrylamide-glyoxal resins. For polyethyleneimine, no mechanism was clearly established. Some electrically neutral and low weight molecules (formaldehyde, glyoxal) can impart wet strength if they are thermally activated (during the drying operation of the paper machine). However, these chemicals cannot be used at the wet end of the paper machine, since their retention is low (Espy, 1995). Moreover, small molecules can penetrate the porous structure of the fibre wall, thus inducing fibre stiffening and brittle papers.

Typically, paper treated with wet strength resins retains at least 15%, whereas untreated paper retains less than 5% of their paper's dry strength (when considering their tensile force) after complete wetting with water. The wet strengthened papers keep their integrity due to the effect of the wet strength additives. However, these cross-

linked polymers make them resistant to re-pulping unless they are attacked with the right combination of chemicals and mechanical energy.

In this work, a permanent wet strength resin (PAE) was studied. To summarize, these resins generally present the following properties:

(i.) water soluble (or water dispersible) thus allowing even dispersion and effective distribution on the fibres;

(ii.) cationic thus facilitating adsorption onto anionic pulp fibres usually by an ion-exchange mechanism;

(iii.) thermosetting with relatively high molecular weight polymers being more completely adsorbed and forming stronger bonds;

(iv.) reactive thus promoting the formation of cross-linked networks (with themselves or with cellulose / hemicelluloses macromolecules), that resist to water dissolution.

Indeed, PAE resin is still the most used permanent wet strength additive. However, there is a lack of data concerning the characteristics and properties of this chemical in the open literature. Thus, the main aims of the Part I of this thesis are:

(i.) a study of the PAE resins including their: structure, charge and cross-linking mechanisms;

(ii.) a study of the main properties of carboxymethylcellulose (CMC) salts (a chemical normally used in combination with PAE for preparing PAE-based wet strengthened papers);

(iii.) a study of the interactions between PAE and CMC. In this case CMC will be used as a model compound of cellulosic fibres and PAE-CMC interactions as a model of the PAE-fibres interactions.

CHAPTER I: LITERATURE REVIEW

Figures 1.1 and 1.2 present a literature review of papers being published from the 1980s related to PAE resins. As it can be observed, for example, reaction mechanisms were proposed only at the beginning of the 1990s. This is partly due to problems of confidentiality in a strongly competing market. Some articles date before 1980s (not included in this review) and mainly describe the good performance of the PAE resin in the papermaking applications (Westfeldt, 1979; Bates, 1969; Stannett, 1967).

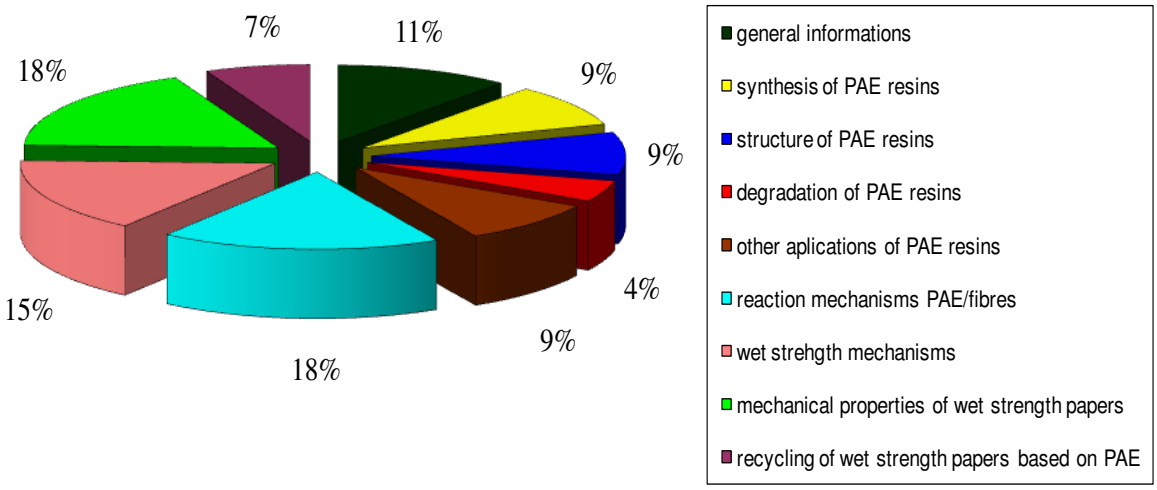

Fig.1.1: Literature review of papers being published from 1980s related to PAE resins (reviewed at 2012).

The articles recently published by Obokata *et al.* (2005; 2004a,b) describing synthesis reactions show a renewed interest for this subject. On the other hand, patents are deposited regularly demonstrating an important activity of the suppliers. The patents frequently deal with new products or new formulations limiting the environmental impacts, the ways of increasing recycling ability of PAE-based wet strengthened papers

and the association of several additives or new agents for an improvement of their performances. Thus, there are still considerable efforts on researches in this domain to understand the properties and the characteristics of these additives and to optimize their performances.

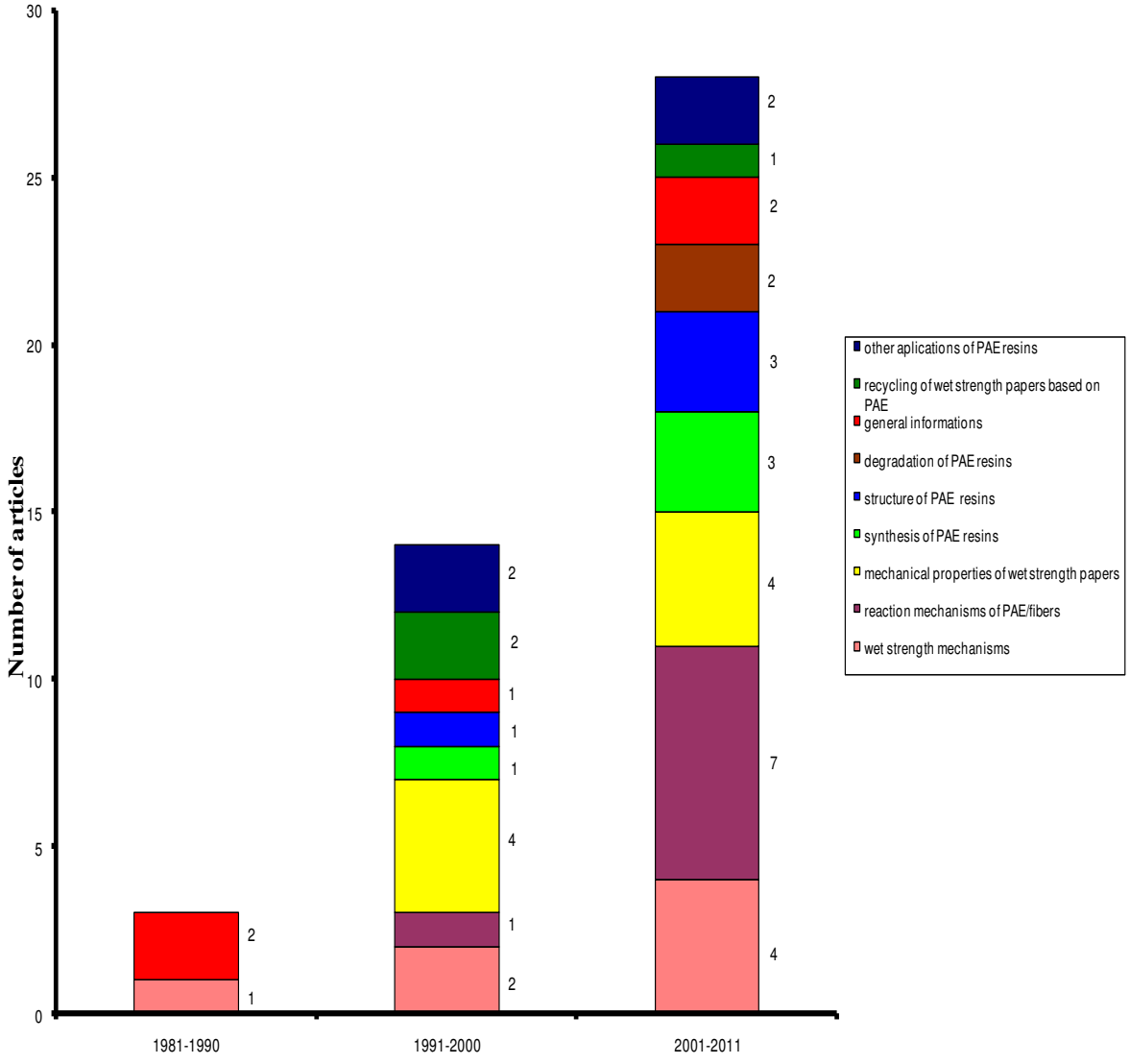

Fig.1.2: Bibliography study as a function of decade from 1980s related to PAE resins (reviewed at 2012).

The subsequent sections are a description of the main wet strength additives used in the papermaking process. A resume of the main characteristic and properties of

these resins described in the literature as: synthesis mechanisms, chemical structure, cross-linking reactions will be briefly presented as well as their application in the papermaking industry and effects on the papers prepared thereof. A special attention will be paid to a literature review of PAE resin, which is the chemical used during this thesis to prepare wet strengthened papers.

1. POLYELECTROLYTES

Polyelectrolytes are polymers that develop substantial charge when dissolved or swollen in a highly polar solvent such as water. These polymers are also commonly termed polyions because their charge arises from many ionized functional groups positioned along the chains (Dautzenberg *et al.*, 1994; Castellan, 1986). Electrostatic interactions between the ionized groups, as well as the presence of small electrolyte ions in the nearby solution, convey to polyelectrolyte systems a host of properties distinct from those displayed by neutral polymer systems. Unfortunately, describing and modeling these properties has proven to be difficult, and many key properties remain poorly understood. Industrial applications and academic interests focus on polyelectrolyte behaviour in solutions, gels and adsorbed layers. Polyelectrolytes frequently form complexes with co-solutes such as multivalent ions, surfactants and other polymers, or small colloidal particles.

Even in water, which possesses a high dielectric constant, electrostatic forces strongly oppose the dissociation and physical separation of unlike charges. When the dissociation occurs, a diffuse cloud of small counter-ions closely surrounds the dissolved polyelectrolyte chain, and this cloud accumulates sufficient charge to compensate for the polyelectrolyte's fixed charge. Ions within the diffuse cloud dynamically exchange with small ions present as added or ambient low molecular weight electrolytes in the surrounding solution, but this exchange does not affect the net excess of countercharge which could be accumulated by the cloud (Dautzenberg *et al.*, 1994).

The size of the diffuse cloud reflects a balance between electrostatic energy, favoring the cloud's collapse onto the oppositely charged chain, and entropy, favoring

the cloud's expansion. Counter-ions in the diffuse cloud, as well as other small ions of an added electrolyte, screen electrostatic interactions, a phenomenon reducing the length scales over which electrostatic interactions remain important. Adding electrolyte to a polyelectrolyte solution contracts the counter-ion cloud, and at sufficiently high electrolyte concentrations, the cloud's shrinkage onto the chain transforms many polyelectrolyte properties to those of a neutral polymer. Conversely, with no added electrolyte and thus only liberated counter-ions present, a special condition termed "salt free", distinctive polyelectrolyte behaviours are strongly magnified (Dautzenberg *et al.*, 1994; Castellan, 1986).

The electrostatic interactions of polyelectrolytes with nearby small ions have frequently been addressed using theoretical methods and approximations adapted from studies of colloids or simple electrolytes. However, polyelectrolytes introduce new and complicating features, most notably, molecular flexibility/orientation, chain entanglement, and a necessity for modeling electrostatic interactions consistently over a large range of length scales. Additional theoretical difficulties may include specific ion interactions, hydrogen bonding of water, unknown values of the local dielectric constant, and ordered placement of charges along the backbone.

Polyelectrolytes are commonly used as additives in papermaking industry to control colloidal stability and adhesives properties of surfaces. One classic example of the latter is the use of cationic polyelectrolytes as retention aids, and as dry and wet strength additives in papermaking. The dry strength of paper is often increased by the addition of cationic polyelectrolytes to the fibre furnish (cationic starch is a typical example). The cationic polymer adsorbs onto the negatively charged fibres, and induces an increase of the number of fibre-fibre bonds. It has been reported that the dry strength of the paper increases with decreasing charge density of the polymer, presumably due to increased polymer-polymer interpenetration and their increased viscoelastic losses that occur during the rupture of the paper sheet under strain (Claesson *et al.*, 2003).

Although DNA is perhaps the best-known biological polyelectrolyte, many additional examples are found among common proteins and polysaccharides. Polyelectrolytes are produced by polymerization of charged monomers or by chemical functionalization of both natural and synthetic neutral polymers. Apart from natural systems, where polyelectrolytes perform an enormous number of biological functions,

polyelectrolytes are mostly employed to modify solution rheology, control the aggregation of colloidal particles, or change the nature of surfaces by adsorption including in papermaking. As a consequence, there are a growing number of applications for polyelectrolytes and no single use or class of uses dominates.

1.1. MAIN WET STRENGTH RESINS

In order to produce papers that retain some of their original dry strength when wetted, it is necessary:

(i.) add to or strengthen existing bonds;

(ii.) protect existing bonds;

(iii.) form bonds that are insensitive to water; and

(iv.) produce a network of material that physically entangles with the fibres.

To achieve this, wet strength additives have been developed. Their chemical reactivity can be of two kinds acting or not together:

(i.) preservation, restriction or homo-cross-linking mechanism: the wet strength additive is adsorbed by cellulosic fibres and form a self-cross-linked network when the paper is dried. When the paper next comes in contact with water, rehydration and swelling of the paper is restricted by the resin network. Thus, a portion of the original dry strength is preserved.

(ii.) reinforcement, new bond or co-cross-linking mechanism: it is suggested that there is cross-linking of the fibres by the wet strength resins, i.e., they can react with cellulosic fibres. The bonds then persist after any naturally occurring bonding has been destroyed by water (Roberts, 1991).

1.1.1. Formaldehyde based resins

Urea formaldehyde (UF) and melamine formaldehyde (MF) are the most common formaldehyde-based resins. They are used in acid conditions in papermaking. UF resins are condensation products of urea and formaldehyde, with polyamine added in small amounts to make them cationic in acidic conditions. During synthesis, and when the UF resins are dried to an insoluble state, their methylol ($-CH_2OH$) groups undergo intermolecular dehydration reaction to form methylene ($-CH_2-$) and/or methylene ether ($-CH_2OCH_2-$) bridges between urea units (Hill *et al*. 1984).

Figure 1.3 depicts the reactions for melamine-formaldehyde resins. The methylol groups on trimethylolmelamine or hexamethylolmelamine form bridges between melamine units to generate a three-dimensional cross-linked structure (Dankelman *et al*., 1986; Tomita *et al*., 1979).

Apparently, wet strength development by UF resins arises only by self-cross-linking of the resin (Espy, 1995). Chemical investigations with cellulose (Jurecic *et al*., 1958) or methyl α-glucoside, a cellulose model compound (Jurecic *et al*., 1960), indicate that UF resins do not react appreciably with these substrates, and this conclusion is supported by spectroscopic methods. Moreover, the activation energy of wet strength development on heat curing showed to be independent of the fibre substrate for a variety of pulps, including cellulose and glass fibres.

Although the curing reactions of MF resins are similar to those of UF, the MF resins show more signs of reacting with cellulose by a reinforcement mechanism. Model experiments with methyl α-glucoside suggest that MF can react with cellulosic hydroxyl groups (Bates, 1966). Photomicrographs of MF-based wet strengthened papers show wet tensile failure occurring in the fibre wall rather than at fibre-fibre contacts (Taylor, 1968).

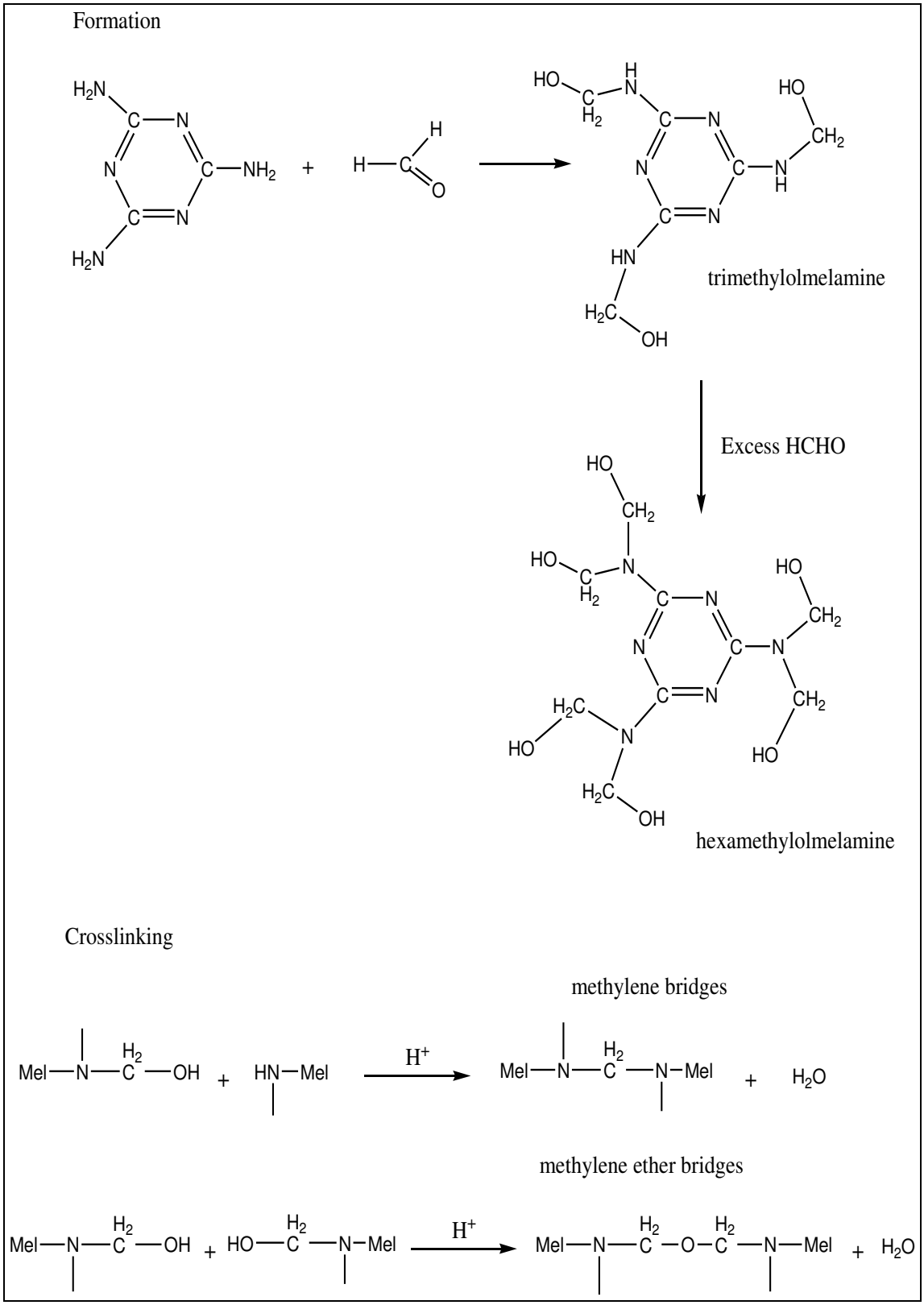

Fig.1.3: Formation and cross-linking of melamine-formaldehyde resins from Espy (1995).

1.1.2. Polyamideamine epichlorohydrin resins (PAE)

For PAE resins more explanations and detailed descriptions will be discussed in the section 1.2 (structural parameters, cross-linking reactions and use in the papermaking process). Here, we will only describe synthesis reactions.

Azetidinium resins are neutral/alkaline curing resins and are produced by condensing a polyamine (e.g., diethylenetriamine) with a dicarboxylic acid or its ester to form a poly(amideamine), as seen on Figure 1.4. Most of the amine groups of this precursor are secondary, but a minority (<5%) of primary amine is present, as well as carboxylic end groups (Espy, 1995). Epichlorohydrin reacts with primary and secondary amine groups to form secondary and tertiary aminochlorohydrins, respectively. At neutral pH and at temperatures above ambient (60^{o}C), the tertiary aminochlorohydrin groups cyclise to form 3-hydroxyazetidinium groups. These strained rings confer both reactivity and cationic charge in the resin.

The exact nature of the cross-linking between polymer chains remains unclear. NMR and FTIR signals of cross-link reaction sites are overlapped by other spectroscopic signals arising from functions present in the resin molecule, and from by-products normally present in PAE solutions after synthesis. For instance, it is difficult to detect signals of the cross-link reactions in the complex liquid ^{13}C-NMR spectra.

It is generally assumed that, during resin synthesis, new formed azetidinium rings can react with the remaining secondary amine groups of polyamideamine or aminochlorohydrin structures. The role of the tertiary amine groups (from initial alkylation of the original secondary amine) as a cross-linking site is still unclear (Obokata and Isogai, 2004b).

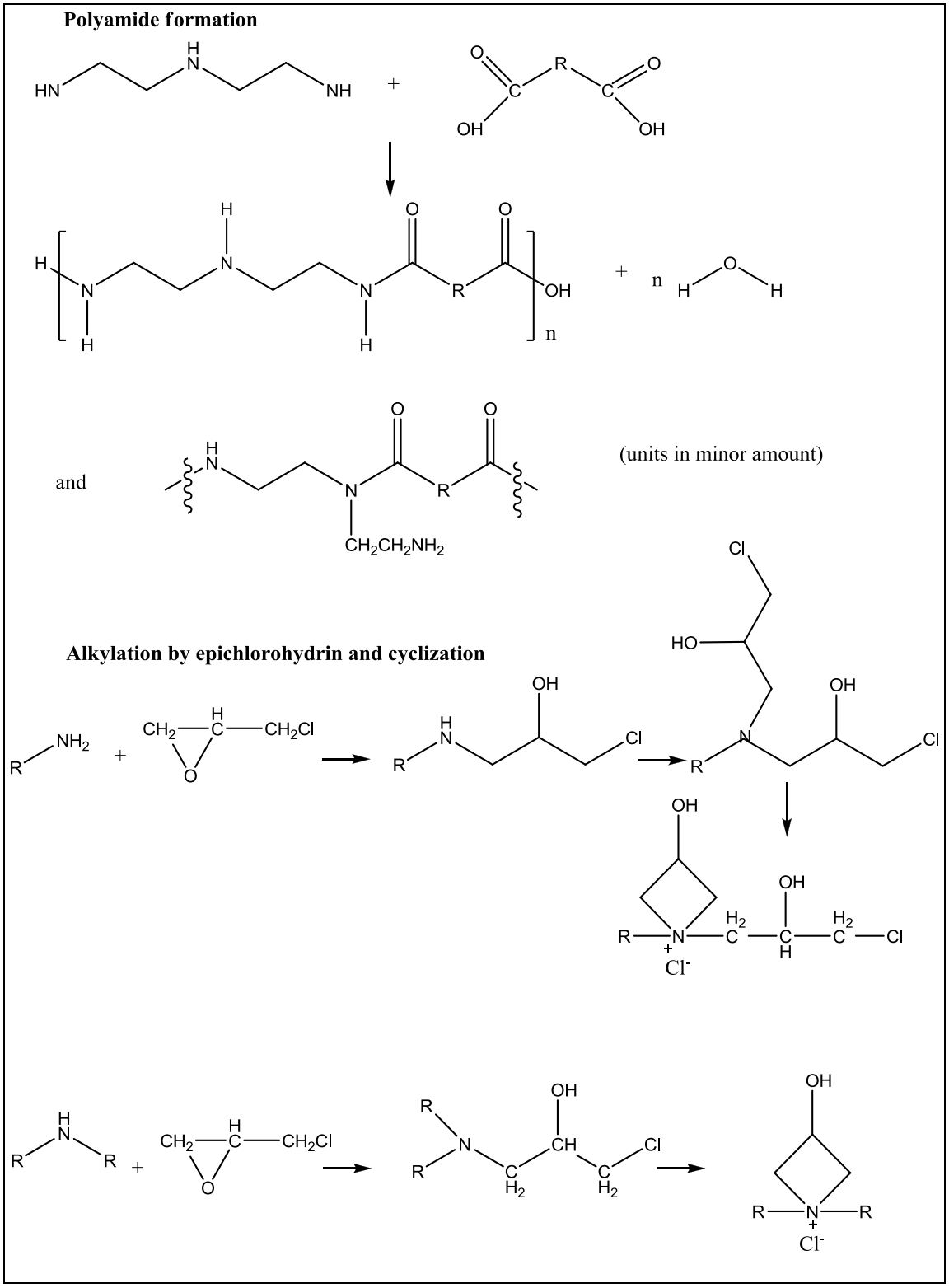

Fig.1.4: Structure of PAE resin from Espy (1995).

1.1.3. Epoxy resins

In some grades of neutral/alkaline curing resins, epichlorohydrin reacts with a backbone polymer containing tertiary amine groups rather than that bearing secondary amines. The resulting reactive functional group is then a quaternary ammonium epoxy. Because the epoxy group is more reactive than its 3-hydroxyazetidinium counterpart, resins that bear such a moiety will lose effectiveness by hydrolysis on storage unless they are stabilized as the corresponding chlorohydrins (Espy, 1995). Treating the resin with alkali in dilute solution re-forms the epoxy groups and restores its full reactivity. Figure 1.5 shows the formation of quaternary ammonium epoxy resins.

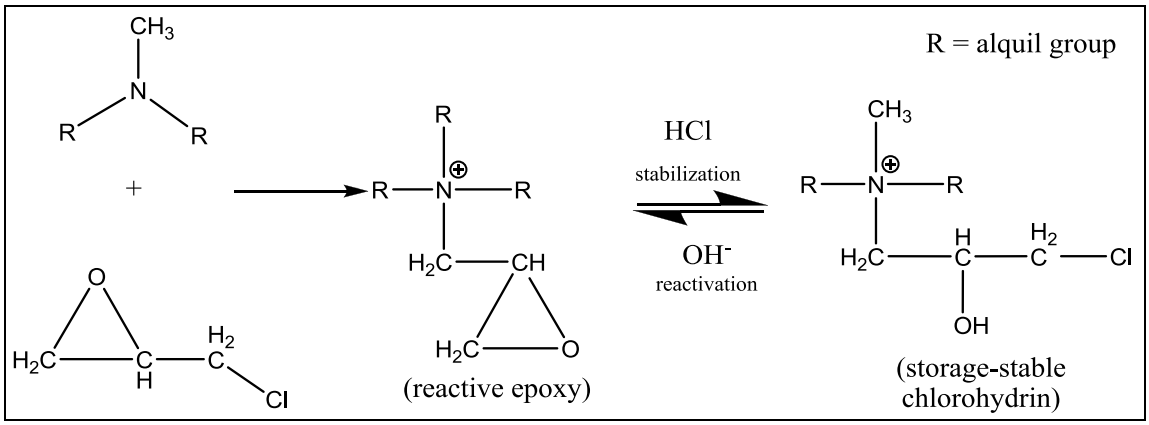

Fig.1.5: Formation of quaternary ammonium epoxy resins from Espy (1995).

One obvious potential self-cross-linking route is the reaction of an epoxy with a residual tertiary amine to form a three-carbon cross-link between two quaternary ammonium groups (see Figure 1.6b). However, it is uncertain how much the consequent generation of the adjacent second positive charge would inhibit this route. Hydrolysis of one epoxy group to a glycol followed by reaction with a second epoxy is possible, but its relative importance is unknown (see Figure 1.6a). As with azetidinium resin it is difficult to characterize small number of cross-linkages among the signals detected by spectroscopic methods for similar reactive groups born by polymer backbone.

In general, epoxy resins react qualitatively like azetidinium resins but quantitatively faster. In many paper grades, they impart higher wet strength (after curing or ageing). They also react faster with water in their epoxy form. In a comparative study of their mechanism, an epoxy resin (with an amine-resistant backbone), partly insolubilized cellulose in cupriethylenediamine solution ("CuEn"), unlike an azetidinium resin with a similar backbone (Espy, 1998). This fact suggests that epoxy resins may react with hydroxyl groups to form ether bonds, which are inert toward aminolysis (Espy, 1995).

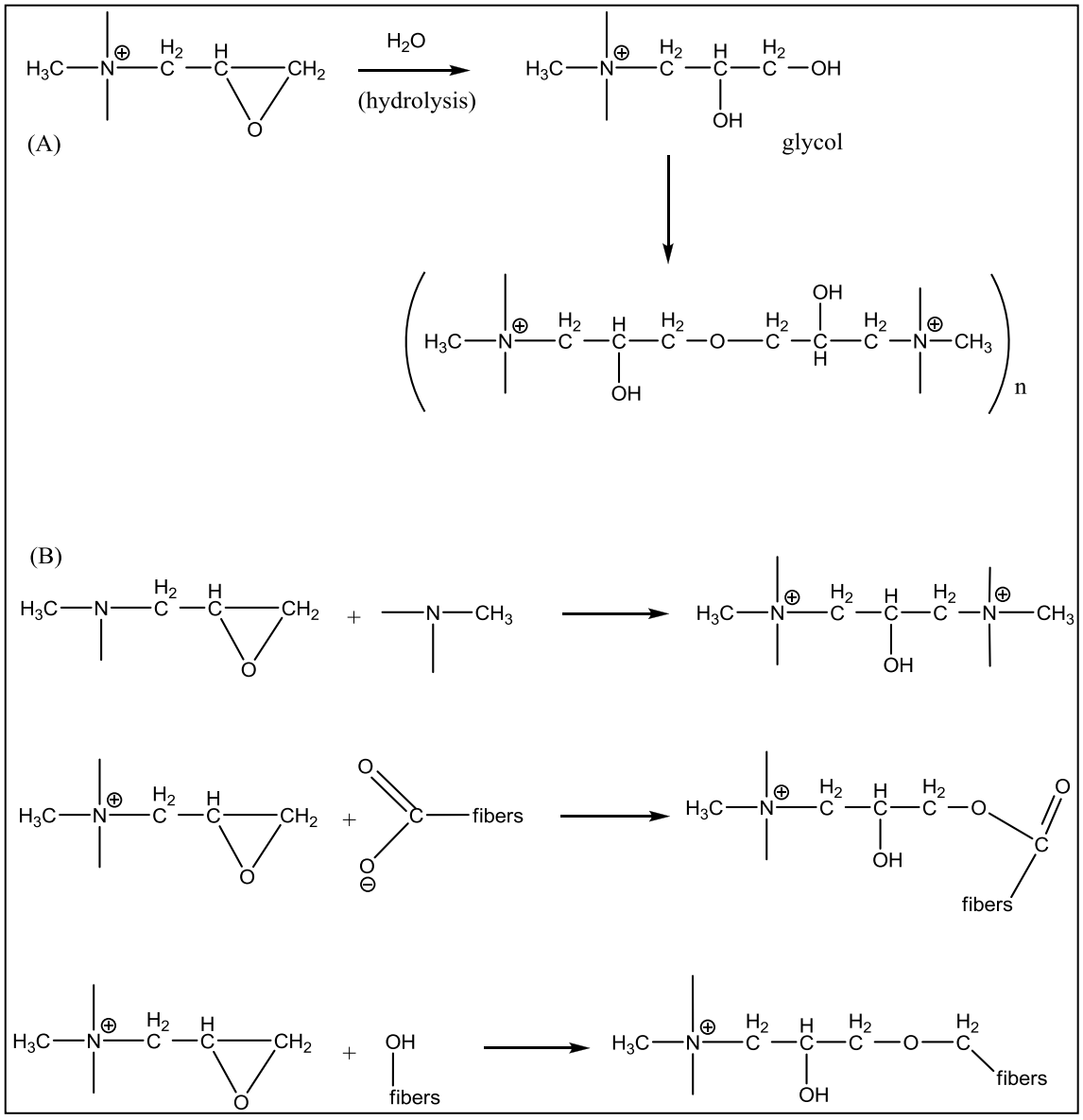

Fig.1.6: Potential crosslinking routes of epoxy resins from Espy (1995).

1.1.4. Aldehyde resins

Aldehyde resins encompass subgroups, characterized by the formyl or aldehyde (-CH=O) groups as the reactive functional group. The first commercial resin was dialdehyde starch, used either as a cationic derivative (Hamerstrand *et al.*, 1963) or with a cationic retention aid (Borchert and Mirza, 1964). Later, glyoxal-modified polyacrylamide resins were introduced. Another development is starch derivatives bearing acetal groups, which are hydrolyzed in acidic pulp suspensions to unblock their reactive aldehyde groups (Solarek *et al.*, 1988). All are temporary wet strength additives. Long-soaking of paper treated with such wet end agents reduces the wet strength at about 30-50%, compared with only 10 to 20% for formaldehyde-based and polyamideamine epichlorohydrin resins (Espy, 1995).

All aldehyde resins are acid-curing (Espy, 1995). The dialdehyde polysaccharides lose effectiveness rapidly at a pH value above 4.0 to 4.5. However, glyoxal-modified polyacrylamide resins maintain their effectiveness up to pH value of 6, so they can be classified as acid/neutral-curing additives.

Figure 1.7 summarizes the chemistry of glyoxal-modified polyacrylamide resins. Cationic monomers in the polyacrylamide backbone help the resin to be adsorbed on pulp. Addition of glyoxal to some of the amide groups introduces reactive functionality to the macromolecule. Some glyoxal units react with end groups, cross-linking the backbone molecules and increasing the molecular weight of the resin. The hydrated formyl groups can also react with hydroxylated compounds such as cellulose, losing water to form hemiacetal bonds. In the same way, in dialdehyde starch, hemiacetal formation between formyl groups and backbone hydroxyls can cross-link the polysaccharide resin, besides its bonding to cellulose macromolecules (Espy, 1995).

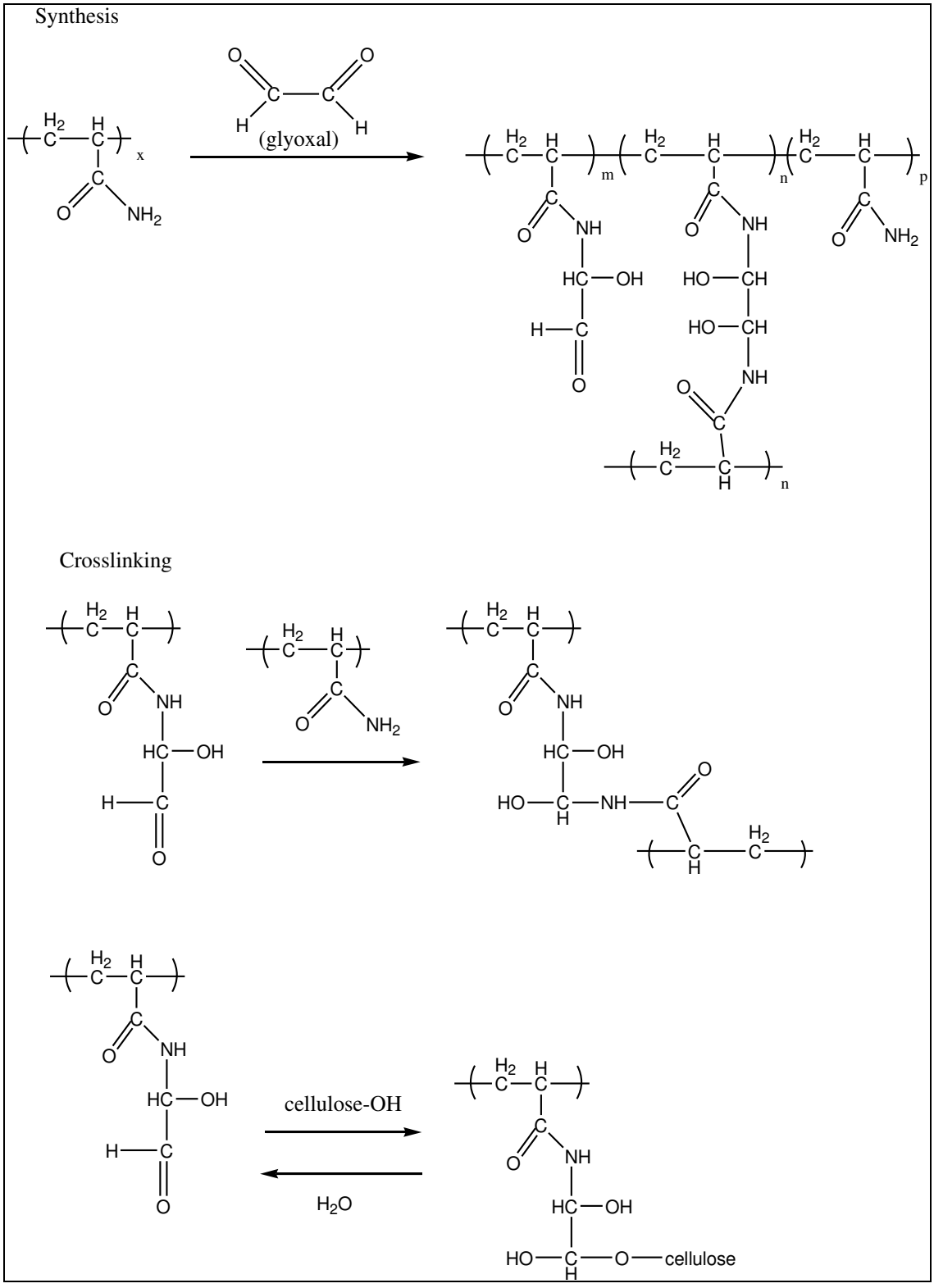

Fig.1.7: Synthesis and cross-linking of polyacrylamide-glyoxal resins from Espy (1995).

Aldehyde resins (including aldehyde derivatives of polysaccharides and glyoxilated polyacrylamides) are believed to react with cellulose groups to form hemiacetal linkages. At first glance, the pH dependence of these resins does not agree with textbook descriptions of aldehyde chemistry, given in Figure 1.7. The equilibrium formation of an aldehyde with an alcohol to form a hemiacetal is catalyzed by either acid or base (see Figure 1.8). However, wet strength development by these resins, especially dialdehyde starch, is only acid-catalyzed. Moreover, alkali rapidly degrades the wet strength imparted by these resins. If alkali catalyzes the reverse reaction, why does it not catalyze the forward reaction? One possible explanation is that of "full" acetal formation, since only acids can catalyze the reaction of a hemiacetal with a second equivalent of an alcohol to form an acetal. However, acetals are stable to base, so any significant acetal formation should impart alkali proof wet strength.

Strength imparted by aldehyde resins probably develops by way of hemiacetal formation. In a reaction catalyzed by either acid or base, the point of minimum rate (where changing pH in either direction accelerates one route more than it slows the other) needs not to be at pH value of 7. It is possible that the base-catalyzed route requires a pH value high enough to degrade the additive by other side reactions of the formyl group, or to alter the behaviour of the cellulose. If this is the case, then only the acid-catalyzed hemiacetal formation would be observed within the range of pH conditions usual in papermaking.

As the pH of a papermaking system increases above value of 4.0 to 4.5, polyacrylamide glyoxal resins maintain more of their effectiveness than does dialdehyde starch. This may occur because of the cross-linking of amide groups by glyoxal becomes faster as pH rises in the value range of 7 to 9. It seems plausible that as acid-catalyzed cross-linking of cellulose by the aldehyde becomes slower with rising pH, it is supplemented by base-catalysed self-cross-linking of the additive. Under re-pulping conditions with an excess of water, both reactions could be reversed with alkali catalysis, and hemiacetal formation could also be reversed with acid (Espy, 1995).

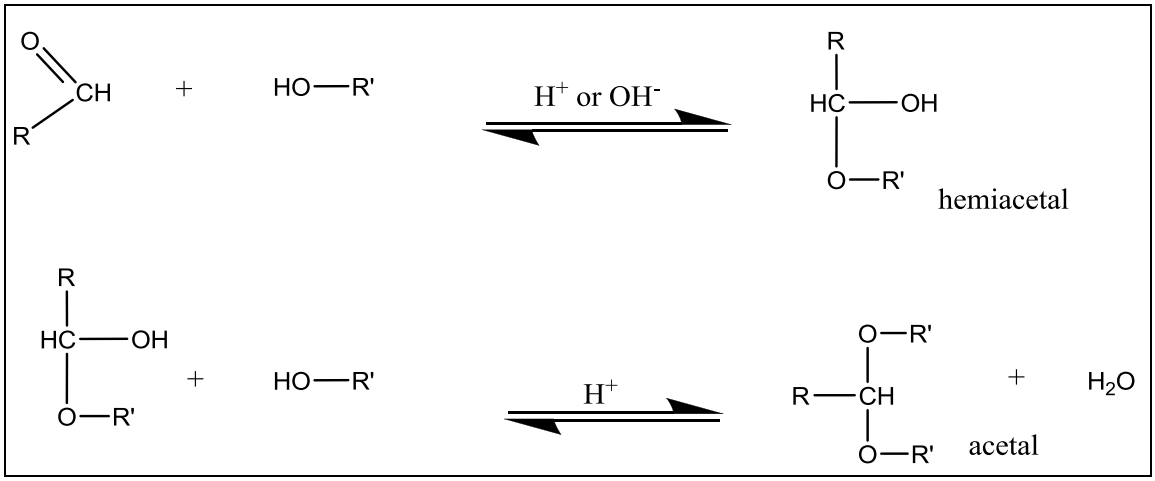

Fig.1.8: Hemiacetal and acetal formation from Espy (1995).

1.1.5. Polyethyleneimine (PEI) and chitosan resins

This pair of polymers challenges the understanding of wet strength mechanism, since both impart substantial wet strength to the paper without bearing any obviously reactive cross-linking groups. A number of explanations have been offered for the wet strength effects of PEI, but none of them completely convincing (Espy, 1995).

One explanation refers to the higher number of ionic bonds resulting from the protonated amine groups of PEI, that the water cannot break all of them (Neogi and Jensen, 1980; Sarkanen *et al.*, 1966). Similarly one can involve a multiplicity of hydrogen bonding again so numerous that water does not cleave their totality. It could be also postulated that the wet strength agent interacts with cellulose forming a sterically complex structure. The so-called "jack-in-the-box" mechanism postulates that PEI diffuses into micro-cracks and pores in the fibre surface, where it becomes stuck because its molecular volume expands when pH value changes (Allan and Reif, 1971). This mechanism and electrostatic interactions neatly and plausibly explains why PEI once adsorbed onto (or diffused into) a fibre, is difficult to remove.

Finally, another potential explanation is based on amide formation between amine groups of the additive and carboxylic groups of the pulp. However this condensation reaction usually requires substantially higher temperatures than those achieved on normal paper machine dryers. The observed amide formation warrants confirmation before this explanation can be entirely satisfying (Espy, 1995). Nevertheless these polymers are not commonly used to prepare wet strengthened papers and there is a lack of data in the literature about them.

1.2. POLYAMIDEAMINE EPICHLOROHYDRIN RESINS (PAE)

The PAE resin is a water soluble additive which has been developed and commercialized from the end of the 1950s, and nowadays occupies above 90% of the market of wet strength agents in neutral-to-alkaline pH paper furnishes. Because of its good performance, PAE is used as a wet-end strength additive in the papermaking process (Obokata *et al.*, 2005; Devore *et al.*, 1993). PAE resins can also be used as retention aids (Fukuda *et al.*, 2005; Kim *et al.*, 2001; Kitaoka *et al.*, 2001; Isogai, 1999; Isogai, 1997; Hasegawa *et al.*, 1997).

Some reports concerning analyses of PAE resins have been published so far. Carr *et al.* (1973) and Devore and Fischer (1993) reported signal assignment of liquid ^{1}H- and ^{13}C-NMR spectra of PAE. The method that the authors used to isolate the PAE for NMR analysis was precipitation by pouring a PAE aqueous solution into acetone and re-dissolving the dried precipitate in dimethylsulfoxide-d_6 (DMSO-d_6). However, isolation of PAE from its aqueous solution should be avoided, because the AZR groups are unstable and PAE undergoes easily cross-linking reactions. Kricheldorf (1981) reported signal assignment of NMR spectrum of a PAE aqueous solution by comparing it with a model compound (1,1-diethyl-3-hydroxyazetidinium chloride) and Obokata *et al.* (2007; 2005; 2004a,b) studied the NMR spectra of PAE aqueous solutions using distortionless enhancement by polarization transfer (DEPT) and C-H correlation spectroscopy (COSY) methods. PAE solutions synthesized by these authors were submitted to ^{1}H- and ^{13}C-NMR analysis simply by addition of small amounts of D_2O.

Apparently, this method allows more accurate and easier determinations of the PAE structure compared with the conventional one, requiring time-consuming titration methods or precipitation / isolation / re-dissolution procedures.

Using NMR, the content of four-membered azetidinium ring (AZR), and the number-average degree of polymerization (DP_n) of PAE macromolecules were determined by Obokata and Isogai (2004a) and Devore and Fischer (1993). The determination of weight and number average molecular weights was carried out by size-exclusion chromatography equipped with a multi-angle laser light scattering detector (Obokata *et al.*, 2005). Structural changes as the content of AZR groups and DP_n of PAE solutions during storage were studied by colloidal titration and ^{1}H and ^{13}C-NMR analyses (Obokata *et al.*, 2005). Colloidal titrations were carried out using sodium polyvinylsulfate (Obokata *et al.*, 2005; Devore and Fischer 1993; Wang and Shuster, 1975) and 2-mercaptoethanol (Bates, 1969) as indicator. The effects of added salts and free carboxyl group concentrations in the fibres on PAE adsorption by pulps were demonstrated by Bates (1969) and Fisher (1996).

The wet-strength improvement of cellulose sheets treated with PAE resins were studied by several authors (Obokata and Isogai, 2007; Fisher, 1996; Espy, 1995; Devore and Fischer, 1993; Wagberg and Björklund, 1993; Fredholm *et al.* 1983; Bates, 1969). Obokata and Isogai (2004a) analysed the wet strength improvement of handsheets prepared with the PAE *vs.* storage times. The influences on the properties of the treated papers and correlations on wet and dry tensile strength data from cured handsheets were studied by Devore and Fischer (1993), Wagberg and Björklund (1993), Espy (1987) and Neogi and Jensen (1980). The sheet-making process was also investigated by Obokata and Isogai (2004a), Wagberg and Björklund (1993), and Bates (1969). However, the preparation and characterization of PAE-based wet strengthened papers will be discussed in details in the Part II of this thesis.

Finally, the properties and characteristics of PAE films were studied by Obokata and Isogai (2007) and Bates (1969). Even after these studies some results concerning structural properties, reactivity, cross-linking and mechanisms of wet strength development of PAE-based papers are still not well understood. Thus, efforts of research can be still made in these topics.

1.2.1. Synthesis of PAE resins

As described previously, the PAE resin is synthesized by the following three steps:

(i.) condensation between adipic acid and diethylenetriamine to form polyamideamine;

(ii.) addition of epichlorohydrin at the secondary amine group in polyamideamine to form N-(3-chloro-2-hydroxypropyl) polyamideamine; and

(iii.) formation of four-membered azetidinium ring (AZR) from the 3-chloro-2-hydroxypropyl group.

Cross-linking between polyamideamine chains occurs partly during the AZR formation, leading to an increase in molecular weight of PAE. When adipic acid is used as one of the starting materials, high temperatures (around 170ºC) are generally required for polyamideamine synthesis. These severe conditions often give relatively large amounts of by-products in the polyamideamine solutions. However, Obokata and Isogai (2004b) used dimethyladipate to substitute adipic acid, as the starting material for PAE synthesis, thus reducing the reaction temperature. The scheme of preparation of PAE used by these authors is shown in Figure 1.9.

After the synthesis, the pH value of PAE aqueous solutions is adjusted to 3-4 with sulphuric and formic acids, in order to increase the PAE stability. Free epichlorohydrin remaining in the PAE solution is then partly converted to 1,3-dichloro-2-propanol and other by-products. Due to unstable AZR groups, PAE suppliers recommend that commercial PAE solutions must be stored in dark conditions and at around 20ºC. In such storage conditions, PAE solutions could be used within 3 to 4 months after purchasing. The deterioration of PAE resins can mostly be restricted within a year, when stored at 4^{o}C (Obokata and Isogai, 2004a).

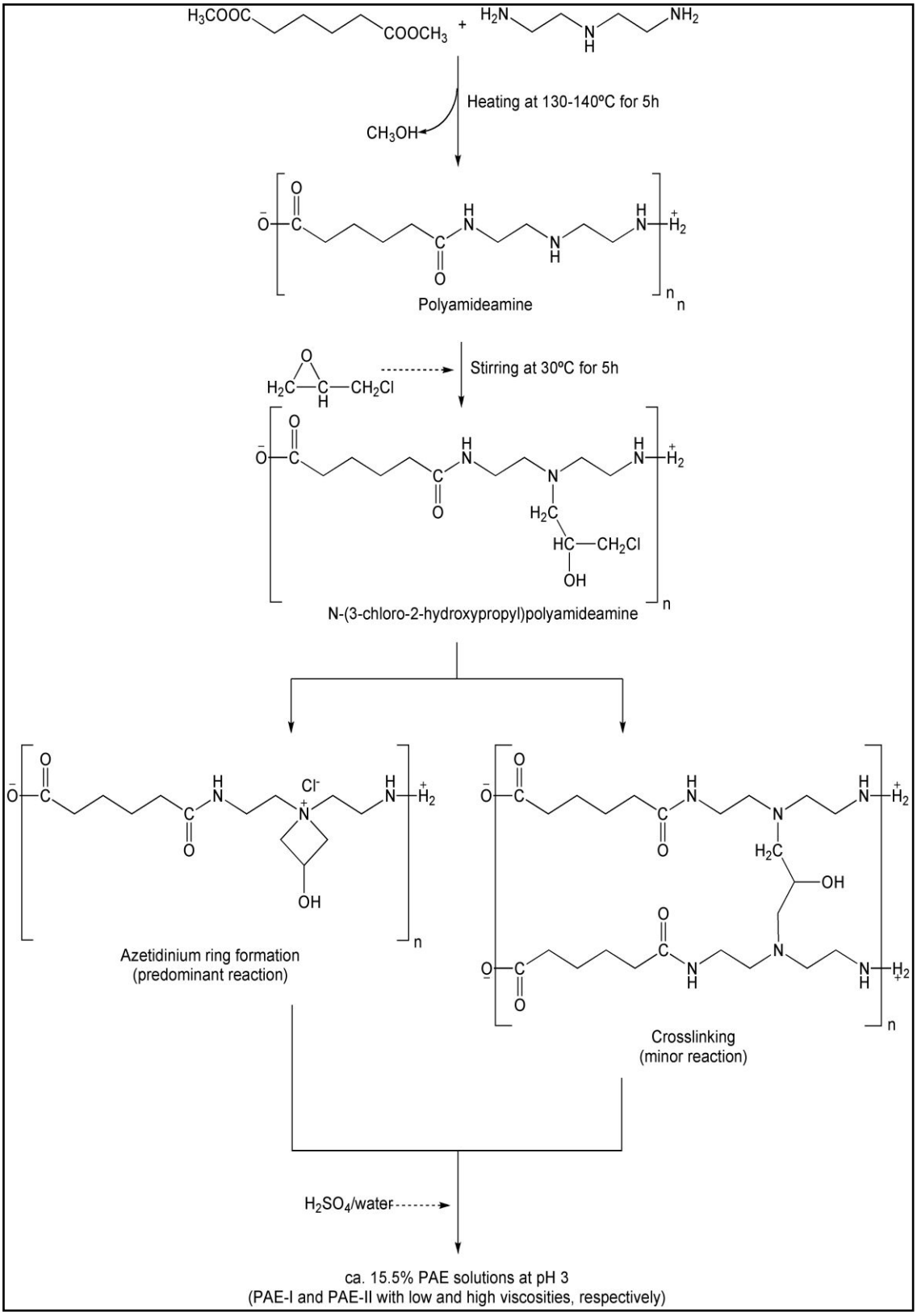

Fig.1.9: Synthesis of PAE resins from Obokata and Isogai (2004b).

The changes in DP_n of polyamideamine main chains during the PAE preparation process, the dosage in epichlorohydrin at the initial stage, the degree of cross-linking and the amount of tertiary amine groups are the relevant parameters for understanding the synthesis as well as the properties of PAE resins. Normally, due to a wide distribution of the molecular weight values, the PAE molecules have extremely large polydispersity (M_w/M_n) (Yoon, 2006).

The molecular weight of the intermediates increases with the reaction time. This phenomenon is responsible for increasing in wet strength of the handsheets prepared thereof, thus indicating that the molecular weight of PAE has a strong influence on the ensuing wet strength performance when used as an additive in papermaking. Then, PAE molecules in commercial solutions are cross-linked and highly dense polymers with, for example, weight and number average molecular mass values of 1.140.000 and 27.000 respectively, and polydispersity of 42 (Obokata and Isogai, 2007; Yoon, 2006).

1.2.2. PAE resins as wet strength agents

The mechanism of wet strength development of cellulose sheets prepared with PAE resins has been extensively studied but has not yet been totally explained (Fischer, 1996; Espy, 1995; Devore and Fischer, 1993; Bates, 1969). Generally, 0.1 to 1% PAE (based on dry weight of pulp), is added to pulp slurries as a wet end additive in papermaking, and sufficient wet strength appears on the PAE-treated paper after thermal drying process of the wet webs (Obokata *et al.*, 2005). As previously mentioned, two mechanisms acting or not together by which PAE resins may impart wet strength to the paper have been proposed: the formation of an independent resin-resin "homo-cross-linked" network (resin-resin covalent bonding), and/or the formation of a resin-fibres "co-cross-linked" network (resin-fibres covalent bonding) (Espy and Rave, 1998; Devore and Fischer, 1993).

Pioneer investigations (NMR studies) of polyamideamine resins assumed that the reactive functional groups were amine-epoxy-based moieties. Model-compound studies using sucrose (Bates, 1966), or methyl glucoside (Bates, 1969) found evidences supporting the first mechanism resin-resin covalent linkages only, indicating the absence of covalent linkages between PAE and the cellulose fibres. Another evidence of this mechanism was found by Devore and Fischer (1993) through the ^{1}H and ^{13}C NMR spectra of PAE solutions.

On the other hand, Espy and Rave (1998) have carried out solubility tests of wet strength paper in cupriethylenediamine solutions, electrophoretic mobility measurements of the pulp suspensions and dry strength behaviour of PAE/CMC combinations, and evidenced the co-cross-linking mechanism. More recently, the existence of the second mechanism (i. e., bonds formation between azetidinium groups of PAE and carboxyl groups of cellulosic fibres) was also confirmed by Obokata *et al.* (2007; 2005; 2004a,b) who used ^{1}H and ^{13}C NMR spectra, FTIR analysis, cellulase treatments, SEC-MALS and colloidal titration techniques. However, as also observed by these authors, the two mechanisms are not mutually exclusive but a combination of the two processes is possible. The results obtained showed that carboxyl groups in cellulose fibres behave first as anionic retention sites of cationic PAE molecules through electrostatic interactions (addition of PAE to the pulp or soaking treatment of once-dried cellulose sheets with PAE aqueous solutions), and after there is the ester bond formation between carboxyl groups of cellulose fibres and azetidinium groups of PAE. Wägberg and Bjorklund (1993) studied PAE-treated sheets prepared from carboxymethylated cellulose with degree of substitution (DS) of 0.69. These authors reported that ester bonds were formed between azetidinium groups of PAE and carboxyl groups of the carboxymethylated cellulose and these covalent bonds directly contributed to wet strength development of the sheets.

The ester bond formations between carboxyl groups of the polyamineamide chains and azetidinium groups of PAE, i.e., within PAE molecules, is also possible to occur, but the contribution of this bonds for wet strength development of PAE-based papers is not clear.

1.3. Carboxymethylcellulose (CMC)

CMC is the most widely used water-soluble derivative of the cellulose. It is produced by reacting cellulose with monochloroacetate or monochloroacetic acid, and resulting on a partial substitution of the hydroxyl groups at the 2, 3 and/or 6 positions of cellulose macromolecules by carboxymethyl groups. Different routes of modification and raw materials may lead to different degrees of substitution. Generally, 0.6 to 0.95 derivatives per monomer unit are possible (Li *et al.*, 2009).

CMC is made up of linear β-(1→4) linked glycanes which exhibit polyelectrolyte properties due to the presence of weakly acidic groups (Tong *et al.*, 2008; Mutalik *et al.*, 2006). It is in free acid form (neutral) at pH value of 3.5, and the acid groups are ionized (negatively charged) at about pH value of 7.0 (Wang and Somasundaram, 2005). Figure 1.10 shows the monomer of the CMC structure.

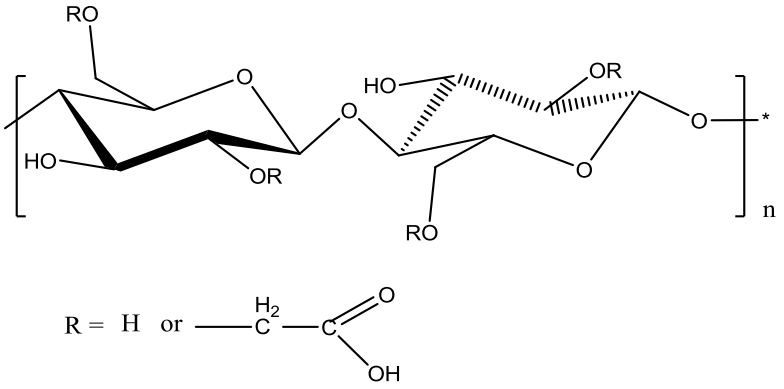

Fig.1.10: Structure of the linear CMC chains: β (1→4)-glucopyranose.

CMC is generally used in its sodium salt form (NaCMC) as stabilizer and protective colloid in detergents, paper coatings, pharmaceuticals, cosmetics and foods.

In papermaking, CMC is an alternative to improve dry strength of the paper. Its great advantage is that it can improve dry strength properties without beating of the fibres, which is very useful for the production of tissue paper that requires softness and good adsorption. In such a context, reffining should be limited because it gives stiffer and denser paper (less porosity) (Gärdlund *et al.*, 2003). In every way due to the economical reasons starch is normally used to replace CMC (Gärdlund and Norgren, 2007; Reynolds and Wasser, 1980).

In normal papermaking conditions, a fixing agent (cationic chemical) needs to be added to ensure that CMC can be adsorbed onto the fibre surface. CMC can also be attached to cellulose in specific conditions (high temperature and in the high electrolyte concentration) (Laine *et al.*, 2002; 2000). A salt is used to shield the repulsion between negatively charged fibres and CMC, making possible for CMC to approach the fibres surfaces and to be attached to them. This irreversible adsorption is believed to follow a co-crystallization mechanism, which is thermodynamically stable.

The temperature has a strong effect on CMC adsorption for cellulosic fibres, which increases rapidly with temperature up to 120ºC. High concentration of electrolyte makes the adsorption less pH dependent. Moreover acidic conditions are more favourable. The adsorption depends on the DS of CMC. Normally, the adsorption decreases for CMC with high DS, due to the charge repulsion between the polyelectrolyte and the fibres. The co-crystallisation mechanisms are more efficient with pure cellulose fibres compared to that occurring with fibres containing appreciable amounts of lignin and hemicelluloses (Watanabe *et al.*, 2004).

1.4. Polyelectrolyte complexes: CMC/PAE

Polyelectrolyte complexes are predominantly formed by electrostatic interactions between oppositely charged polyelectrolytes in solution. Studies regarding complex formation have been reported over the last twenty years (Enarsson and Wägberg, 2007; Gärdlund *et al.*, 2003; Gernandt *et al.*, 2003; Kramer *et al.*, 1997).

When the solutions containing different polyelectrolytes are prepared, different kinds of complexes can be obtained, depending on several factors such as the mixing molar ratio, acid/basicity of the polyelectrolytes used, ionic strength of the medium, chain length or accessibility of the charged sites of the polyelectrolyte, etc. Properties such as charge density, position and type of functional groups, flexibility of the polymeric chains to mention a few among many factors, also affect the formed complex (Gärdlund *et al*., 2003; Gernandt, 2003).

In papermaking and during the preparation of PAE-based wet strengthened papers, anionic CMC is usually introduced before the addition of the PAE solution into the fibre pulp suspension, in order to increase the saturation adsorption of cationic PAE. A complex is supposed to be formed between the two oppositely charged polyelectrolytes. This complex exhibits a positive net charge that is lower than that associated to PAE macromolecules. The combined addition of CMC and PAE is then a way to adsorbs more PAE onto the fibres before reaching the neutralization or saturation of the fibre surface.

Detailed static light scattering studies showed that the polyelectrolyte complexes between PAE and CMC have a spherical shape, and therefore may to be very useful as a wet strength additive considering their bridging ability (Gärdlund *et al*., 2003; Gernandt *et al*., 2003). If the formed complexes are small enough, then they may also penetrate into the fibre wall and in this way strengthen it. This parameter was proved to be important for improving the wet strength of the paper, which is not only dependent on the joint strength between the fibres but also on the cohesive properties of the fibre wall (Espy, 1995; Taylor, 1968). In addition, CMC-PAE complexes also improve the dry strength of the paper (Obokata and Isogai, 2004a; Laine *et al*., 2002; Bates, 1969).

In this work CMC, was used as a model compound for cellulosic fibres, and PAE-CMC interactions was used as a model to study PAE-fibres interactions. The main aim of this study was to ask questions discussed in the literature but no completely answered as the mechanism related to PAE wet-strengthened papers ("protection" and/or "reinforcement" mechanisms), and the type of interaction between CMC-PAE (opposite electrostatic interactions, hydrogen bonding and/or covalent bonds).

1.5. Main objectives

Based on these initial assumptions, the objectives of the Part I of this thesis are:

(i.) a study of the properties of aqueous PAE solutions. The charge of PAE will be determined by colloidal titration as a function of the pH values and of the conductivity of the medium using a particle charge detector and PES-Na as an anionic standard polyelectrolyte. Liquid ^{1}H and ^{13}C NMR will be performed in order to confirm the PAE structure described in the literature. Other basic analyses as solubility tests will be also carried out to clarify PAE properties in aqueous medium;

(ii.) in order to find out new insights about PAE cross-linking reactions, analyses of PAE films will be performed. In this case, effects of a post-thermal treatment and ageing under controlled conditions on cross-linking reactions of PAE resins will be studied. Analytical techniques as: solid state ^{1}H and ^{13}C NMR, FTIR on ATR mode, thermal and thermomechanical analysis (DSC and DMA, respectively), and microscopy (SEM) will be used to study PAE films. New evidences of PAE cross-linking reactions will be proposed;

(iii.) a preliminary study of PAE degradation will be performed with the main aim of increasing the repulpability of PAE-based wet strengthened papers. Thus, the PAE degradation efficiency will be studied without PAE fibres. The effects of some repulping agents such as NaOH, H_2SO_4, H_2O_2 and persulfates salts will be determined for degrading thermal post-treated PAE films. However, these results will be presented and discussed in the Part II of this thesis and related to the repulping of industrial PAE-based papers.

(iv.) a study of the main properties of carboxymethylcellulose (CMC) salts. This chemical is normally used in combination with PAE for preparing PAE-based wet strengthened papers. Thus, analyses of CMC solutions (optical microscopy and colloidal titration) and of CMC films (solid state ^{1}H and ^{13}C NMR, FTIR on ATR mode, SEM, EDS, DMA and DSC) will be performed; and

(v.) a study of the interactions between PAE and CMC (in this case CMC is used as a model compound of cellulosic fibres and PAE-CMC interactions as a model of the PAE-fibres interactions), after preparing films of polyelectrolyte complexes. Analytical techniques as described above for PAE and CMC characterizations will be carried out. Thus, attempts to clarify the mechanism related to PAE resin ("reinforcement" and/or "protection" mechanisms of cellulosic fibres), for preparing PAE-based wet strengthened papers will be proposed.

CHAPTER II: MATERIALS AND METHODS

2.1. Characteristics of PAE resins and NaCMC salts

In this study, PAE commercial aqueous solutions were used and characterized. Table II.1 shows some of the characteristics of these products.

***Tab. II.1*:** Characteristics of PAE commercial aqueous solutions (data from the suppliers).

	KYMENE 20XCELL	**MARESIN T35AS**	**KYMENE 625**	**EKA WS505**
Solid content (%)	19.8	13.5	25.0	20.0
pH (25°C)	2.5	2 to 3.5	2.9	2.5 to 3.5
Density g/L	1.1	1.05	1.1	1.05

Two salts of CMC (NaCMC) were tested in this study. The first one is a conventional product used for the industrial production of wet strengthened papers (Niklacell P70 UC from Mare), and the second one is a purified chemical (Fluka from Biochemica). Table II.2 shows some of the properties of the two products.

***Tab.* II.2:** Characteristics of commercial NaCMC (data from the suppliers).

	Niklacell P70 UC Mare	**Fluka Biochemica**
Solid content (%)	90	85 to 90
Degree of substitution	0.5 to 0.65	0.6 to 0.95

2.2. Films of PAE, CMC and PAE/CMC complexes: preparation and characterization

All the films were prepared by casting in Teflon plates (diameter 5 cm), for a week under controlled conditions (25°C and 50% RH).

For PAE, 60 mL of the commercial aqueous solutions (EKA WS505) were used, and films of about 1 mm thickness were obtained. The PAE films were then heated in an oven (105°C) for varied time intervals in order to study the kinetics of the cross-linking reaction as a function of the duration of the thermal treatment.

For CMC, 1 and 2% aqueous solutions were prepared by dissolving NaCMC powder in distilled water at room temperature. Moderated magnetic stirrer was used until a clear solution was obtained (c.a. 24 h). 100 mL of 1% CMC aqueous solutions were used and films with thickness of about 0.2 mm were obtained.

In order to eliminate by-products of synthesis, a purification of NaCMC Niklacell was carried out by acidifying a 1% CMC solution left to pH value of 2 with HCl under moderated magnetic stirring. After, 1 L of ethanol was added and the solution decanted for 30 min. Then, the acidic form of CMC was filtered on a Whatman paper (number 4) and washed several times with distilled water until neutral pH. The precipitated was re-solubilized with ultra-sound treatment for 1 h and at pH value of 10 continuously adjusted with NaOH. Then, films of purified CMC Niklacell were prepared as described above.

Polyelectrolyte complexes (PAE/CMC) were made by mixing the two polyelectrolytes at room temperature (25°C) under moderated magnetic stirring for 30 min. The mixture was then transferred to the Teflon plates, and films with thickness of about 1 mm were obtained. Variations of PAE/CMC mass ratios were carried out, and thermal treatments were performed for 24 h at 105°C in an oven in order to study the interactions between these polyelectrolytes induced by the heating.

2.3. Moisture content and drying kinetics

The solid contents were determined by drying the PAE aqueous solutions (c.a. 1.0 g) and the CMC powders (c.a. 1.0 g) in an oven at 105°C for 48 h. The solid percentage was calculated from weight difference.

The drying kinetics of the PAE and CMC films were carried out by weighing the CMC and PAE aqueous solutions in Teflon plates until constant mass during preparation of the films. The drying rates were measured under constant temperature and relative humidity (25°C and 50% RH), and the water loss percentage was plotted against time.

2.4. Colloidal titration

The charge of the PAE and CMC aqueous solutions was determined by colloidal titration using a particle charge detector (PCD-03 - Mütek). 10 mL of diluted solutions of CMC and PAE resins (approximately 0.5 g/L) were poured into the cell of the PCD-03 and titrated with polydiallyldimethylamonium chloride (polydadmac / Sigma Aldrich) and sodium polyethylenesulfonate (PES-Na / Noviprofibre) at 22 ± 3°C, respectively. The standard solutions were injected until the PAE and CMC in solution were neutralized by the oppositely charged polyelectrolyte giving rise to a potential value of 0 mV. For PAE solutions a complete study of the variation of the PAE charge as a function of pH and conductivity values was carried out. Three measurements for each sample were performed at least.

2.5. Liquid and solid states Nuclear Magnetic Ressonance (NMR)

NMR spectra of industrial PAE aqueous solutions and commercial CMC were recorded at 25°C on Varian spectrometers, UNITY400 and MERCURY400. ^{1}H and 2D experiments were performed with a 5 mm id-pfg (indirect detection – pulse field

gradients) probe; ^{13}C, DEPT 135, and ^{23}Na experiments with a 10 mm BB (Broad Band) probe.

For PAE solutions, amounts of D_2O-DCl were added to the aqueous solutions to obtain a NMR-lock signal. For commercial CMC, heavy water solutions were prepared. Concentrations were about 10% (w/w) for carbon, sodium and 2D experiments, and about 2 to 5% (w/w) for proton experiments.

^{1}H spectra were obtained at 399.959 MHz using a solvent presaturation sequence; the spectral widths were adjusted to the area of presence of signals, relaxations delays and pulses used allowing quantitative measurements. Zero-filling, but no apodization functions were applied before FT. Chemical shifts are referenced to TMS (0 ppm).

^{13}C quantitative spectra were obtained at 100.580 MHz with proton decoupling applied only during acquisition time to avoid nOe (nuclear Overhauser effect), with 11 s relaxation delay, and 30^{o} pulse; 4 Hz line broadening was applied before FT.

DEPT experiments were carried out with a delay $d_2 = 1/(2J)$ optimized for a coupling constant $^{1}J_{CH} = 130$ Hz, 3 s relaxation delay and 14.5 s for a 90^{o} pulse. The last pulse was 135^{o} allowing CH_2 negative signals, and CH, CH_3 positive ones. Chemical shifts were referenced to TMS (0 ppm).

^{23}Na spectra were obtained at 105.802 MHz, without proton decoupling. Relaxations times T_1 were measured with recovery method. Chemical shifts are referenced to NaCl (0 ppm).

2D experiments were conducted with spectral widths used for 1D spectra.

COSY ($^{n}J_{HH}$ correlations): 2K data points, 3 s relaxation delay, 265 experiments, forward linear prediction, zero filling and sinebell apodisation, to obtain symmetrised 4K x 4K matrix.

HMQC ($^{1}J_{CH}$ correlations): 2K data points, 2.5 s relaxation delay, 128 experiments, without ^{1}H decoupling during acquisition, delay was optimized for $^{1}J_{CH} = 130$ Hz. A forward linear prediction on 512K in the ^{13}C dimension was applied prior sinebell apodisation and zero filling in both dimensions to obtain 4K x 2K matrix.

HMBC ($^{n}J_{CH}$ correlations): 2K data points, 2.5 s relaxation delay, 128 experiments, delay were optimized for $^{1}J_{CH}$ = 130 Hz and $^{n}J_{CH}$ = 5 Hz. A forward linear prediction on 512K in the ^{13}C dimension was applied prior sinebell apodisation and zero filling in both dimensions to obtain 4K x 2K matrix.

Chemical structures of insoluble materials were studied with ^{13}C solid-state NMR experiments. Carbon spectra were recorded on a Bruker AVANCE400 spectrometer equipped with a 4 mm CP/MAS probe, operating at 79.490 MHz for ^{13}C. Samples were placed in 4 mm ZrO_2 rotors, with 12 kHz spinning rate. All the spectra presented were recorded using a combination of cross-polarization, high-power proton decoupling and magic angle spinning (CP/MAS). Recycle delay were 5 s, contact times were 2 ms for CMC studies and 0.5 ms for PAE resins ageing studies. These latter were performed at 233 K with 7 kHz spinning rate to avoid that spinning side bands overlap some interesting NMR signals. 10 Hz line broadening was applied before FT. Chemical shifts are referenced to TMS (0 ppm) with glycine sample (C=O signal at 176.03 ppm) (Brus *et al.*, 2002).

2.6. Fourier transformed infra-red spectroscopy (FTIR)

FTIR spectra of heated and unheated PAE and PAE/CMC complexes films were collected using a FTIR Spectrometer Paragon 1000 (Perkin Elmer) in ATR mode (Attenuated Total Reflection). The films were scanned from 400 to 4000 cm^{-1} at resolution of 4 cm^{-1}. Each spectrum represents an average of 16 consecutive scans.

FTIR spectra of NaCMC powder and CMC films were collected using the same spectrometer but in transmission mode. The samples (c.a. 2 mg) were dried in an oven for 24 h at 105°C, thoroughly triturated, mixed with 200 mg of spectroscopic grade KBr, and pressed into pellets for recording the spectra.

2.7. Optical microscopy (OM), scanning electron microscopy (SEM) and energy dispersive X-ray spectroscopy (EDS)

CMC solutions were analyzed in an optical microscope (Axio Imager Mim) between glass thin plates. Micrographs with different resolutions were recorded.

A scanning electron microscope (Quanta 200) was used to examine the representative regions of the surface and the cross-section of PAE, CMC and PAE/CMC complexes films. The samples were conditioned in desiccators and coated with gold under vacuum (Emitech K550x) before analyses.

The X-ray microanalysis (EDS) was carried out with the X-Flash 5010 detector (silicon drift detector).

2.8. Differential scanning calorimetry (DSC)

DSC analyses of PAE, CMC and PAE/CMC complexes films were performed in a DSC analyzer Q - 800 (TA Instruments) under a flow rate of nitrogen during the scans (50 mL/min). The samples (c.a. 5 mg) were studied in open aluminum pans with a scan rate of 5°C/min. Two consecutive scans were performed for each sample: the first scan from -90 to 120°C and the second scan from -90 to 300°C.

2.9. Dynamic mechanical analysis (DMA)

Dynamic mechanical analyses of PAE, CMC and PAE/CMC films (10 x 5 mm^2) were carried out using a Rheometric System Analyzer III (TA Instruments) in tension mode at 1 Hz scanning frequency, and with a temperature rate of 5°C/min. A flow rate of nitrogen was used during analyses. The glass transition temperature (*Tg*) was determined as the temperature at the peak of the *Tan* δ curve.

2.10. Swelling ratio

The swelling ratio of unheated and heated PAE films was determined under isothermal conditions (25°C). The films were immersed in distilled water and the gel weighed until saturation (constant mass). The swelling percentage was determined by the following relation:

$$swelling \quad ratio = \frac{m_f - m_i}{m_i} \times 100$$

with m_f : final weight

m_i: initial weight

2.11. Ageing study

The effects of ageing on heated and unheated PAE and PAE/CMC complexes films (mass ratio 50 : 50) were studied until six and three months, respectively. The films were conserved under controlled conditions (25°C and 50% RH), and analyzed by ^{13}C and ^{1}H NMR in solid state, FTIR working in ATR mode, DMA, DSC, SEM and EDS, as described in the previous sections.

CHAPTER III: RESULTS AND DISCUSSION

3. CHARACTERIZATION OF POLYAMIDEAMINE EPICHLOROHYDRIN (PAE RESIN)

The chemicals used in this study are commercial aqueous solutions (KYMENE 20XCELL, KYMENE 625, MARESIN T35AS, and EKA WS505). They are cationic polyelectrolytes polyamideamine epichlorohydrin (PAE) resins. Their solid content was found to be in agreement with the suppliers data presented in "Materials and Methods". These commercial solutions showed the same properties and characteristics after preliminary tests such as colloidal titration, FTIR spectroscopy and DSC analyses. It was, therefore, decided to study EKA WS505 as a representative chemical reagent for PAE commercial solutions.

3.1. CHARACTERIZATION OF PAE COMMERCIAL AQUEOUS SOLUTIONS

3.1.1. Nuclear magnetic resonance (NMR)

As the starting materials used in this work are industrial products, it was essential to characterize them properly before further studies. Thus, EKA WS505 solution was studied by NMR and colloidal titration.

The NMR characterization of this chemical was carried out by adding deuterated solvent into the initial industrial solution and recording the main corresponding resonances. The evaporation of the starting aqueous solutions was not possible: indeed any attempt of isolation induces cross-linking reaction leading to the insolubility of PAE resin. Thus, it was therefore decided to add directly heavy water (D_2O) in aqueous commercial solutions and deuterated hydrochloric acid (DCl) to adjust the pH to acid range, then following the procedure of Obokata and Isogai (2004b).

Figure 3.1 A and B presents the ^{1}H and ^{13}C NMR spectra, respectively, for EKA WS505 commercial aqueous solution. Proton spectrum was recorded with moderate solvent suppression, whereas carbon homologue was recorded in quantitative mode. As it can be seen in the spectra, the product displayed the presence of several impurities. Thus, as expected, the purity of this compound is low.

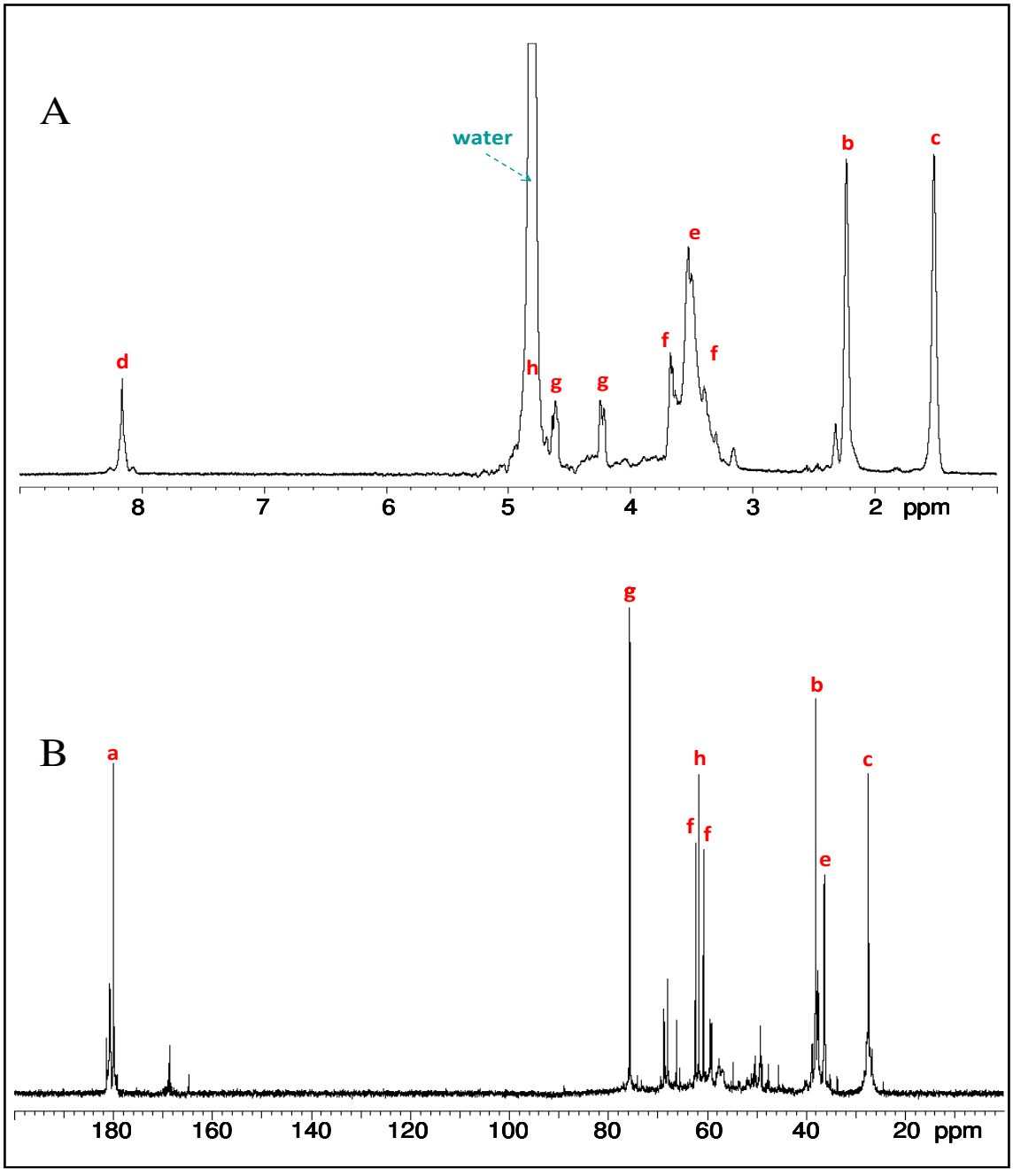

Fig. 3.1: **A)** ^{1}H and **B)** ^{13}C-NMR spectra for EKA WS505 commercial aqueous solutions in D_2O/DCl, at 25°C.

Initially, we were interested in characterizing the main constituent, the PAE monomer presented in Figure 3.2. To elucidate this point, various experiments were carried out as DEPT, COSY, HMQC and HMBC. The combination of these studies permitted the signals assignment, as summarized in Table III.1.

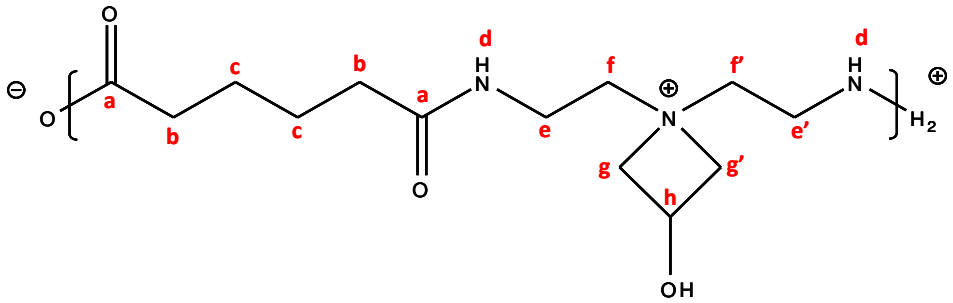

Fig. 3.2: Labeling atoms for PAE monomer unit.

Tab. III.1: Experimental NMR liquid data.

a (NHCO)	**h**	**g**	**f**	**i**	**e**	**b**	**C**	**d**	
180	61.7	75.65	62.35 60.8		36.25	38.1	27.4		δ ^{13}C
	CH	**CH_2**	**CH_2**		**CH_2**	**CH_2**	**CH_2**		**DEPT 135**
1	0.5	1	2x0.5		1	1	1		Integrals (^{13}C)
	4.8	4.6 4.2	3.7 3.4		3.5	2.2	1.51	8.16	δ ^{1}H $^{1}J_{CH}$ HMQC **correlations**
3.5 2.2 1.5	4.6 4.2	4.8 3.7 3.4	4.8 3.5 4.6 4.2		8.16 3.7 3.4	1.5	2.2		^{1}H
	75.7 62 60	61.7 62.3 60.8	75.7 61.7 36.3		180 60.8	180 27.4	180 38.1	36.25	$^{n}J_{CH}$ HMBC **correlations** ^{13}C
	4.6 4.2	4.8 4.2 4.6	3.5		8.16 3.7 3.4	1.51	2.2	3.5	^{1}H $^{n}J_{HH}$ COSY **correlations**

The carbon chemical shifts allow unambiguous assignment. DEPT 135 (see Figure 3.3) confirms the **C**(h) at 61.7 ppm, the only positive peak, as the only CH group present in the chemical structure. The nitrogen ion N^+ (in β position) reduces the hydroxyl electronegative effect for this carbon. The measured integrals are in agreement with the expected structure.

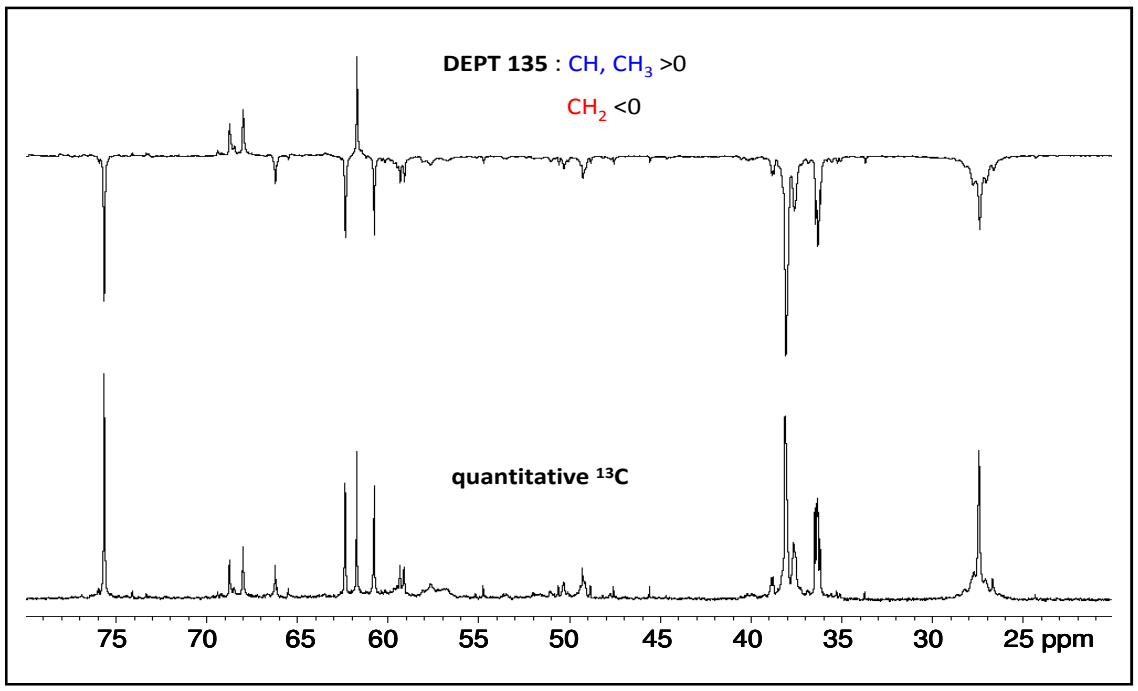

Fig. 3.3: ^{13}C NMR spectra: **A)** DEPT 135 (**C**H and **C**H_3 give positive signals, and **C**H_2 negative signals) and **B)** quantitative ^{13}C.

HMQC experiments (without any proton decoupling during the acquisition time), allow detecting what carbon is linked to what proton, and enable all proton assignments (see Figure 3.4). It is worth to point out the carbon – proton correlation at 61.7 and 4.8 ppm, respectively. It could be noticed that the proton **H**(h) at 4.8 ppm is totally overlapped by the water signal on the 1D proton spectrum (see Figure 3.1A). This assignment is confirmed by COSY (proton – proton correlations) and HMBC (proton – carbon correlations via $^nJ_{CH}$) experiments (see Table III.1).

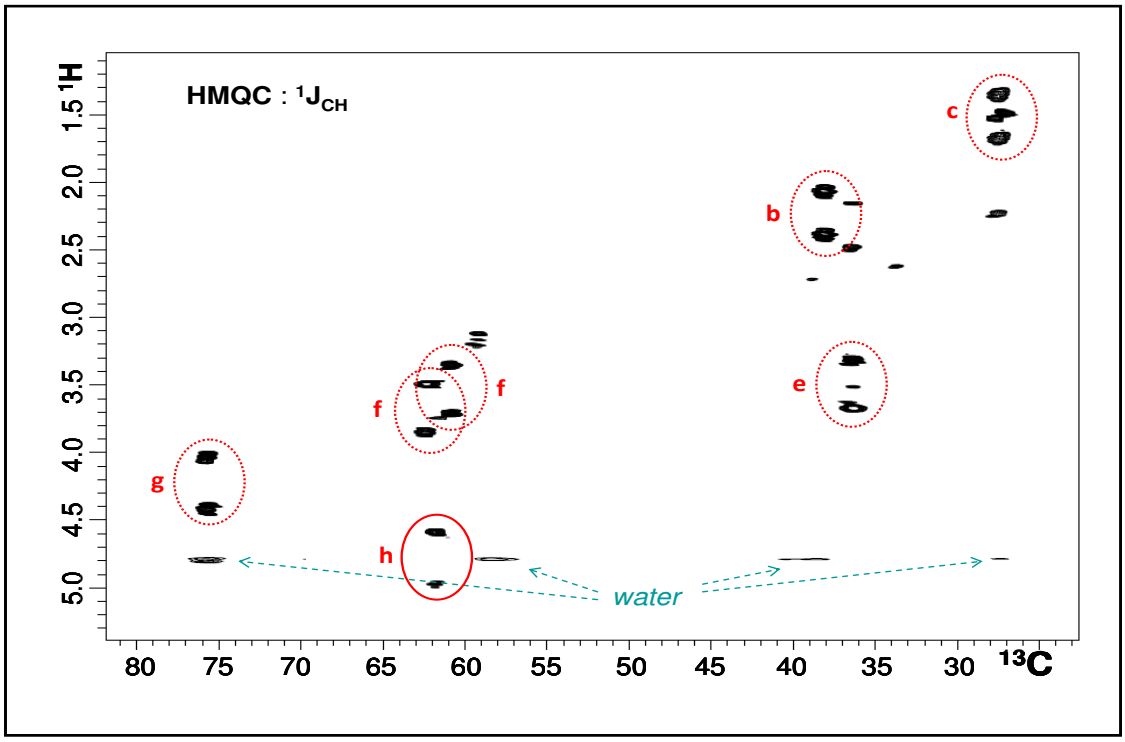

Fig. 3.4: HMQC without any ^{1}H decoupling during the acquisition time.

The signal at 8.24 ppm (see Figure 3.1 A) is assigned to the proton borne by amide **H**(d). Because these protons are exchangeable in the presence of D_2O, they do not appear quantitatively (deuterium cannot be detected in ^{1}H NMR). No amide protons were detected by Obokata and Isogai (2004b) in ^{1}H NMR spectrum of synthesized PAE in 100% D_2O resulting from complete deuterium exchange. In our case, only small amount of D_2O is observed, because the major part of the solvent consists in water molecules.

All the chemical shifts for PAE carbons obtained in this work were consistent with those reported by Obokata and Isogai (2004b) and Kricheldorf (1981). On the other hand, proton assignments for PAE were close to those reported by Obokata and Isogai (2004b) for synthesized PAE in D_2O/D_2SO_4, but different from those reported by Carr *et al.* (1973) and Devore and Fischer (1993) for PAE/DMSO-d_6/CH_3CO_2Na solutions. As postulated earlier by Obokata and Isogai (2004b), chemical shifts for PAE protons in deuterated DMSO present remarkable differences probably due to the pH influence on the protonation of nitrogen atoms.

Obokata and Isogai (2004b) made quantitative NMR measurements to obtain the azetidinium ring (AZR) rate and the DPn. For this purpose, they have used the integrals of peculiar peaks from synthetic products. For example the DPn of the repeating unit has been calculated from signals areas of carbonyl **C**(a) and carboxyl **C**(a') carbons at 179.6 and 180.2 ppm, respectively. Figure 3.5 presents the spectrum in carbonyl-carboxyl region for EKA WS505 solutions.

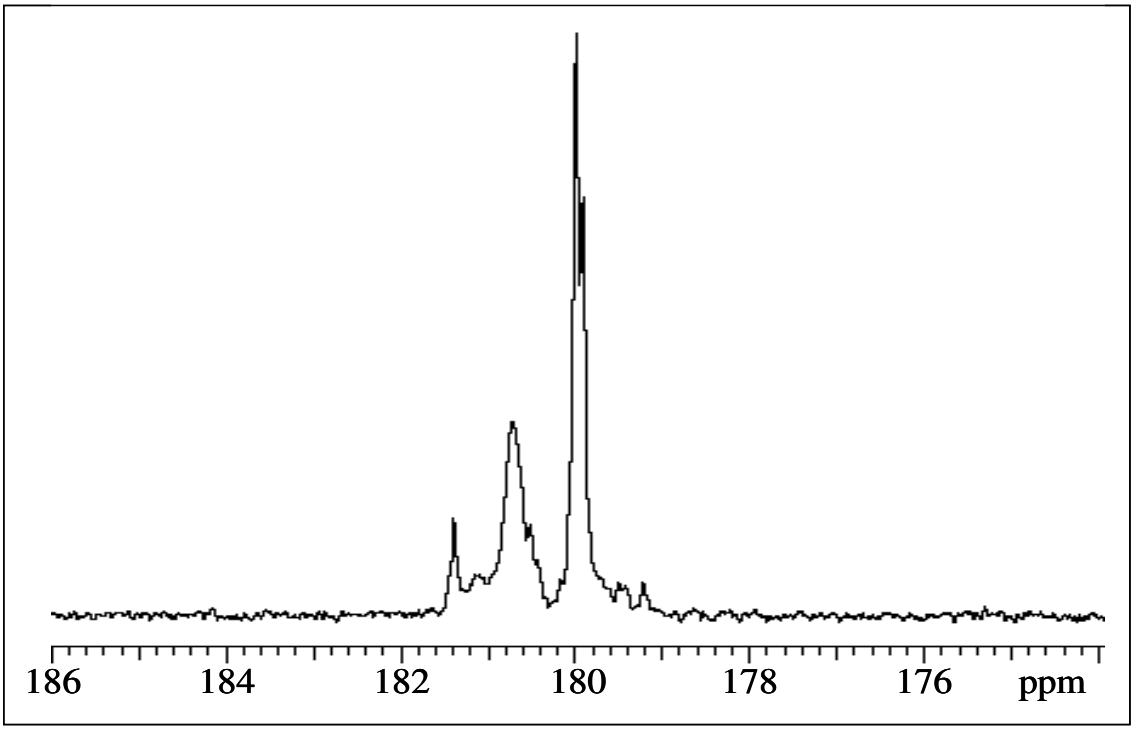

Figure 3.5: Carbonyl-carboxyl region of ^{13}C NMR spectrum for PAE commercial aqueous solutions.

During PAE synthesis, many by-products can be formed. In our case, we work with commercial solutions whose doubtless the major component is PAE. Nevertheless, they also contain many other products (called "impurities"), as observed from NMR analyses (Figure 3.6). These impurities display several peaks which hinder those arising from PAE macromolecules, thus making impossible any quantitative measurements because of peaks overlapping.

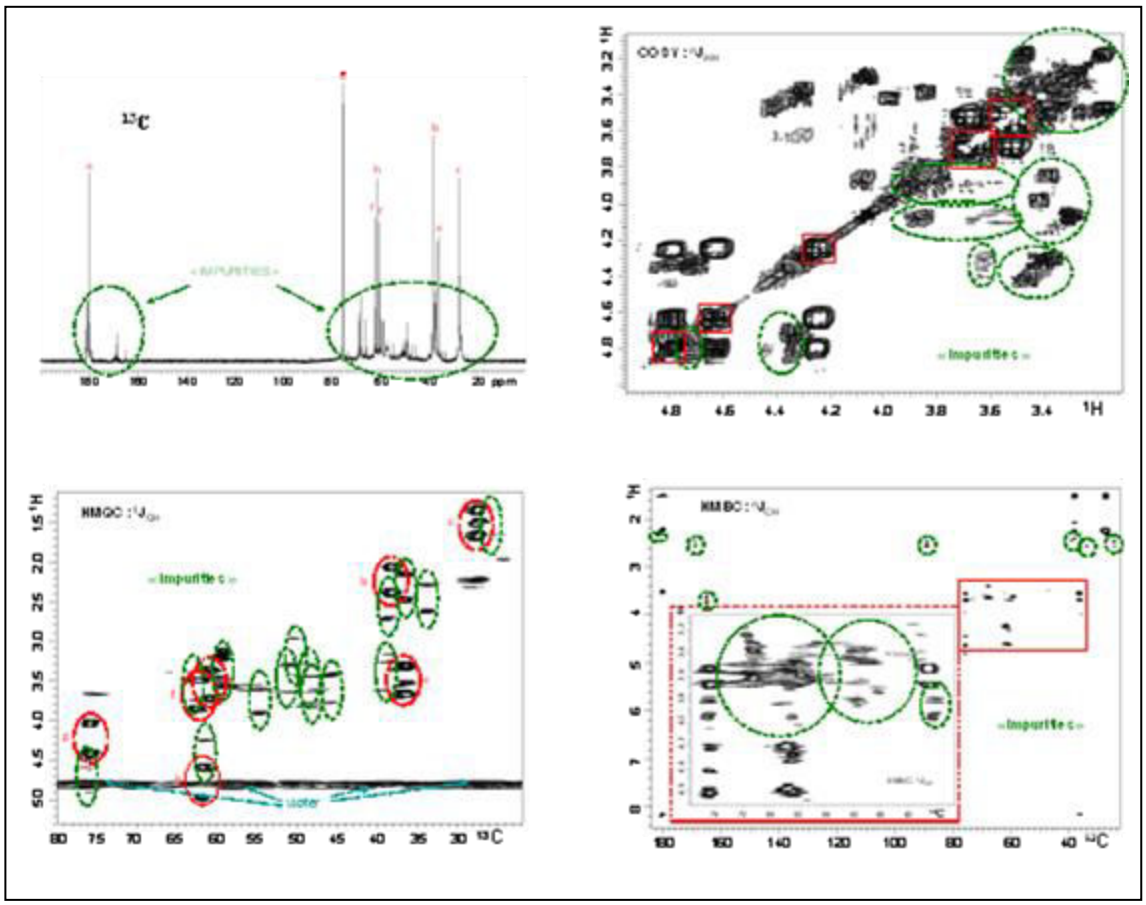

Fig. 3.6: By-products detection on ^{13}C spectrum, and COSY, HMQC and HMBC experiments.

Although quantitative measurements are not possible, we tried to elucidate the assignments of these "impurities" (or by-products). When adipic acid is used as one of the starting materials, high temperatures around 170°C are generally required for polyamideamine synthesis. Such severe conditions often give relatively large amounts of by-products. However, we do not have access to any information neither about the starting monomers nor concerning the synthesis route of these commercial products. Figure 3.7 shows the structure of some by-products in PAE aqueous solutions after synthesis, as reported by Obokata and Isogai (2004b).

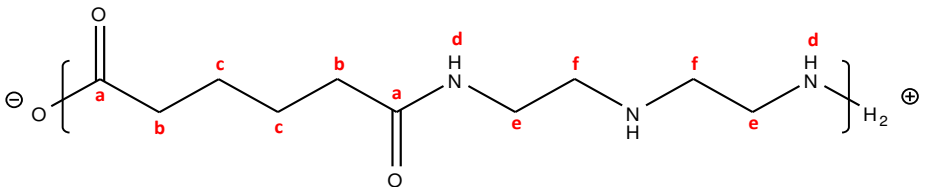

Polyamideamine ***(PAA)***

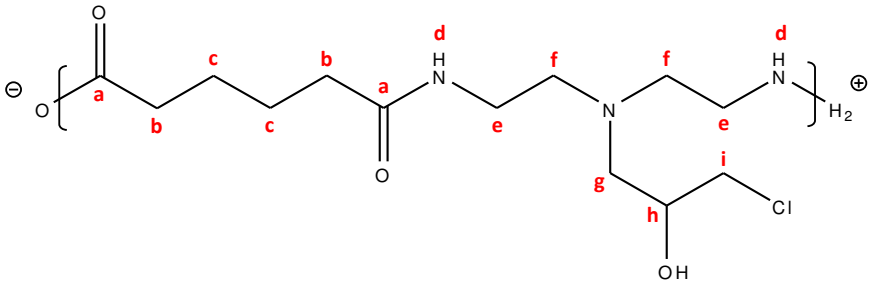

N-(3-chloro-2-hydroxypropyl)Polyamideamine ***(Cl-PAA)***

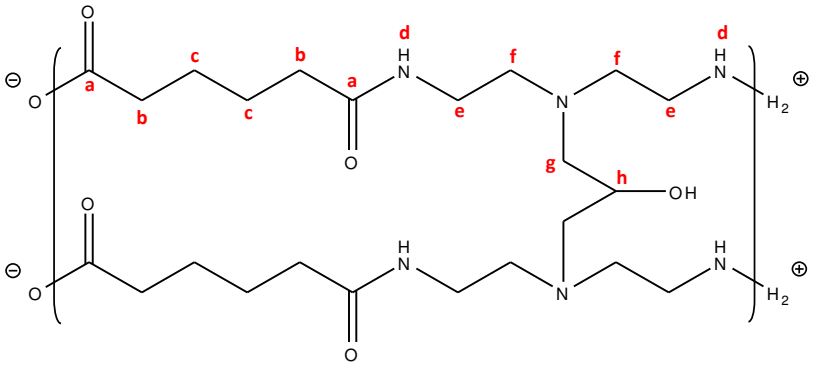

Crosslinked PAE ***(CrL-PAE)***

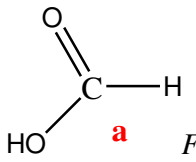

Formic acid ***(FA)***

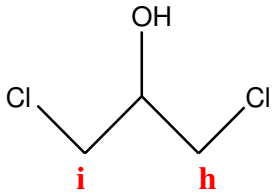

1,3-dichloro propanol ***(Cl_2POH)***

Fig. 3.7: Some by-products normally present in PAE commercial aqueous solutions.

Comparing our NMR results with the literature data (Obokata and Isogai, 2004b) and theoretical spectra predicting PAE NMR patterns (see Table III.2), we can make certain hypothesis about the chemical structure of some "impurities". Small amount of unmodified polyamideamine (**PAA)** and 3-chloro-2-hydroxypropyl group may be present as intermediate compounds in the PAE samples, even after heating of the N-(3-chloro-2-hydroxypropyl)polyamideamine (**Cl-PAA)** solution to form the azetidinium ring from the 3-chloro-2-hydroxypropyl precursor. The presence of the latter may be confirmed by the $^{1}J_{CH}$ correlation between carbon atoms in the 49 to 46 ppm region with the protons at 3.6 to 3.8 ppm attributed to the **C**H_2(i). **Cl-PAA** structures are confirmed also by two other correlations, namely:

(i.) **C**H(h) at 68 to 67 ppm in $^{1}J_{CH}$ correlations with C**H**(h) at 4 ppm and $^{n}J_{CH}$ correlations with C**H**$_2$(i) at 3.6 to 3.8 ppm; and

(ii.) **C**H_2(f and g) at 59 to 60 ppm in $^{1}J_{CH}$ correlations with C**H**$_2$(f and g) at 3.2 ppm and in $^{n}J_{CH}$ correlations with C**H**$_2$(i) at 3.6 to 3.8 ppm.

The unmodified polyamideamine **PAA** structures exhibit $^{n}J_{CH}$ correlations between the carbonyl **C**(a) at 180.7 ppm and the C**H**$_2$(b) at 2.3 ppm and several **C**H_2(f and e) in the 45 to 50 ppm region. From our experiments it is difficult to conclude the presence or not of cross-linked units.

After synthesis, the pH of PAE aqueous solutions is adjusted to 3-4 with sulphuric and formic acids in order to improve the stability of the PAE aqueous solutions justifying the presence of **FA** (Obokata *et al.*, 2005). The necessity of adding formic acid was not commented in the literature.

A more detailed study was not performed based on ^{1}H and ^{13}C NMR analyses to determine the structures of impurities, but we must keep in mind their presence because of their possible influence on the results of this work especially on the preparation and characterization of PAE films, the cross-linking reaction as well as on their ageing.

Table III.2: Theoretical ^{13}C and ^{1}H chemical shifts for by-products present in PAE commercial aqueous solution.

	a'	a	h	g	f	I	e	b	c	d
PAA pH 8 Obokata 2004	180	179			51 2.8		44 3.38	38 2.14	27 1.61	 7.8
Cl-PAA pH 3 Obokata 2004	179	180.7	68 4.4	59.3 3.5	57.1 3.5	49.2 3.8	37.7 3.7	38 2.3	27.4 1.61	 8.3
CrL-PAE ACD-NMR predictor	180.1	178.6	66.5 4.1	58.84 2.67 2.68	53.57 2.46		37.45 3.08 3.09	39 2.14	27.4 1.61	 7.8
FA ACD-NMR predictor	168 9.18									
Cl2POH ACD-NMR predictor			71.78 4.06			45.12 3.74				
PAE experimental		180	61.7 4.8	75.65 4.6 4.2	62.35 60.8 3.7 3.4		36.25 3.5	38.1 2.2	27.4 1.51	 8.16

3.1.2. Colloidal titration

In order to determine the specific charge of the PAE structure, diluted solutions were studied by colloidal titration using a particle charge detector (PCD-03 Mütek). Figure 3.8 shows the specific charge at electrical conductivity range of 100-500 µS/cm and pH values varying from 2 to 12. Below a pH value of 4 and above a pH 10, the samples showed conductivity values close to 1000 µS/cm. This high conductivity induces difficulties on stabilization of the streaming potential during the beginning of the experiment, making hard to detect the equivalent point (or endpoint). As a

consequence, a poor reproducibility of the results was observed. All samples showed after the endpoint a cloudy solution due to the precipitation of polyelectrolyte complexes formed between PAE resin and PES-Na (anionic standard polyelectrolyte). A decrease of the conductivity by one order of magnitude was also observed. The specific charge values of 3.0, 2.0 and 1.5 μeq/g were obtained on pH values of 4, 7 and 10, respectively, for PAE samples.

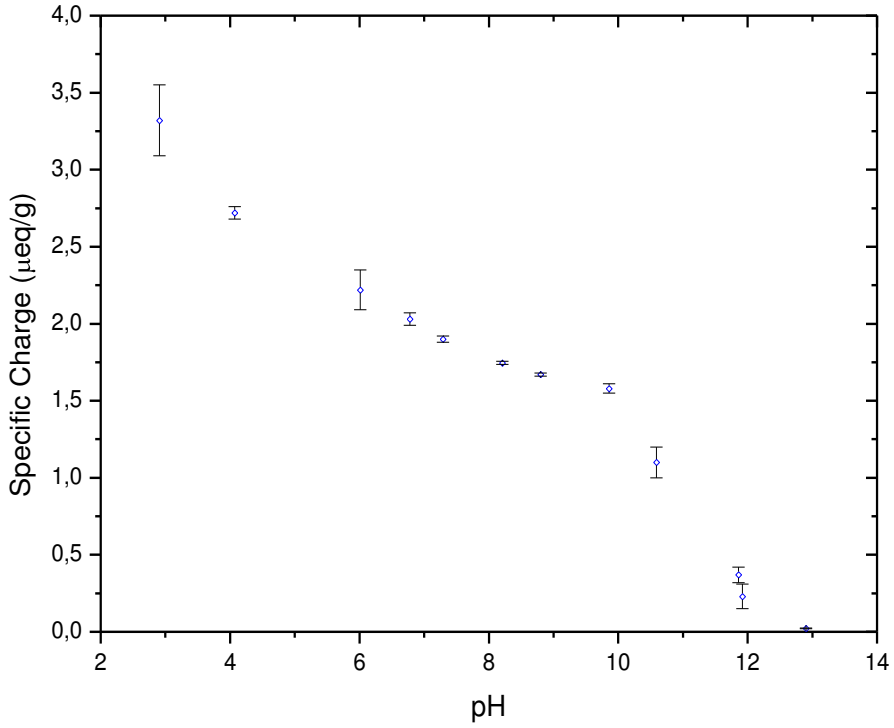

Fig. 3.8: Colloidal titration for diluted PAE aqueous solutions determined using a particle charge detector (PCD-03 Mütek) and PES-Na as anionic standard polyelectrolyte as a function of the pH of the medium.

The colloidal titration method is convenient but it represents indirect values, and it depends on the mechanism of formation of polyion complexes and differences in charge density between the polyelectrolytes. Another two important parameters that should be considered are the conductivity and the pH values of the solutions. The cationic charge densities around pH values of 4 (c.a. 3.0 μeq/g) indicate the total

amounts of protonated secondary/tertiary amino groups in the PAE structure and quaternary ammonium groups. In contrast, the cationic charge densities around pH 10 (c.a. 1.5 μeq/g), reflect only the amount of quaternary ammonium groups. Above a pH value of 10, another phenomenon must be considered to explain the specific charge decrease (as for example PAE cross-linking). However, as stated before, there is a poor reproducibility in this pH range due to an increase in conductivity of the solution.

Table III.3 presents the specific charge values described in the literature for PAE resins as well as the corresponding determination method used to obtain them. However, to the best of our knowledge, a complete study of the PAE charge, as a function of pH and conductivity have never been reported yet.

Table III.3: Specific charge of the PAE resins.

	Colloidal titration	**Specific charge (μeq/g)**	**pH**
Enarsson and Wägberg, 2007	with toluidine blue as an indicator	2.19	7
Yonn, 2007	with PCD and PES-Na as an indicator	5.0	7
Obokata *et al.*, 2005	with potassium polyvinylsulfate and toluidine blue as an indicator	3.3	4
Gernandt *et al.*, 2003	with polystyrenesulfonate and toluidine blue as an indicator	1.7	7
Gärdlund *et al.*, 2003	with PCD and potassium polyvinyl sulphate as an indicator	Not available	Not available
This work	with PCD and PES-Na as an indicator	3.0 2.0 1.5	4 7 10

3.2. PREPARATION OF PAE FILMS

PAE commercial aqueous solutions were lyophilized and re-precipitated in non-solvents in order to eliminate water and by-products. Freeze drying technique (Freeze dryer Alpha 2-4 L D plus Bioblock Scientific) was carried out until constant weight, after c.a. 15 days. The solid obtained showed an intense yellow color and it was insoluble in acetone and ethanol. On the other hand, in water, the lyophilized product losts its intense yellow color and resembles a gel. Partial re-solubility was however observed with the presence of filaments and fragments of the gel. After filtration and drying of this sample under ambient conditions for 24 h, the solid reacquired its initial aspect. One possible explanation for insolubility is the PAE cross-linking during water elimination.

Precipitation of PAE solutions was carried out in different organic solvents (methanol, ethanol, DMSO, dichloromethane and acetic acid), and the products obtained were studied using FTIR analyses. Spectra of the precipitated samples with methanol, ethanol and after freeze-drying showed the same absorption bands, although the spectra of the sample precipitated in acetone presented intense absorption bands attributed to the presence of water and bad clearness. After precipitation in different solvents, all the samples were insoluble in water. Table III.4 shows the results of re-solubilization of PAE precipitated for 48 h in acetone under ambient conditions (the acetone was changed after 24 h).

The preparation of PAE films was carried out with different PAE/methanol/acetone ratios, and by the evaporation of PAE commercial aqueous solutions (without organic solvents), under ambient and controlled conditions (25^{o}C and 50% RH). Visual inspection of the films showed presence of bubbles and holes in the films prepared from the mixture of organic solvents or evaporation under room temperature. However, neither bubbles nor holes were observed in the films prepared by evaporation under controlled conditions. These materials were partially soluble in water at moderated stirring for 1 h. The films prepared by evaporation of water under room temperature or in mixture of organic solvents were no longer soluble. After these initial studies we decided to prepare PAE films by casting under controlled conditions. Similar results were obtained by Obokata and Isogai (2007). The films casted in these studies

under room temperature and for several days were swollen but no longer soluble in water indicating the formation of some cross-linking during the drying process.

Tab. III.4: Re-solubility tests for PAE after precipitation in acetone.

Solvents	***Solubility***	***Visual aspects***
methanol	Insoluble	yellow
ethanol	Insoluble	yellow
DMSO	Insoluble	yellow
dichloromethane	Insoluble	yellow
water	partially soluble	formation of a colorless and translucent gel
water + methanol (50 : 50)	partially soluble	formation of a colorless and translucent gel
acetic acid	insoluble	yellow

Suppliers of PAE commercial aqueous solutions recommend avoiding freezing. In order to store PAE aqueous solution for a long time, EKA WS505 was frozen at c.a. -10°C to prevent cross-linking reactions. Colloidal titration of PAE commercial aqueous solution, and DMA and FTIR analysis of PAE films were performed to study possible physico-chemical modifications after freezing of the solutions. Figure 3.9 presents FTIR spectra before and after freezing of PAE aqueous solutions for 48 h, whereas Figure 3.10 presents DMA tracings. No modifications of the specific charge by colloidal titration were observed. The characteristic absorption bands obtained from FTIR analysis and the mechanical relaxations derived from DMA curves were also the same before and after freezing of EKA commercial solutions. One possible explanation to avoid freezing could be postulated: conserving the action of microorganisms that are added in PAE aqueous solutions after synthesis to degrade toxic by-products formed as 1,3-dichloro-2-propanol (Obokata *et al.*, 2005).

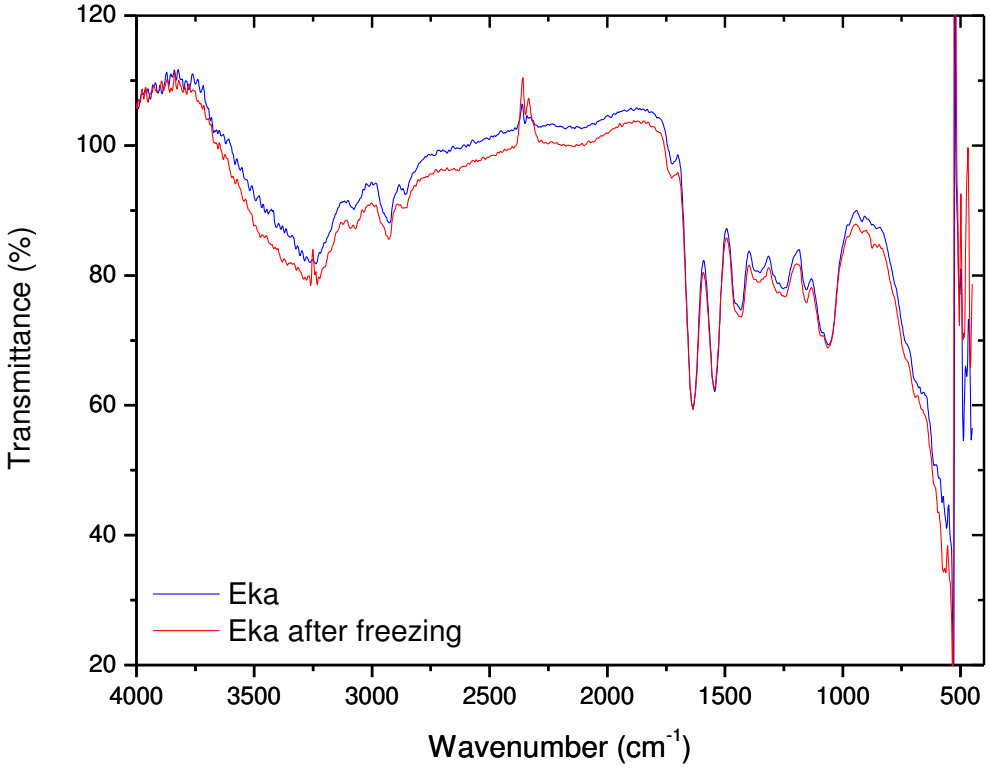

Fig. 3.9: FTIR analysis of films prepared with EKA aqueous solutions before and after freezing.

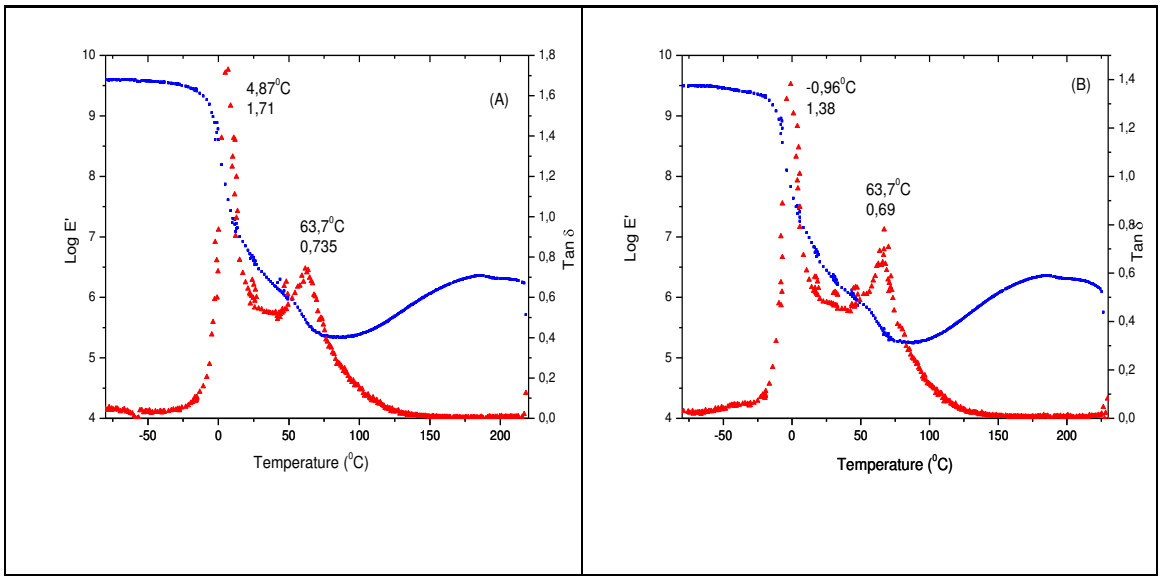

Fig. 3.10: DMA analysis of films prepared with EKA aqueous solutions before **(A)** and after freezing **(B)**.

Figure 3.11 shows the drying profile of PAE films. After a week, they still contain water molecules (c.a. 13%), probably due to interactions between water molecules and polar groups in the PAE structure or trapped water molecules during the formation of the films.

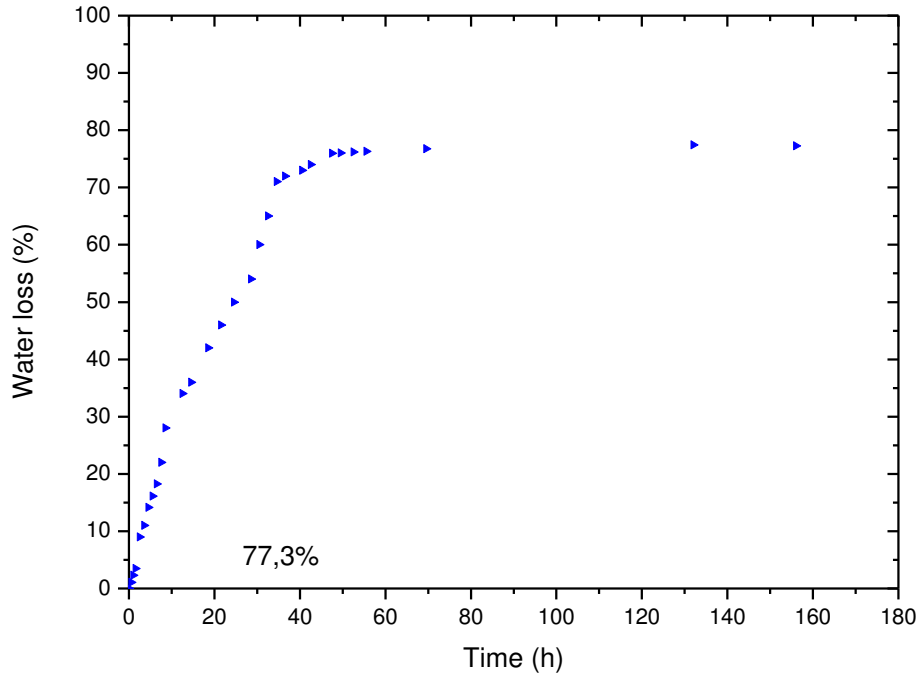

Fig. 3.11: Drying profile of PAE films (Eka WS 505) prepared in Teflon mould, for a week under controlled conditions (25°C and 50% RH).

Figure 3.12 shows the swelling rate at 30°C for heated (105°C for 24h in an oven) and unheated PAE films. The obtained curves show a plateau value at about 5 and 24 h for unheated and heated PAE films, respectively. A remarkable increase in the temperature of the distilled water during the swelling, probably due to a high affinity of PAE and water was observed but not measured. Unheated film showed formation of a translucent gel during swelling, and the heated film broken down into small pieces and it displayed a yellow color. The swelling ratios for the unheated and heated PAE films, after saturation, were found to be situated at about 5000 and 270%, respectively.

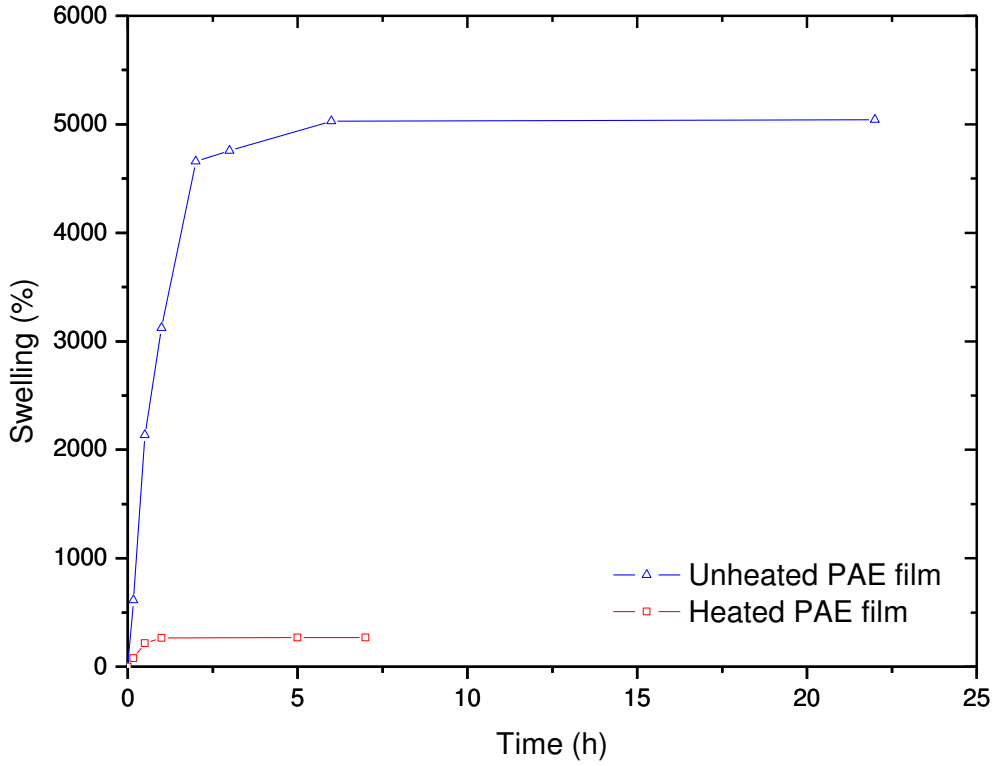

Fig. 3.12: Swelling rate at 30°C of heated (105°C for 24h) and unheated PAE films.

3.3. MORPHOLOGICAL, THERMAL AND MECHANICAL CHARACTERIZATIONS OF PAE FILMS

Figure 3.13 presents the micrographs obtained by SEM of unheated PAE films. Cross-section micrographs (see Figure 3.13 C and D) show the formation of films without internal porosity. Some pores can be observed on the surface of the films, but they seem to be closed pores (see Figure 3.13 C).

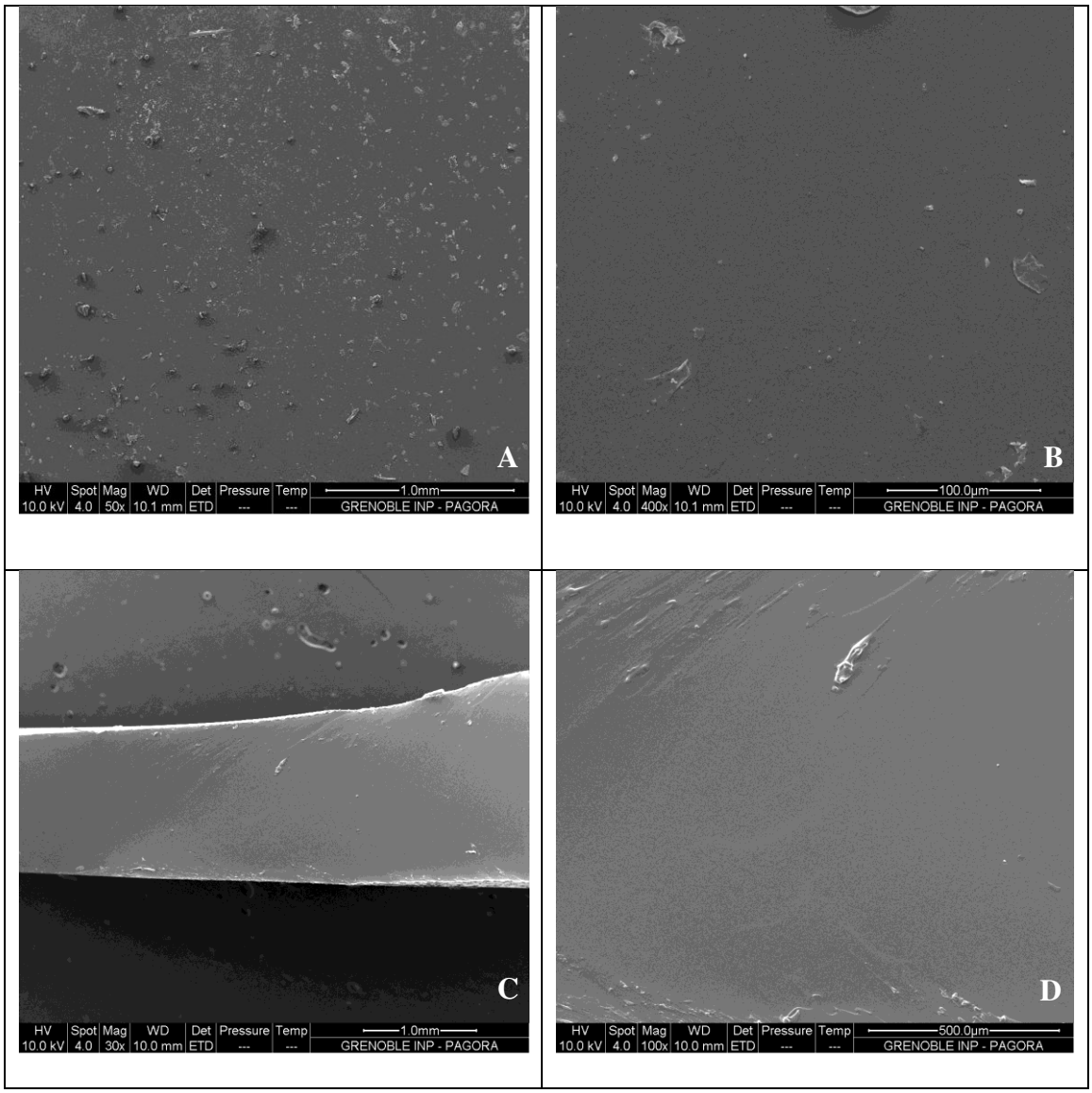

Fig. 3.13: Micrographs obtained by SEM of unheated PAE films **(A)** and **(B)** surface, and **(C)** and **(D)** cross-section.

PAE films were heated in an oven at 105°C for 24 h in order to study thermally induced PAE cross-linking. Figure 3.14 presents FTIR spectra of unheated and heated PAE films. These spectra show typical amide I and II absorption bands of polyamide-6 at 1636 and 1542 cm^{-1}, respectively, already observed by Obokata and Isogai (2007) and Costa *et al.* (1999a,b).

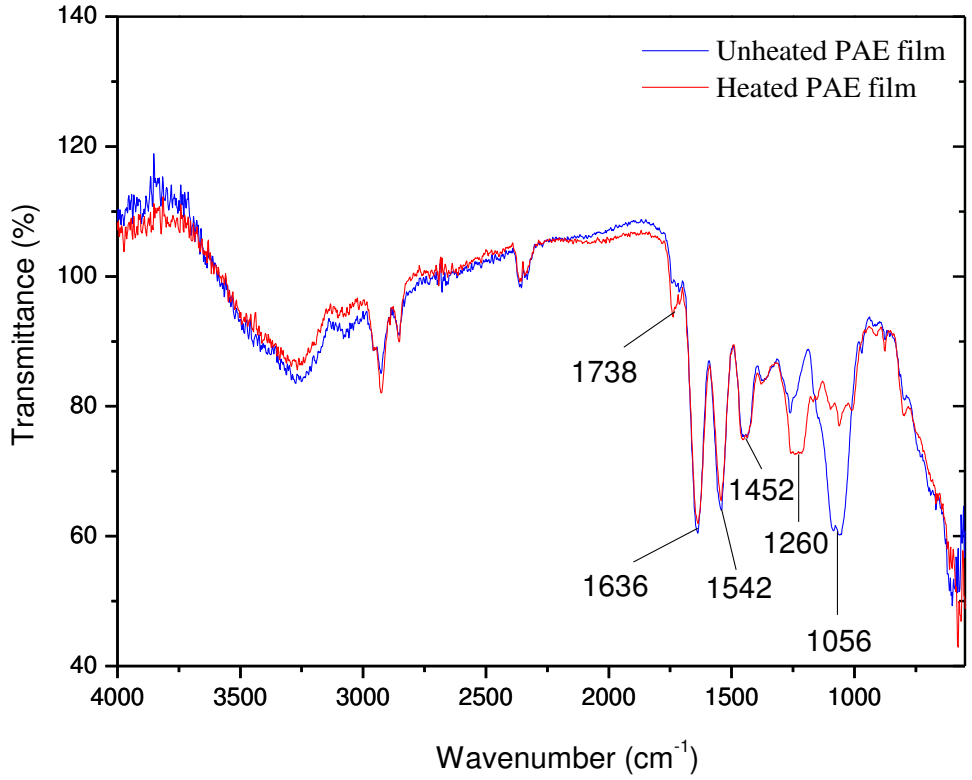

Fig. 3.14: FTIR analysis of PAE films before and after thermal treatment in an oven at 105°C for 24h.

The main differences induced from thermal treatment are related to the absorption bands at around 1060 and 1260 cm^{-1}. The band at 1060 cm^{-1} was attributed to the breathing of AZR and to OH stretching vibrations of secondary alcohols (Dyer, 1965). The intensity decrease of this absorption band with the thermal treatment is related to the opening of AZR (Russel *et al.*, 1997). The band at around 1260 cm^{-1} was attributed to C-N stretching vibration of tertiary amine and CO stretching vibrations of secondary alcohols (Silverstein *et al.*, 2005; Dyer, 1965). The intensity increase of this band after thermal treatment is probably due to cross-linking of PAE macromolecules.

Figure 3.15 describes a possible cross-linking reaction between PAE-PAE and/or PAE-unmodified polyamideamine residues from synthesis. Table III.5 shows the absorption bands described in the literature for PAE resin and polyamide.

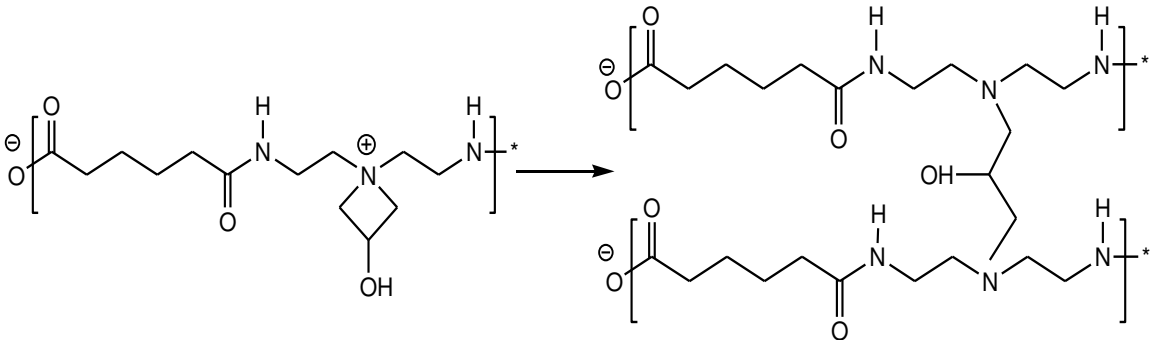

Fig. 3.15: Cross-linking reaction between PAE-PAE and/or PAE-unmodified polyamideamine macromolecules.

According to our results, the main cross-linking reaction occurs between the AZR and secondary amine groups in the PAE structure and/or in the unmodified polyamideamine, which gives rise to the:

(i.) formation of 2-propanol bridges between PAE-PAE or PAE-unmodified polyamideamine;

(ii.) decrease of AZR percentage in the PAE structure; and

(iii.) increase of percentage of tertiary amine bonds.

A little increase of the intensity of the absorption band at 1738 cm^{-1} was also observed which is attributed to C=O stretching vibration of ester groups. Then, it is required to consider the secondary contribution of ester linkages to the PAE cross-linking which will be studied in detail in the next section "Ageing of PAE films".

Table III.5: Attribution of the absorption bands obtained from FTIR analysis of PAE resin and polyamide.

Bande (cm^{-1})	**Obokata and Isogai, 2007**	**Cooper *et al.*, 2001**
916		C-CO stretching and CH_2 rocking
1058		Skeletal C-C stretching
1256	C-O stretching vibrations of ester groups	Amide III coupled with hydrocarbon skeleton, CH_2 wagging or twist
1350		Amide III, CN stretching + in plane NH deformation, coupled with hydrocarbon skeleton. Also CH_3 end group symmetric deformation. CH_2 wagging or twist + amide III. Regular fold band
1434		CH_2 scissoring next to CO group trans conformation, CH_2 scissoring for all methylenes not adjacent for to amide groups, CH_2 scissoring next to NH group trans conformation
1546	Amide II	Amide II. Mainly in plane NH deformation (+CO and CN stretching)
1636	Amide I and symetric deformation of H_2O	Amide I. Mainly CO stretch (+in plane NH deformation + possibly CN stretching)
1724	C=O stretching vibrations of ester groups	
2854		CH_2 α- CO symmetric stretching, CH_2 β- NH and γ- NH symmetric stretching , CH_2 α- NH symmetric stretching
2934		CH_2 γ-NH and β-CO asymmetric stretching, CH_2 α- CO asymmetric stretching + CH_3 symmetric stretching, CH_2 β- NH asymmetric stretching, CH_2 α- NH asymmetric stretching
3270		N-H stretch

Until today, the cross-linking mechanism for PAE resins is a matter of discussion within the scientific community. Obokata and Isogai (2007) attributed the absorption bands at around 1728 and 1260 cm^{-1} detected in heated PAE films (105°C for 10 min), to C=O and to C-O stretching vibrations of ester groups, respectively. These authors stated that ester bonds are formed from partial cross-linking during synthesis, and/or are formed during drying and preparation of PAE films under room temperature. Thus, as discussed in the section "Ageing of the PAE films" there is experimental evidence of what pointed out by solid-state NMR and associated to the main contribution of the cross-linking mechanism of PAE, as sketched in Figure 3.15. In certain conditions, PAE-PAE ester bonds can be formed but their contribution is rather secondary. Any way, it is necessary to keep in mind that low amount of carboxylic end groups is present in the resin, thus making negligible the possible formation of ester bonds from these groups.

DSC analyses were performed to study the thermal transitions in the PAE structure. Films of PAE were submitted to two consecutive temperature scans on the same sample, namely: **(i.)** the first step was carried out on the temperature range of -90 to 120°C; whereas **(ii.)** the second one involved a wider range, i.e., -90 to 350°C.

The determination of the glass transition temperature (Tg) was performed by exploiting the DSC tracings of the two scans. Table III.6 presents Tg of the samples and the calorific capacity associated to these transitions.

Table III.6: Glass transition temperature (Tg) of PAE films, as determined by DSC analysis.

PAE film	***First Scan***		***Second Scan***	
	Tg (°C)	**Calorific Capacity J/(g °C)**	**Tg (°C)**	**Calorific Capacity J/(g °C)**
Unheated	1,18	0,0959	14,4	0,104
Heated	63,3	0,251	62,6	0,346

The Tg obtained from the first scan is different for unheated films from that of the second scan. This difference can be related to a incomplete cross-linking reaction. After heating during the first scan and consequently additional cross-linking, unheated and heated PAE films show Tg temperatures at around 14 and 62°C, respectively. The endothermic transition at 100°C of the unheated films on the second scan was attributed to the residual water elimination and the exothermic transition between 150 to 300°C was assigned to the cross-linking process and to the degradation of the PAE structure. The heated film (105°C for 24 h) showed, on the second scan, an exothermic transition at 220 to 300°C related to the degradation of the cross-linked PAE structure.

Unheated and heated PAE films were also characterized by DMA analyses. These tests provide accurate assessment of thermodynamic transitions in the material structure. Figure 3.16 shows the storage modulus (E') and tan δ curves of thermally treated films at 105°C for different time intervals.

Unheated PAE films show two relaxations on tan δ curve. It is worth nothing that they exhibit relaxations in the same regions to polyamide and polyepichlorohydrin in pure forms, i.e. at 60 and -10°C respectively (Costa *et al.*, 1998a,b). This phenomenon may result from the presence in the film of unmodified polyamideamine as a by-product from PAE synthesis, as confirmed previously by liquid NMR analyses and FTIR spectra.

Films heated for 10 min and 1 h show a shoulder close to the first relaxation. This behaviour is probably related to the formation of intermediate chemical structures partially cross-linked and/or interfaces, induced by the thermal treatment, between PAE-PAE and/or PAE-unmodified polyamideamine. An increase of E' was observed after 100°C for unheated films and films heated for 10 min due to a cross-linking reaction. After 4 h treatment, the films still showed thermodynamic relaxations influenced on minimum by two phases. However a shift of the relaxations to high temperatures and a smaller decrease of the E' values were observed with the increase of the temperature when one compare the samples unheated and heated for 10 min and 1 h. Such a feature is expected and it suggests that PAE cross-linking is developed as a function of the time and of the temperature.

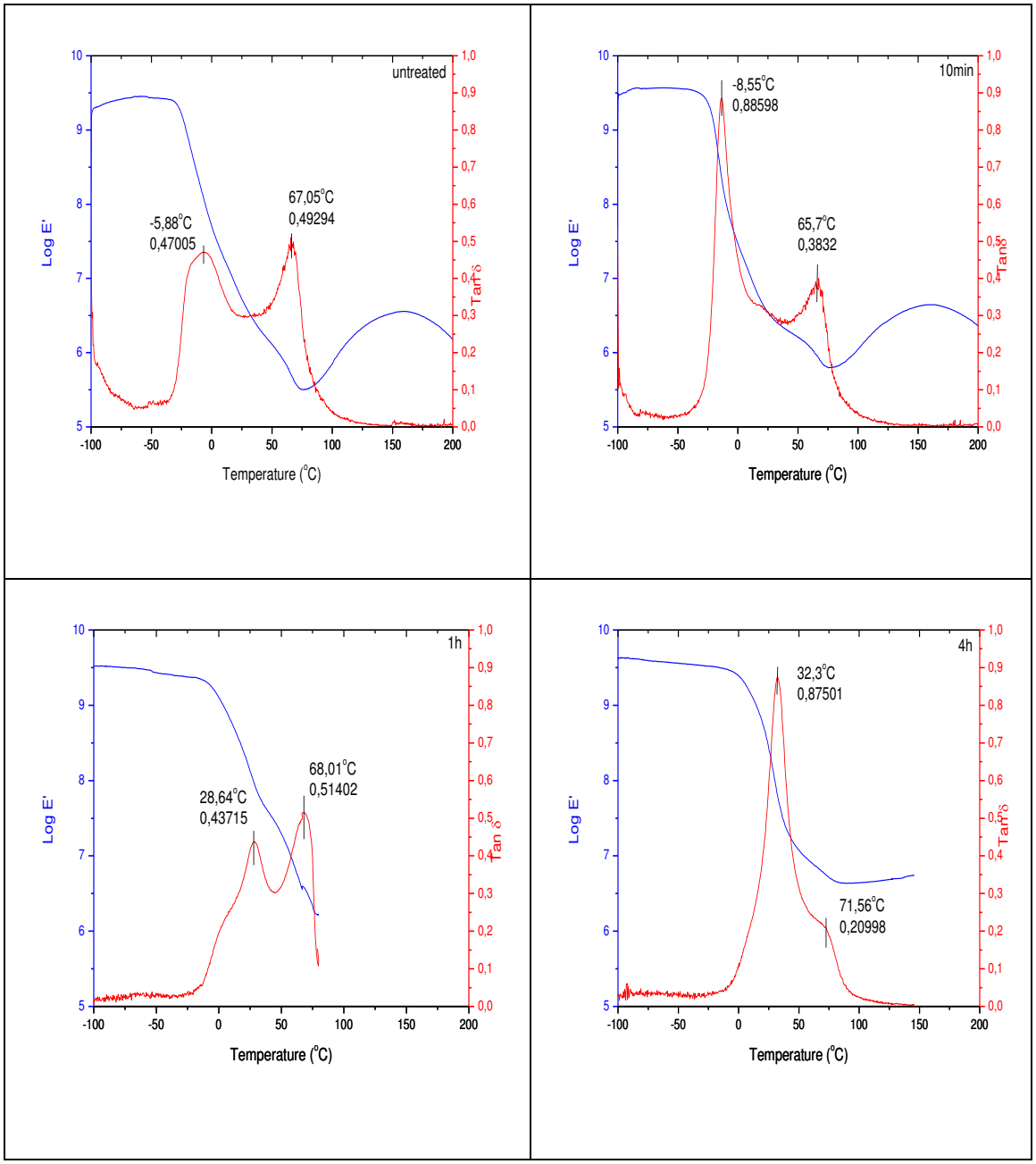

Fig. 3.16: Log E' and tan δ curves obtained by DMA analysis for unheated and heated PAE films.

From these experiments, we can conclude that the first relaxation is attributed to a polyamideamine phase modified by epichlorohydrin (PAE phase), whereas the second one is proper relaxation of the polyamideamine phase (normally present in PÀE solutions as a by-product from PAE synthesis).

Figure 3.17 (A) and (B) show DMA analysis of unheated and heated PAE films (105°C for 24 h), respectively. The thermally post-cured film showed only one well defined Tg temperature at 80°C. Thus, we can conclude that during the thermal treatment, the PAE phase related to the first relaxation undergoes chemical reactions, due to the opening of the AZR, thus resulting in PAE cross-linking. As previously discussed, intermediate cross-linked phases between PAE-PAE and/or PAE-polyamideamine phases, associated to shoulders close to the relaxations, are formed and influence the thermodynamic behaviour of the PAE films. However, after 24 h treatment, there is only one value of Tg suggesting that the PAE cross-linking reached its ultimate state and the thermodynamic relaxations are determined only by this cross-linked phase.

Finally, we can postulate that differences in the transitions during characterization of PAE films by DSC and DMA analyses are due to the sensitivity and principles related to these techniques. DMA analyses are more sensitive to determination of Tg, relaxations and transitions caused by physico-chemical reactions and interactions in the material structures (Biddlestone *et al.*, 1986; Gradin and Bäklund, 1981). The Tg shows a variation of few J/g ºC of calorific capacity and a remarkable variation of the E' (10^3-10^4 Pa). Based on this assumption, the thermodynamic technique is more sensitive to the determination of Tg in comparison with the calorimetric techniques.

Another advantage is that the DMA technique is a direct method for measuring Tg and Tm because it is directly related to the macromolecules motions. In some cases, as in blends or composites, in which one of the components is present in low concentration, their Tg can be detected only by thermodynamic-mechanical analysis (Wunderlich, 1997). However, these techniques cannot replace each other and should be considered as complementary tools.

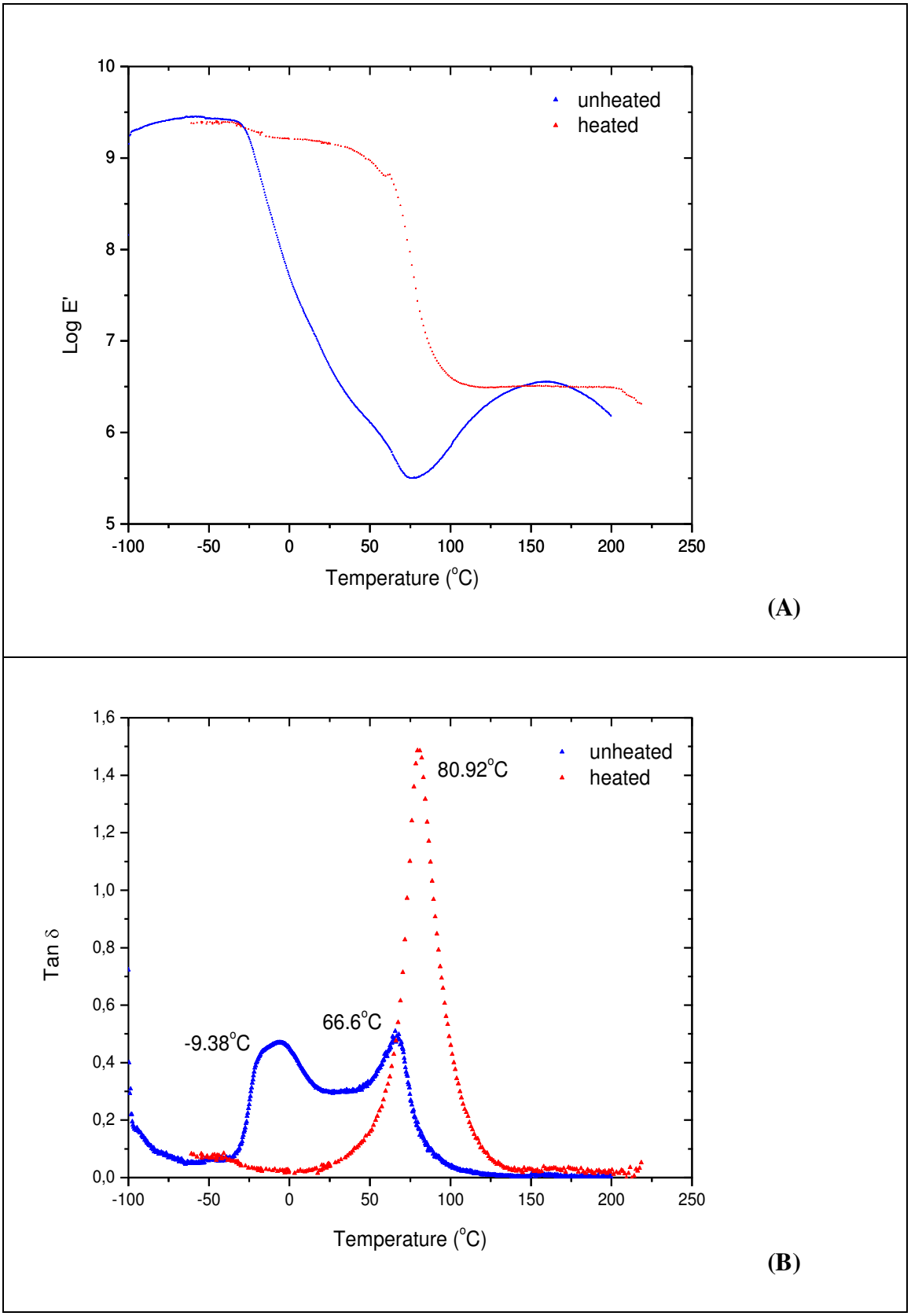

Fig. 3.17: DMA analyses of unheated and heated PAE films at 105°C for 24h **(A)** E' *vs* T and **(B)** tan δ *vs* T.

3.4. AGEING STUDY OF PAE FILMS

In order to study PAE cross-linking mechanisms, heated (at 105°C for 24 and 48 h), and unheated PAE films were aged under controlled conditions (25°C and 50% RH), and studied by NMR spectroscopy. Figure 3.18, 3.19 and 3.20 show the spectra of solid state ^{13}C NMR analyses of unheated PAE films aged up to one year.

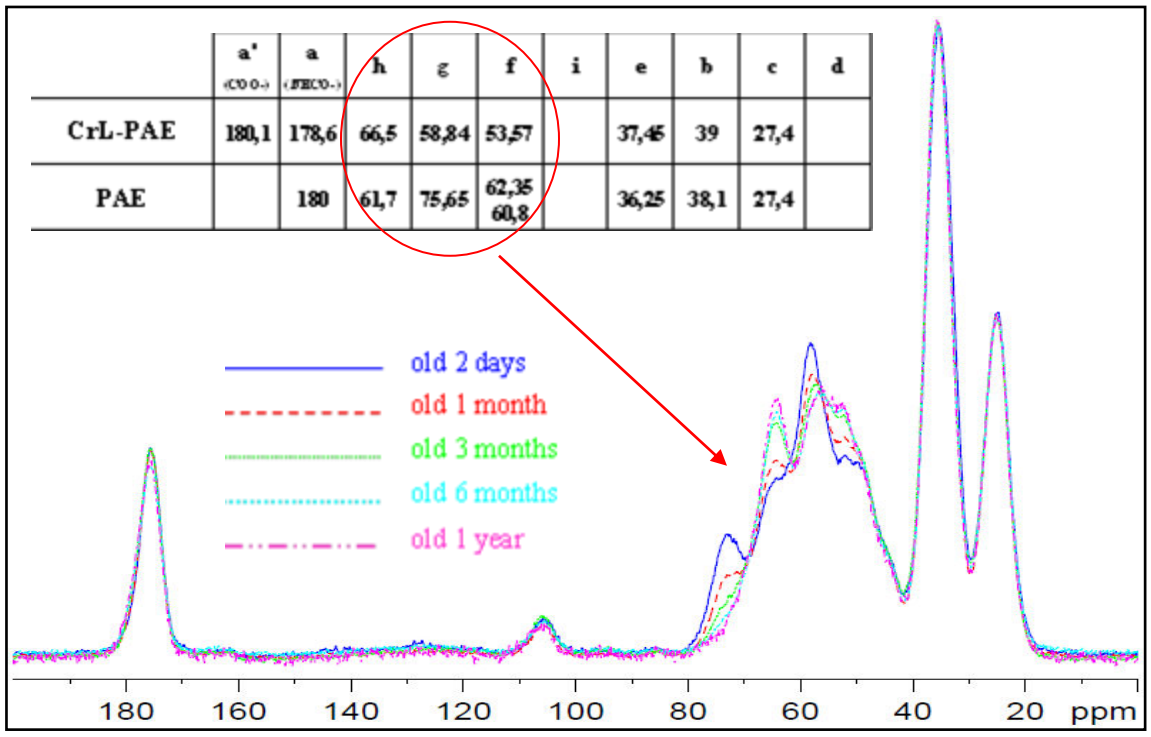

Fig. 3.18: Solid state ^{13}C NMR recorded at 243 K of aged unheated PAE films.

The carbons signals of carbonyl **C** (a) and carboxyl **C** (a') at 178.6 and 180.1 ppm, respectively, did not suffer any substantial change during ageing of the unheated PAE films up to one year as shown on Figure 3.19, which represents a strong magnification of this region. Thus, in the conditions employed we can postulate that the carbonyl and carboxyl groups of PAE do not participate to the cross-linking reaction during the ageing of unheated PAE films. In fact, these spectra suggest that there is no ester bond formation. However, several clear changes on the signals associated to the AZR group appearing at 40-80 ppm were observed as shown on Figure 3.20.

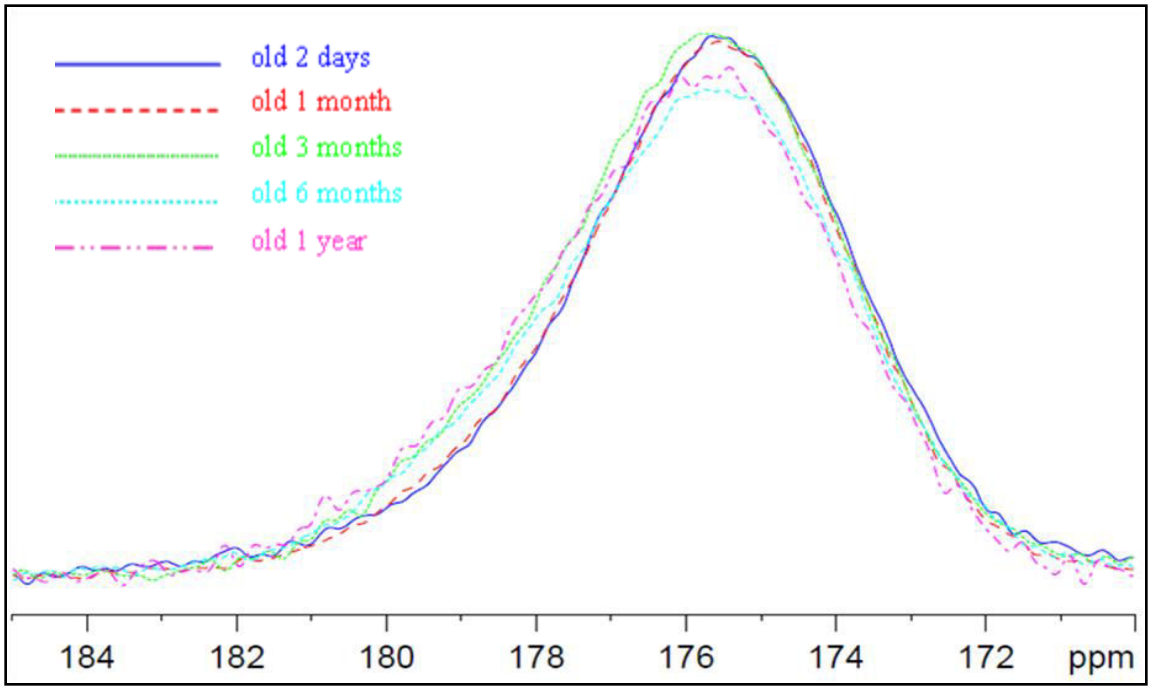

Fig. 3.19: CP-MAS ^{13}C NMR spectra of aged unheated PAE films recorded at 243 K (carbonyl-carboxyl region: 170 to 182 ppm).

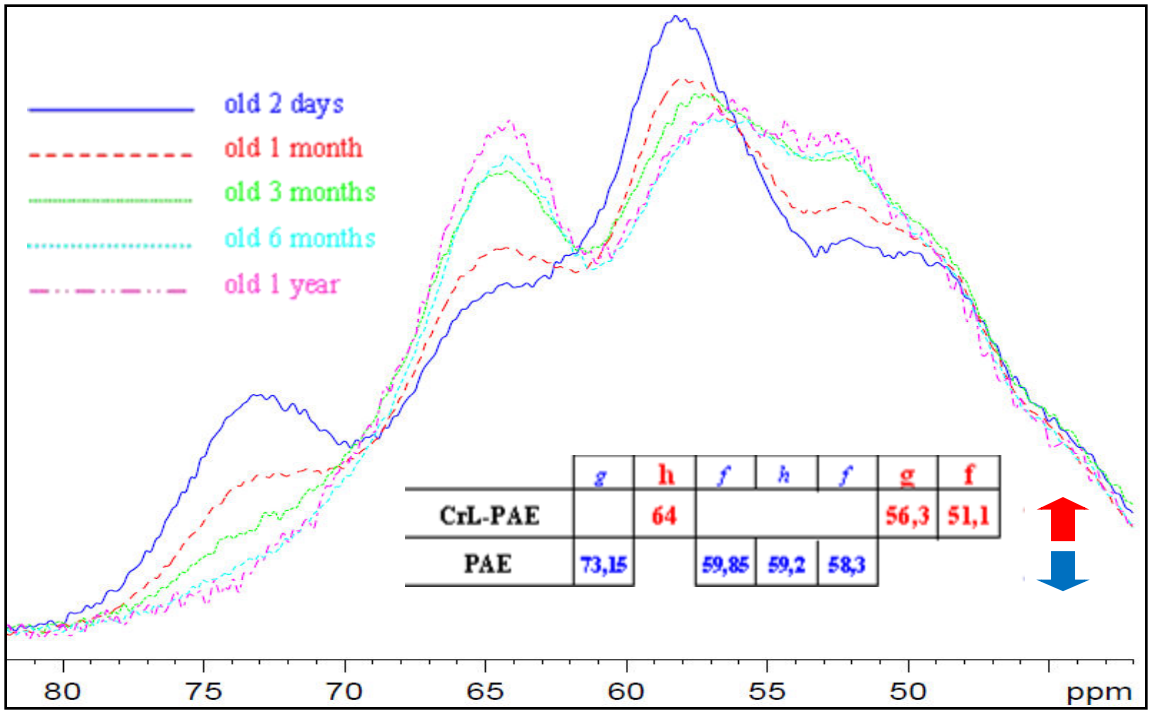

Fig. 3.20: CP-MAS ^{13}C NMR spectra of aged unheated PAE films recorded at 243 K (AZR region: 40-80 ppm).

During the ageing of unheated PAE films, the carbon signals areas, associated to the AZR at 73.15 (g), 59.85 (f), 59.2 (h) and 58.3 (f') ppm decrease, and the carbon signal areas at 64 (h), 56.3 (g) and 51.1 (f) ppm increase. Thus, based on the assignments on the Figure 3.21, we can point out that the cross-linking reaction of unheated PAE films proceeds by a nucleophilic attack of N atoms in the PAE and/or polyamideamine structures on the carbons g and g' of the AZR, which leads to the ring opening reaction and the formation of 2-hydroxy propanol bridges between the polyamideamine chains.

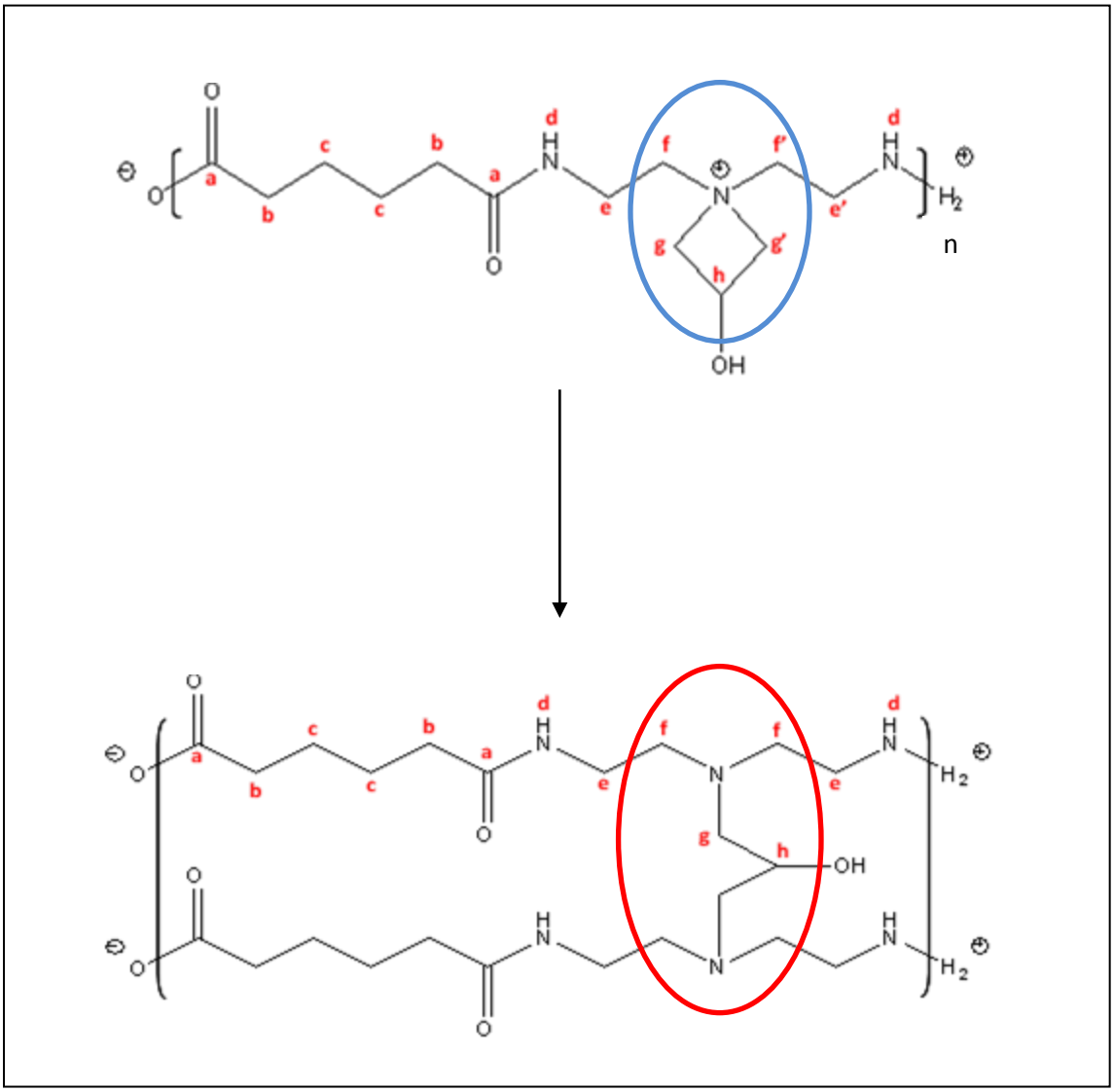

Fig. 3.21: Cross-linking reaction of unheated PAE films during ageing.

Figure 3.22 (A) and (B) presents the FTIR spectra of aged unheated PAE films for 2 days, 1 and 3 months and shows that several changes have occurred during ageing, namely:

(i.) a decrease in the absorption band at around 1050 cm^{-1} (attributed to the breathing of AZR);

(ii.) an increase in the absorption signal at around 1260 cm^{-1} (attributed to CN stretching vibrations of tertiary amine groups and CO stretching vibrations of secondary alcohols); and

(iii.) the appearance of the absorption peak at around 1150 cm^{-1}, which corresponds to the region of CO stretching vibrations of secondary alcohols and CN stretching vibrations of tertiary amines.

After 3 months and up to one year, the differences on the intensity of the absorption bands are negligible.

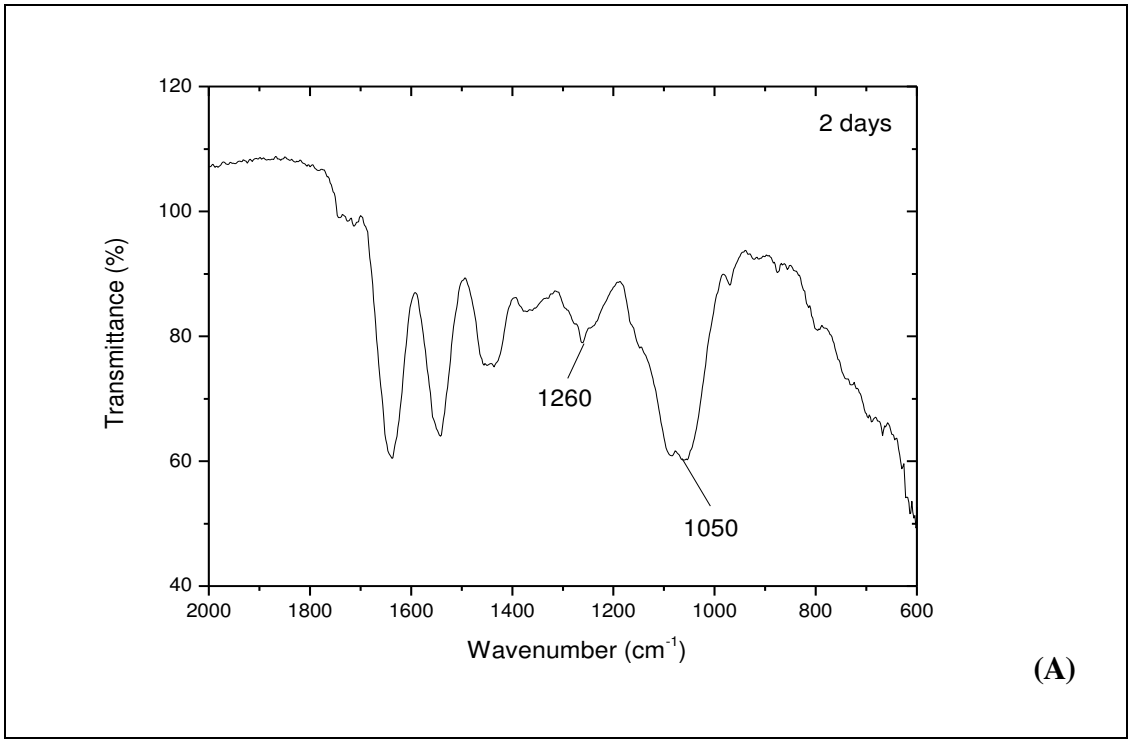

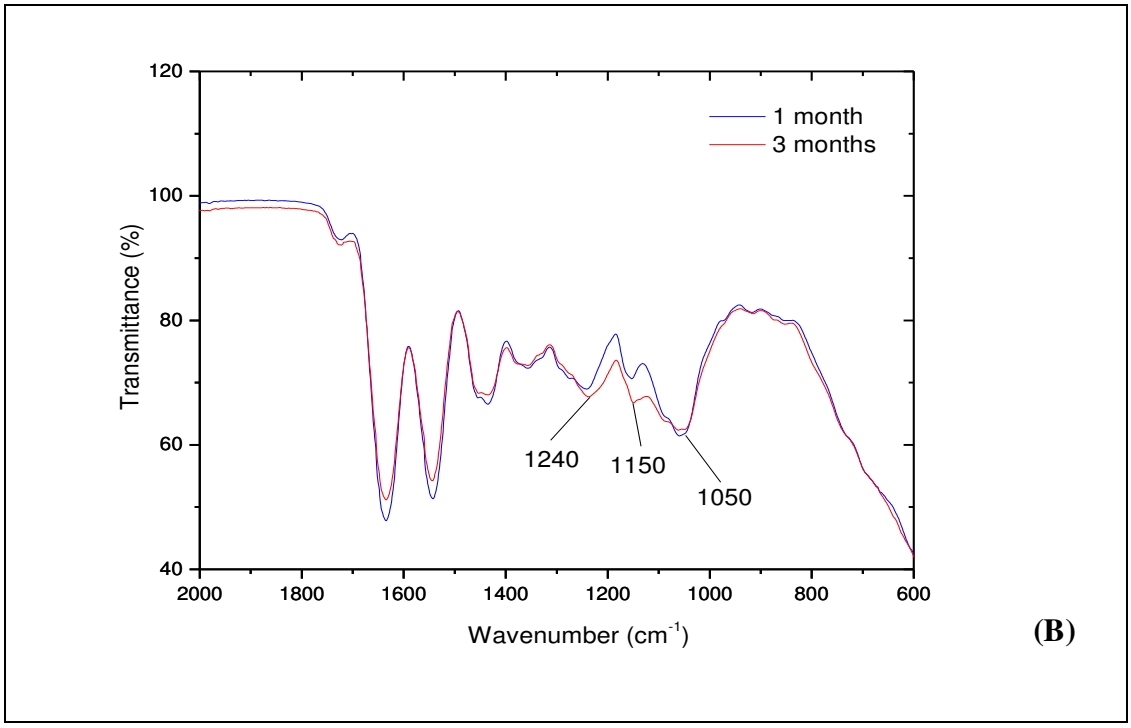

Fig. 3.22: FTIR spectra of aged unheated PAE films for **A)** 2 days, and **B)** 1 and 3 months.

DMA experiments of aged unheated PAE films were carried out (see Table III.7). 1 month aged films showed two relaxations:

(i.) at 4.9°C attributed to the PAE phase; and

(ii.) at 69.1°C attributed to the polyamideamine phase.

As observed in the NMR experiments and from FTIR spectra, even after one month of ageing there is still AZR remaining groups in the unheated PAE structure. This phase influences the thermodynamic relaxations of the PAE during DMA experiments. Films aged for 3 months up to one year showed only a relaxation, at around 81°C, attributed to the cross-linked PAE phase.

Table III.7: DMA experiments of aged unheated PAE films.

	First Tg (^oC)	***Second Tg (^oC)***
2 days	-9.38	66.6
1 month	4.9	69.1
3 months	-	80.9

Solid state ^{13}C NMR, FTIR and DMA experiments revealed that the cross-linking of the unheated PAE films reached its ultimate state between 1 to 3 months of ageing. After 3 months up to one year, remaining AZR in the PAE structure can be considered negligible indicating the complete cross-linking.

Figure 3.23, 3.24 and 3.25 present CP-MAS ^{13}C NMR spectra of aged heated (at 105°C for 24 h) PAE films (red line) and show that the signals associated with AZR groups did not suffer appreciable changes even after storage during six months (green line). Thus, we can conclude that the cross-linking reactions induced by opening of AZR (see Figure 3.21), reach their final state with this thermal post-treatment and that the ultimate cross-linking stage is achieved at 24 h at 105°C. Two other experimental evidences that support this assumption are, namely:

(i.) a similarity of the FTIR spectra of heated PAE films aged for 1 up to 6 months (see Figure 3.27 A); and

(ii.) a presence of only a one thermal transition (Tg), at around 80°C on tan δ curves deduced from DMA experiments after the thermal treatment, and attributed to the cross-linked PAE phase (see Figure 3.18).

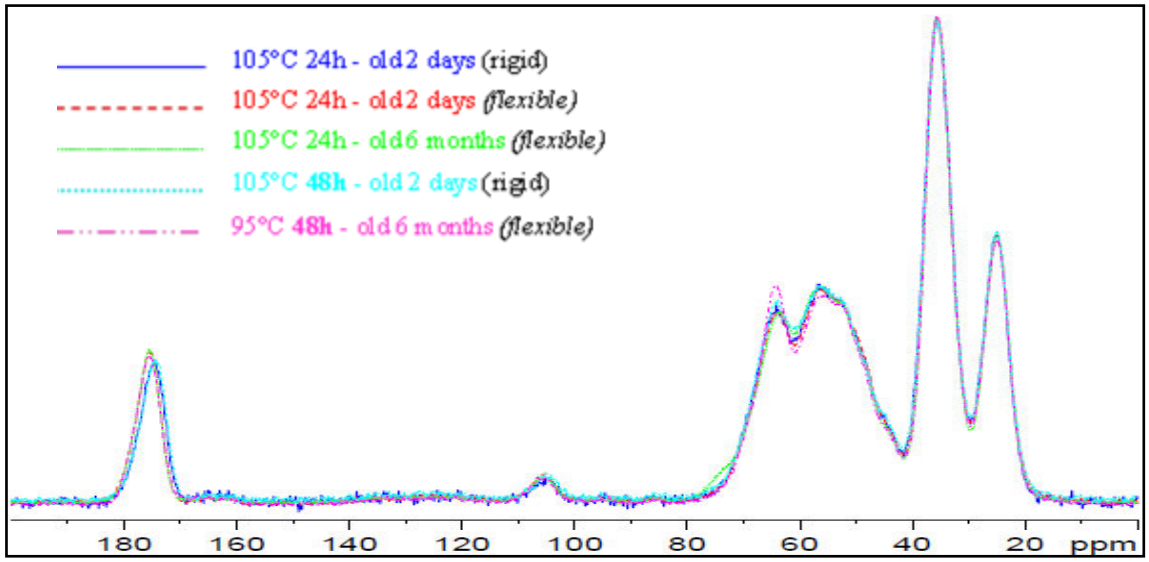

Fig. 3.23: Solid state ^{13}C NMR spectra of aged heated PAE films at 243 K.

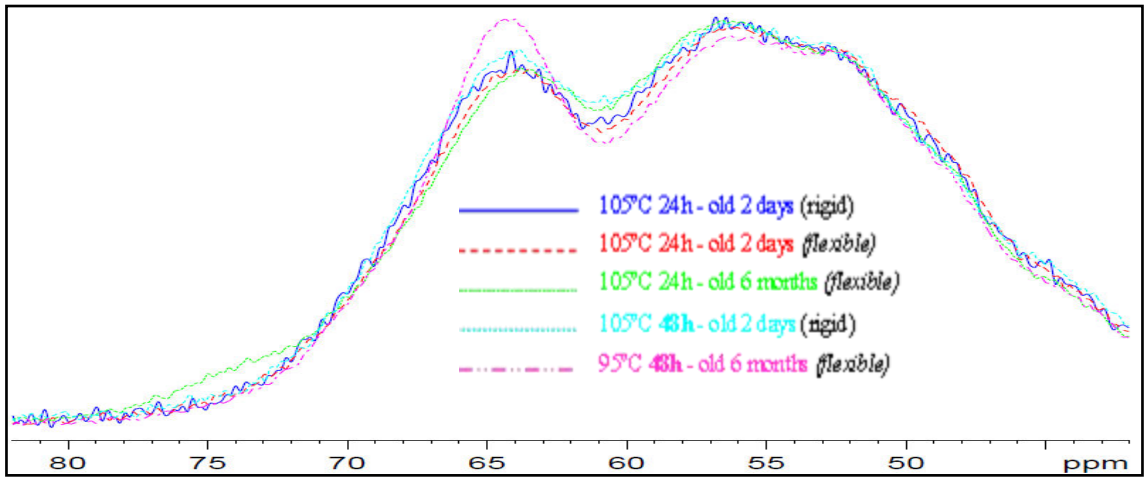

Fig. 3.24: Solid state ^{13}C NMR spectra of aged heated PAE films at 243 K (AZR region: 40 to 80 ppm).

The NMR spectra of the aged heated PAE film (rose) in the Figure 3.24 showed an increase in the peak at 64 ppm, i.e., that is associated with C (h) (see Figure 3.21) signal area, suggesting cross-linking reactions up to 6 months. However, this sample underwent a thermal post-treatment at 95°C for 48 h and in a closed NMR rotor during the experiments. These particular conditions justify the possible presence of remaining AZR in the PAE structure and the incomplete thermally induced cross-linking reaction based on its opening.

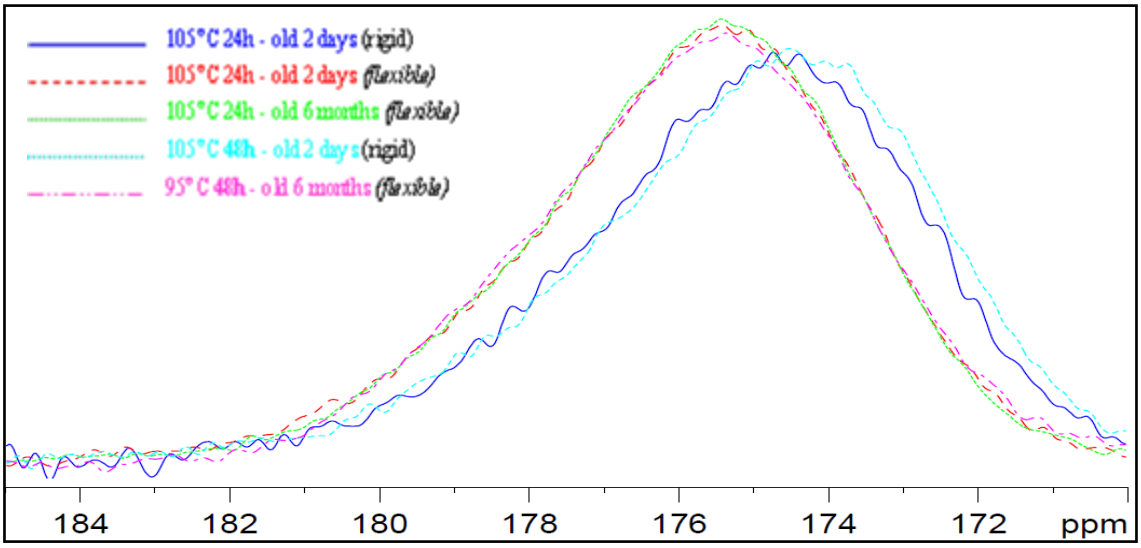

Fig. 3.25: Solid state ^{13}C NMR spectra for aged heated PAE films at 243 K (carbonyl-carboxyl region: 170-182 ppm).

In the Figure 3.25, the signal areas of carbonyl **C**(a) and carboxyl **C**(a') of two samples of heated PAE films aged for two days display a shift of around 1 ppm when compared to the other samples, namely:

(i.) a sample heated at 105°C for 24 h (dark blue); and

(ii.) a sample heated at 105°C for 48 h (light blue).

However, there is no clear modification in the AZR region (40 to 80 ppm) as observed for other samples (see Figure 3.24). These two samples also showed specific behaviour in terms of rigidity. Differently from the other flexible samples that were stored before NMR analyses under controlled conditions (25°C and 50% RH), these two rigid samples were kept in desiccators after the thermal post-treatment (anhydrous conditions), and showed moisture content of c.a. 1%. Nevertheless, under ambient conditions for a period of time of approximately 24 h, they become flexible like the samples conserved under controlled conditions, and moisture content of c.a. 10%. The observed shift in the carbonyl-carboxyl region (170 - 182 ppm) together with the flexibility/rigidity behaviour let us to assume that a secondary thermally induced cross-linking occurs. Figure 3.26 shows the reaction between carboxylic end groups and hydroxyl groups of AZR in the PAE structure yielding the formation of ester bonds (Fischer esterification). Apparently, this additional cross-linking with ester bonds

formation together with the plasticizing effect of water is the responsible of flexibility/rigidity behaviour of the PAE structure. In contact with humidity of ambient atmosphere, the chemical equilibrium is displaced toward the alcohol and the carboxylic acid (hydrolysis of the ester bonds), and it gains flexibility and behaves as the other samples.

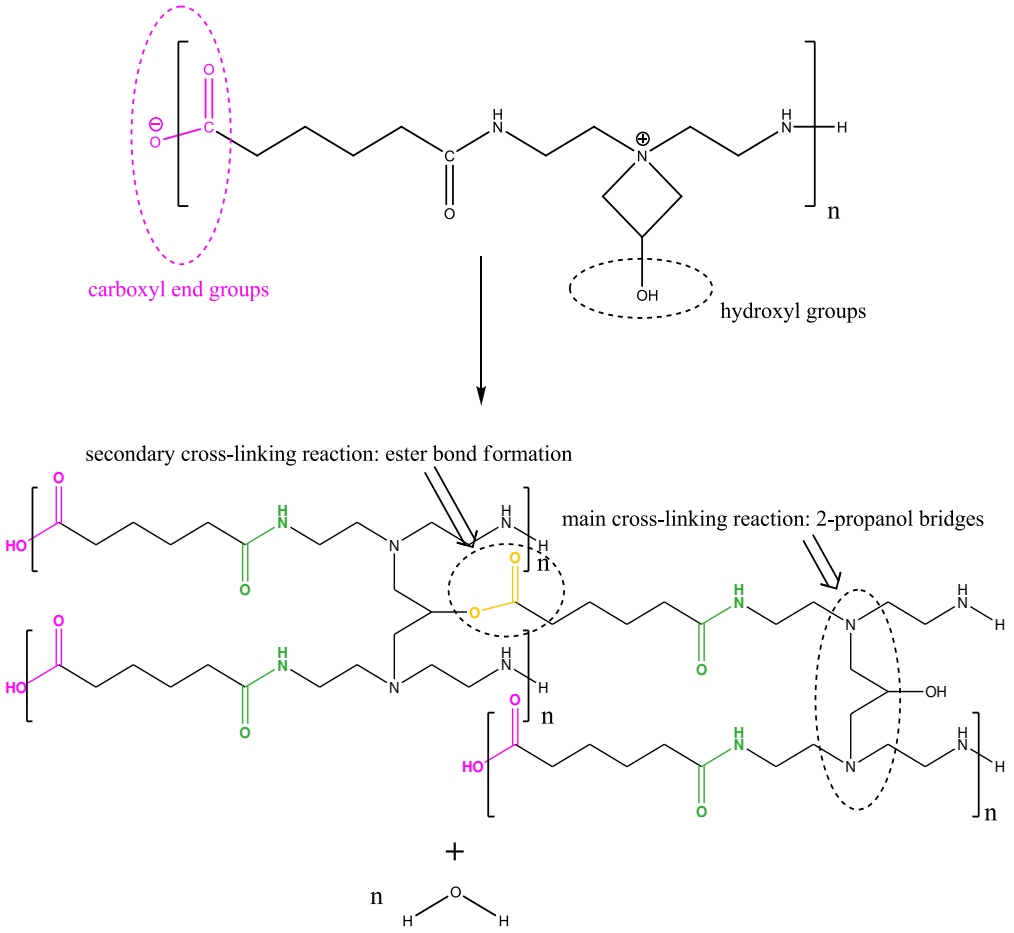

Fig. 3.26: Cross-linking reaction based on ester bond formations (Fischer esterification), between carboxylic end groups and OH groups of AZR in PAE structure.

Fischer esterification occurs when refluxing a carboxylic acid and an alcohol in the presence of an acid catalyst like sulfuric acid. The reaction was first described by Emil Fischer and Arthur Speier in 1895. Most carboxylic acids are suitable for the reaction, but alcohols should generally be a primary or secondary. The reaction is often carried out without solvent particularly when a large reagent excess (e.g. when methanol is used), or in a non-polar solvent (e.g. toluene), to facilitate the Dean-Stark water removal. Typical reaction times vary from 1 to 10 h at temperatures of 60 to 110°C. The

main disadvantage of direct acylation is the unfavourable chemical equilibrium (hydrolysis of the ester bonds reforming the acid and the alcohol), that must be attenuated e.g. by a large excess of one of the reagents, or by the removal of water (Solomons, 2007).

The PAE ester bond formation can also be confirmed from FTIR spectra of unheated and heated PAE films (see Figure 3.27 B). A small increase in the absorption band at around 1738 cm^{-1} was observed, and attributed to CO stretching vibrations of ester groups. This cross-linking mechanism was already extensively discussed by several authors, but not clearly experimentally confirmed (Obokata and Isogai 2007; 2005; 2004a,b; Fisher, 1996; Espy, 1995; Devore and Fischer, 1993; Wägberg and Björklund, 1993; Fredholm *et al.* 1983; Kricheldorf, 1981; Carr *et al.*, 1973; Bates, 1969). An explanation is that these studies were carried out in aqueous medium and/or environmental conditions that are unfavourable to a Fischer esterification due to presence of water and consequently hydrolysis of ester bonds. In the present study we worked on solid state, and by investigating the effects of ageing, thermal post-treatment and storage conditions (controlled and anhydrous), the PAE cross-linking mechanisms were elucidated.

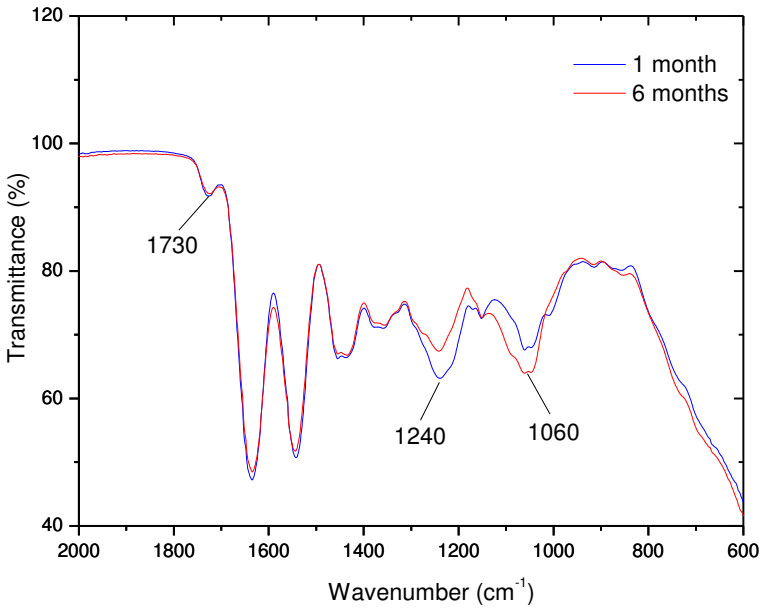

(A)

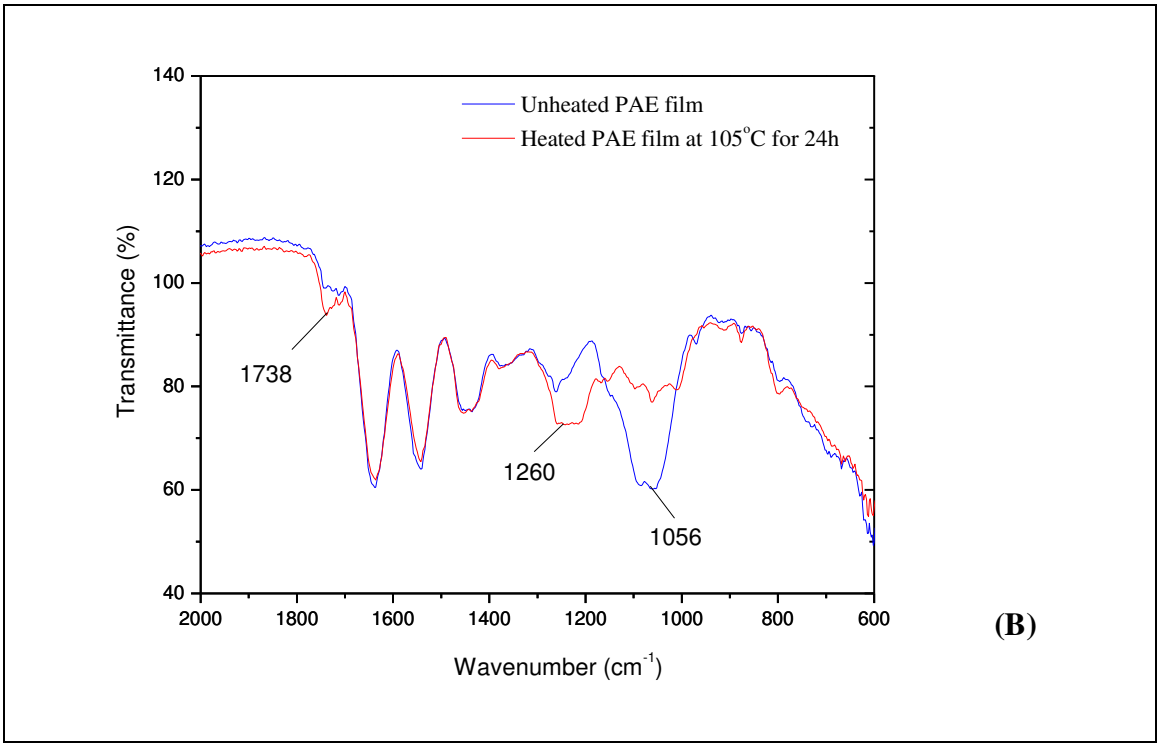

Fig. 3.27: FTIR spectra of aged heated PAE films: **A)** heated PAE films (at 105°C for 24h) aged for 1 and 6 months, and **B)** unheated and heated PAE films aged for 2 days.

Based on these experimental results, some important and unpublished findings concerning PAE cross-linking can be made:

(i.) the main reaction can be described from a nucleophilic attack of the N atoms (in the PAE and/or polyamideamine a common by-product from PAE synthesis), by the AZR group leading to the tertiary amine bond formations and 2-propanol bridges between PAE macromolecules;

(ii.) this cross-linking reaction can be boosted by a thermal post-treatment for 24 h at 105°C (above the Tg of the polyamideamine phase determined from DMA analyses), yielding a completely cross-linked network. However, it is possible to reach the same cross-linked stable network by ageing the unheated PAE films for c.a. 1 to 3 months;

(iii.) a reaction with a secondary contribution between carboxylic end groups in the PAE structure and hydroxyl group of AZR can take place during cross-linking. However, this reaction requires energy input (thermally induced), and occurs under particular conditions (for 24 – 48 h and at 105°C).

3.5. Conclusions

In order to characterize PAE polymers, direct evaporation of the starting PAE aqueous solutions or precipitation in organic solvents were tested. These procedures are not adequate, because they induce a PAE cross-linking reaction leading to the insolubility of PAE resin. Thus, liquid state ^{1}H and ^{13}C NMR was performed adding directly heavy water in aqueous commercial solutions and deuterated hydrochloric acid to adjust the pH. The PAE resin spectra displayed the presence of several impurities. To elucidate the PAE structure, various experiments were carried out as DEPT, COSY, HMQC and HMBC. The combinations of these studies permitted the signals assignment and all the chemical shifts for PAE carbons obtained in this work were consistent with those early reported by Obokata and Isogai (2004b) and Kricheldorf (1981). The presence of small amount of unmodified polyamideamine and pendant like 3-chloro-2-hydroxypropyl group in PAE solutions was also detected. However, from our experiments it was difficult to conclude the presence or not of cross-linked units from PAE synthesis because of the NMR signals overlapping.

The specific charge of PAE resin was determined as a function of pH values and of conductivity of diluted solutions from colloidal titration using PES-Na as a titrant reagent and a particle charge detector to determine the equivalent volume. Specific charge values of 3.0, 2.0 and 1.5 μeq/g were obtained for pH values of 4, 7 and 10, respectively. The charge at pH close to 4 gives the total amount of protonated secondary/tertiary amine groups in the PAE structure and quaternary ammonium groups. In contrast, the cationic charge around pH 10 reflects only the amount of quaternary ammonium groups.

After initial studies based on solubility tests, PAE films were casted under controlled conditions. After a week, the films still contain c.a. 13% of water. Cross-section micrographs show the formation of films without internal porosity. Some closed pores are observed on the surface only, probably resulting from water elimination.

FTIR analyses show that the main differences induced by thermal treatment of PAE films are related to the absorption bands at around 1060 and 1260 cm^{-1}. The band at 1060 cm^{-1} was attributed to the breathing of AZR and to OH stretching vibrations of

secondary alcohols. The band at around 1260 cm^{-1} was attributed to C-N stretching vibration of tertiary amine and CO stretching vibrations of secondary alcohols. The decrease in intensity of the band at 1060 cm^{-1} is related to the opening of AZR with the thermal post-treatment and to the cross-linking of PAE macromolecules. Thus, according to our results, the main PAE cross-linking reaction occurs by a nucleophilic attack of N atoms in the PAE and/or polyamideamine structures, which gives rise to the: **(i.)** decrease of AZR percentage in the PAE structure; **(ii.)** formation of 2-propanol bridges between PAE-PAE or PAE-unmodified polyamideamine macromolecules; and **(iii)** increase of percentage of tertiary amine bonds.

A little increase of the intensity of the absorption band at around 1738 cm^{-1} in FTIR spectra of heated PAE films was also observed, which is attributed to C=O stretching vibration of ester groups. Then, it was necessary to consider the secondary contribution of ester linkages to the PAE cross-linking. ^{13}C NMR and FTIR experiments as a function of the ageing of PAE films showed that ester bonds formation is a reversible reaction. In contact with water, as for example the humidity of ambient atmosphere, the chemical equilibrium is displaced toward the alcohol and the carboxylic acid (hydrolysis of the ester bonds). Apparently, the ester bonds formation is also responsible for flexibility/rigidity behaviour observed for some PAE film samples together the plasticizing effect of water: the films that presented rigidity after thermal post-treatment and storage under anhydrous conditions recover flexibility when stored under ambient or atmosphere conditions and there is no more experimental evidences of ester bonds. This cross-linking mechanism was already extensively discussed by several authors, but not clearly experimentally confirmed and definitely accepted (Obokata *et al.* 2007; 2005; 2004a,b; 2003; Fischer, 1996; Espy, 1995; Devore and Fischer, 1993; Wägberg and Björklund, 1993; Fredholm *et al.* 1983; Kricheldorf, 1981; Carr *et al.*, 1973; Bates, 1969). An explanation is that these studies were carried out in aqueous medium and/or ambient conditions that are unfavourable to a Fischer esterification reaction due to presence of water. In this study, we worked in conditions which allowed elucidating the PAE cross-linking mechanism. Even if we consider ester bond formation as secondary contribution to the PAE-cross-linking, it is also necessary to keep in mind the low amount of carboxylic end groups in PAE structure able to form these bonds. This fact and an unfavourable chemical equilibrium already discussed are probably the

main responsibles for experimental difficulties in determining ester bonds formation during PAE-cross-linking.

Unheated PAE films show two relaxations on tan δ curve, as determined by DMA analyses, which were close to Tg for polyamide and polyepichlorohydrin in pure forms. This phenomenon results from the presence in the film of unmodified polyamideamine, as a byproduct from PAE synthesis, as confirmed from liquid NMR analyses and FTIR spectra. Thus, we can conclude that the first relaxation at c.a. -10°C is attributed to a polyamideamine phase modified by epichlorohydrin (PAE phase), whereas the second one at c.a. 80°C is a proper relaxation of the polyamideamine phase. An evolution of the thermally induced PAE cross-linking as a function of time is observed. The thermally post-cured film (105°C for 24 h), showed only a well defined Tg at 80°C. Thus, we can conclude that during the thermal treatment, the PAE phase related to the first relaxation undergoes chemical reactions, due to the opening of the AZR, thus resulting in PAE cross-linking. However, after 24 h treatment, there is only one value of Tg suggesting that the PAE cross-linking reached its ultimate state.

As observed in the NMR experiments and the FTIR spectra, even after one month of ageing there are still remaining AZR groups in the unheated PAE structure and this phase influences the thermodynamic relaxations of the PAE during DMA experiments. Solid state ^{13}C NMR, FTIR and DMA experiments revealed that the cross-linking of the unheated PAE film reaches its final state between 1 to 3 months of ageing. On the other hand, no experimental evidences were found of AZR presence in heated PAE films when analyzed by the same techniques. Thus, we can conclude that the cross-linking reactions are boosted by a thermal treatment and that the reaction is complete after 24 h at 105°C (above the Tg of the polyamideamine phase determined from DMA experiments).

CHAPTER IV: CHARACTERIZATION OF CARBOXYMETHYLCELLULOSE (CMC) SALTS

As discussed before, CMC is used in the papermaking industry as dry strength additive or more frequently in conjunction with PAE for enhancing the wet strength of papers. In this case, CMC is added in the pulp suspension before PAE resin. It is recognized that there is a synergistic effect between CMC and PAE on regard to the wet strengthening properties of the resin. This effect was attributed mainly to the increased amount of PAE adsorbed due to the weaker charge of the PAE/CMC complexes when compared to PAE charge (Laine *et al.*, 2002).

There are different grades of CMC. Highly purified products, i.e., with low salt content are used mainly in the food and pharmaceutical areas, whereas large amounts are produced in crude commercial grades without any refining for use in detergents, oil drilling, and paper industry (Heinze and Koschella, 2005).

The chemical bond formation between the cellulose fibres and the PAE resin has been extensively studied but a clear cut-mechanism is still not proposed (Obokata *et al.*, 2007; 2005; 2004a,b; Devore and Fischer, 1993; Kricheldorf, 1981; Carr *et al.*; 1973; Bates, 1969). Thus, in order to study the mechanism related to the development of wet strength properties of PAE-based papers, CMC was used as a model compound of cellulosic fibres. This subject will be discussed in the Chapter V.

Chapter IV describes characterizations of NaCMC considering both a crude product used in the papermaking industry to prepare PAE-based wet strengthened papers (Niklacell P70 UC from Mare), and for comparison, an analytical grade homologue, supplied by Biochemica (Fluka). Studies of NaCMC in solid state and liquid solutions will be performed in order to determine the main properties of these chemicals.

4.1. Preparation of CMC solutions

Figure 4.1 presents micrographs of 1% Fluka and Niklacell CMC solutions, as obtained by optical microscopy. The micrographs show the presence of residual fibres with a symetrical pattern of modification. To the best of our knowledge, these structures have never been described before.

Elementary fibrils of cellulose consist of crystallites and intercalated less ordered (amorphous) domains. Cellulose fibres differ in terms of their crystalline content, size and orientation, as well as in the amorphous domains, the size and shape of the voids, and the number of inter-fibrillar lateral tie molecules (Stana-Kleinschek *et al*., 2001). It can be postulated that all these properties have an influence on accessibility of the chemical reagents. Thus, during NaCMC preparation, monochloroacetic acid penetrates more easily the amorphous domains, thus yielding the formation of modified and unmodified phases within the cell wall of cellulosic fibres. Consequently, more and less swollen regions alternate along the main axis of the carboxymethylated fibres. As observed on the micrographs, when NaCMC is stirred in water (1% w/w), modified domains of the fibre structure swell in a great extent. The unmodified and/or slightly modified domains do not swell as much, which gives rise to the formation of small rings along the remaining fibres. CMC solutions at 0.01, 0.5 and 2% w/w concentration also showed the same structures even after heating (at 80^{o}C for 24 h). This is a typical characteristic of NaCMC commercial grades at least in the DS range used, which varied from 0.5 to 0.65 and 0.65 to 0.95 for Niklacell and Fluka NaCMC, respectively.

Heinze and Koschella (2005) postulated that the variation in hemicelluloses concentration in fibres may influences the quality of the NaCMC prepared. Thus, insoluble residues may appear, and their amount seems to be influenced mainly by the reactive fraction of cellulose in the pulp.

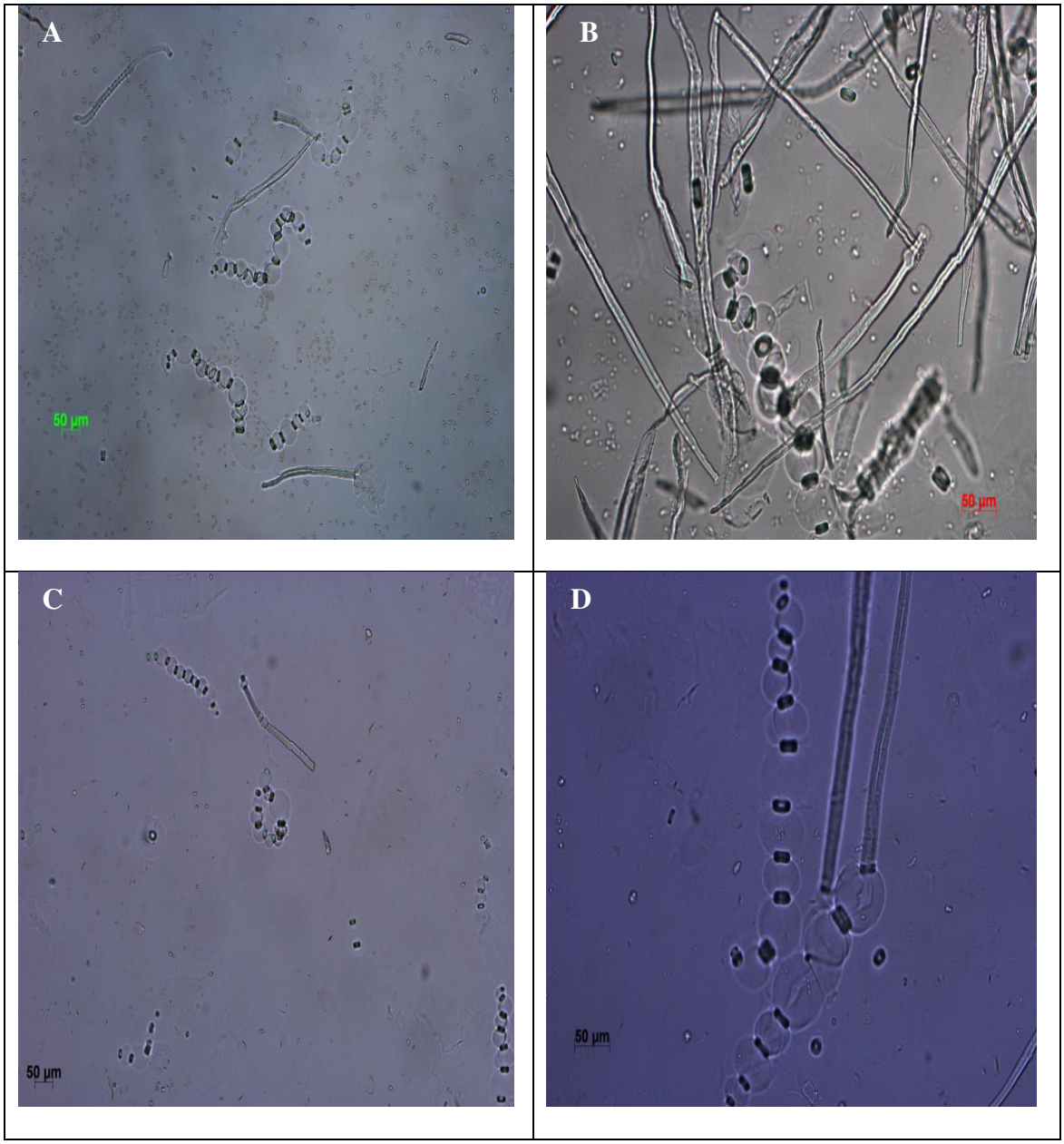

Fig. 4.1: Optical microscopy micrographs of 1% CMC solutions: **(A)** and **(B)** Niklacell and **(C)** and **(D)** Fluka chemicals.

4.2. Preparation and characterization of Fluka and Niklacell CMC films

Figure 4.2 shows the drying kinetics under controlled conditions (25°C and 50% RH) of Fluka (CMC-fF) and Niklacell films (CMC-fN). A sigmoidal curve was obtained when the % water loss was plotted *versus* log of the time (in hours). The Fluka

film shows a slower kinetics of water loss due to its highest DS value. After one week, CMC films prepared from the two grades still showed a small residual amount of water (around 3%) resulting from the presence of polar groups in the CMC structure able to form hydrogen bonds with water molecules.

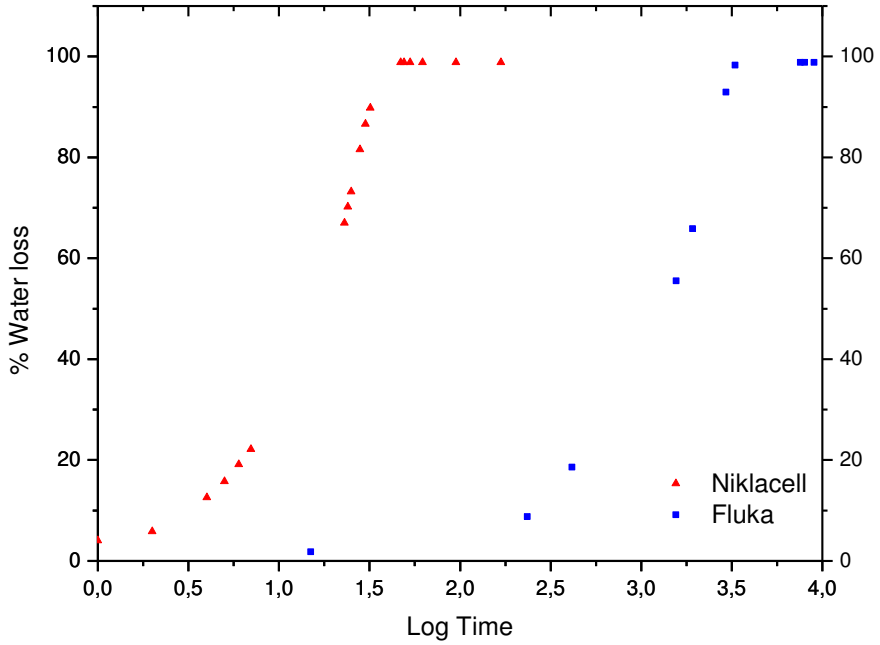

Fig. 4.2: Drying kinetics of CMC films prepared in Teflon moulds for one week under controlled conditions (25°C and 50% RH).

Films prepared from Fluka are flexible and transparent, and easily removed from the Teflon mould without breaking, whereas films prepared from Niklacell are more brittle (although without cracks), visually heterogeneous and show formation of two domains: **(i.)** opaque; and **(ii.)** semi-transparent regions.

In order to explain the observed differences of the CMC, the CMC powders and the films prepared thereof were analyzed:

(i.) NaCMC Fluka on powder state (**CMC-F**);

(ii.) CMC Fluka film (**fF**);

(iii.) NaCMC Niklacell on powder state (**CMC-N**);

(iv.) opaque region of CMC Niklacell film (**CMC-fNo**);

(v.) semi-transparent region of CMC Niklacell film (**CMC-fNt**); and

(vi.) film of purified CMC Niklacell (**CMC-fNp**).

Figure 4.3 shows micrographs obtained by SEM of the surface (A and B) and cross-section (C and D) of opaque Niklacell CMC film (CMC-fNo). Salts are present on the film surface whereas the cross-section displayed phase segregation. The semi-transparent Niklacell CMC film (CMC-fNt) shows the same features.

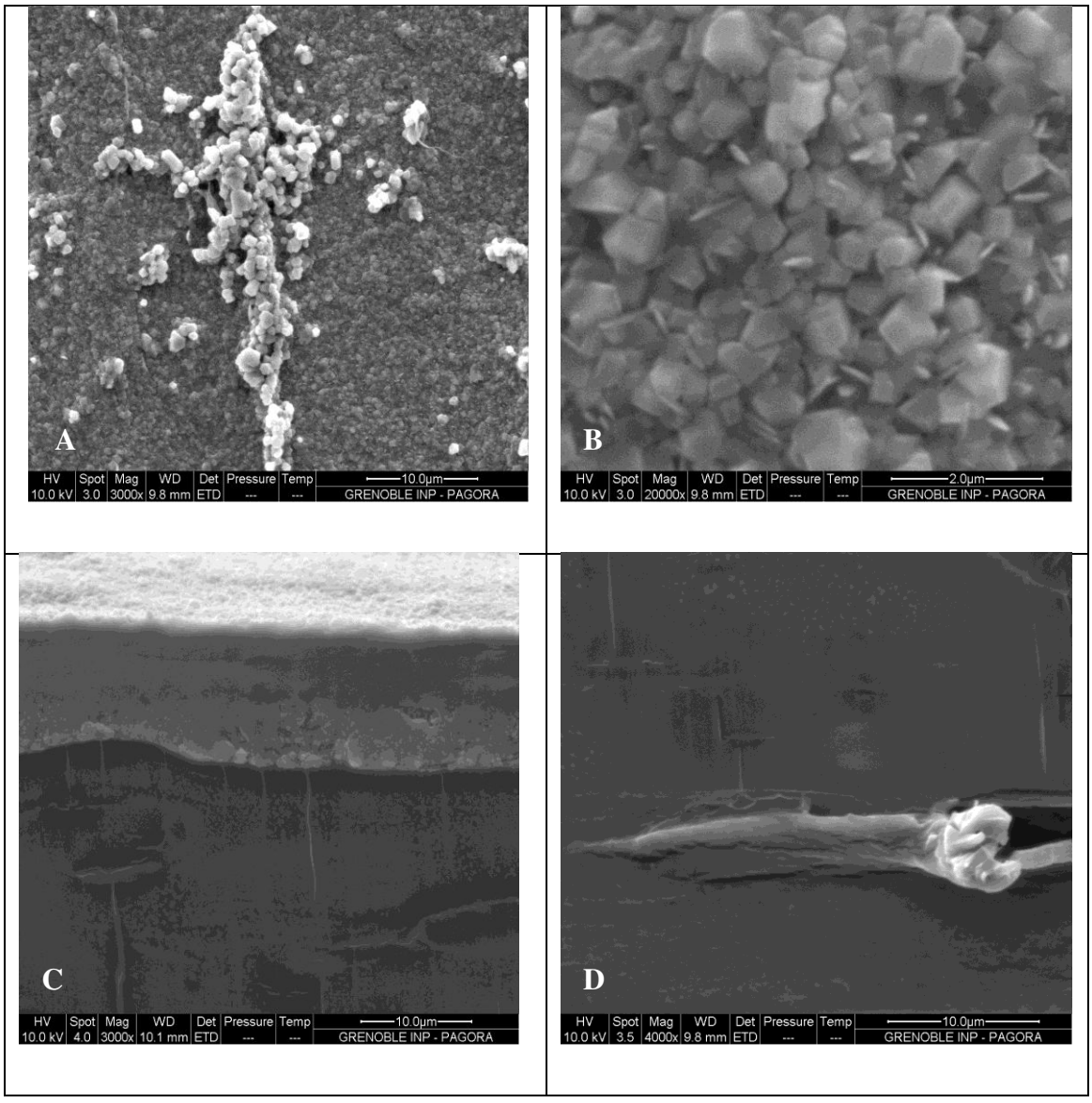

Fig. 4.3: Micrographs obtained by SEM of CMC-fNo: **(A)** and **(B)** surface and **(C)** and **(D)** cross-section.

The observed upper side of the film on the cross-section micrograph (Figure 4.3 C) was in contact with the Teflon mould during film preparation. With water elimination of the CMC solution, salts precipitated and deposited on the mould surface. The bottom side was in contact with the atmosphere. X-ray microanalysis shows that the upper side is rich in Na and Cl, whereas the bottom one contains mostly C, O, Na and Cl atoms. Thus, we can affirm presence of NaCl from Niklacell CMC preparation. During film preparation by evaporation (casting), there is a segregation of at least two phases: a rich NaCl layer and a mixture CMC / NaCl layer.

Figure 4.4 shows micrographs obtained by SEM of the surface of mould and atmosphere contacts (B and A micrographs, respectively), and cross-section (micrographs C and D) of the purified Niklacell CMC (CMC-fNp) film. As observed, the surface which was in contact with the mould (micrograph B) presents an entanglement of fibres when compared to the other side (micrograph A). Cross-section micrographs also show the presence of fibres, but not clearly the formation of salt layers or phase segregation when compared to the Niklacell films (see Figure 4.3) prepared without purification (CMC-fNo and CMC-fNt).

X-ray microanalysis confirms the presence of C, O and Na atoms as the major components on both sides. However, the presence of Cl was still observed, although in small amount, when compared to the unpurified Niklacell films. Thus, we can conclude that the purification process used decreases the salt content and probably the polydispersivity of the Niklacell CMC when compared to the crude form.

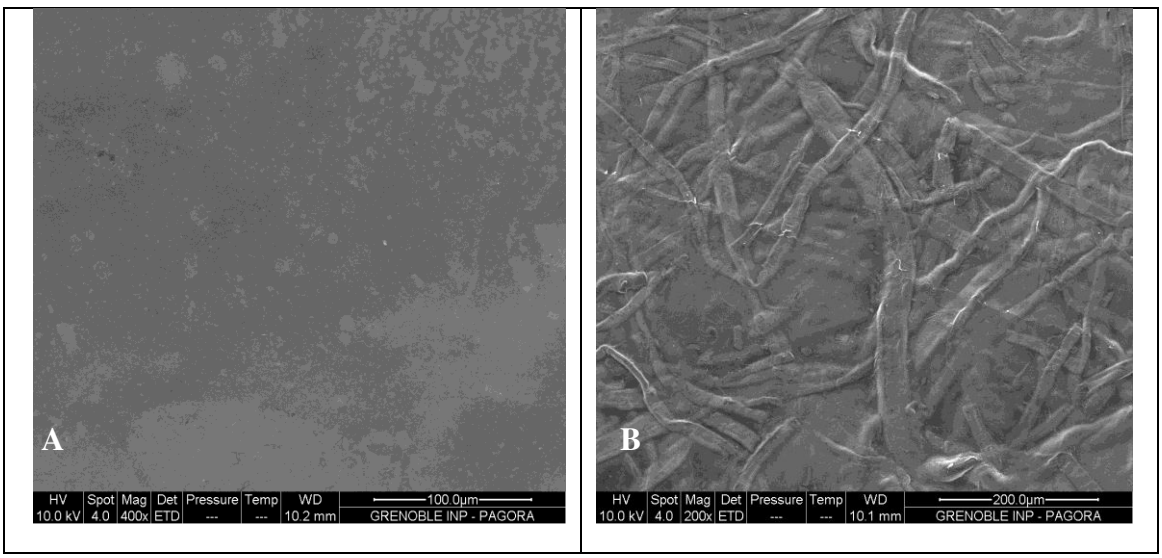

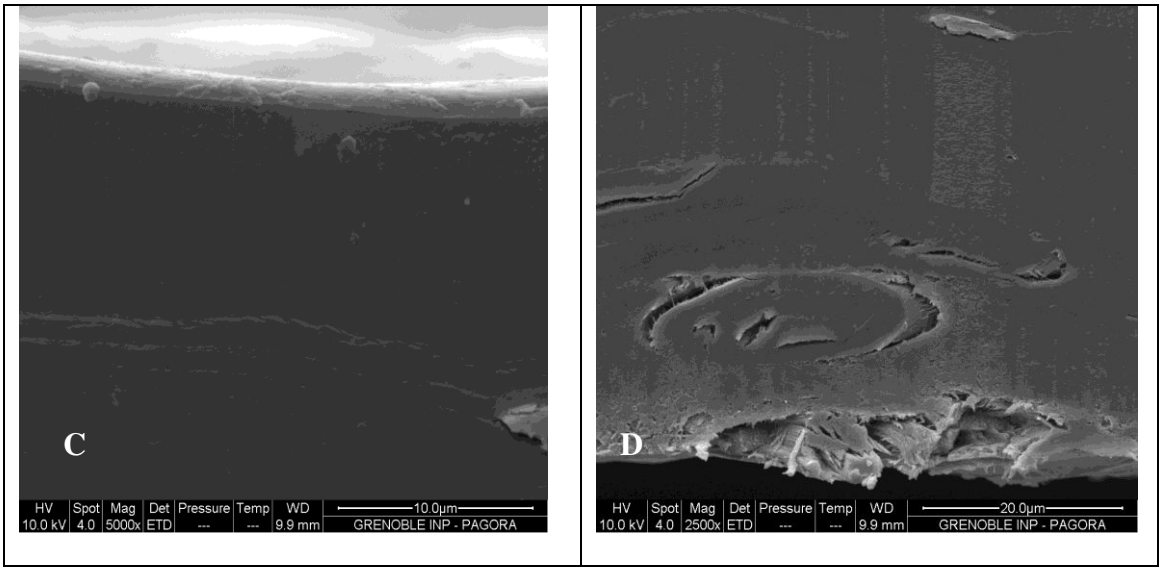

Fig. 4.4: Micrographs obtained by SEM of the surface (A) atmosphere and (B) mould contacts, and (C) and (D) cross-section of the purified Niklacell CMC film.

Figure 4.5 A and B presents the surface and the cross-section micrographs, respectively, obtained from SEM of Fluka CMC film (CMC-fF). As expected, the formation of a homogeneous film without the presence of salt layers and segregation of phases is observed from the micrographs. X-ray microanalysis shows that C, O and Na are the major elements forming CMC structure and confirms the purity degree of this chemical.

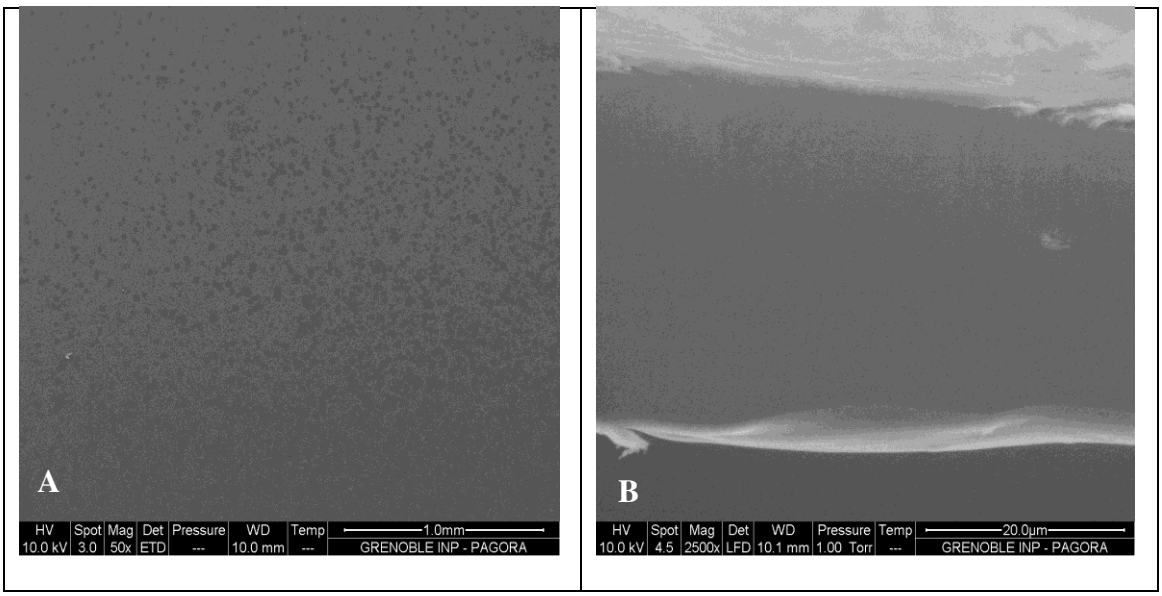

Fig. 4.5: Micrographs obtained by SEM of Fluka CMC film: **(A)** surface and **(B)** cross-section.

Powder and films CMC samples were studied by NMR. Table IV.1 shows quantitative integrals data from ^{13}C NMR spectra at 298 K (quantitative measurements determined from cross-polarization curves) of the CMC samples. Three other commercial purified CMC with known DS values were added for comparisons (CMC 0.7, 0.9 and 1.2).

Tab. IV.1: Quantitative data from solid state ^{13}C NMR at 298 K of CMC samples (C_{6u} represents unsubstituted C_6 of AGU and C_{6s} substituted C_6 of AGU).

region (in ppm)	190 - 170	110 - 95	95 - 67	67 - 50
assignment	**C=O**	**C_1**	**C_4, C_2, C_3, C_5, C_7,C_{6s}**	**C_{6u}**
FLUKA				
CMC-F	0.88	1.00	5.15	0.89
CMC-fF	0.95	1.00	5.21	0.90
NIKLACELL				
CMC-N	0.87	1.00	4.64	1.23
CMC-fNo	1.10	1.00	4.66	1.20
CMC-fNp	0.86	1.00	4.59	1.04
CMC-fNt	0.53	1.00	4.58	0.93
COMMERCIAL				
CMC-0.7	0.83	1.00	5.05	0.88
CMC-0.9	0.90	1.00	5.20	0.86
CMC-1.2	1.26	1.00	5.73	0.82

In this table the intensities of the carbon peaks associated to anhydroglucose moiety are given according to the labeling of this unitary group, as sketched in the Figure 4.6:

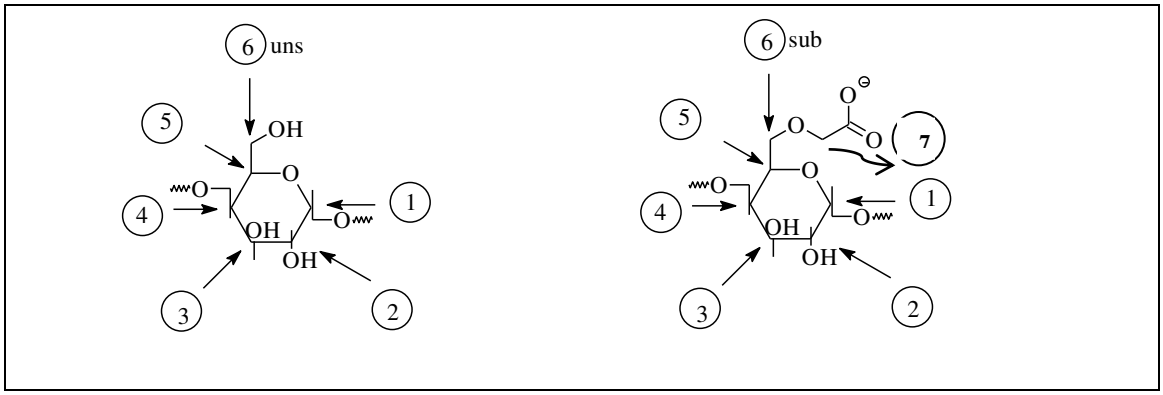

Fig. 4.6: Labeling of the anhydroglucose moiety.

From the ^{13}C CP/MAS NMR spectra, the DS value can be calculated from the ratio of carboxyl (C=O) to C_1 signal area. CMC-F and CMC-fF exhibit close DS values of 0.88 and 0.95, respectively, which are in the range of the supplier data (0.6 to 0.95) and close to commercial purified **CMC-0.9**.

DS values of CMC Niklacell samples (CMC-N, CMC-fNo, CMC-fNp, CMC-fNt) vary in a greater extent. The DS of the CMC-fNt sample (0.53) is close to that of the supplier data range (0.5 to 0.65). An explanation of the variations of the DS values is the presence of impurities and/or by-products like NaCl which affect all the resonances intensities by spurious effects such as concentration and ionic strength (Capitani *et al.*, 2000).

Although NaCl presence is well known, some liquid state ^{23}Na NMR measurements were performed on CMC aqueous solutions samples. ^{23}Na has a nuclear spin of 3/2, and its relaxation is mostly controlled by the interaction between the nuclear quadrupole moment and local electric field gradients. The line width of the peak was conventionally used as a measurement of the mobility and/or of the symmetry of the electric field gradient around the sodium ion. The line width at half height ($\Delta\nu_{1/2}$) is related to the transversal relaxation time T_2 through an apparent relaxation time T_2^* from the equation:

$$\mathbf{1/T_2 = 1/T_2^* + C \quad and \quad \Delta\nu_{1/2} = 1/(\pi \times T_2^*)}$$

where C is a constant.

Bansal *et al.* (2000) investigated ^{23}Na relaxation data (T_1, T_2^* or $\Delta\nu_{1/2}$) as a function of the sodium concentration and fitted their experimental curves with monoexponential functions. In the same way, Minato and Satoh (2004) studied the evolution of ^{23}Na line width at half height as a function of CH_3COONa concentration as calibration curves. So we have applied an exponential fit to our results (see Figure 4.7), which show similar profile to the Minato's calibration curves.

The width at half height ($\nu_{1/2}$) and the longitudinal relaxation time (T_1) were measured. These two parameters depend on the sodium bond type: **(i.)** NaCl or **(ii.)** COO^-Na^+. Some measurements were also carried out after hydrochloric acid addition in order to release Na in salt form. These results are presented in Table IV.2.

Tab. IV.2: Na parameters obtained by liquid state ^{23}Na NMR for CMC aqueous solutions samples.

Compound	$\nu_{1/2}$ Na (Hz)	T_1 Na (ms)
NaCl	10.0	46.9
FLUKA		
CMC-F	50.2	9.5
CMC-F-HCl	10.5	45.1
CMC-fF	49.2	9.6
CMC-fF-HCl	10.4	45.1
NIKLACELL		
CMC-N	**34.4**	**14.1**
CMC-fNo	**23.0**	**21.2**
CMC-fNo-HCl	19.0	45.2

With Fluka samples (CMC-F and CMC-fF), practically all the Na is present in sodium carboxylate bonds. After HCl addition, Na is present in salt form as indicated by the NMR studies of CMC-F-HCl and CMC-fF-HCl samples which are similar to those of standard NaCl.

With Niklacell samples, Na is present either in sodium carboxylate or in NaCl salt forms. From Figure 4.7, it appears that the initial **CMC-N** powder contains 25% of Na as NaCl and 75% as COO^-Na^+ forms. During the film formation, there is a phase segregation and the salt concentration in the opaque region of CMC Niklacell film sample (**CMC-fNo)** shows Na values of 50% as NaCl and 50% as COO^-Na^+ forms.

These results confirm the initial statements of the NaCl presence as a by-product from synthesis in the Niklacell samples. Other experimental evidences about NaCl in the Niklacell samples were observed from conductivity values of the CMC solutions. 1% NaCMC Fluka and Niklacell solutions show conductivity values of 187 and 4810 µS/cm, respectively.

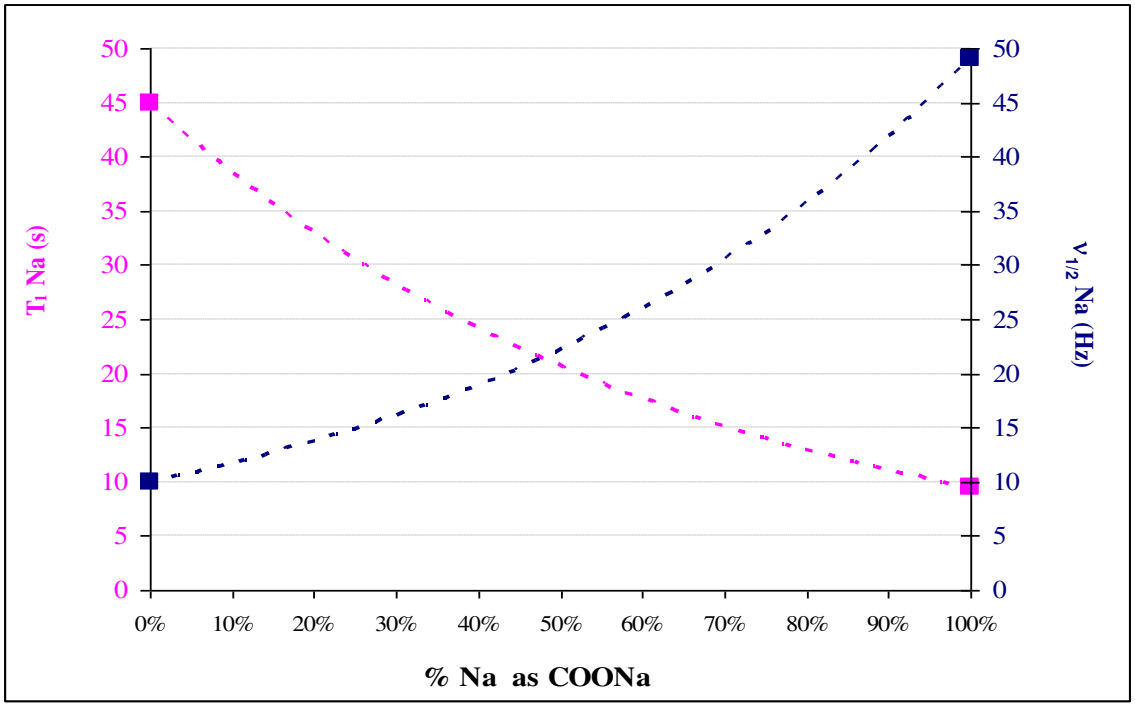

Fig. 4.7: Curves of relaxation time (T) and width at half-height ($\nu_{1/2}$) *versus* Na % as COO^-Na^+ obtained from liquid state ^{23}Na NMR.

Heterogeneous reaction of cellulose (Williamson ether synthesis) yields CMC with a statistic distribution of substituted units. Detailed investigations on the distribution of the carboxymethyl groups by means of ^1H NMR spectroscopy reveal a

reactivity in the order O-2 > O-6 >> O-3 (Heinze and Pfeiffer, 1999; Heinze and Koschella, 2005).

The resolution in liquid state ^{13}C NMR spectra of the samples is significantly increased, which enables spectra recorded in this way to be evaluated for determining the total and the partial DS at C_2, C_3 and C_6 positions (Heinze and Koschella, 2005). As proposed by Capitani *et al.* (2000) from ^{13}C NMR studies of CMC solutions in D_2O at 363 K, the chemical shift of C_6 (labeled C_{6u}) at 64 ppm is displaced toward C_4, C_2, C_3, C_5, C_7 region at 72.8 ppm after carboxymethylation (labeled C_{6s}), as shown in Table IV.3 and in Figure 4.8. From these data, we can also notice that the C_1 and the C=O resonances of substituted AGU in position 6 were shifted toward low frequencies compared to those of substituted AGU in position 2 and 3.

Tab. IV.3: Chemical shifts (ppm) of liquid state ^{13}C NMR (D_2O at 363K) of cellulose and CMC prepared thereof (from Capitani *et al.*, 2000).

	C1			**C4**		**C2**	**C5**		**C3**			**C6**	**cellulose**
	105,3			82,3		78,7	78,0		76,8			64,0	
C=O	**C1**	**C*2**	**C3**	**C4**			**C5**			**C7**		**C6**	**CMC-C2**
174,1	105,6	87,3	85,9	82,3			78,0			74,8		64,0	
C=O	**C1**		**C*3**		**C4**		**C5**	**C2**		**C7**		**C6**	**CMC-C3**
174,4	105,8		85,9		81,5		77,5	77,0		75,1		64,0	
C=O	**C1**			**C4**		**C5**	**C2**		**C3**		**C7**	**C*6**	**CMC-C6**
172,5	105,3			82,3		80,0	78,7		76,8		74,3	72,8	

The lack of resolution of solid state compared to that obtained with liquid state NMR restricts any precise measurement of the partial DS at C_2, C_3 and C_6 positions. However, data of Table IV.1 and spectra of Figure 4.8, allow extracting some information. In the absolute way, there are less C_6 substituted units in Niklacell CMC than in Fluka ones. The C_{6u} area is higher for CMC-N samples, but substituted units are less numerous. Based on NMR studies, other statements can be also made:

(i.) Fluka CMC is very similar to commercial CMC-0.9;

(ii.) DS value of CMC-F is 0.9, with 11% substitution at C_6 position and 89% at C_2-C_3 position; and

(iii.) Niklacell CMC is less substituted, and contains considerable amounts of Na as NaCl. DS value of CMC-fNt is 0.55, with 9% substitution at C_6 position and 91% at C_2-C_3 position if we consider that results obtained from CMC-fNt are the most representative of CMC-N.

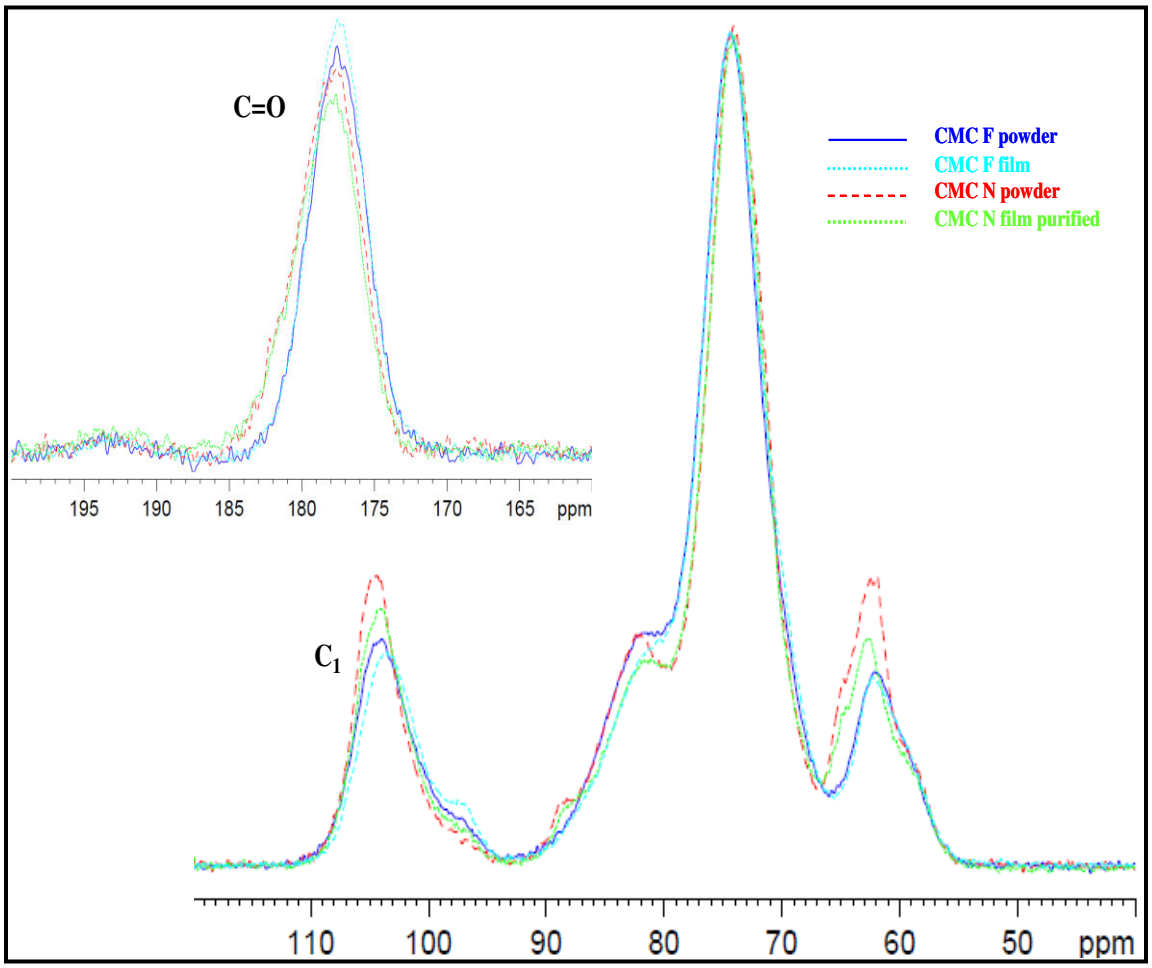

Fig. 4.8: Solid state ^{13}C NMR spectra at 298 K of CMC samples.

Thus, the main differences between Niklacell and Fluka CMC are not in the partial DS values (solid state NMR does not allow differentiation between substitution at C_3 and C_2 positions), but in the total DS values and on the remarkable presence of NaCl.

Figure 4.9 presents FTIR spectra of Niklacell and Fluka CMC films (CMC-fN and CMC-fF, respectively), obtained using ATR mode and the assignments of the main absorption bands are reported in Table IV.4.

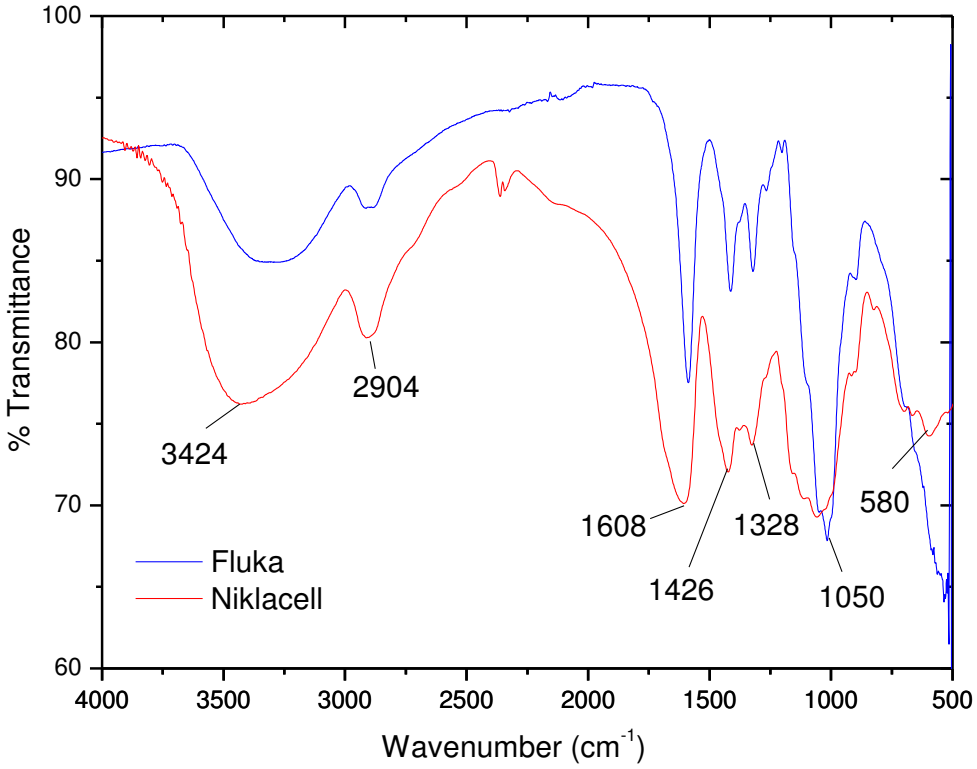

Fig. 4.9: ATR-FTIR spectra of CMC films prepared for one week under controlled conditions (25°C and 50% RH).

Bands associated to Niklacell sample are larger than those of Fluka probably due to the presence of salts. Characteristic signals of ester groups in the region of 1600 cm^{-1} (C-O) and 1100-1000 cm^{-1} (O-R) are lower, showing new evidences of the lowest DS of Niklacell samples as already observed in the NMR measurements.

Table IV.4: Main CMC absorption bands obtained by FTIR analysis in ATR mode.

Bands (cm^{-1})	**Assignments**
580	Ring stretching and ring deformation of α – D – (1-4) and α – D – (1-6) linkages
1050	$-CH_2$ twisting vibrations, primary alcoholic $-CH_2OH$ stretching and $CH-O-CH_2$ stretching (Pushpamalar *et al.*, 2006)
1328	-OH bending vibration (Tong *et al.* 2008; Pushpamalar *et al.*, 2006); symmetrical deformations of $–CH_2$ (Wang *et al.*, 2005)
1426	symmetric vibrations for COO^- group (Tong *et al.* 2008; Wang *et al.*, 2005) and $–CH_2$ scissoring (Pushpamalar *et al.*, 2006)
1606	Anti-symmetric vibrations for COO^- groups (Tong *et al.* 2008; Pushpamalar *et al.*, 2006); ring stretching of glucose (Wang et al., 2005) and of non hydrated C=O groups
2904	C-H stretching of the –CH2 groups (Tong *et al.* 2008; Pushpamalar *et al.*, 2006)
3424	O-H stretching and intermolecular/intramolecular hydrogen bonds (Tong *et al.* 2008; Pushpamalar *et al.*, 2006; Wang *et al.*, 2005)

Fluka and Niklacell samples were studied from DSC analyses and the Figure 4.10 shows an example of DSC tracings corresponding to CMC Fluka powder (CMC-F). As described in Materials and Methods, two consecutive temperature scans were carried out on the same sample. The first scan was performed from -100 to 120°C. An isothermal step of 5 min at 120°C was carried out before cooling and starting a second scan within the temperature range of -100 to 400°C.

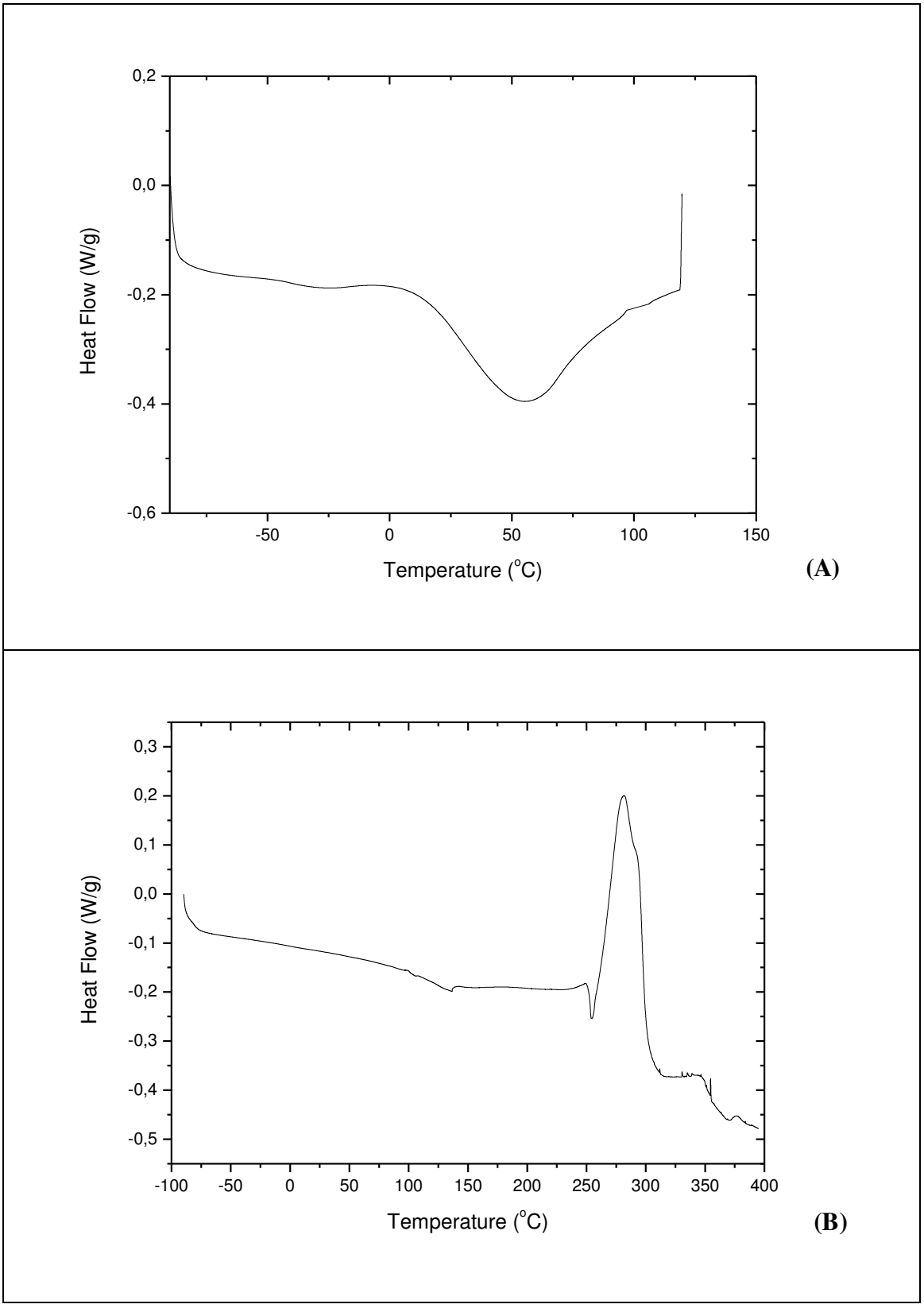

Fig. 4.10: DSC analysis of Fluka CMC powder (CMC-F) during: **(A)** first and **(B)** second scans.

Table IV.5 presents the temperature ranges of the thermal transitions of CMC-fNo and CMC-fNt and shows that the main transitions are:

(i.) an endothermic transition during the first scan between 30 and 120°C attributed to water evaporation;

(ii.) an endothermic transition during the second scan between 90 and 220°C related to residual water not eliminated during the first scan;

(iii.) an endothermic transition during the second scan close to 250°C attributed to the melting temperature (Tm) of crystalline regions of the CMC structure; and

(iv.) an exothermic transition between 250 and 320°C attributed to the combustion of the CMC structure.

Tab. IV.5: DSC analysis of Niklacell CMC films (opaque and semi transparent regions).

		Endothermic (°C)	***Exothermic (°C)***
Opaque	***First scan***	**35-120**	**-**
	Second scan	**95-210** **250**	**255-320**
Semi transparent	***First scan***	**30-120**	**-**
	Second scan	**100-215** **250**	**215-305**

Table IV.6 presents the temperature range of the thermal transitions of CMC Fluka (CMC-F) and purified CMC Niklacell films (CMC-fNp). Probably, due to the elimination of hygroscopic salts (NaCl), during purification, water elimination in the CMC-fNp occurs only during the first scan when compared to CMC-fNo and CMC-fNt. However, as expected, CMC-fNp presents thermal transition temperatures close to those of CMC-F.

Tab IV.6: DSC analysis of purified Niklacell CMC films and Fluka CMC.

		Endothermic (^oC)	***Exothermic (^oC)***
Purified	***First scan***	**25-120**	**-**
	Second scan	**-** **265**	**270-310**
Fluka	***First scan***	**30-120**	**-**
	Second scan	**-** **255**	**260-300**

Fluka and Niklacell CMC films were studied from DMA analyses and these two purified products present similar relaxations. Figure 4.11 shows E' and Tan δ curves of the Fluka CMC films (CMC-fF) and of the purified Niklacell CMC films (CMC-fNp). CMC-fF presents two relaxations:

- at 30°C attributed to Tg and at 260°C attributed to Tm.

CMC-fNp presents three relaxations:

- at 35°C attributed to Tg; at 240°C attributed to Tm; and

- between 90 and 120°C attributed to the effects of water elimination on the thermomechanical properties of the film.

A relaxation related to the influence of water elimination in CMC-fF was not observed probably because of the high purity of this chemical (very small amount of salts from CMC preparation). The E' of CMC-fNp was found to increase during the second relaxation (between 90 and 120°C). Probably, due to water elimination there is a long-range cooperative segmental mobility in the amorphous phase of neighboring regions. Effects like additional organization of the polymer chains with or not crystallization and increase of the density due to water elimination can be induced and these parameters acting or not together can restrict molecular motion in the film causing an increase on the E'.

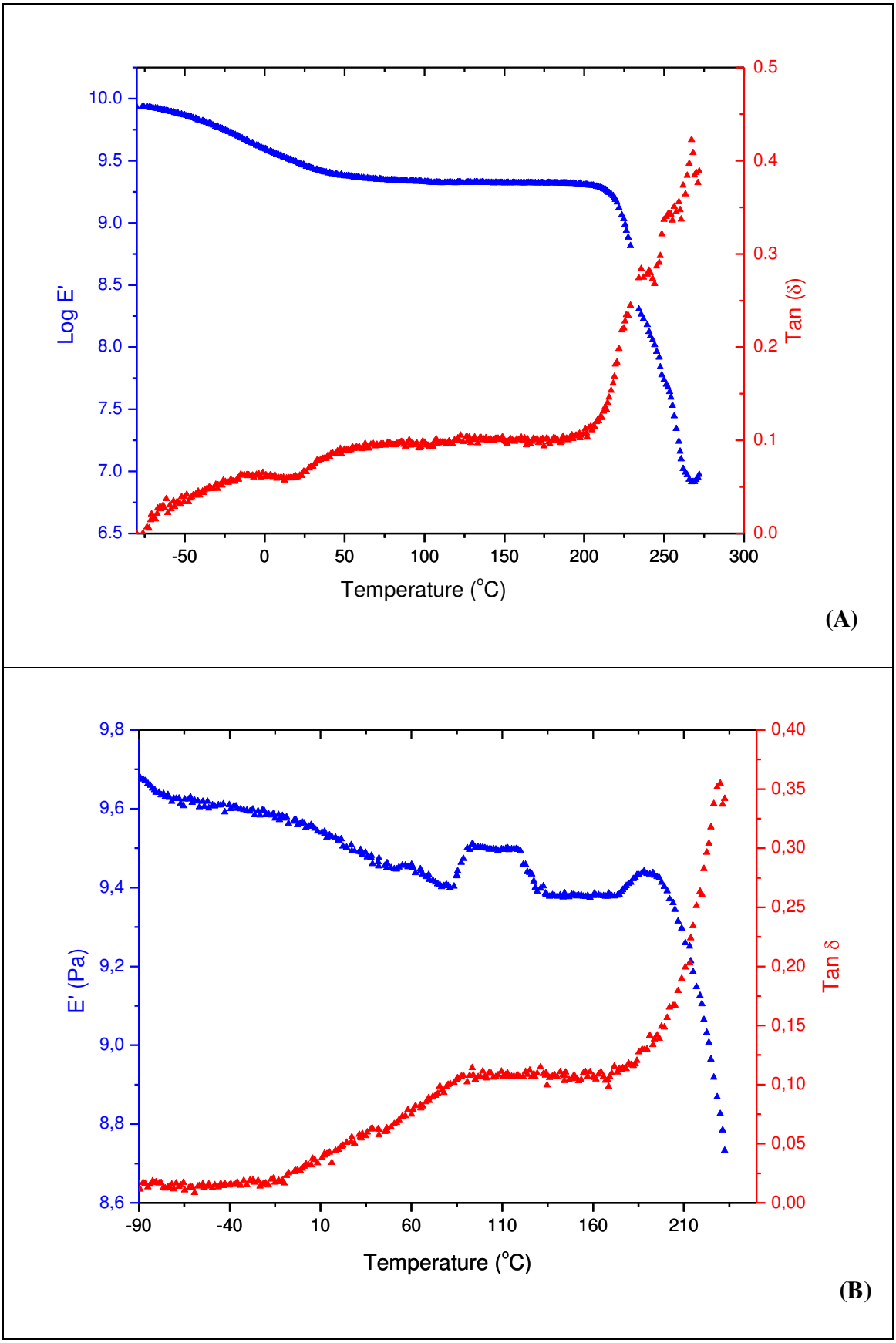

Fig. 4.11: Storage modulus and Tan δ curves obtained by DMA analysis of CMC films prepared with A) Fluka and B) purified Niklacell.

Figure 4.12 shows storage modulus (E') and Tan δ curves obtained from DMA analysis of opaque (CMC-fNo) and semi-transparent (CMC-fNt) regions of CMC-fN. The samples present three relaxations as observed on the Tan δ curves. The relaxations between 70 and 100°C and between 70 and 170°C are attributed to Tg of CMC-fNt and CMC-fNo, respectively, and to the effects of water elimination. The broadening of the relaxation is probably due to higher amount of salts and their influences on the mobility of the polymeric chains in the amorphous domains and a high polydispersivity. A relaxation at around 240 and 230°C of CMC-fNt and CMC-fNo samples, respectively, is attributed to Tm of the crystalline regions of the CMC structure. An endothermic transition was also observed close to this temperature on the curves obtained from DSC analyses (see Table IV.5).

The first relaxation at around -20 and -15°C of CMC-fNt and CMC-fNo, respectively, is probably due to impurities from synthesis in these crude grades. An evidence of this assumption is the absence of these relaxations in the purified CMC grades. However, the nature of these impurities was not determined.

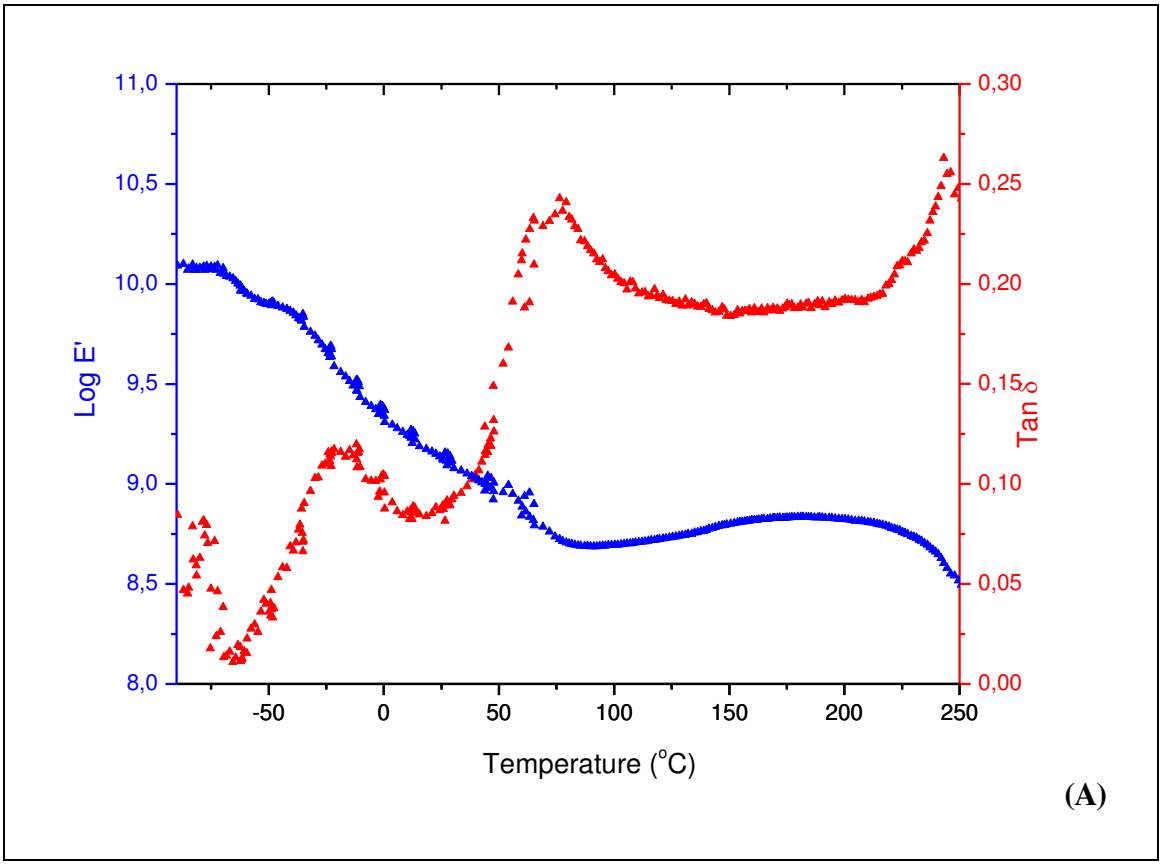

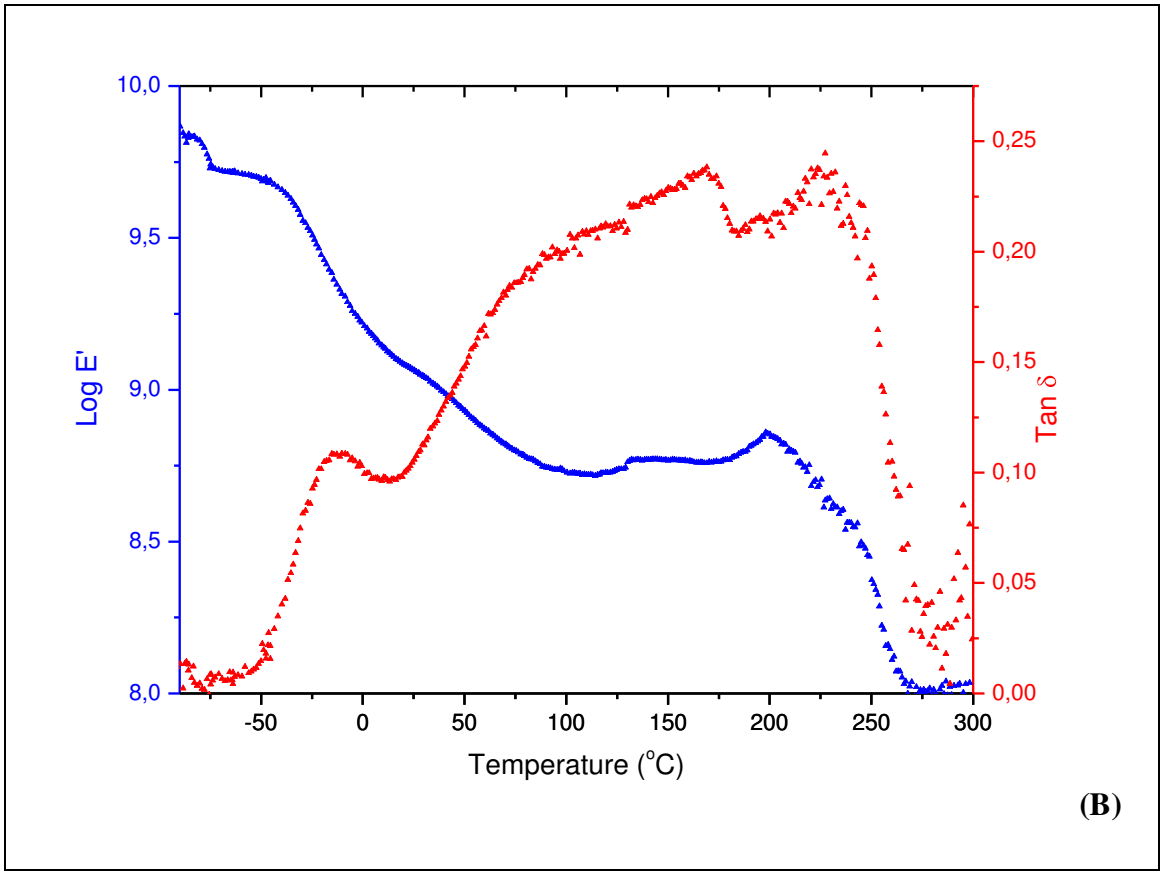

Fig. 4.12: Storage modulus and Tan δ curves obtained by DMA analysis of CMC films prepared with Niklacell **(A)** transparent and **(B)** opaque parts.

4.3. Conclusions

In this study two CMC chemicals were characterized: Fluka (a purified grade) and Niklacell (a crude grade used in papermaking industry). Micrographs obtained from optical microscopy of Fluka and Niklacell CMC solutions showed the presence of residual fibres with a symmetrical pattern of modification. Films prepared from Fluka were flexible and transparent whereas films prepared from Niklacell were more brittle and visually heterogeneous (opaque and semi-transparent regions).

Micrographs obtained from SEM of the surface of opaque and transparent Niklacell CMC samples showed the presence of salts, whereas those corresponding to the cross-section displayed phase segregation. During film preparation there was a segregation of at least two phases: a rich NaCl layer and CMC / NaCl layer as confirmed from X-ray microanalysis technique. For Fluka CMC, the obtained films are homogeneous and do not exhibit the presence of salt layers or phase segregation. X-ray microanalysis showed that C, O and Na atoms constitute the majority of elements.

From the ^{13}C CP/MAS NMR spectra, the DS value could be calculated from the ratio of carboxyl (C=O) to C_1 signal area. CMC Fluka samples showed DS values in the range of the supplier data. CMC Niklacell samples showed greater variations of DS values due to the presence of impurities and/or by-products as NaCl. From liquid state ^{23}Na NMR measurements performed on CMC aqueous solutions samples, we showed that practically all the Na is present as sodium carboxylate in Fluka samples. With Niklacell samples, Na is present either in sodium carboxylate or in NaCl salt forms.

From solid state NMR and FTIR, some information could be extracted. CMC Niklacell is characterized by a high content in NaCl and a lower DS when compared to Fluka CMC.

Niklacell and Fluka CMC films were analyzed from DSC and DMA techniques. The observed differences were attributed mainly to the presence of salts and impurities in the crude grade. Nevertheless, after purification of Niklacell, the product showed properties close to those of Fluka samples.

CHAPTER V: PREPARATION AND CHARACTERIZATION OF PAE/CMC FILMS

Complex formation between anionic and cationic polyelectrolytes (PEL) has been known for a long time. The driving forces in this kind of complexation are mainly the interactions between the oppositely charged macromolecules, but hydrophobic interaction, van der Waals forces and hydrogen bonding can also play a role. The stoichiometry, *i.e.*, the molar ratio between the anionic and the cationic groups of these compounds is important for describing these polyelectrolytes complexes (PEC). Such a parameter is mainly determined from the nature of ionic groups in the polymers, their respective density, their molar weight distributions, and fromf the reaction conditions. We can find 1 / 1 stoichiometric polysalts, but recent publications have given more attention to the deviation from this stoichiometry (Sang *et al.*, 2010; Ankerfors *et al.*, 2009; Lindqvist *et al.*, 2009; Enarsson and Wägberg, 2007; Gärdlund and Norgren, 2007; Alince *et al.*, 2006; Vainio *et al.*, 2006; Eriksson *et al.*, 2005; Megan *et al.*, 2005; Gärdlund *et al.*, 2003; Gernandt *et al.*, 2003; Wägberg and Hägglund, 2001; Wägberg *et al.*, 1998; Krammer *et al.*, 1997; van de Steeg *et al.*, 1992).

As discussed before, the aim of our work is not to study complex formation between CMC and PAE, but to use CMC (an anionic polyelectrolyte) as a model compound of cellulosic fibres, and PAE/CMC interactions to study PAE-fibres interactions. Films of polyelectrolyte complexes were prepared at pH value of 6-7, as described in Materials and Methods, and using a variation of CMC/PAE mass ratios. Fluka CMC macromolecules posses a higher charge (5.5 μeq/g determined from colloidal titration using PCD03 and polydadmac like a cationic polyelectrolyte standard) than that of the PAE resin.

5.1. Results and discussion

In order to study the interactions between CMC and PAE macromolecules, heated (at 105°C for 24 h) and unheated CMC/PAE films were aged under controlled conditions (25°C and 50% RH), and studied from NMR spectroscopy. Figure 5.1 shows

the solid state ^{13}C NMR spectra of unheated CMC/PAE films at 50% w/w. A theoretical SUM spectrum was obtained from the addition of experimental spectra data of the CMC Fluka and PAE films with the same ageing time. All the experimental spectra were performed at 243K.

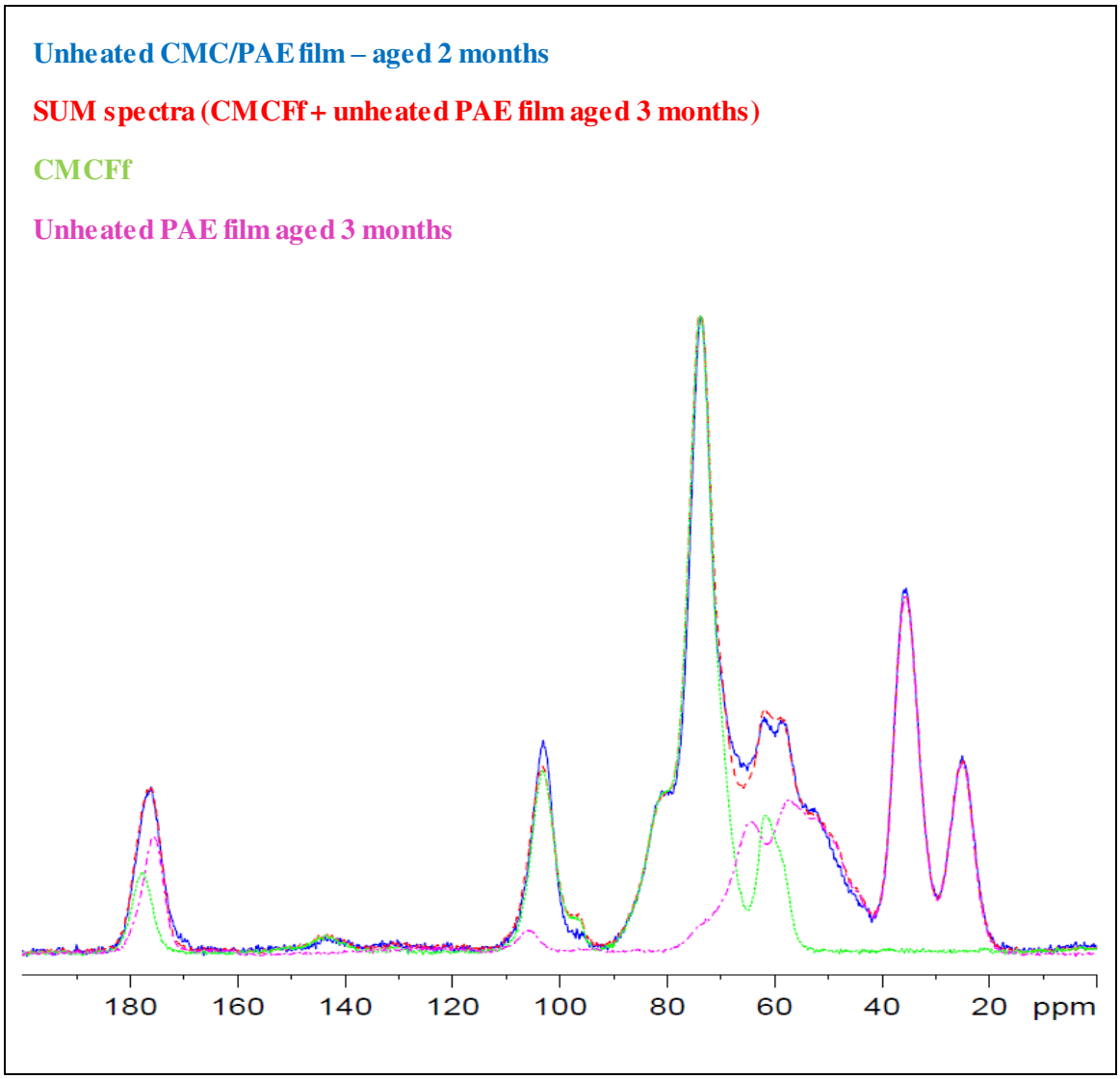

Fig. 5.1: CP/MAS ^{13}C NMR spectra recorded at 243 K of aged unheated CMC/PAE films.

Several remarks can be drawn, namely:

(i.) the ageing of the prepared films from 2 days to 2 months did not induce modifications in the carbonyl-carboxyl region (190-165 ppm) of the unheated PAE/CMC films (spectra not shown);

(ii.) the strong magnification of the carbonyl-carboxyl region (see Figure 5.2), shows an excellent adequacy between experimental CMC/PAE and theoretical SUM spectra. Thus, we can postulate that in this frequency region, the experimental CMC/PAE film spectrum presents the same tracings as that yielded from mathematical addition for C=O bands of CMC and PAE films. In fact, these spectra suggest that there is no ester bond formation between CMC and PAE in these conditions.

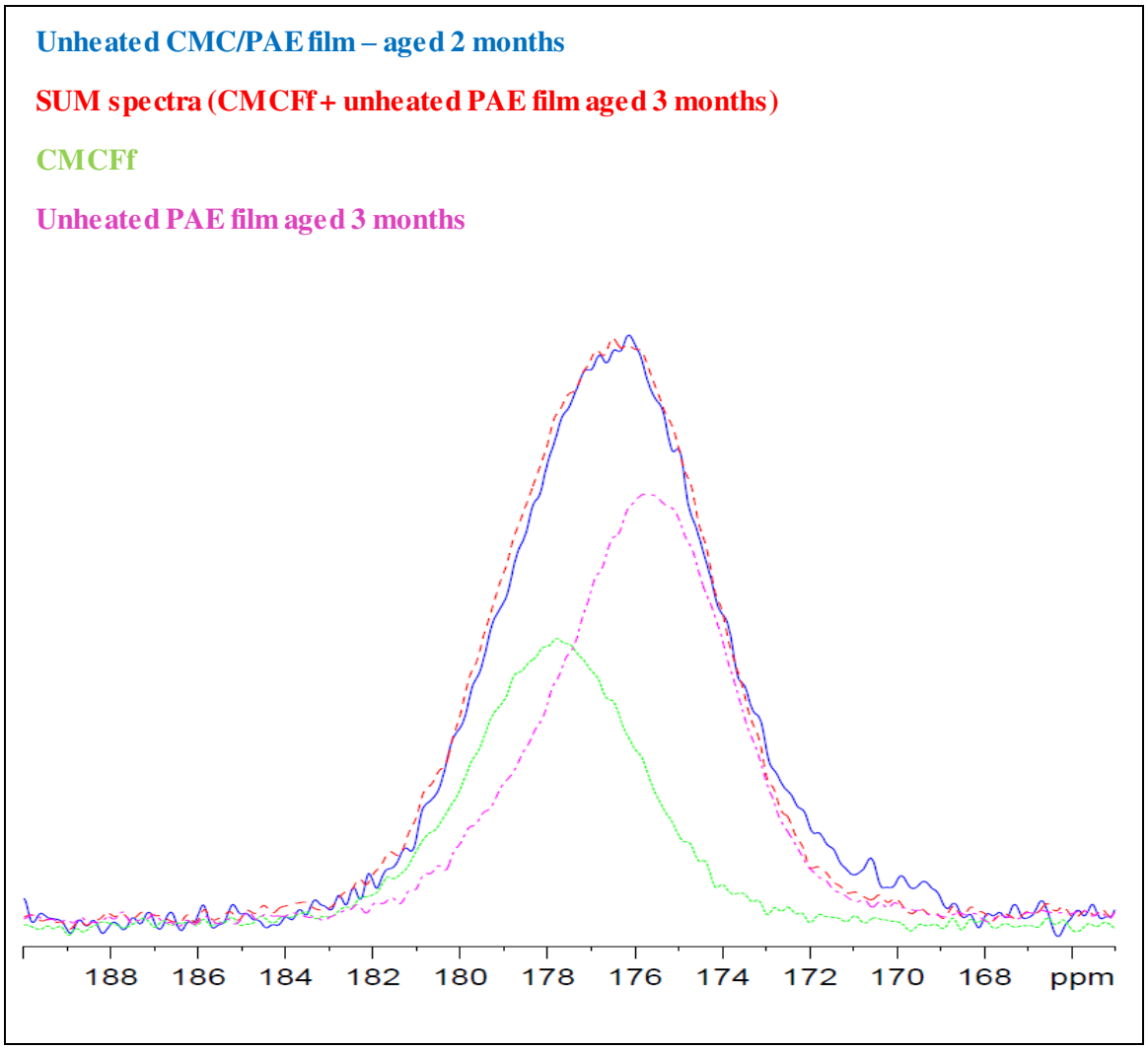

Fig. 5.2: CP-MAS ^{13}C NMR spectra of unheated CMC/PAE films recorded at 243 K (carbonyl-carboxyl region: 170 to 184 ppm).

(iii.) The ageing from 2 days to 2 months induces modifications in the AZR region (92-40 ppm) of CMC/PAE film spectra (see Figure 5.3 **A** and **B**).

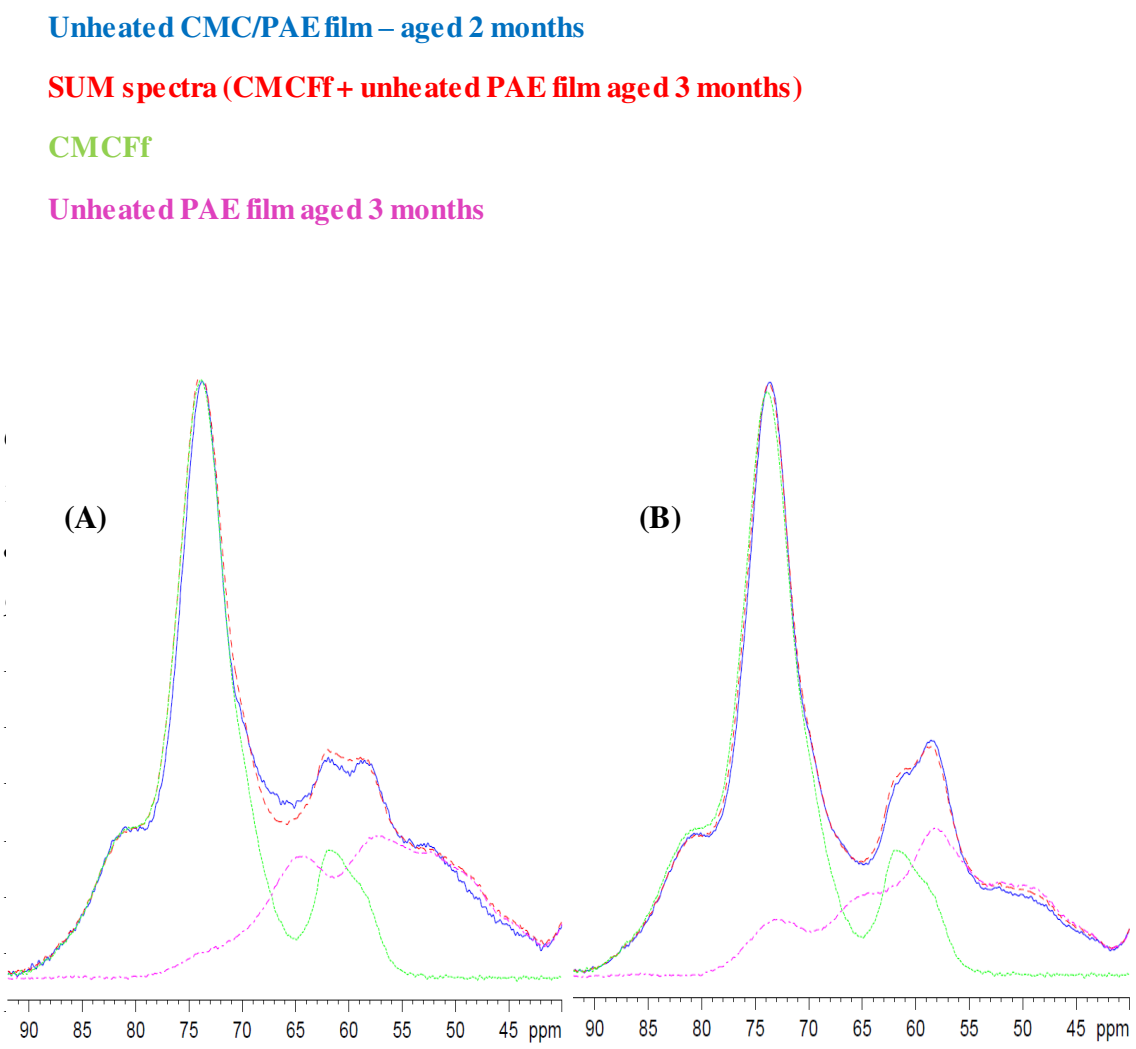

Fig. 5.3: CP-MAS ^{13}C NMR spectra of unheated CMC/PAE films recorded at 243 K in the AZR region (40-90 ppm) aged for: **A**) 2 months and **B**) 2 days.

(iv.) from the strong magnification of AZR region (92-40 ppm) we observe an excellent adequacy between experimental and theoretical spectra. Thus, as discussed before, we can point out that the modifications observed as a function of the ageing correspond only to the cross-linking of the PAE resin derived from the opening of the AZR ring. These spectra confirm that no ester bond formation between PAE and CMC takes place.

Figures 5.4 shows the experimental and theoretical solid state ^{13}C NMR spectra of heated (at 105°C for 24 h) CMC/PAE films at 50% w/w. Theoretical SUM spectra were derived from a mathematical addition of the spectra corresponding to CMC Fluka film and to rigid (storage in dissicator: anhydrous conditions) or flexible (storage under controlled conditions: 23°C and 50% RH) heated PAE films, respectively. After the thermal treatment, CMC/PAE films spectra aged for 2 days up 6 months do not show differences in AZR region. Thus, we can conclude that, as in the case of PAE films, the reactions in CMC/PAE films are boosted by a thermal post-treatment (105°C for 24 h) to a final state.

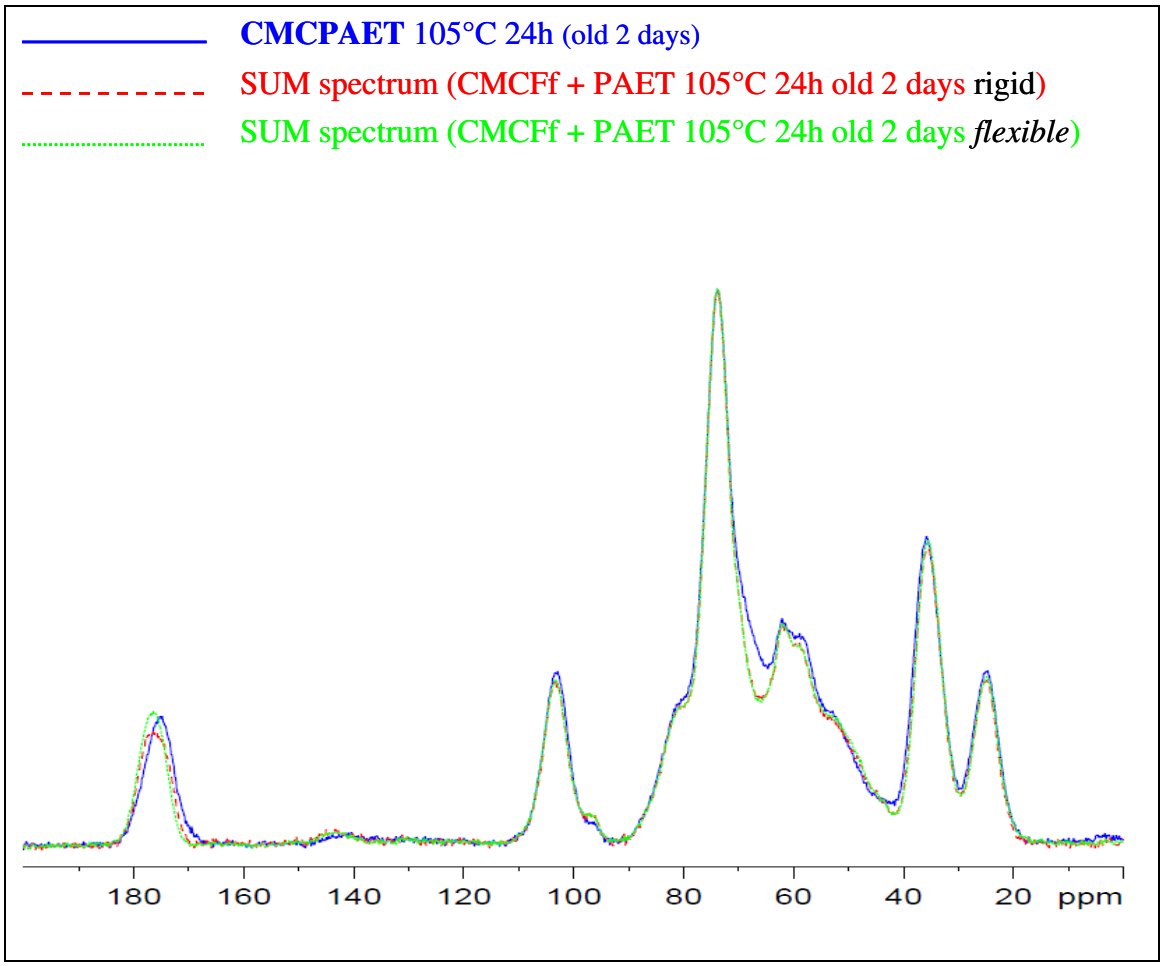

Fig. 5.4: Solid state ^{13}C NMR recorded at 243 K of heated CMC/PAE films.

Figure 5.5 represents a magnification of the solid state ^{13}C NMR spectra of the carbonyl-carboxyl region associated to the heated CMC/PAE films. As observed, with the thermal post-treatment, the heated CMC/PAE films spectrum is not in total adequacy with the SUM spectra. The experimental band is shifted towards weaker frequencies. This is in agreement with a carboxylate signal derived from a reaction of OH group in the AZR and a carboxylic group in the CMC. Thus, we can postulate that with the thermal post-treatment there is ester bond formation between PAE and CMC. As explained before, the Fischer esterification reaction is promoted by a heating treatment (between 1 and 10 h and temperatures between 60 and 110°C).

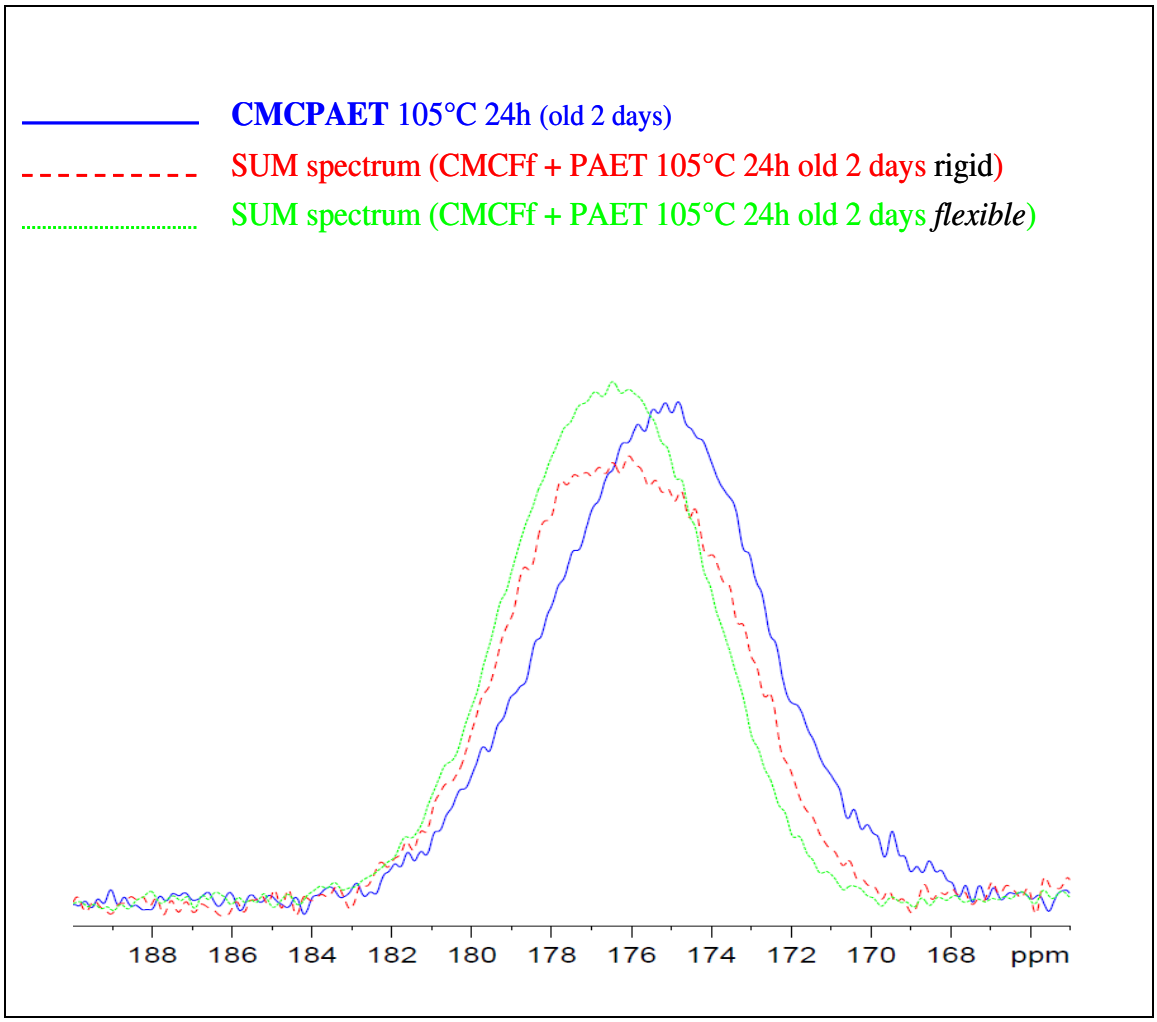

Fig. 5.5: CP-MAS ^{13}C NMR spectra of heated CMC/PAE films recorded at 243 K (carbonyl-carboxyl region: 170 to 184 ppm).

Figure 5.6 represents a magnification of the AZR region (62-72 ppm), and some changes can be observed, probably due to the ester bond formation. However, numerous signals overlap making impossible any assignment.

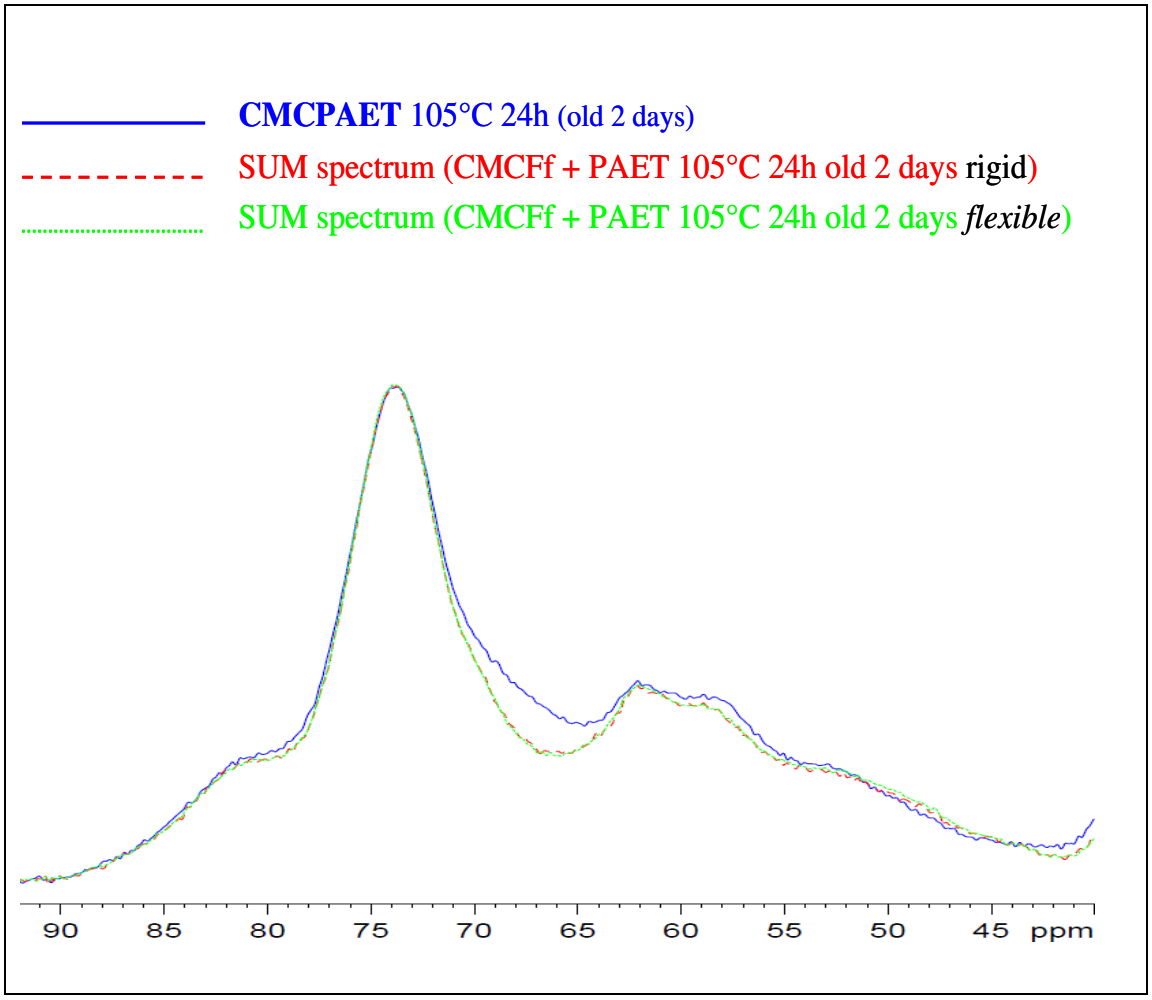

Fig. 5.6: CP-MAS ^{13}C NMR spectra of heated CMC/PAE films recorded at 243 K (AZR region: 40 to 90 ppm).

The ester bond formation is confirmed from FTIR spectroscopy. Thus, Figure 5.7 and 5.8 shows FTIR spectra of heated and unheated CMC/PAE films, as a function of the CMC amount (% w/w: 5, 15, 50 and 75%).

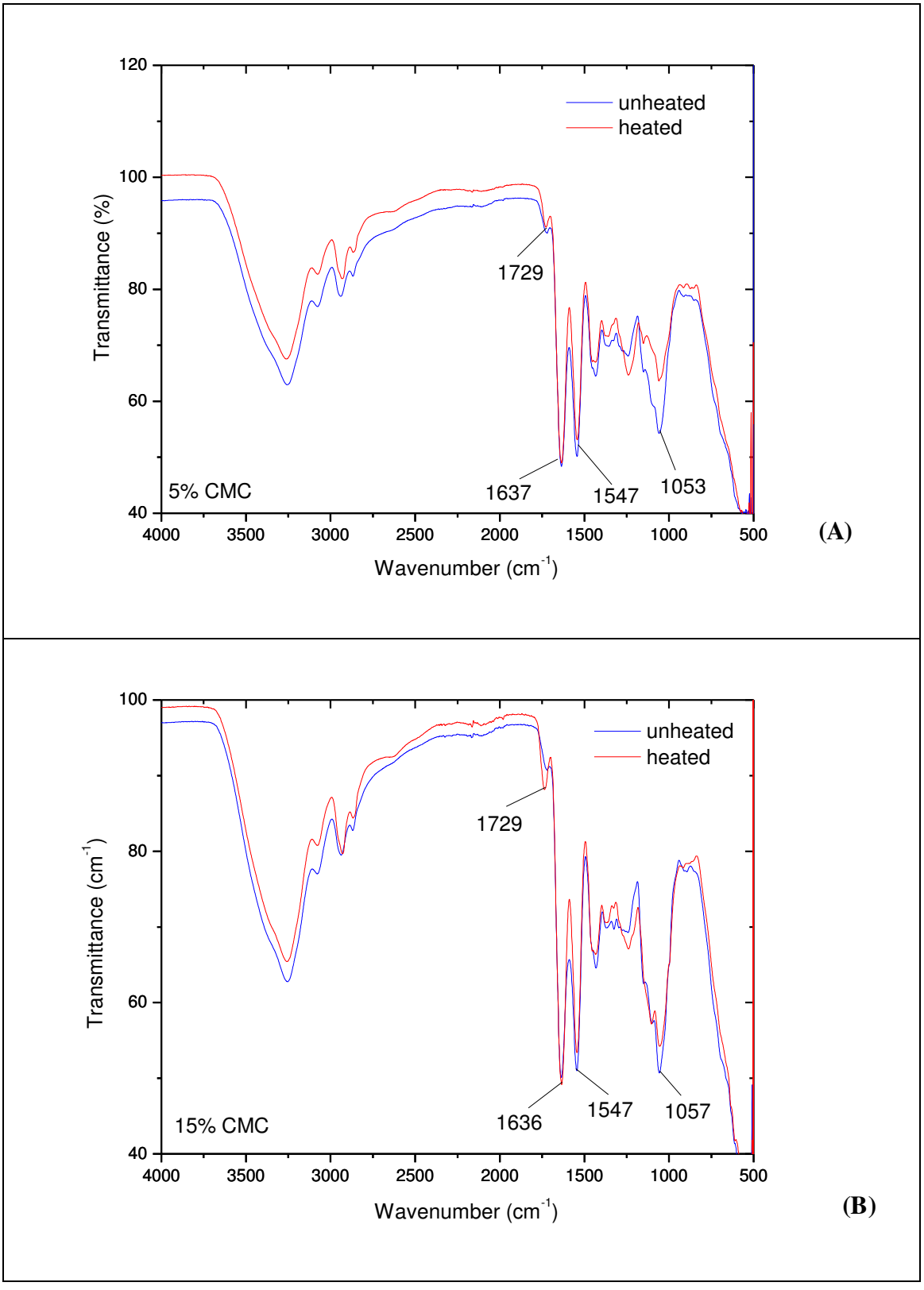

Fig. 5.7: FTIR spectra of heated and unheated CMC/PAE films: (**A**) 5 and (**B**) 15 % w/w CMC.

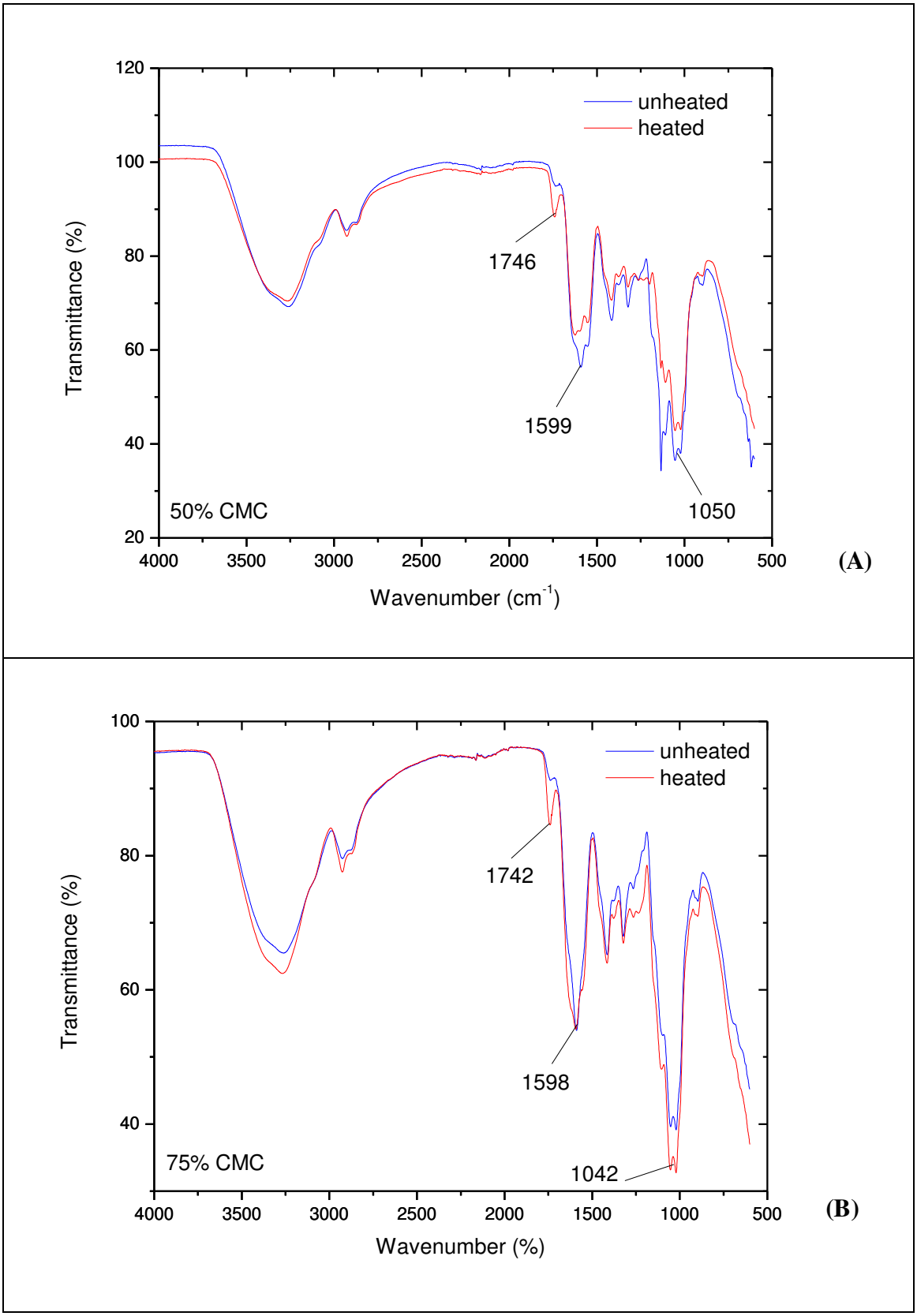

Fig. 5.8: FTIR spectra of heated and unheated CMC/PAE films: **(A)** 50 and **(B)** 75 % w/w CMC.

After thermal post-treatment, one can observe an increase of the absorption band at around 1730 cm^{-1}, which is characteristic of C=O stretching vibrations of aliphatic carboxylic ester functions (Silverstein *et al.*, 2005). This signal is not present in the FTIR spectra of CMC or unheated CMC/PAE films. The intensity of this band increases proportionally with increasing the CMC ratio. Thus, these experiments allow confirming that the ester bond formation between CMC and PAE in CMC/PAE films is boosted by a thermal post-treatment and increases with the carboxylic group concentration, as already established from NMR analyses.

The absorption bands at around 1547 and 1636 cm^{-1} in CMC/PAE spectra are present in the PAE FTIR spectrum and attributed to amide II and I vibrations, respectively. For high CMC dosages these bands are overlapped by the absorption band at 1606 cm^{-1} present in CMC FTIR spectrum and assigned to anti-symmetric vibrations of COO^- group, ring stretching of glucose and non hydrated C=O.

The absorption band at around 1050 cm^{-1} is attributed to the breathing of AZR in PAE FTIR spectrum. Its relative intensity increases proportionally with an increase of the CMC concentration due to overlapping with CMC absorption bands, i.e., those correponding to $-CH_2$ twisting vibrations, primary alcoholic $-CH_2OH$ stretching mode and $CH-O-CH_2$ stretching.

For concluding, important evidences related to the interaction between PAE and CMC were determined in this work. The experiments confirmed ester bond formation between CMC and PAE, which were boosted from a thermal post-treatment and increased with the CMC concentration even with storage of the films under controlled conditions (25°C and 50% RH). For PAE resin (see Chapter III) we also observed experimentally ester bond formation but only under anhydrous condition. In this case, it was difficult to determine spectroscopically ester bonds in PAE films probably due to the small amounts of carboxylic end groups able to form ester bonds and the hydrolysis of these bonds when films were stored at 50% RH. CMC polymer bears a high amount of carboxylic groups (CMC charge is 2.5x greater that PAE charge). So, it is easier to detect them even if they can be hydrolized as a function of storage time in the used conditions. These results confirm the work of Wägberg and Björklund (1993) which observed from FTIR experiments the formation of a saturated ester in cured PAE-based

sheets made from a carboxymethylated pulp. However, as other authors, it was not possible for them to determine ester bonds during self-cross-linking of PAE resin.

SEM micrographs of the surface and cross-section of heated and unheated CMC/PAE films with different % w/w of CMC (5, 15 and 50%) are presented in Figure 5.9, 5.10 and 5.11. The formation of various crystal-like structures can be observed. These 'crystals' may be polyelectrolytes complexes salts formed during preparation of CMC/PAE films, and they are thermally sensitive and disappear with the thermal post-treatment. Huang *et al.* (2003) and Lii *et al.* (2002) also observed the formation of wide leaf-like and cypress leaf-like structures when preparing and characterizing protein-CMC complexes films.

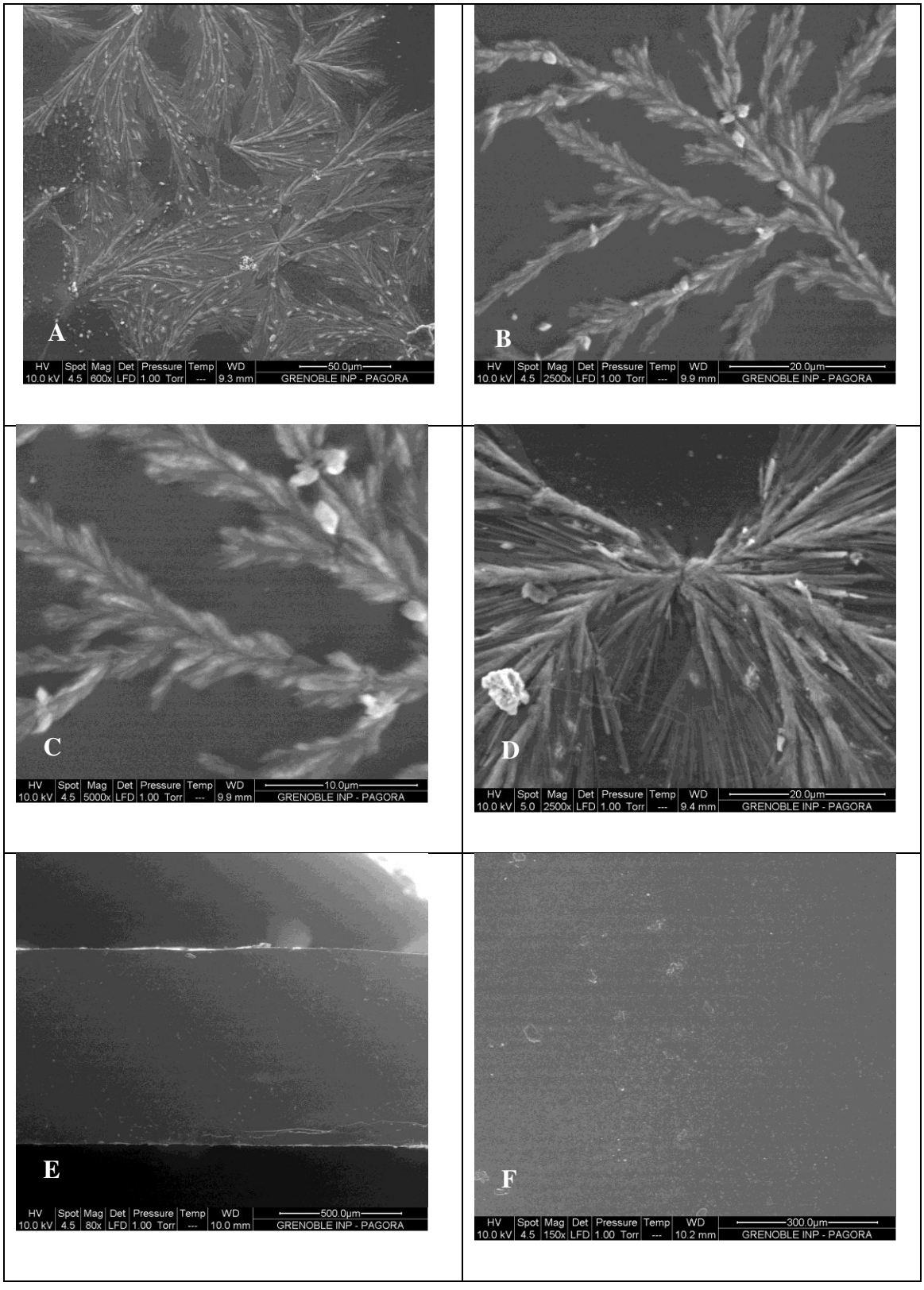

Fig. 5.9: SEM micrographs for **(A)**, **(B)**, **(C)** and **(D)** surface, **(E)** cross-section of unheated and **(F)** surface of heated CMC/PAE films (5% CMC w/w).

More detailed studies of the properties of these structures were not carried out. However, due to the interesting behaviour of CMC in contact with amino-polyelectrolytes this can be the focus of future studies.

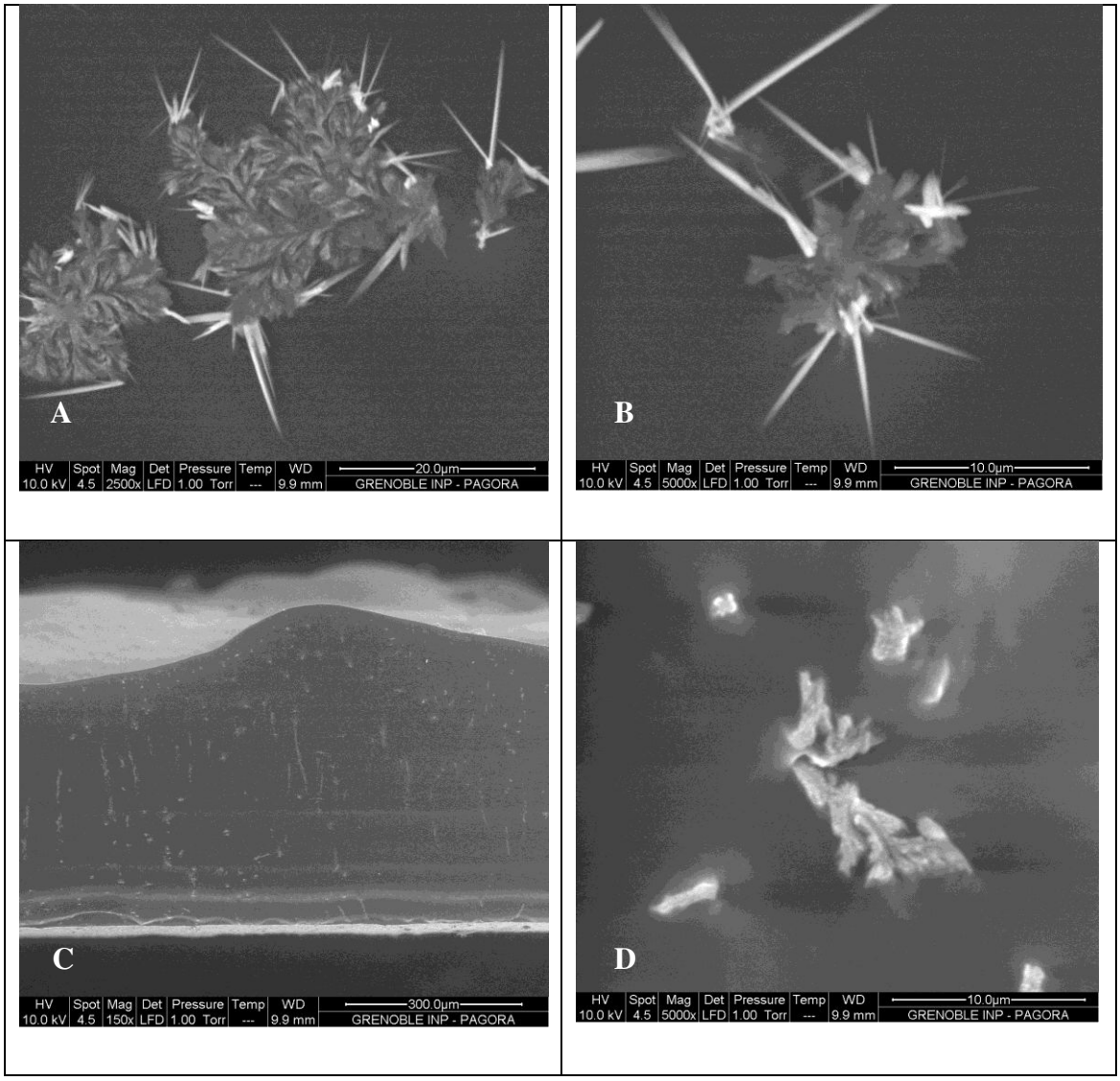

Fig. 5.10: SEM micrographs for **(A)** and **(B)** surface, **(C)** cross-section of unheated and **(D)** surface of heated CMC/PAE films (15% CMC w/w).

From the Figure 5.11 we can observe a formation of at least three phases in the unheated CMC/PAE film (50% w/w). After heating, there is only a homogeneuos phase with some NaCl rich crystals as established from EDS technique.

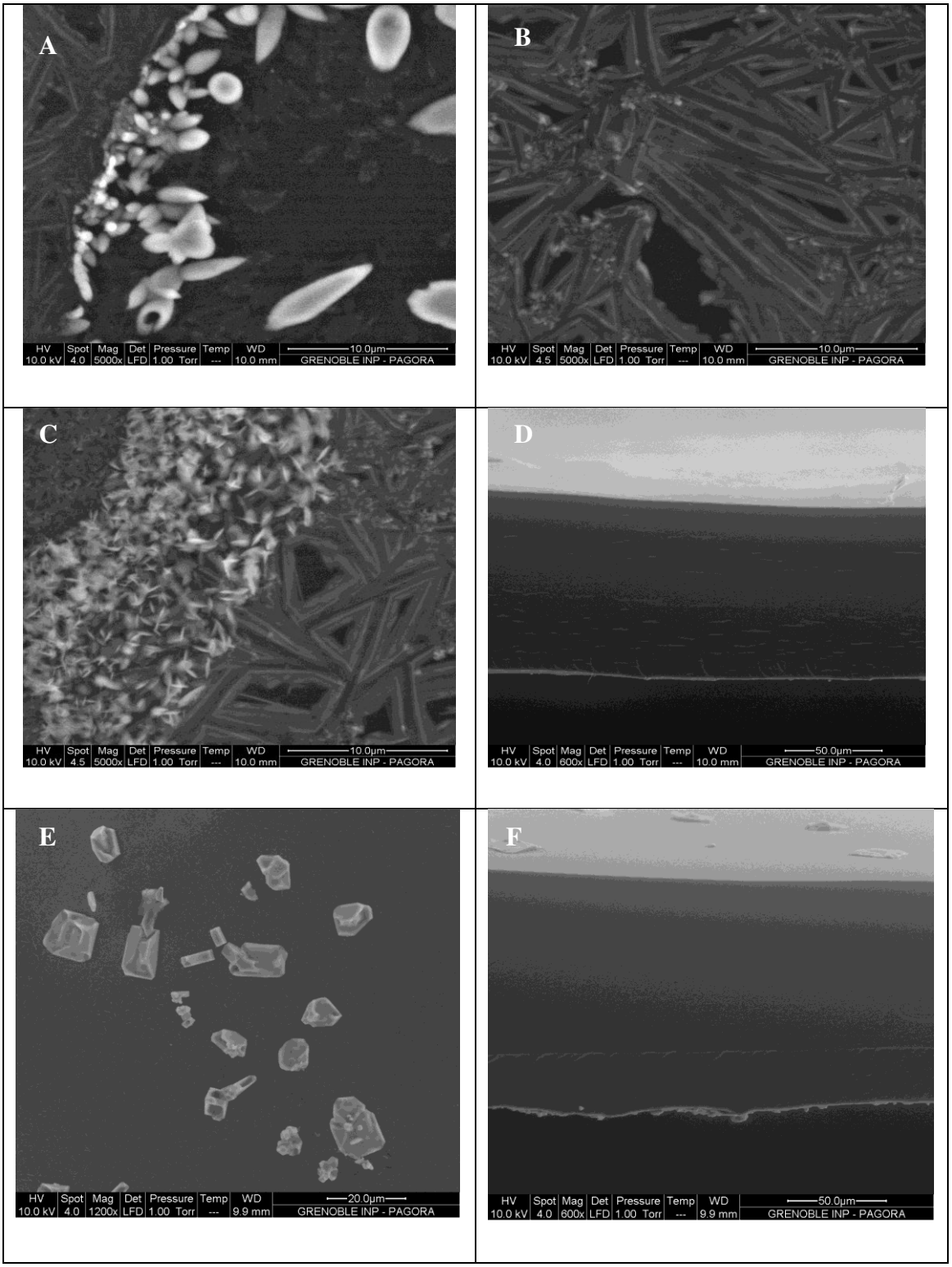

Fig. 5.11: SEM micrographs of **(A)**, **(B)** and **(C)** surface, **(D)** cross-section of unheated and **(E)** surface and **(F)** cross-section of heated CMC/PAE films (50% CMC w/w).

DMA analyses of heated and unheated CMC/PAE films (50% w/w) were performed and the experimental data are shown on Figure 5.12. Unheated CMC/PAE films showed a relaxation at around 75°C, with a first shoulder at around 0°C, and a second well defined relaxation at 200°C. The unheated PAE films show two relaxations:

(i.) at -5.0°C attributed to the Tg of the polyamideamine epichlorohydrin phase; and

(ii.) at 67.0°C associated with the Tg of the polyamideamine phase.

Fluka CMC films showed two relaxations at 30 and 230°C, attributed to the Tg and the Tm, respectively. The CMC/PAE (50% w/w) are non-stoichiometric films, because the Fluka CMC macromolecules posses a higher charge (2.5x greater) than that of the PAE resin. We can therefore consider that the CMC is in excess to neutralize all the PAE macromolecule charges. Thus, a minimum of three relaxations is expected in CMC/PAE films related to each phase. Probably, the first relaxation (at around 75°C) can be attributed to the formation of CMC/PAE polyelectrolyte complexes salt mainly derived from electrostatic interactions forming a physical non-stoichiometric mixture of polymers. The presence of a shoulder is probably due to uncross-linked PAE (polyamidemine epichlorihydrin phase). The relaxation at around 200°C can be attributed to the Tm of CMC.

For heated CMC/PAE films (Figure 5.13 B), a broad relaxation is observed at around 50°C probably related to a phase derived from the cross-linking of the PAE (opening of the AZR cycle), and the reaction of CMC and PAE (ester bond formations). The second relaxation observed at around 200°C is probably attributed to the Tm of the CMC, as in the case of unheated CMC/PAE films. This behaviour also suggests that thermally induced reaction between CMC and PAE has occurred.

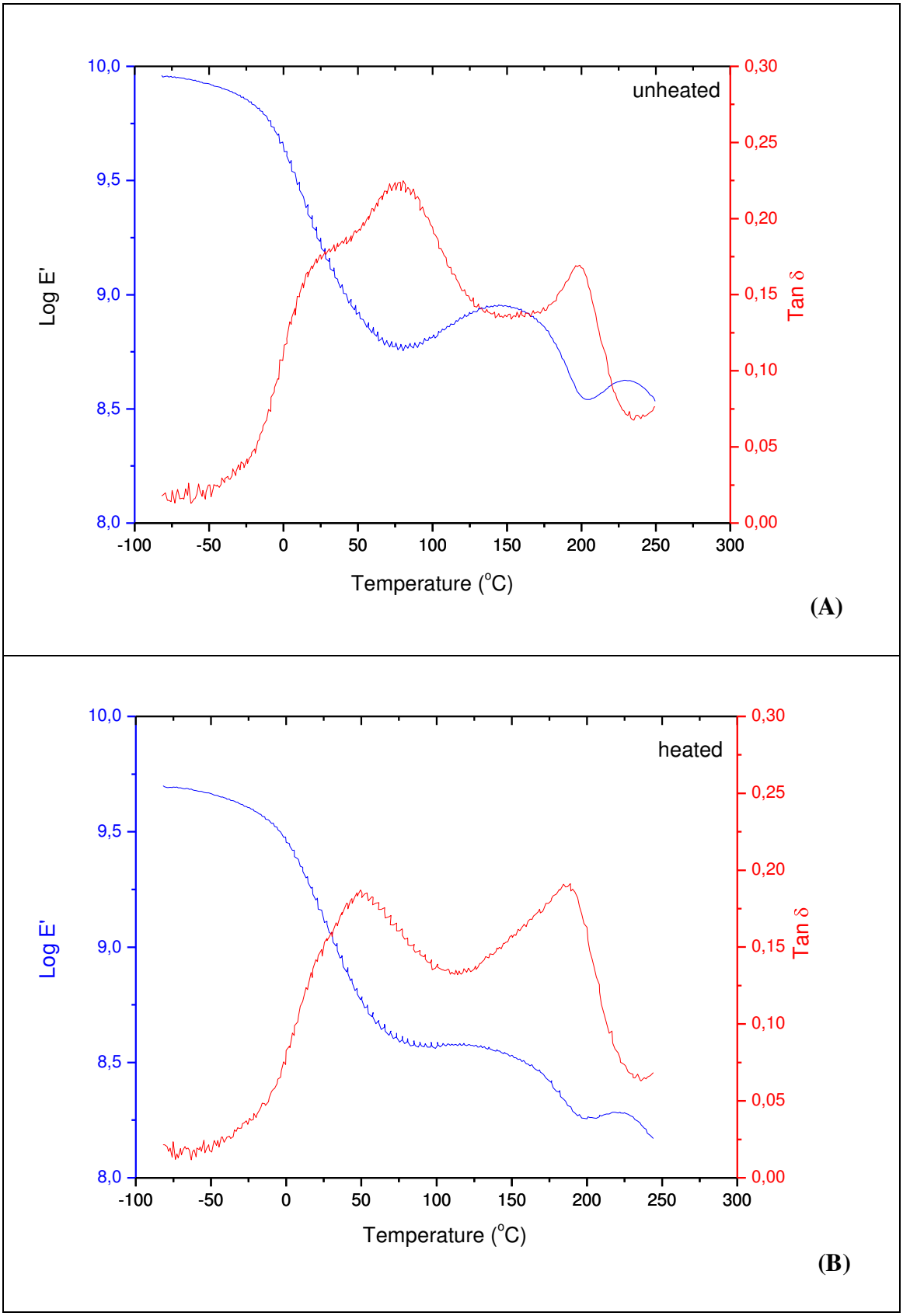

Fig. 5.13: DMA curves (Log E' and Tan δ) of **(A)** unheated and **(B)** heated CMC/PAE films (50% CMC w/w).

5.2. Conclusions

After individual characterizations of PAE and CMC polymers in the Chapter 3 and 4, respectively, we used CMC as a model compound for cellulosic fibres and PAE-CMC interactions as a model to study PAE-fibres interactions. Films of polyelectrolyte complexes were prepared using different CMC/PAE mass ratios and evidences of the reaction mechanism between PAE and CMC were observed.

Solid state ^{13}C NMR showed that ageing of the unheated PAE/CMC films from 2 days up to 2 months did not induce any modification in the carbonyl-carboxyl region. However, for the same ageing time, modifications in the AZR region occur. From the strong magnification of both regions, it was observed an excellent adequacy between experimental CMC/PAE and theoretical SUM spectra. Thus, in these conditions, there was no ester bond formation between CMC and PAE. The observed modifications for unheated CMC-PAE films correspond only to the cross-linking of the PAE resin resulting from the opening of AZR.

Heated and aged CMC/PAE films spectra obtained from ^{13}C NMR for 2 days up to 6 months did not exhibit any tracing difference. From a magnification of the carbonyl-carboxyl region of the NMR spectra, it appears that heated CMC/PAE film spectrum was not in total adequacy with the SUM spectrum. The carbonyl-carboxyl experimental band was shifted toward weaker frequencies, which is in agreement with a carboxylate signal derived from a reaction between a OH group in the AZR and a carboxylic group in the CMC. Thus, in these conditions (thermal post-treatment), ester bond formation between these polymers may occur. The ester bond formation was also clearly confirmed from FTIR spectroscopy. After thermal post-treatment, the CMC/PAE film spectra showed an increase of the absorption band at around 1730 cm^{-1} which is characteristic of C=O stretching vibrations of aliphatic carboxylic ester functions. This signal was not present in the FTIR spectra of CMC or unheated CMC/PAE films. The intensity of this band increased proportionally with an increase of the CMC ratio.

SEM micrographs of the surface and cross-section of unheated CMC/PAE films with different amounts of CMC (5, 15 and 50% w/w) showed the formation of different structures. Apparently these “crystals”, which are thermally sensitive, are

polyelectrolytes complexes salts formed during preparation of CMC/PAE films. From Tan δ curves obtained from DMA analyses, we observed that unheated CMC/PAE films present the thermomechanical properties of a physical mixture between these polyelectrolytes. After heating, the relaxations showed signs of chemical reaction between CMC and PAE. This behaviour also suggests that thermally induced reaction between CMC and PAE has occurred.

Based on our results we can postulate that PAE can react with carboxyl groups in the fibres in similar way of that observed with CMC. However, the small amount of carboxylic groups present in the fibres can make impossible determining ester bonds from spectroscopic experiments. On the other hand, even if these bonds are formed we can consider that their contribution to wet strength of papers is negligible due to their hydrolysis in contact with water.

.

PART II

USE OF PAE RESIN IN PAPERMAKING: IMPROVEMENT OF THE PREPARATION AND REPULPING OF PAE-BASED PAPERS

CHAPTER I

The pulping and papermaking processes application to the production of wet strengthened papers

The paper industry is often referred as capital-intensive (because it uses large and expensive equipments), water-intensive (almost all of the processing operations use aqueous suspension of fibres or chemical solutions), and energy-intensive (the paper industry consumes large amount of energy in the refining and drying stages).

Paper is manufactured from a suspension called the papermaking furnish or stock whose composition depends on the grade of paper being manufactured. However, a papermaking furnish usually contains both: fibrous and nonfibrous constituents.

Wood pulp is the most important source of fibres used in paper manufacturing. Pulps are classified according to their method of manufacture and the wood species. These two factors determine the chemical composition and the morphological characteristics of the fibres which, in turn, influences the properties of paper produced from them. Pulps can be classified as virgin or recycled. It is worth noting that more than 50% of the fibres used for manufacturing paper and board are recycled fibers.

1. The pulping and papermaking processes

1.1. Fibrous raw materials in papermaking

A large number of different wood species are used for the production of wood pulps. The species can be classified into two main groups:

(i.) the softwoods (or conifers), such as pines, spruces, firs, and hemlocks; and

(ii.) the hardwoods (or deciduous trees) such as gum, aspen, oak, hickory, maple, *Eucalyptus* and cottonwood (Sixta, 2006; Scott and Abbot, 1995).

Softwood (SW) and hardwood (HW) fibres differ in their morphology such as length and width, but also in terms of content and chemical structure of hemicelluloses. The SW fibres have typical lengths between 2 and 4 mm, while HW fibres have lengths between 1 and 2 mm long on average (Scott and Abott, 2005). Generally, SW fibres present higher aspect ratios (length to width ratio) than HW fibres. Table I.1 summarizes the chemical composition and the main morphological characteristics of HW and SW fibres.

Tab. I.1: Chemical composition and morphological characteristics of softwoods (SW) and hardwoods (HW) fibres from Sixta (2006).

Characteristics		***SW***	***HW***
Chemical composition (%)	***Cellulose***	40-44	43-47
	Hemicelluloses	25-29	25-35
	Lignin	25-31	16-24
Cell dimensions	***Length average (mm)***	3.3	1.0
	Length range (mm)	1.0-9.0	0.3-2.5
	Diameter average (µm)	33	20
	Diameter range (µm)	15-60	10-45

In SW, the fibres perform both functions of providing structural strength and conducting fluids. On the other hand, HW gain structural strength from fibres but have additional elements called vessel elements that conduct fluids. Vessel elements are very large and often appear as pores in a cross-section of a given wood piece (Sixta, 2006).

From a papermaking point of view, we can deduce that papers or boards produced from HW and SW fibres will exhibit different properties. Thus, HW fibres produce smooth and dense papers that are suitable for printing and coating, while SW

produce rough, bulk and high tearing strength papers that are excellent for linerboard and sack papers. These differences are largely a function of the corresponding coarseness of the fibres, which is controlled primarily by the thickness of the fibre wall (Sixta, 2006; Scott and Abbot, 1995).

Papers made from fibres with high aspect ratio (SW) are generally stronger, particularly in terms of tearing resistance. Fibres with high aspect ratio also tend to produce more open sheets (with higher porosity), having higher bulk, and air permeability. These properties are related to the fact that fibres with high aspect ratio have a greater tendency to flocculate which is detrimental to the sheet paper formation (Scott and Abbot, 1995). Because of this, it is common to use mixtures of HW and SW fibres in order to improve the sheet formation.

Another fibre property that contributes to paper properties is the intrinsic fibre strength. There is no doubt that fibre strength contributes significantly to all mechanical properties. However, there is a long-standing controversy over whether the fibres or the fibre-to-fibre bonds are the limiting factors (Lindstöm *et al.*, 2005).

1.1.1. Chemical composition of wood fibres

The chemical composition of wood impacts many properties of the papers produced from their fibres. Wood fibres mainly consist of three macromolecules: cellulose, hemicelluloses and lignin. Extracts are also present but are mostly removed by chemical pulping and bleaching processes (Gandini and Belgacem, 2008; Wägberg et Annergren, 1997).

The principal constituent of a wood fibre is cellulose, which is a polymer that yields glucose when broken down by chemical means. Cellulose is the structural material of which the fibre is built. It is a white substance, insoluble in most solvents, and resistant to the action of most chemicals except strong acids (Gandini and Belgacem, 2008; Zhang *et al.*, 2008). In addition to its importance as the main structural material of wood fibres, cellulose is also very important for paper properties because the attraction between cellulose, at the fibre surfaces, is the principal source of fibre-to-fibre

bonding in paper (Lindstöm *et al.*, 2005). Figure 1.1 shows the monomer unit of the cellulose structure.

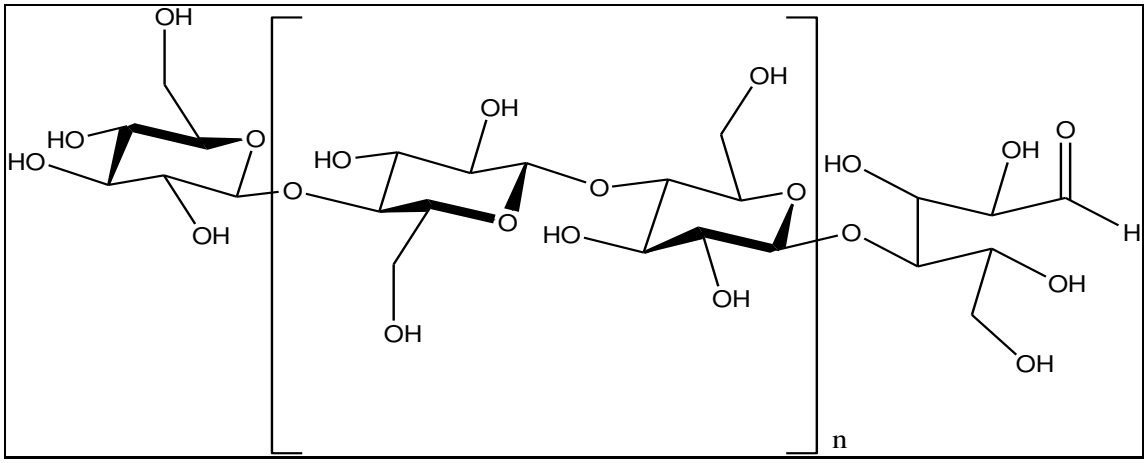

Fig. 1.1: Monomer unit of the cellulose structure.

According to Sjoström (1981) native cellulose in wood has a DP value of approximately 10.000 glucopyranose units and it is around 15.000 for native cellulose in cotton. However, Bledzki and Gassan (1999) show that purification procedures usually reduce the DP, e.g. a DP of 14.000 in native cellulose can be reduced to about 2.500. As resported by Daniel (1985), valonia fibres present a DP of 26.500 and white cotton fibres present a DP ranging from 14.000 and 20.000 depending on the part of the fibre where the analysis was performed. It is therefore important to keep in mind that the length of polymer chains varies according to the source of cellulose or even to the part of the plants.

The hemicelluloses are the second major chemical constituents of wood fibres. They are heteropolysaccharides and differ from cellulose mainly because they consist of several sugar moieties, mostly branched, and have lower molecular masses with a DP of 50 to 200 (Gandini and Belgacem, 2008). The sugar units (anhydro-sugars), making up the supramolecular structures of hemicelluloses (within the biosynthetic pathways), can be subdivided into groups such as pentoses (xylose and arabynose units), hexoses (glucose and manose units), hexuronic acids (glucuronic acid) and deoxy-hexoses (rhamnose units). The main chain of hemicelluloses can consist of only one unit

(homopolymer, e.g., xylans), or two or more units (heteropolymer, e.g., glucomannans). Some of the units are side groups of a main chain (backbone), for example 4-O-methylglucoronic acid, galactose (Sixta, 2006). Examples of sugars constituting hemicelluloses structure are shown in Figure 1.2.

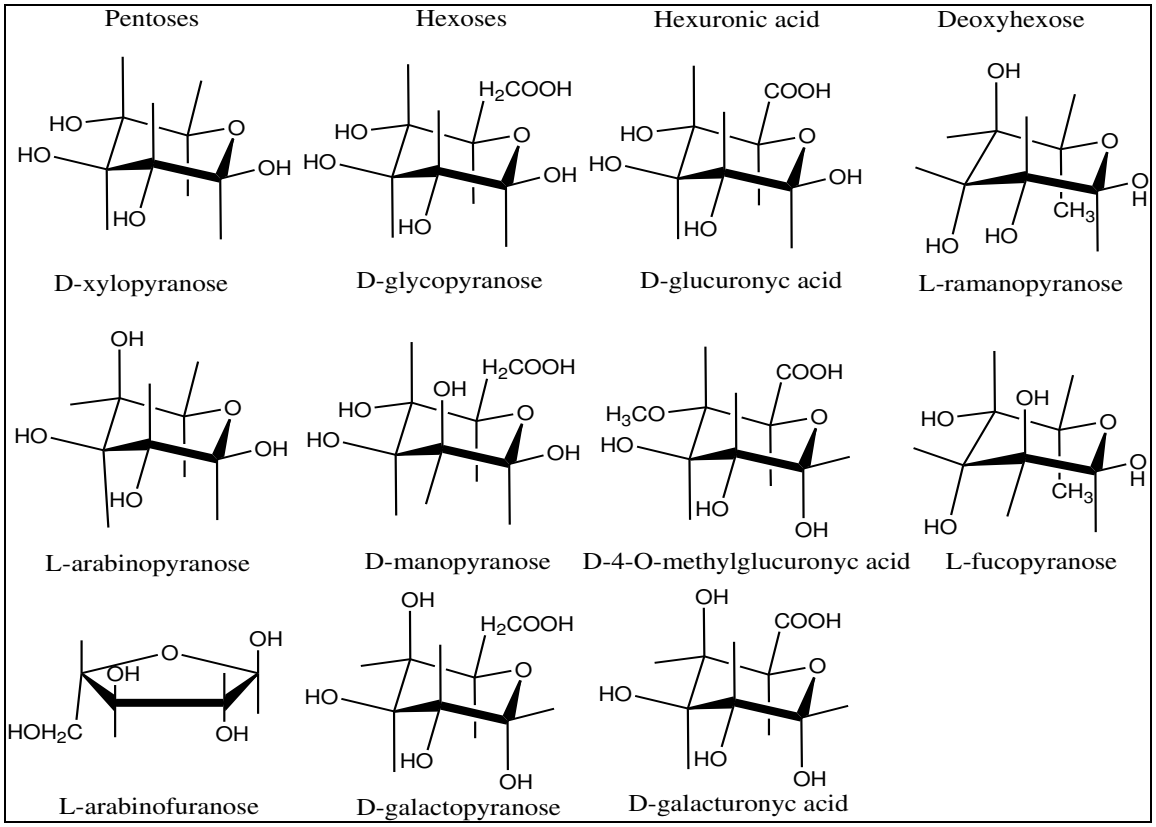

Fig. 1.2: Sugar constituents of hemicelluloses.

There are significant differences between SW and HW fibres related to the type and content of the hemicelluloses. SW fibres have a high proportion of mannose units and more galactose units than HW, whilst HW fibres have a high proportion of xylose units and more acetyl groups than SW. In HW, the xylan chain are placed at irregular intervals with groups of 4-O-methylglucoronic acid with an α-(1,2)-glycosidic linkage at the xylose units. Furthermore, many of the OH-groups at C2 and C3 of the xylose units are substituted by O-acetyl groups producing O-acetyl-4-O-methylglucurono-xylan, the main hemicelluloses component in HW fibres (10-35%). HW xylans contain

small amounts of rhamnose and galacturonic acid. Further studies showed that the reducing end of xylans consists of a combination of xylose, rhamnose and galacturonic acid units which is seen to be responsible for the alkali resistance of the xylan molecule. In general, SW xylans differ from HW xylans by the lack of acetyl groups and by the presence of arabinose units linked by α-(1,3)-glycosidic bonds to the xylan backbone. Thus, the 10 to 15% of SW xylans are arabino-4-O-methylglucuronoxylans. Mannans from wood are characterized by a heteropolymer backbone consisting of mannose and glucose units (so-called glucomannans). The simplest structure is shown in HW glucomannans, as they consist only of glucose and mannose units linked by β-(1,4)-glucosidic bonds forming slightly branched chains. SW fibres contains about 15-25% mannans that consist of a glucomannan backbone to which acetyl groups and galactose residues are attached, forming O-acetylgalactoglucomannans (Sixta, 2006).

Many hemicelluloses are removed by mild chemical action. In wood, they are associated with cellulose, and they are very important in papermaking because they promote the development of fibre-to-fibre bonding through their influence on the ability of fibres to take up water during processing and their direct participation in the bonding (Lindström *et al.*, 2005).

The lignin is the third major chemical found in wood. In nature, much of the lignin is located between the fibres where it serves as a binding agent. It also occurs within the fibre wall. Lignin is a very complex material that does not have a simple structure. It is insoluble in water and in most common solvents, but can be made soluble by chemical action (Gandini et Belgacem, 2008; Sixta, 2006). There are three monomers methoxylated to various degrees: *p*-coumaryl alcohol, coniferyl alcohol, and sinapyl alcohol. These lignols are incorporated into lignin in the form of the phenylpropanoids *p*-hydroxyphenyl (H), guaiacyl (G), and syringyl (S), respectively. Figure 1.3 shows the precursors of the lignin and the Figure 1.4 presents the lignin structure of *Fagus sylvatica* proposed by Nimz (1974).

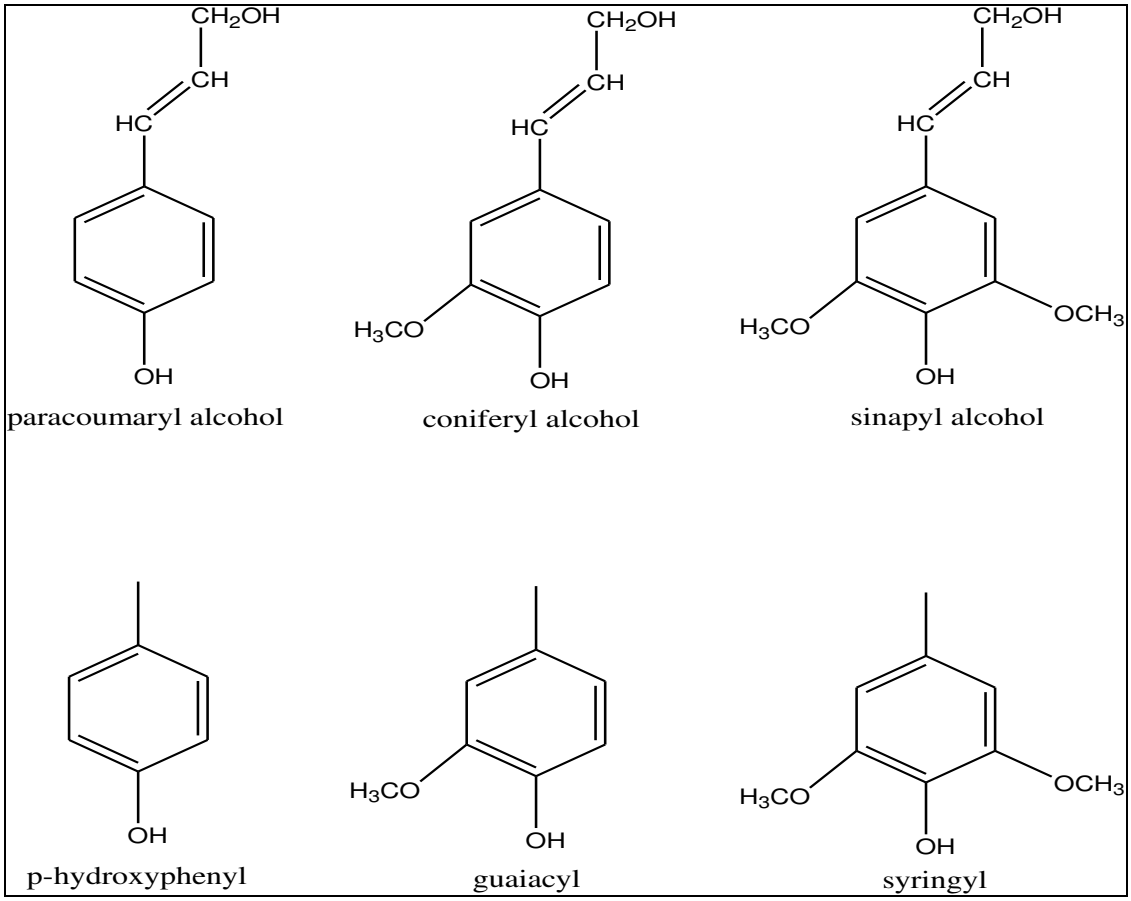

Fig. 1.3: Methoxylated monomers and phenylpropanoids precursors of the lignin structure.

All chemical pulping processes are based on reactions, which solubilize lignin. However, no practical method has been found to completely remove lignin by pulping. In the kraft process (described in this chapter), the modified lignin that remains gives a brownish color to papers made from unbleached pulps. If white paper is desired, the remaining lignin must be removed or dissolved by bleaching. Lignin actually hinders the formation of fibre-to-fibre bonds in paper and, as such, decreases paper strength (Lindström *et al.*, 2005). As one travels from the outside of the fibre to the lumen, the lignin concentration decreases while the cellulose concentration increases.

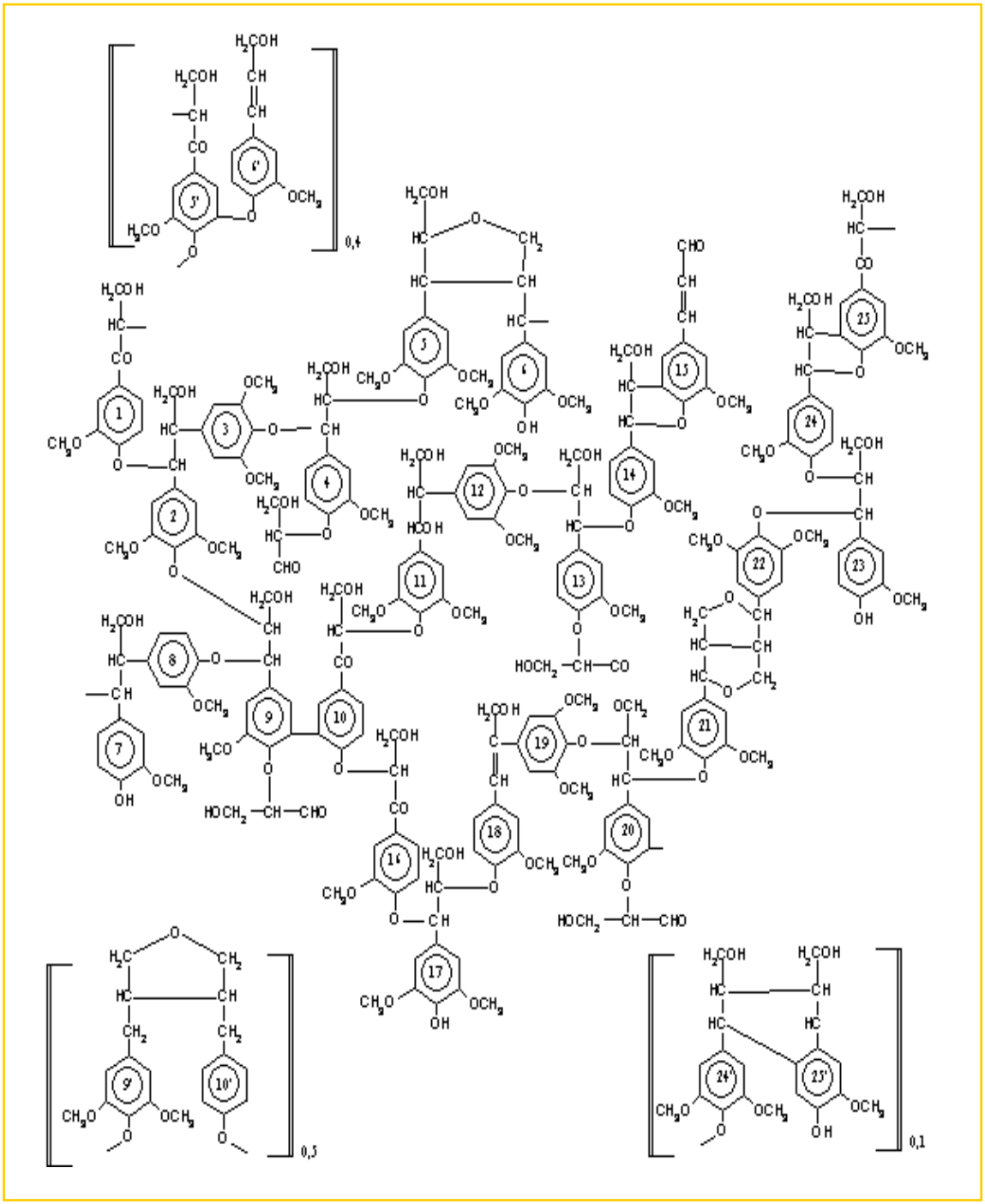

Fig. 1.4: Structure of the lignin (*Fagus sylvatica)* proposed by Nimz (1977).

The acidic functional groups associated with wood consist of:

(i.) carboxylic acid groups with a pKa comprised between 4 and 5;

(ii.) phenolic hydroxyl groups with an approximate pKa value of 10; and

(iii.) weakly acidic hydroxyl groups present in polysaccharides with a pKa of roughly 14.

With the exception of pulps that contain significant levels of sulfonate groups, carboxylic acid groups on the hemicelluloses are the main functional groups that give rise to the generation of charged sites on the fibres under typical papermaking conditions (Dang *et al*., 2006; Fras *et al*., 2004; Bardwaj, 2004; Lindgren and Öhman, 2000; Lloyd and Horne, 1993; Katz *et al*., 1984; Sjöström and Enström, 1966).

During kraft pulping of wood, a significant proportion of the initial 4-O- methylglucoronic acid side group (MeGlcA) of xylan are converted to hexenuronic acids (HexA) which can contribute to the fibre charge of kraft brownstock. Pulping conditions and green liquor pretreatment, prior to pulping, strongly affect the formation and stability of HexA. Alkaline pulping also results in the formation of new polysaccharide carboxyl groups, generated from the peeling reaction which is stopped by the formation of metasaccharinic acid or other alkali-stable carboxyl groups. The residual lignin in kraft pulps is well-known to contain carboxylic acid groups. The bleaching of kraft pulps is directed at removing residual lignin, hexenuronic acids, and other chromophoric compounds. The kraft pulping process and bleaching processes including oxygen delignification, peroxide bleaching, and ozone bleaching not only remove these components but also generate new carboxylic acid groups (Dang et al., 2006).

1.2. Pulping processes

Theoretically, all natural fibrous materials can be used to manufacture paper, and many have been tried but only a few have proved to be practical. Wood pulp is by far the most important source of papermaking fibres. Pulping processes can be grouped into three categories according to the form of energy used for the “detachment” of the fibres (Sixta, 2006):

(i.) mechanical pulping processes "liberate" fibres by the application of pure mechanical energy with little or no chemical added;

(ii.) chemical pulping processes "liberate" fibres by using chemicals reacting with the lignin. As a result, the lignin, that binds the fibres together, is either dissolved or softened to the point that the fibres will fall apart with only mild mechanical treatment; and

(iii.) semi-mechanical pulping processes combine chemical and mechanical means. Examples of processes are the neutral sulfite semi-chemical, and kraft semi-chemical processes used in the production of corrugating medium and linerboard, respectively.

Each pulping has its advantages and disadvantages related to wood species, yield and relative strength, and consequently, different pulping processes may be used to prepare pulps for different paper grades. For instance, fibres obtained by mechanical pulping processes are generally shorter than those obtained through chemical pulping. Similarly, mechanical pulps contain high amounts of fine elements. All these characteristics directly impact the properties of the produced papers.

Besides, there are large chemical differences between groundwood and chemical pulps, namely their lignin and hemicelluloses contents and distributions. Investigations have shown that lignin restricts fibre swelling in water, decreases fibre-to-fibre bonding, and acts to stiffen fibres, all of which contributing to the low strength, high bulk, and high opacity of papers made from groundwood pulps. As a result of lignin removal, bleached chemical fibres swell more rapidly during beating and become more flexible. Additionally, surface enlargement occurs and numerous interfibre bonds can form (Sixta, 2006; Scott and Abott, 1995). Moreover, the different mechanisms by which the lignin is removed in the various chemical pulping processes result in property differences among pulps.

The major influence of pulping processes on cellulose is to decrease the average polymer chain length, which does not seem to affect significantly the strength properties of the fibres until a particular critical value is reached, after which this strength decreases rapidly. The extent of depolymerization varies greatly with different pulping

processes, being less with mechanical pulps and greater in acid sulfite pulps (Sixta, 2006).

The hemicelluloses content and distribution in the fibre wall can be also modified by the pulping processes. In general, we can say that hemicelluloses is known to improve interfibre bonding, and removing some of them allow obtaining papers for which high tear, sheet softness, and opacity are essential. HW pulped by a neutral sulfite semi-mechanical process contain high hemicelluloses content, and provide the stiffness properties required for corrugating medium. On the other hand, alpha-pulps produced by hot alkali purification of sulfite pulps or prolonged acid sulfite cooking are essentially free of hemicelluloses and produce soft and opaque papers (Sixta, 2006).

Regarding now the production of pulps, almost 360 million tonnes of fibres (virgin wood pulp, other fibre pulps and recovered paper) were used as fibre furnish in 2009. The amount has more than tripled since 1965, and the recovered paper has sustained most of the growth: in 2009, 182 million tonnes were collected and processed. Non-wood and other types of pulps accounted for a minor share with 18 million tonnes (5%) in 2009.

Tab. I.2: Shares of global used by grade (1999-2009) from FAOSTAT (2011).

Wood pulp grade	***2009 production (million tonnes)***	***Share by volume (%)***		
		1999	***2004***	***2009***
Chemical	118.7	38.0	36.2	33.0
Mechanical	28.5	11.3	10.3	7.9
Dissolving	3.6	0.9	0.9	1.0
Semi-chemical	9.2	2.5	2.5	2.5
Other fibre pulp	17.8	4.8	4.8	5.0
Recovered paper	181.6	41.8	45.4	50.5
Total	359.3	100.0	100.0	100.0

The production of virgin wood pulp was 160 million tonnes in 2009 (44.5% of fibre furnish). Between 2004 and 2009 wood pulp output decreased by 9%, and the

economic crisis in 2008-2009 caused a 10% fall year-on-year. Northern America is still the largest producer region with 40.6% of the world total. Europe is the second with 27.6% and Asia and Latin America follow with 15 and 13.5% shares, respectively. Expansion of Latin America's wood pulp production was 48% from 2004 to 2009. Northern America closed one fifth of its output in the same period (see Table I.3).

Tab. I.3: Production of wood pulp in 2009 (regional shares and changes) from FAOSTAT-ForeSTAT (2011).

Region	*2009 production (million tonnes)*	*Shares (%) 2009*	*Change (%) 2004/2009*	*Change (%) 2008/2009*
Africa	2.7	1.7	1.6	-9.7
Northern America	64.9	40.6	-19.7	-11.5
Latin America	21.6	13.5	48.4	6.4
Asia	23.9	14.9	-4.9	-16.0
Europe	44.2	27.6	-11.7	-11.1
Oceania	2.7	1.7	0.04	-9.6
World	**159.9**	**100.0**	**-9.1**	**-10.0**

Chemical wood pulp dominates the production with 74% share of all wood pulps. Mechanical pulp accounts for most of the rest with 18%. Dissolving and semi-chemical wood pulps are of lesser importance.

The rise of fast-developing nations is obviously changing the regional breakdown of wood pulp production. The so-called "BRICs" (Brazil, Russia, India, China), have maintained a steady growth rate in wood pulp production, whereas the developed countries have closed uncompetitive capacity in their old mills. Northern America and the Nordic countries have not built new production lines in the past 15-20 years. Asian countries have built new production capacity in the recent times: in East and South Asian countries this happened already in the 1990's, while in China more actively only since 1997.

Latin America's expansion has been impressive in chemical wood pulp, led by Brazil where production has increased from 9.6 million tonnes in 2004 to 13.9 million

tonnes in 2009. In the last five years, the world's biggest and modern pulp mills have been built in Brazil, Uruguay, China and Indonesia. These countries are expected to be favored destinations for greenfield projects also in the near future, accompanied by projects in Russia, Oceania and Africa. Emerging biorefinery investments in Northern America and in Europe will be brownfield investments, i.e., alterations of existing pulp mills.

The United States hold a 30% global share of wood pulp output, ahead of Canada (11%) and Brazil (9%). The following nine countries account for 29% of the world production (see Figure 1.5), and among them Sweden, Finland, Japan, Russia are the leading ones. The rise of China's paper consumption is feeding growth in pulp industry especially in Asia and in Latin America. China's virgin fibre availability from domestic sources continues to be constrained in spite of massive planting of new forests.

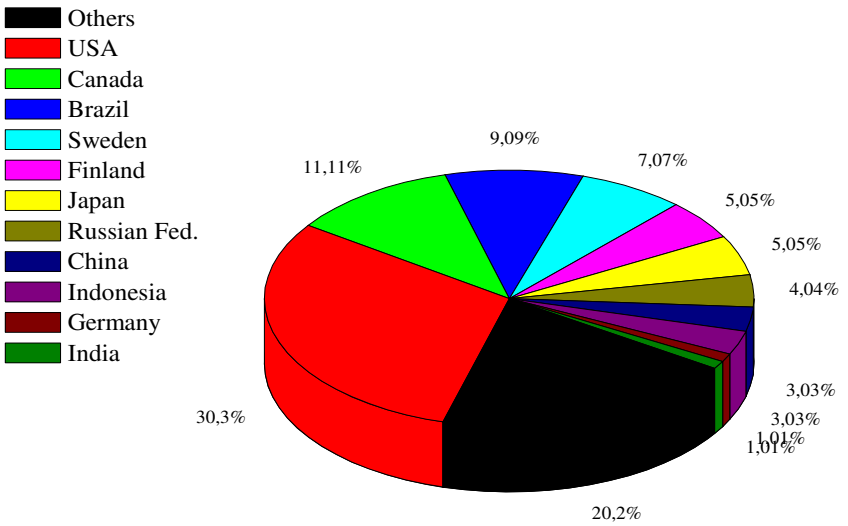

Fig. 1.5: World's leading producers of wood pulp in 2009 from FAOSTAT (2011).

1.2.1. Mechanical pulping processes

Mechanical pulping processes are carried out with SW fibres, and they show 90-95% yield. Their main advantages are low costs and high pulping yields, as well as good printability of the produced papers. On the other hand, the main disadvantages are low aging qualities and low strength of the papers (Sixta, 2006).

The oldest mechanical pulping process is the stone groundwood. In this process, a bolt of wood is pressed lengthwise against a roughened grinding stone revolving at peripheral speeds of 1000 to 12000 m/min. The slurry of fibres and fibre fragments is screened to remove shives and other oversized particles. Subsequently, it is thickened by removal of water to form a pulp stock suitable for papermaking. The principle is simple, but efficient production of a uniform and good quality pulp requires careful control of the stone surface roughness, pressure of the wood against the stone, and shower water temperature and flow rate (Scott and Abbott, 1995).

In the 1950s, a mechanical pulping process have been developed involving shredding and grinding of wood chips between the rotating discs of a device called a refiner. Refiner mechanical pulping usually produces pulps with longer fibres than stone groundwood. Mechanical pulps allow the production of highly opaque sheets having excellent printing properties. However, the paper is weak and discolors readily on exposure to light (Scott and Abbott, 1995).

1.2.2. Thermomechanical and chemitermomechanical pulping processes

The basic refiner mechanical pulping process has undergone many enhancements. Today, most installations employ pre-softening of the chips with steam to modify both energy requirements and the resulting pulp properties. The obtained pulp, called thermomechanical pulp or TMP, is usually much stronger than the common refiner mechanical pulp and contains very little screen reject material (Scott and Abbott, 1995).

In addition to steam pretreatment, chemicals such as sodium hydroxide and sodium sulfite, can be used to pretreat wood chips prior to defibering them in a refiner. Chemical pretreatments can lead to improvements in pulp strength and brightness. Pulps

produced in this way are referred to as chemithermomechanical pulps or CTMP (Scott and Abbott, 1995).

1.2.3. Kraft chemical pulping processes

Chemical pulping processes involve cooking wood chips with chemicals at high temperature and pressure in an enclosed vessel called a digester. The cooking chemicals soften and dissolve the lignin holding the fibres together in wood, resulting in their ready separation when the pulp is expelled from the digester. These fibres are capable of producing stronger papers than those made from mechanical pulps. There are two types of chemical pulps produced today: kraft and sulfite (Scott and Abbott, 1995).

In the kraft process, which is by far the most widespread, wood chips are cooked in the presence of sodium hydroxide and sodium sulfite. Kraft cooking times depend upon the intended use of the pulp: about 1 h for used in the production of sack paper or linerboard and up to 5 h for bleachable pulps used for fine papers. As expected, the pulp yield is inversely related to the cooking time. For example, the yield for a bleachable pulp will be on the order of approximately 50% (Sixta, 2006).

One of the principal advantages of the kraft process is the existence of an efficient chemical and energy recovery system. Without such a system, the kraft process would not be economical, and it would adversely affect the environment. The functions of the kraft recovery system are:

(i.) recovery of chemicals from the spent cooking liquor (black liquor) in order to form fresh cooking liquor (white liquor),

(ii.) recovery of energy from the incineration of dissolved lignin and other wood components in the black liquor like hemicelluloses, and

(iii.) consequently minimization of air and water pollution.

1.3. Bleaching processes

The color of unbleached pulps is predominantly caused by the lignin remaining in the fibres after pulping. Consequently, the bleaching process is designed to react with lignin and either remove it or convert it to a colorless form. The former approach is taken with kraft pulps, while the latter approach is applied to mechanical pulps.

Sodium peroxide and sodium dithionite are bleaching agents commonly used for high yield pulps. Single-stage bleaching is practiced. By this way, only moderately high brightness is achieved, and the bleaching effect is not permanent. The pulp undergoes brightness reversion over time. Lignin-removal bleaching methods are applied to low yield kraft pulps. Various chemicals (ClO_2, O_2, H_2O_2 and O_3) can be used, and multi-stage bleaching is practiced (Sixta, 2006). Very high brightness can be achieved, and the bleaching effect is permanent.

A bleaching stage consists of three steps:

- the mixing step: the pulp is mixed with bleaching chemicals and steam may also be added in the mixer if an elevated temperature is required.
- the reaction step: chemicals and pulp fibres are allowed to react in a large tank called a bleaching tower. The residence time in the bleaching tower, coupled with chemical charge and temperature, determines the degree of bleaching
- the washing step: excess bleaching chemicals and reaction products are separated from the bleached pulp (Sixta, 2006).

1.4. The papermaking process

Papermaking is a process in which several steps or unit operations succeeding: stock preparation, sheet forming, pressing, and drying stages. In the stock preparation area, non fibrous components (chemical additives and fillers or pigments) are mixed with recycled or virgin fibres and broke. Broke corresponds to papers, which are not shipped from the mill. Examples are paper trimmed from edges in various finishing

operations, paper produced during paper machine breaks, paper having holes and other defects, and so on. It is not unusual for a mill to internally recycle as much as 30% of the paper that it produces.

Figure 1.6 shows a scheme of this papermaking process steps.

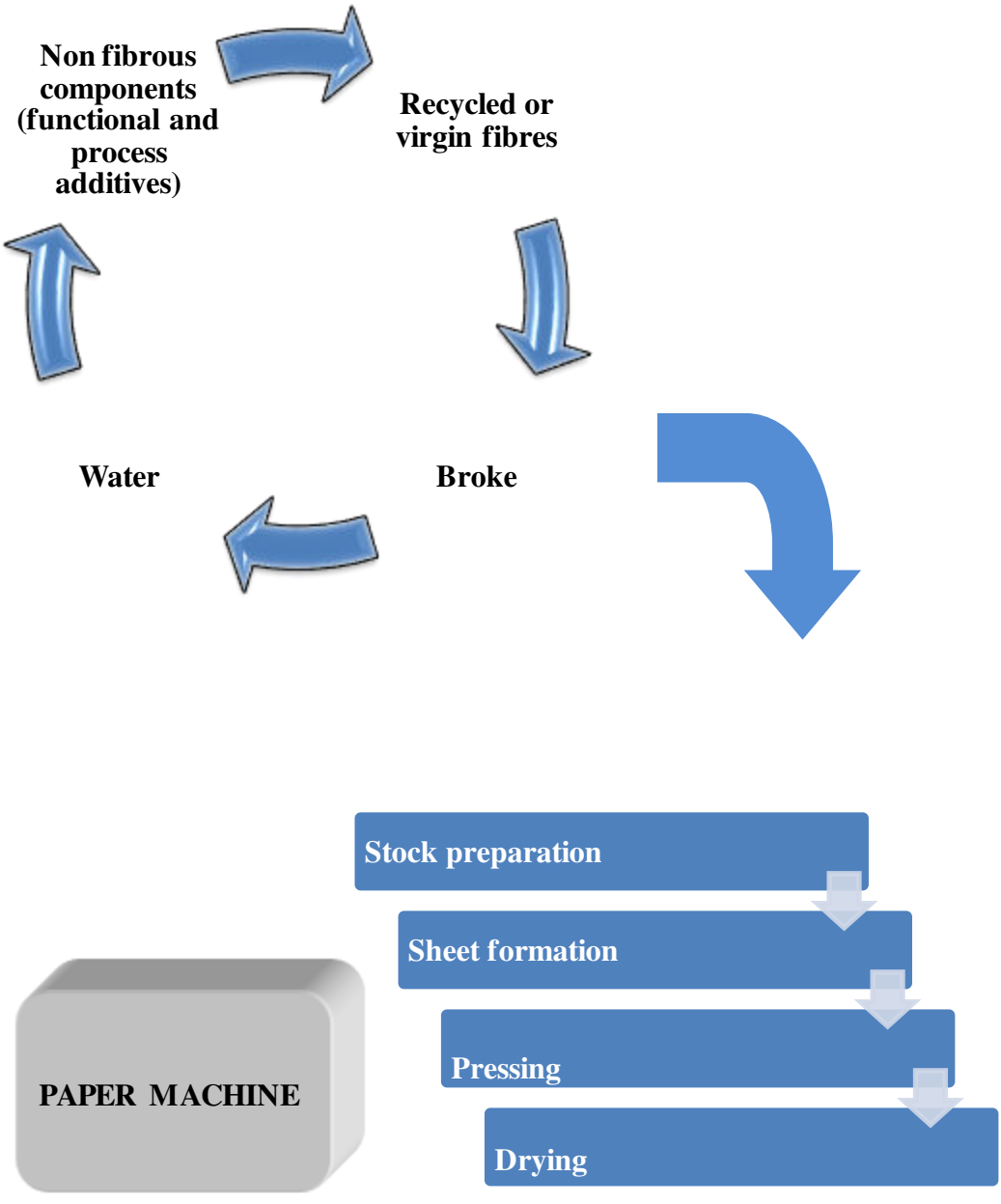

Fig. 1.6: Scheme of papermaking process steps.

1.4.1. The stock preparation area

The stock preparation area is the location in a paper mill where furnish is prepared for papermaking. Several functions are required to do this. Table I.4 shows the equipments commonly employed to achieve these functions.

Tab. I.4: Functions and related equipments employed in stock preparation from Scott and Abbott (1995).

Function	***Equipment***
Pulping or defibering of dry pulp or broke	Pulper
Storage of pulp and furnish slurries	Stock chests
Adjustment of stock consistency	Consistency regulators
Fibre refining to develop properties	Beaters, jordans, disc refiners
Metering and blending of furnish ingredients	Stock proportioners, magnetic flow
Removal of dense contaminants from stock	Forward cleaners, reverse cleaner, through cleaners
Removal of oversized contaminants	Pressure screens
Removal of air from stock	Stuffbox, deculator

Fibre slurries are prepared at approximately 4-5% consistency either by defibering market pulp in a pulper or by diluting high consistency stock slurries pumped directly from the pulp mill (Sixta, 2006). After, the slurries are stored in stock chests. If secondary fibres are to be incorporated in furnish, they are treated more or less in the same way, but the cleaning operations (centrifugal cleaning and pressure screening described hereafter) are more intensive and deinking stage may be added to the process.

The step immediately following the preparation of pulp slurries is usually beating or refining to develop pulp and paper properties. Three types of equipment can be used for this purpose: Hollander beaters (cigarette papers), conical refiners, and disc refiners (most common). In all three cases, the fibres are subjected to mechanical action from bars passing over one another in the presence of water (Scott and Abbott, 1995). The repeated passage of pulp through zones of compression and shearing cause fibre surfaces to become frayed while the internal layers of the fibre wall separate. Consequently, the fibres absorb very large amount of water: the fibres swell, and become more flexible and conformable. Then, in the formed web, the contact surface between fibres is enhanced and the fibre-to-fibre bonded area increases (Lindström *et al.*, 2005). To summarize, the main actions of refining can be described as follows:

(i.) internal fibrillation caused by the breakdown of fibres walls into separate lamellas, which increases the flexibility of fibres so that during the sheet formation the fibres conform to each other producing large areas of intimate contact;

(ii.) external fibrillation described as the creation and/or exposure of fibrils on the fibre surface; and

(iii.) the generation of fines from fibres when these are not able to sustain compressive and/or shear forces during the treatment anymore.

Schopper-Riegler degree (^{o}SR) is used to evaluate the refining level. It gives the ability of water to drain away from pulp slurry under conditions of a forming pad. The greater the degree of refining the slower the water drains from the slurry. Typical values for refined pulps range from 20 to 40^{o} SR, even if very high levels of refining are required for certain paper grades (tracing papers for example). In general, HW tends to have lower drainability than SW fibres.

The papermaker has the choice of either refining different types of fibres separately or together. In modern mills, separate refining of HW and SW fibres is always practiced. Once refined, the fibres are stored in refined fibres chests. After that, the fibres are pumped to a metering and blending system and finally to the machine chests. Then, the stock is sent through a stuffbox, which is a device that provides a constant flow of stock to the basis weight valve. The basis weight valve would be

located immediately after the stuffbox, and serves to control the amount of furnish pumped to the paper machine. As its name implies, the basis weight valve controls the average basis weight of the paper made on the machine. Sometimes, a conical refiner is used to cut the fibres to a certain degree. This shortening improves the fibres distribution in the formed web, but tends to slow down the water drainage rate on the forming section of the paper machine. A dilution is carried out in a stream labeled "whitewater from paper machine". Before this dilution step, the pulp slurries in the stock preparation system are all above 3 to 4% consistency. After the dilution step, the furnish consistency is 0.5 to 1% (Scott and Abbott, 1995).

Centrifugal cleaning refers to a multiple-stage operation that removes small particulate contaminants having densities greatly different from fibres. The contaminants whose densities are greater, such as sand, pipe scale, and other small dense particles are removed by devices known as forward cleaners. The contaminants whose densities are much less than fibres are removed by devices called reverse cleaners. In both cases, the operating principle is the same. For example, in a forward cleaner, the stock is introduced tangentially to the upper cylindrical body of the cleaner under high pressure. The stock swirls down through the body of the cleaner, subjecting the particle in the slurry to high centrifugal forces. Under these forces, dense particles tend to migrate toward the walls. Upon striking the walls, the particles slide down and are removed at the lower tip. Meanwhile, the lighter fibres and other light furnish components migrate toward the center of the cleaner where they reverse their flow direction. The separation of dense contaminants from fibres is not perfect, and a certain quantity of fibres is lost. In order to minimize the loss of fibres and other desirable materials, rejects from the first stage of cleaners (the primary stage) are used as input to a second cleaner stage, and rejects from the secondary stage are usually taken to a third, or tertiary stage. Sometimes a fourth stage is used, also. Accepts from the second, third and fourth stages are recycled to the input streams of the preceding stages (Scott and Abbott, 1995). Rejects from the final stage are discarded. By using such a multiple-stage cleaning system, it is possible to minimize fibre loss and still ensure that most of the dense contaminants are removed from the stock prior to the paper machine.

In modern papermaking systems, accepts from the first centrifugal cleaner stage go to a deaerating step where dissolved and entrained air is partially removed. This decreases the tendency of furnish to foam and also ensures that water will drain rapidly

when the sheet is formed. The deaerator operates by subjecting furnish to vacuum, which causes the air to boil out.

After the cleaners, the deaereted furnish is pumped to a pressure screen that removes oversized contaminants. There are several different configurations of pressure screens in use today. They require the accepted stock to pass through holes or slots. Rejects too large to pass through the screen openings leave through a rejects port. Since the stock has a tendency to blind over the screen openings, a hydrofoil unit rotates within the screen and acts to keep the slots and holes free of fibres and other materials. From the screen, the stock travels to the headbox, which is the initial component of the paper machine (Scott and Abbott, 1995).

1.4.2. Paper machine

The invention of papermaking in A.D. 105 is often attributed to Ts'ai Lun, a member of the Chinese Emperor's Court. From that time, all paper was made by hands until 1798 when the paper machine was invented by Nicholas Louis Robert, a French papermaker. Robert's machine was improved by Bryan Donkin and John Gamble in England. Their work was financed by the Fourdrinier brothers, after whom the machine was named. The Fourdrinier paper machine consists of the headbox, fourdrinier forming section, press section, drying section and reel. The stock flows from the stock preparation area to the headbox, and then onto the forming section. The resulted wet fibrous mat is conveyed through the press and drying sections. The paper is finally wound up on the reel.

1.4.2.1. Headbox and forming section

The headbox has three basic functions:

(i.) to spread the stock over the width of the machine,

(ii.) to achieve uniform distribution of fibres and other materials throughout the sheet of paper,

(iv.) to ensure that the stock is traveling as fast as the forming section when the fibres come into contact with the forming fabric, even if small differences can be manipulated to modify paper properties (Scott and Abbott, 1995).

It is worth noting that the headbox affects the directional characteristics of the sheet in two ways. First, the acceleration of the fibre slurry in the slice region causes many of the fibres to rotate so that their long axes are more parallel to the direction of flow. This produces the machine direction fibre orientation preference found in most paper sheets. Second, if the slurry is not travelling at the same velocity as the Fourdrinier wire, the fibre orientation will be affected. For example, if the slurry is travelling slower than the wire, the wire tends to align the fibres more in the machine direction. If the slurry is moving faster than the wire, the fibres are slowed when they hit the wire and turn crossways, along the cross direction. In practice, the ratio between the slurry velocity and wire speed is kept very close to 1.0. Thus, the major contributor to fibre orientation is flow acceleration in the slice (Scott and Abbott, 1995).

On the forming section of the paper machine, the distribution of fibres can be influenced to some degree by drainage disturbances. On slower machines, the upper end of the forming wire is often shaken back and forth in an attempt to randomize the fibre orientation and make the paper less directional in character. On the other hand, local severe drainage conditions on the wire can move the fibres and lead to poor formation. In addition to the machine direction/cross direction unevenness induced by the paper machine, the drainage conditions on typical Fourdrinier and cylinder machines produce a variation in the composition of the sheet from the top to the bottom, which causes two-sidedness (Scott and Abbott, 1995). This is a result of draining the sheet from one side only during formation.

When the first layer of fibres are deposited on the forming fabric, fines, filler, and other small particles pass on through, leaving the longer fibres to form the web. As succeeding fibres are deposited, they form a tighter mesh, which is more efficient at retaining small particles in the web. Thus, concentration of small-sized material

increases when moving through the sheet from the wire side to the felt side (Scott and Abbott, 1995). The effect can be minimized but never completely overcome:

(i.) retention aids properly used may limit the two sidedness by flocculating small elements (that is increasing their apparent size), and by attaching small elements to fibres which are well retained; and

(ii.) twin-wire formers allow the drainage from both sides of the sheet and lead to a more symmetrical distribution of fines and filler through the sheet.

Thus, the headbox and forming section determine the sheet formation and directional unevenness of the paper sheet.

1.4.2.2. Press section

After the forming section, the wet paper web is transferred to a press felt and conveyed into the press section. In the press section, the web is dewatered by squeezing it between pairs of large rolls. The press felt absorbs water as it is expressed from the sheet. Pressure from the presses compact the sheet and forces fibres to come into closer contact. In this manner, pressing is an essential step for the subsequent formation of fibre-to-fibre bonds in the drying section (Lindström *et al.*, 2005). If too much pressure is applied very rapidly, the water inside the sheet will actually move fibres about and disrupt the sheet formation. This phenomenon is called crushing and should be avoided since it adversely affects paper properties (Scott and Abbott, 1995).

1.4.2.3. Drying section

When the sheet leaves the press section, it typically contains 40% solids and 60% water by weight. The fibres can accommodate large amounts of water inside their structure. Many fibres also hold much water in the pores and interstices of their walls. This water is held very tightly and evaporative drying is necessary to remove further water from paper and bring it to its final moisture content of 4 to 7% (Scott and Abbott, 1995).

An important function of the drying section is the "setting" of interfibre bonds in the sheet. It is believed that, as the moisture content of the web approaches its final value, strong capillary pressures are established inside the sheet that force the fibres into the very close contact required for the establishment of fibre-to-fibre bonds. These forces are often referred to as "Campbell forces".

After sheets leave the dryers, the draw tensions are released, but the internal stresses at the fibre crossings remain because the fibres are now bonded tightly together. These internal stresses significantly affect the relative values of machine direction and cross direction mechanical properties (Scott and Abbott, 1995). These internal stresses are also a source of dimensional instability in paper whenever a sheet is exposed to increased relative humidity. This results in fibre swelling which relaxes the stresses at fibre-to-fibre bonding points, causing the sheet to become wavy or cockled. From this discussion, it appears that the drying section influences many other properties of paper sheets besides its moisture content.

1.4.2.4. Reel section

Once the sheet has been formed, pressed, and dried, it is collected on a large roller at the reel of the paper machine. The paper is wound around a spindle until a large diameter roll is built up. The paper is then broken and transferred to a fresh spindle and the completed roll or log of paper is removed from the machine for further treatments. A log may contain as much as 20 tonnes of paper. The transfer of paper from one spindle

to another is known as a "turn-up" and may be done by hand on slower paper machines. On modern high-speed machines, reel turn-up is carried out automatically (Scott and Abbott, 1995).

1.4.2.5. Machine calendering

The final paper machine operation that we will consider is machine calendering. Here, dried paper is passed through one or more nips formed by chilled steel rolls under pressure. One of the major functions of the calender stack is to adjust the uniformity and value of the thickness of paper. Smoothness is another property that is improved by machine calendering. The response of the paper web depends on the moisture content of the sheet. The higher the moisture content, the more pliable and plastic are the fibres and the greater are the effects of calendering (Scott and Abbott, 1995).

1.5. Nonfibrous raw materials in papermaking

Only a limited range of properties can be achieved in manufactured papers from wood fibres only. Because of this, the papermaker combines the choice of wood fibres with a wide array of chemical additives when preparing furnish. These additives fall into two categories: functional and processing additives (Scott and Abbott, 1995). Some examples of nonfibrous additives in the papermaking furnish are: wet strength resins (improving strength of paper when saturated with water), dry strength agents (improving dry strength), dyes (tinting and shading of paper), fillers (improving opacity, brightness, smoothness of paper), sizing agents (imparting resistance to penetration by aqueous liquids), retention aids (improving retention of fillers and fines during sheet formation), pitch control agents (preventing pitch deposits on machinery), defoamers (preventing foaming of paper stock), slimicides (preventing growth of slime and other biological substances in the papermaking system), etc.

1.5.1. Functional additives

Functional additives are chemicals that either enhance an existing property or impart a new property to paper. Some examples are: sizing agents such as rosin size, alkyl ketene dimers (AKD) and alkenyl succinic anhydride (ASA); dry-strength agents such as cationic starch, gums and polyacrylamides; wet-strength resins such as formaldehyde based resins and polyamideamine resins; coloring and tinting agents such as acid, basic and direct dyes, and colored pigments; fillers such as talc, clay and calcium carbonate.

1.5.2. Chemical processing aids

The chemical processing aids promote the performance of a functional additive or assist the papermaker in maintaining the cleanliness and runnability of a paper machine system. Some examples are: retention aids such as cationic and anionic polyacrylamides, polyamines and cationic starch; defoamers; microbiological control agents; pitch control agents such as talc, alum and dispersants; drainage aids; formation aids such as high molecular weight anionic polymers.

1.6. The production of wet strengthened papers

1.6.1. Adsorption phenomena during preparation of wet-strengthened papers

The adsorption of polyelectrolytes from solution onto solid, liquid, or gas interfaces defines a vast field, one that encompasses innumerable phenomena and many technologies. Thus, only some important considerations will be described here. Figure 1.7 displays how flexible polyelectrolyte homopolymers interact with a flat and charged surface. The left-hand side of this scheme indicates the behaviour at low concentration of salts (cs) (a condition typically dominated by electrostatic interactions), while the right-hand counterpart illustrates the behaviour at high cs (a condition requiring additional consideration of the segment–surface interaction energy χs and possibly the segment–solvent interaction energy χ).

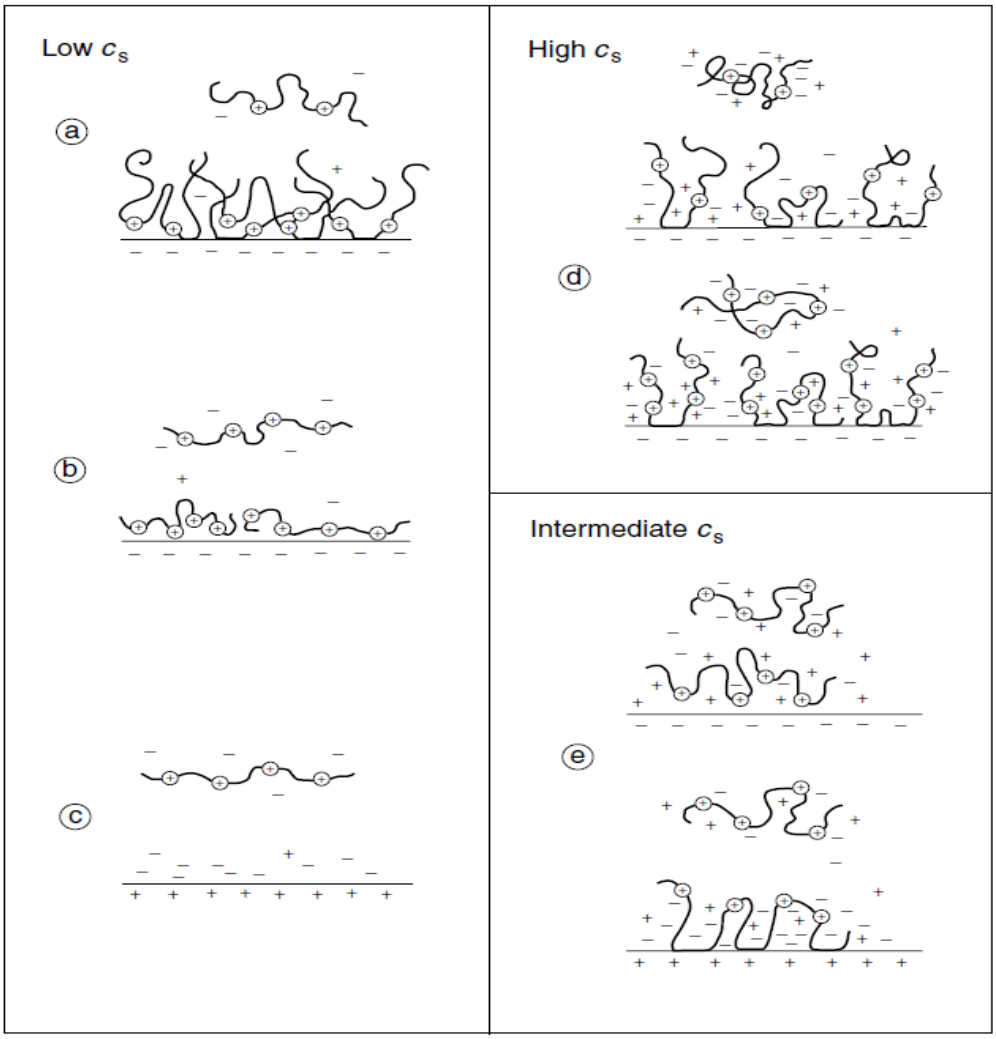

Fig. 1.7: Pictorial representations of polyelectrolyte adsorption for conditions of surface charge density, polymer charge density, and ionic strength from Dautzenberg (1994).

Diagram 'a' represents the adsorption of a lightly charged polyelectrolyte from dilute solution onto an oppositely charged surface. In this case, there is a compensation of the surface charge by the polyelectrolyte, the adsorbed amount is high, and the adsorbed layer is thick (thickness ~ R_g). When the polyelectrolyte is more highly charged, as sketched in diagram 'b', there is again charge compensation, but the adsorbed amount is lower and the adsorbed layer is much thinner (thickness << *R*g). Diagram 'c' shows that polyelectrolytes typically do not adsorb onto similarly charged surfaces when cs is low because electrostatic repulsions cannot be overcome by even large positive segment–surface contact energy. Turning to the right-hand side of the

Figure 1.7, the top portion of diagram 'd' shows the adsorption at high cs for a lightly charged polyelectrolyte attracted to an oppositely charged surface by positive segment–surface interaction energy. The bottom portion of the same diagram shows the analogous situation for a more strongly charged polyelectrolyte. The strong screening of electrostatic interactions yields similar features for both cases, including the adsorbed amounts and the layer thicknesses. Electrostatic interactions are essentially irrelevant. The bottom of the right-hand side, diagram "e", describes behaviour at intermediate cs and either electrostatics (top portion) or segment–surface interaction energy (bottom portion) can dominate. In the latter case, a polyelectrolyte adsorbs to a similarly charged surface with its fixed charges positioned as far as possible from the surface (Dautzenberg *et al.*, 1994).

Combining steric (i.e. configurational), osmotic, and electrostatic contributions, adsorbed/attached polyelectrolytes can modify interparticle forces in complex ways. Stabilization typically ensues when polyelectrolytes are irreversibly adsorbed/attached to particle surfaces at high density and in such a way that the chains extend significantly into the solution phase. It is important for stabilization that the thickness of the adsorbed/attached polyelectrolyte layer exceeds the distance to the primary minimum of the van der Waals attraction. Charge neutralization is effective when a polyelectrolyte of low molecular weight and high charge density is introduced to a dispersion of oppositely charged particles. The chains adsorb as a thin layer to an adsorbed amount that effectively compensates for the particle charge.

1.6.2. Main parameters affecting the wet strength of PAE-based papers

Generally speaking, wet strength agents like PAE are added to the stock suspension after the refining step. They are usually introduced before the mixing chest. If a high wet strength is required, CMC (carboxymethyl cellulose) is added just before in order to increase the adsorbed amounts of PAE as previously discussed (Part I). As the effect of the addition of CMC will not be studied in this work, we will not describe related studies from the literature.

1.6.2.1. Preparation of PAE-based papers and wet strength determination

From an analysis of the literature data (see Table I.5), the pulps used for preparing PAE-based papers are bleached or unbleached HW or SW kraft pulps or mixtures of them, refined at different levels but with Schopper Riegler degrees rarely exceeding a value of 35. In certain cases, the fine fraction is removed before the treatment with PAE and the tested pulps may be protonated. In order to study the mechanisms of wet strength development, some works are based on the use of specific pulps with various content in carboxylic groups (TEMPO-oxidized or carboxymethylated pulps, linter pulps and methylamidated pulps). Internal addition of PAE is the most common procedure for obtaining wet strength papers but, in some studies, a soaking treatment of the handsheets is also performed in PAE aqueous solutions. Handsheets are produced on standard former or on dynamic former in order to limit the influence of the pulp flocculation induced by the PAE addition. The drying conditions of the handsheets may vary as well as those of the thermal post-treatment (if this treatment is carried out). Finally, the soaking time in water of the paper strips before the measurement of the wet tensile strength is also a variable parameter. Table I.5 reports the main experimental conditions encountered in a selection of published works.

Tab. I.5: Experimental conditions encountered in a selection of published works for preparation of PAE-based papers and wet strength determination.

Tested pulp	*Mode of addition, added amount and contact time*	*Drying and /or thermal post-treatment of the handsheets*	*Determination of the wet tensile force*	*Authors*
Commercial bleached SW refined at 25°SR.	PAE added into the pulp suspension (pH=7.5)	Curing at 105°C for 1 h.	Soaking time: 1h in deioni-zed water	Espy and Rave, (**1988**)
Pine unbleached kraft pulps refined at 35°SR; Whole and classified pulps.	PAE (1%) added into a 0.5% pulp suspension (pH=4.5); Contact time: ns*; Soaking of handsheets in aqueous solutions containing PAE; Contact time: 30s.	Drying at 105°C for 7 min	TAPPI T456	Stratton (**1989**)

Tab. I.5 continued

Tested pulp	*Mode of addition, added amount and contact time*	*Drying and /or thermal post-treatment of the handsheets*	*Determination of the wet tensile force*	*Authors*
Commercial bleached SW pulp; carboxymethylated pulps; Fines removing procedure.	PAE added into the pulp suspension (pH=6.6); Contact time: 5 min.	Drying: ns*; Curing at 105°C for 1 h.	Soaking time: 10 s in deionized water.	Wägberg and Björklund, **(1993)**
ns*	ns*	Drying at 105°C for 10 min; Curing at various temperatures and times.	Soaking time: 1 h in deionized water	Devore and Fischer, **(1993)**
Laboratory unbleached SW kraft pulp; Fines removing procedure.	PAE (2%) added into a 0.25% pulp suspension (pH=8); Contact time: 30 min.		SCAN P20:95	Häggkvist *et al*., **(1998)**
Commercial HW bleached kraft pulp (HBKP) refined at 23°SR.	PAE (0.3%) added into a 0.15% pulp suspension (pH=7); Contact time: ns*.	Uncured: drying at 23°C and 50% RH; Cured: 100°C (2 min) + 110° (10 min).	Soaking time: 30 min in deionized water	Obokata and Isogai, **(2004a)**
Laboratory unbleached and bleached spruce kraft pulps; Fines removing procedure.	Soaking of handsheets in aqueous solutions containing 0.5, 0.6 and 6% of PAE (pH=8); Contact time: 1 min.	Dried under restraint and cured for 20 min at 105°C after the impregnation.	ns*	Andreasson *et al.,* **(2005)**
Mixture of SW and HW bleached kraft pulps refined at 25°SR.	PAE added into a 0.5% pulp suspension at pH=7; Various contact times.			Yoon **(2007)**
Commercial HBKP; methylamidated HBKP; Linter pulp; TEMPO-oxidized linter pulp.	PAE added into the pulp suspension (pH=7.8); Contact time: ns*; Soaking of handsheets in aqueous solutions; Contact time: 10s.	Uncured: drying at 23°C and 50% RH Cured: 110°C for 10 min.	Soaking time: 30 min in deionized water.	Obokata and Isogai, **(2007)**
Cotton linters, fibrillated cotton linters (refined in a PFI mill at 42°SR and 61°SR), TEMPO-oxidized cotton linters.	Soaking of handsheets in 0.1% to 0.4% PAE aqueous solutions; Contact time: 10s.	Uncured: drying at 23°C and 50% RH; Cured: 100°C (2 min) + 110°C (10 min).	Soaking time: 30 min in deionized water.	Obokata and Isogai, **(2009)**

*ns: not specified

1.6.2.2. Adsorption of PAE resin

Adsorption of PAE resin is affected by several parameters, which mainly are: the PAE dosage, the charge density of the polymer, its molecular weight and polydispersity, the charge of the fibres, their ability for swelling, the porosity of the fibre wall, and the chemical environment. Some of these parameters can directly impact the polymer conformation in solution and on the fibre surface. Table I.6 shows the main characteristics of PAE solutions used in different studies. One can observe that the charge density of the PAE is close for all the presented studies. Oppositely, the MW is characterized by extremely great variations, probably denoting a certain variability of the available commercial products and the difficulty to compare values obtained in different experimental conditions and techniques.

In order to quantify PAE adsorption (adsorbed amount of PAE / added amount of PAE), two techniques are mainly described in the literature: colloidal titration and nitrogen content determination. The results obtained from all these techniques are more or less influenced by the fact that commercial solutions of PAE contains by-products as discussed in Part I of this manuscript.

Tab. I.6: Characteristics of PAE solutions used in different studies.

AZR content (related technique)	***Charge density (related technique when described)***	***DPn or mean molecular weight, polydispersity (related technique when described)***	***PAE***	***Authors***
	2.27 meq/g at pH=6.6 (colloidal titration).		Commercial solution (Kymene 557H).	Wägberg and Björklund, **(1993)**
16% w/w (^{1}H-NMR).	About 2 meq/g (colloidal titration).	MW about 10^4 Daltons (viscosimetry).	PAE resin synthe-sized at laboratory scale.	Devore and Fischer, **(1993)**
		6700 g/mol; M_W/M_N=3.4 (SEC).	Commercial solution (Kymene 557H).	Swering and Wagberg, **(1994)**

Tab. I.6 continued

AZR content (related technique)	***Charge density (related technique when described)***	***DPn or mean molecular weight, polydispersity (related technique when described)***	***PAE***	***Authors***
	Low MW fraction: 3.1 meq/g (pH = 3) and 1.0 meq/g (pH=8); High MW fraction: 4.0 meq/g (pH = 3) and 2.1 meq/g (pH=8); Unfractionated PAE: 3.8 meq/g (pH=3) and 1.3 meq/g (pH=8); (colloidal titration).		Commercial solution (Akzo Nobel) treated or not by ultra-filtration in order to obtain two PAE fractions: low and high MW fractions.	Häggkvist *et al.*, **(1998)**
		37000 g/mol with fractions down to 350 g/mol (NMR self diffusion).	Commercial solution (Eka Chemicals).	Andreasson *et al,* **(2005)**
	5 meq/g at pH = 7 (colloidal titration).	MW about 500 000.	Commercial solution	Yoon **(2007)**

Elementary analysis allows determining the nitrogen content of the handsheets and from the comparison with the nitrogen content of the PAE solution and that of reference handsheets (non treated handsheets), it is possible to evaluate the PAE adsorption. Obokata and Isogai (2004a) used this technique and studied the adsorption of a commercial PAE solution by a HW bleached sulphate pulp refined at 23°SR and at pH = 7. For an added amount of 0.3% of PAE, the adsorption was about 60% which seems to be low if considering the fact that the pulp is refined and the PAE dosage is low. In another study (Obokata and Isogai, 2007), the same pulp was treated with PAE and the nitrogen content allows determining adsorption varying between 70 and 80% for added amount ranging from 0.3% to 0.9%.

Colloidal titration: after adsorption tests (introduction of the PAE into the pulp), the amount of remaining PAE in solution can be determined by titrating the solution with an anionic polyelectrolyte (titrant such as potassium polyvinylsulfate). The main difficulty of this procedure is related to the method used for the separation of the aqueous solution containing the non-adsorbed PAE from the fibres and fines present

in the suspension. Filtrations followed or not by a centrifugation step are generally performed but the fact that very fine elements are totally removed is not ascertained. Stratton (1989) used this technique and found that the adsorption is 100% for a 1% amount of PAE added to an unbleached kraft pulp refined at 35°SR and with contact time of 5 min. For higher amounts added to the pulp (up 4.5%), the ratio of the adsorbed to the added amount decreases and saturation value is attained at about 2.5%. Wägberg and Björklund (1993) and Yoon (2007) also used polyelectrolyte titrations in order to determine the concentration of non-adsorbed polymer.

Another technique was described by Andreasson *et al.* (2005) who determined the adsorption amount by analyzing the adipic acid content (ion exclusion chromatography) after hydrolysis of the PAE. Nevertheless, they did not present the obtained results.

Adsorption of the PAE may be also monitored by zeta potential measurements of the treated fibres or fines. Stratton (1989) determined the zeta potential of fines after 5 min adsorption time with an electrophoresis technique. The obtained results show that the zeta potential is 0 for a PAE dosage of 0.15%. Moreover, by coupling zeta potential and colloidal titration techniques, it appears that, up to added amounts of 1%, the adsorption remains total even if the zeta potential exhibits a positive value of 14 mV. Finally, for higher dosages, the zeta potential reaches a plateau value of 18 mV. Streaming potential measurements were also performed by Yoon (2007) in order to measure the charge decay of fibre surface after PAE adsorption.

The adsorption of polyelectrolytes by fibre slurries is a time-dependent process often described as a three-stage process: adsorption, reconformation and penetration into the porous wall of the fibre. Very few studies precisely describe this process in the presence of PAE. As discussed above, Yoon (2007) coupled the use of colloidal titration and streaming zeta potential in order to follow the concentration of the non-adsorbed PAE in solution and the zeta potential of the fibres as a function of time. Different PAE dosages were tested between 0.25 and 1%. As expected, this work showed that the adsorbed amount of PAE depends on the contact time. For the lowest dosage, the adsorption is completed after 10 min. For the highest dosage, the needed time is longer (20 min). More surprising is the intensity of the charge decay when the zeta potential is measured. For a dosage of 0.6% of PAE, the zeta potential increases from -20 mV to 70

mV in the first minute, then comes back to nearly 0 mV after 30 min. For the lowest dosage, the zeta potential is stabilized after 20 min and for the highest one, it continues decreasing after 40 min of contact time.

1.6.2.3. Mechanisms of wet-strength development

Paper strength depends mainly on the joint strength between fibres, on the fibre strength and on the sheet formation. It is well accepted that fibre strength can play a role only if the joint strength is high enough. Polyelectrolytes absorbed by the fibres can act by increasing both the bonded area and the bonding strength. When wet strength agents are added to the pulp suspension, it is assumed that the increase in the dry strength results partly from a greater delamination force of the fibre wall induced by an anchoring of the cross-linked network into the fibre. Indeed, these polymers, which are characterized by a high polydispersity and a relative low mean molecular mass, can partially penetrate the porous structure of the wall. If the penetration occurs at a large extent (it is for example the case for small molecules like polycarboxylic acids), the cross-linking leads to brittle papers. Oppositely, if polymers are used and their molecular mass does not allow any penetration, the strength may fall because only the external layers of the fibre walls participate to the strength. A lot of works were published on this subject and among them, Häggkvist (1998) studied the wet strength of handsheets treated with unfractionnated PAE samples and fractionated ones by ultra-filtration (low and high MW fractions). NMR relaxation measurements were also performed on pulp treated with unfractionated and fractionated PAE samples in order to determine the pore size distribution of the fibres. Even if PAE treatment results in a shift towards smaller pores, there is no clear difference between the three samples. Oppositely, the wet strength of the obtained papers is significantly improved when using the high MW PAE solution. The author attributed this behaviour to the penetration to a greater extent of the low MW PAE into the interior of the fibre wall. In this case, the resin is less present onto the fibre surface and cannot create an adequate network. The work of Andreasson *et al.* (2005) reviews the previously published papers and investigates the penetration of wet strength agents into the fibre wall. By using ISEC (inverse size exclusion chromatography) and NMR techniques, the authors show that PAE polymers (at least the fraction characterized by the smaller molecular weights)

can penetrate the fibre wall as the measured average pore size decreases after adsorption. The polymers may then self-cross-link or react with groups in the fibre wall. This behaviour probably contributes to the increase of the wet and dry strengths of PAE-based papers. From these considerations, it follows that an optimal MW of the polymers probably exists. Moreover, it would depend on the characteristics of the fibres (porosity of the fibre wall, swelling ability, etc) and on their chemical environment (pH, salt concentration, for instance).

The reaction of azetidium groups with carboxylic groups of cellulosic fibres has also been largely debated as already mentioned in the Part I of this manuscript. Devore and Fischer (1993) concluded from their experimental study that no covalent bond was formed between azetidium groups of the PAE and carboxylate groups of the cellulosic fibres or CMC. At the same time, Wägberg and Björklund (1993), by using carboxymethylated pulps and FTIR investigation, stated that an ester linkage is formed between the PAE and the carboxylic groups of the fibres. They also showed that, for a constant amount of added PAE (for which the adsorption is supposed to be 100%), the wet strength increases with the degree of substitution of the carboxymethylated fibres which support the hypothesis of a chemical reaction between the carboxyl groups of the fibres and the PAE resin. In 2007, the work of Obokata and Isogai led to the same conclusion. These authors used a commercial HW bleached kraft pulp (HBKP) as such and methylamidated (whose carboxyl groups were converted to methylamide groups). For the same PAE content in the sheet, the wet strength of heated HBKP handsheets is much higher than that of heated methylamidated HBKP. These results were confirmed by comparing the behaviour of linter pulp sheets and TEMPO-oxydized pulp sheet and prepared PAE-based handsheets were subjected to a cellulase treatment. FTIR analysis of the ensuing residues revealed the presence of significant amounts of ester bonds which were attributed to the reaction of AZR with carboxyl groups of the cellulosic fibres. The authors concluded that the carboxyl groups of the fibres partly govern the obtained wet strength. A similar study was performed by the same authors in 2009 with pure cellulose pulp (cotton linters). If the pulp is highly fibrillated, there is a marked improvement of the wet strength of the papers after heating, even in this absence of carboxylic groups. This result proves that the formation of ester bonds (if it occurs) is probably not the only mechanism to consider.

1.7. Repulping of PAE-based wet strengthened papers

The papermaker can reduce raw material costs by blending virgin fibres with broke and clippings instead of discarding them in solid waste landfills. Papers with a high wet strength were traditionally considered unrecyclable, and their repulping is the focus of some studies (Bhardwaj and Rajan, 2004; Fischer, 1997; Espy and Geist, 1993).

For years, sodium or calcium hypochlorite were preferred reagents for repulping PAE-based wet strengthened papers. However, mainly because of concern about chloroform, tetrachlorodibenzodioxins, and adsorbable organic halides (AOX) in mill effluents, there is a growing interest in possible non-chlorinating repulping aids. Persulfate salts are an effective chlorine-free alternative to hypochlorite (OCl^-) for repulping of neutral / alkaline wet strengthened papers prepared from PAE resins and their broke.

Persulfates are salts of peroxysulfuric acid ($H_2S_2O_8$) also known as peroxydisulfuric acid. The ammonium, potassium, and sodium salts are commercially available products. Other monopersulfuric acid salts (H_2SO_5 or Caro's acid) were also prepared, namely: $2KHSO_5$ **:** $KHSO_4$ **:** K_2SO_4 (Espy and Geist, 1993; Kennedy and Albert, 1960). Table I.7 shows some physical properties of sodium, potassium and ammonium persulfate salts.

Tab. I.7: Physical properties of persulfate salts (from Atkins *et al.*, 2006).

	Solubility at 20°C (g/L)	***Density (g/cm^3)***	***pH (1% solution)***
$Na_2S_2O_8$	**560**	**2.40**	**5 to 7**
$K_2S_2O_8$	**60**	**2.48**	**5 to 8**
$(NH_4)_2S_2O_8$	**560**	**1.98**	**4 to 6**

It is well established that aqueous solutions of persulfate decompose by first-order kinetics to yield sulfate and hydroxyl-free radicals. Attack of N-methyl in N,N-diethylamides by free radicals has also been reported (Needles and Whitfield, 1964; Kennedy and Albert, 1960). This suggests that the dealkylations proceed *via* radical attack on α carbon with respect to the amide nitrogen. The observed exothermic feature, high reaction rate, and the reaction products are consistent with the following chain process which is analogous to the oxidation of methanol by persulfate. Figure 1.8 shows a free radical degradation reaction mechanism of N,N-disubstituted amide by potassium persulfate in acidic conditions (pH value between 4.6 and 4.9).

N-substituted and N,N-disubstituted amides were found to undergo dealkylation in potassium persulfate in aqueous dipotassium hydrogen phosphate. This reaction gave amide and N-alkylamides, respectively, in moderate yields (Needles and Whitfield, 1964). The dealkylated group appeared in the reaction mixture as the corresponding aldehyde or ketone.

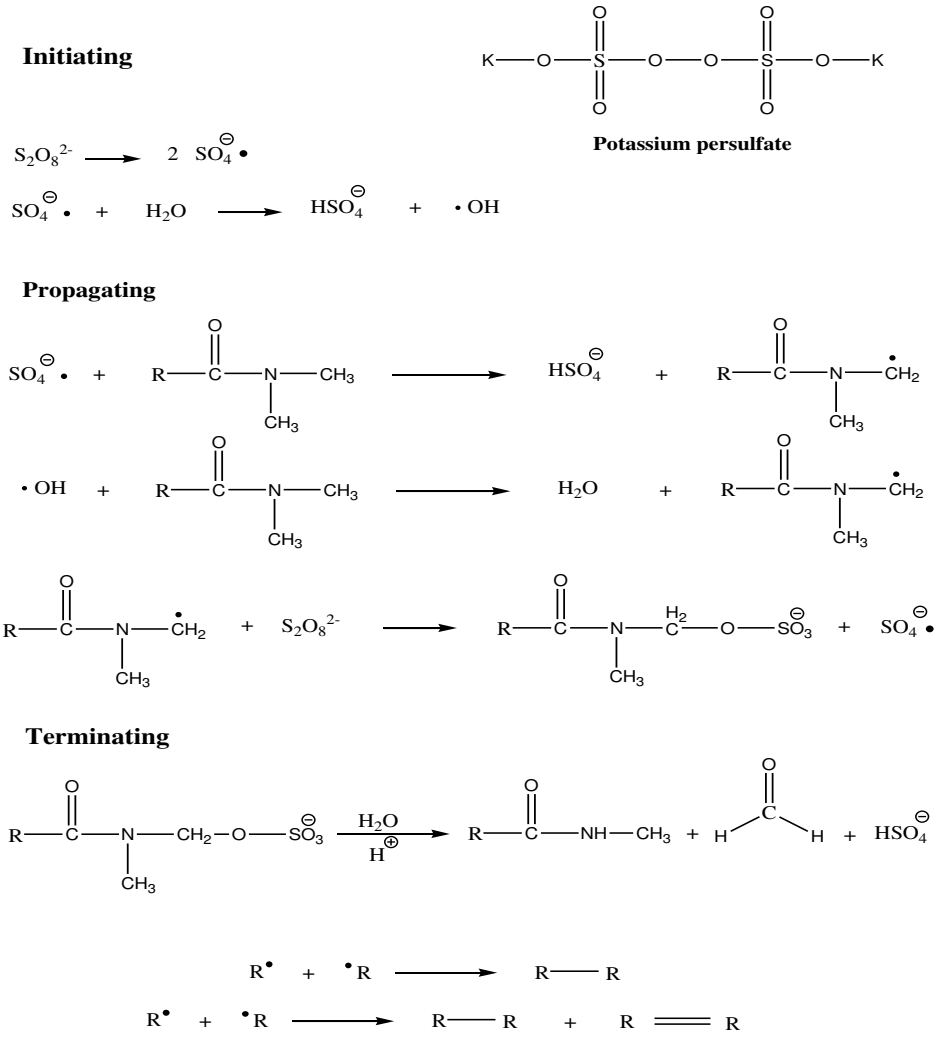

Fig. 1.8: Free radical reaction mechanism of N,N-disubstituted amide degrading by $S_2O_8^{2-}$ from Needles and Whitfield (1964).

The reaction of persulfate with formamide, N-methylformamide, and N,N-dimethylformamide yields a more complex mixture of products. Formamide is oxidized to carbon dioxide and ammonia. N-methylformamide yields carbon dioxide, ammonia, and formamide, whereas N,N-dimethylformamide gives N-methylformamide, in addition to the above listed products. It is though that any formamide resulting from the demethylation of N-methylformamide is further oxidized by persulfate to carbon dioxide and ammonia (Needles and Whitfield, 1964). Another example of an oxidation of organic substrates is a reaction of a simple amino acid in aqueous potassium persulfate. This reaction gives aldehydes containing one less carbon atom than the

starting amino acid and quantitative yields of ammonia and carbon dioxide (Kennedy and Albert, 1960).

There is no recognised standard test method to determine the repulpability of wet strengthened papers and each paper mill seems to have its own method which may meet its individual needs but may not be valid for other mills. The type and amount of wet strength resin will require different chemical treatment and conditions. Table I.8 shows some works concerning the recycling of PAE-based papers, paper types and main parameters used for degrading them.

Tab. I.8: Literature data of recycling of PAE-based papers.

Works	**Paper type**	**Conditions and/or methodology**
Schmalz (1961)	- bleached and unbleached PAE-based broke	- pH value of 10 (NaOH) and temperature of 38°C; - modified TAPPI disintegrator; - a test tube filled with the degraded sample was compared with the diluted standard samples to determine the degree of fibre separation;
Merret (1987)	- PAE kraft linerboard: **(i.)** 170 g/m^2 **(ii.)** 440 g/m^2	- pH value between 11 and 12 and temperatures ranging from 50 to 80°C; - the repulping was carried out in a consistency range of 10 to 17% in a 2.1 m diameter high consistency pulper;
Espy and Geist (1993)	- 0.3 to 0.75% PAE BKP (50/50 and 70/30 HW/SW) and BK chemicothermome-chanical pulp (35/30 HW/SW) - bleached broke	- hypochlorite or sodium persulfate in hot and alkaline medium; - the paper was repulped at 1.3% consistency in a TAPPI disintegrator following TAPPI T205 om 88; - the progress of defibering was charted in six steps, with 6 representing complete defibering;
Fischer (1997)	- unbleached linerboard (0.4, 0.6 and 1% PAE); - bleached poster board (1% PAE); - unbleached seedling paper (1% PAE) - unbleached raising tray paper (1% PAE)	- the effects of pH, time, temperature, rewetters, shear and reagent concentration (NaOH, $Na_2S_4O_8$, $KHSO_5$, H_2O_2, H_2SO_4 and NaOCl) were studied; - the degree of repulping was quantitatively determined by filtering the repulped paper through a slotted vibrating screen and the unpulped paper was dried at 105°C and weighed;

Bhardwaj and Rajan (2004)	- PAE bleached wet strength wastepaper	- effects of variables such as repulping time, pulp stock concentration, soaking time, temperature, and reagent concentration (NaOH, $Na_2S_4O_8$, $KHSO_5$, H_2O_2, H_2SO_4 and NaOCl) in the repulping stage were examined; - British standard laboratory disintegrator; - after repulping, samples of repulped slurry from each trial were screened and the rejects (unpulped paper) were dried at 105°C and weighed. The pulping yield was then calculated. After the repulping stage, the stock was also diluted to about 0.04% for visual observation checking the redispersability of the recycled pulp in water;

Schmalz (1961) and Chan and Lau (1988) observed that hypochlorite ion increased the rate of repulping, this rate being dependent upon the concentration of the oxidizing salt, and the pH and temperature of the slurry. High temperature ($\geq 40^oC$) and high pH values (c.a. 10) increased considerably the repulping. Merret (1987) studied the repulping of wet strength paperboard using high consistency pulper. He also observed that an elevated temperature and high consistency have a considerable influence on defibering. As an example, for repulping wet strengthened 175 g/m^2 linerboard, an increase in temperature from 53 to 73°C decreased both the repulping time and the specific energy consumption by almost half. Moreover, in all these studies, it was observed that when unbleached furnishes were repulped a substantial amount of hypochlorite was consumed for bleaching the papers.

Espy and Geist (1993) showed that, for various PAE-based papers, the best results were obtained with persulfates salts at an alkali pH. Increasing the temperature decreased the repulping time as already observed by other authors. Bleached broke was more rapidly defibered by alkaline persulfate than by alkali alone at the same pH range.

A new repulping process with a nonchlorinating oxidizing and rewetting agents was used by Fischer (1997). The process involves an oxidation step at a low pH, with inorganic or organic peroxides, followed by hydrolyzing the wet strength paper at a high pH. In up-scaling trials, unbleached paper containing high levels of PAE resins was repulped to about 95% in mill pulpers. However, as expected, the dry tensile strength of the handsheets prepared from recycled fibres using the double pH method was weaker than with other treatments (NaOH, $Na_2S_4O_8$, $KHSO_5$, H_2O_2, H_2SO_4 and NaOCl).

Repulping of PAE-based wet strengthened papers with inorganic chemicals was also investigated by Bhardwaj and Rajan (2004). The effects of major variables such as repulping time, pulp stock concentration, soaking time, temperature, and reactant concentration in repulping efficiency were examined. Pulp freeness, zero-span tensile strength, fibre fractionation and physical properties of the handsheets prepared from recycled fibres were analysed. Contradictorily to other studies, these authors concluded that acidic systems were found to be more effective in depolymerising the wet strength resin present in the paper and the best results were obtained when the pH during repulping was less than 3. In this case, a maximum of 98% yield was obtained (even with presence of few bonded fibres after repulping). Considering the contradictory results reported in the literature, one of the aims of this thesis will be then to optimize the recycling of some industrial PAE-based wet strengthened papers.

1.8. MAIN OBJECTIVES

Based on the literature data some studies will be carried out in the PART II of this thesis, namely:

(i.) due to economical and industrial interests a pulp suspension of 100% *Eucalyptus* (Suzano) fibres will be used to prepare PAE-based wet strengthened papers. Some classical characterizations such as refining kinetics of the pulp, morphological characterization of the fibres, as well as their total and surface charges will be determined;

(ii.) studies of PAE adsorption by *Eucalyptus* fibres will be performed under controlled conditions (pH value between 7.5 and 8 and conductivity value between 700 and 800 μS/cm). The adsorption kinetics will be studied by ζ potential measurements (streaming potential and electrophoretic mobility) as a function of the PAE concentration, and mixing and storage times;

(iii.) effects of experimental conditions on the wet and dry strength of the papers will be investigated: PAE dosage, conductivity of the pulp suspension, thermal post-treatment and storage time of the prepared handsheets will be varied;

(iv.) recycling of industrial PAE-based papers and degradation of PAE-films will be studied as a function of the added chemicals and their concentration, time, pH and temperature of the treatment. Attempts to compare the results obtained for the industrial papers and the cross-linked PAE films will be made.

CHAPTER II: PREPARATION AND CHARACTERIZATION OF PULP SUSPENSIONS

HW and SW bleached kraft pulps supplied as dry sheets were used in this study. The pulp suspensions were prepared by standard methods and studied by optical microscopy. Refining was performed for each pulp, and for a mixture of SW (40%) and HW (60%). Total charge of the refined pulps was determined by potentiometric (with NaOH) and conductimetric titrations (with NaOH and $NaHCO_3$). The surface charge was measured by polyelectrolyte titrations using a particle charge detector and ζ potential measurements (electrophoretic mobility and streaming potential techniques).

2.1. MATERIALS AND METHODS

2.1.1. Moisture content

The solid content of the pulps was obtained by drying samples (c.a. 1.0 g) in an oven at 105°C for 48 h. The studied pulps were stored at ambient conditions.

2.1.2. Optical microscopy

The pulps (Sodra Blue and Suzano) were observed by optical microscopy (Axio Imager Mim) in order to determine the wood species of the fibres.

2.1.3. Refining kinetics of the pulp suspensions

The studied pulps were beaten in distilled water in a Valley beater (Weverk) following the NF Q 50-008 standard. 400 g of dried pulp were mixed with 15 kg of deionized water and stirred in a vessel for 20 min. Then, the concentration of the pulp suspension was adjusted at 20 g/L. Before refining, the pulp suspension was brushed for 20 min in the Valley beater. Pulp drainability (Schopper-Riegler degree: °SR) was measured using a PTA machine (PH 019). Refining kinetics of the pulps were studied

by measuring Schopper-Riegler degrees, until a degree of 30°SR was reached, and plotting them against time.

2.1.4. Morphological characterizations of the pulp suspensions

Morphological characteristics of the pulp suspensions, before and after refining, were assessed using a Morfi analyser (LB-01 TechPap S.A.). After introducing a sample with a known weight (300 mg) into the main tank, the pulp suspension is diluted and stirred for homogenization. Then, the pulp suspension flows through the measuring cell, which consists of a transparent vein with a specific geometry (flat channel), and the pictures are recorded using a black and white CCD camera. Finally, these pictures are analyzed and the parameters obtained are: arithmetic and weighed lengths (mm), width (μm), coarseness (mg/m), content in macrofibrils (%) and in fine elements (%). Macrofibrils are elements which were partially detached from the fibre walls during refining. Fines are defined as elements whose size is less than 200 μm and their amount is defined as the ratio of the total length of fines to the total length of the elements present in the suspension (expressed in percentage). Arithmetic (l_A) and weighed (l_W) mean length are calculated as follows:

$$l_A = \frac{\sum_i n_i l_i}{\sum_i n_i} \qquad l_W = \frac{\sum_i n_i l_i^2}{\sum_i n_i l_i}$$

Trials were made in triplicate and the difference between two obtained results did not excess 2%.

2.1.5. Charge measurements of the pulp suspensions

A number of methods are available to analyze the nature, content, and strength of acidic groups in wood materials. The amount of acidic groups (total charge) can be determined by conductimetric and potentiometric titrations, and ion exchange. Adsorption of cationic polyelectrolytes gives information on the accessibility of anionic

groups in the fibres. Because the accessibility of the functional groups may differ depending on their location (inside the fibre wall or on the fibre surface), and on the molecular weight of the polymer, polyelectrolyte adsorption can be used to determine both the surface charge (excluding the pores) and the total charge of cellulosic fibres (including the charges in pores).

In this study, the total charge of the fibres was determined by potentiometric (NaOH) and conductimetric titrations (NaOH and $NaHCO_3$), and the surface charge by polyelectrolyte titration using streaming current, streaming potential and electrophoretic mobility measurements. Before charge measurements, the pulp suspensions were converted to their fully protonated form by soaking them at 1% consistency in 0.01 mol/L HCl for 1 h. The pH of the pulp after this soaking time was close to 2.2. The pulps were then filtered under vacuum using a Buchner funnel and a Nylon sieve (70 μm), and washed several times with distilled water until a pH value close to 7.0. On the beginning of the washing step, the filtrate was re-circulated to avoid loss of fines until the formation of a fibrous mat thick enough. The vacuum was maintained until no more water could be extracted from the pulp mat. After titrations, the amount of fibres in each sample was determined gravimetrically by filtering the pulp on a pre-weighed filter paper and drying in an oven at 105°C for 48 h.

2.1.5.1. Determination of the total charge by conductimetric and potentiometric titrations

The conductimetric titrations of fibre suspensions are similar to that of soluble acids. Figure 2.1 shows the obtained curve for conductimetric titration. The measured parameter is the conductance. Marked increases or decreases in conductance are associated with the changing concentrations of the two most highly conducting ions: the hydrogen (H^+) and hydroxyl (OH^-). It is necessary to carry out the procedure in the presence of a neutral salt because the Donnan equilibrium may cause a very unequal distribution of the mobile ions between the interior of the fibre wall and the external solution (Fras *et al.*, 2004). Prior to the titration, the fibres are first converted to the H^+ form, which means that all acidic groups have proton as a counterion. After this, the fibres are titrated with NaOH and the following reaction takes place (if we consider that only carboxylic groups are present):

Fibre - COOH + Na^+OH^- → Fibre - COO^-Na^+ + H_2O

The conductimetric titration curve of fibre suspensions is characterized by three distinct phases:

Phase 1: neutralization of free excess of protons which slightly lowers the conductivity;

Phase 2: neutralization of carboxylic groups, which does not change the conductivity. The added sodium ions (Na^+) act as counterions to the carboxylic acidic groups, and the dissociated protons are neutralized by the added hydroxide ions (OH^-);

Phase 3: accumulation of NaOH in excess which leads to an increasing conductivity. The total amount of carboxylic groups can be determined from the second intersection point.

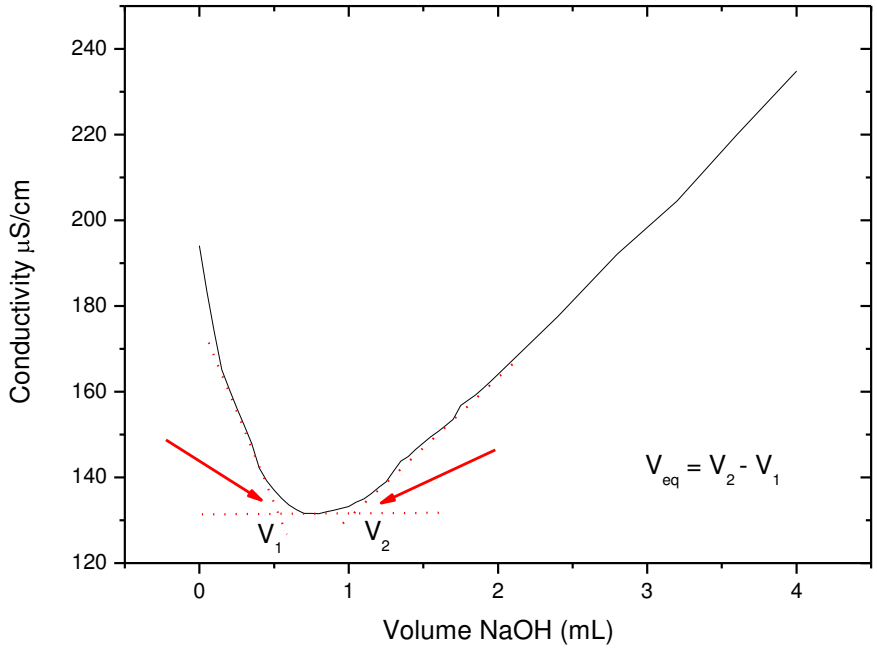

Fig. 2.1: Conductometric titration curve and determination of equivalent volume for Sodra blue pulp.

For conductimetric titrations, approximately 0.5 g of the protonated pulp was dispersed in 100 mL of a 1 mmol NaCl solution, and 0.5 mL HCl 0.05 mol/L (Aldrich) was added before starting the titration. During the titrations, a magnetic stirrer with a Teflon rod was used to mix the pulp suspensions. Two titrants were used, namely: 0.05 mol/L NaOH and $NaHCO_3$ (both supplied by Aldrich). The titration was performed at 25°C using a conductivity meter (Thermo Scientific Orion 4 star), and a conductivity cell (Orion 013005 MD). Measurements were taken after the addition of c.a. 0.05 mL of alkali solution and the stabilization of the conductivity of the medium (between 1 and 2 min). Near the inflexion point, readings were taken drop to drop. The titration gave the conductivity of the suspension, as a function of the added alkali volume. The content in acidic groups c (in µeq/g of o.d. pulp) was given by the additional alkali volume needed to reach the second inflexion point:

$$c(\mu eq\ /\ g) = \frac{(V_2 - V_1)\, C_{NaOH\ /\ NaHCO_3}}{m}$$

with m the mass of the o.d. pulp used for the trial.

Trials were made in triplicate and the difference between two obtained results did not excess 10 and 20% for NaOH and $NaHCO_3$ conductometric titrations, respectively.

Potentiometric titrations were performed by using a combined pH glass electrode (Orion). Calibration of the pH meter using buffer solutions having pH values of 4, 7 and 9 was carried out before titrations. A magnetic stirrer with Teflon rod was used to stirr the pulp suspensions during the titrations, as described for conductimetric method. The potentiometric titrations were performed with 0.5 g of a protonated pulp in 100 mL of deionized water containing HCl and NaCl (0.005 mol/L HCl, 1 mmol/L NaCl). The analyses were performed at 25°C. The volume of titrant for each addition was controlled at c.a. 0.05 mL. The measurements were recorded after the stabilization

of the pH (between 3 and 5 min). A blank titration curve was generated by titrating 100 mL of 0.005 mol/L HCl in 1 mmol NaCl by 0.05 mol/L NaOH in 1 mmol NaCl.

Figures 2.2 show the obtained curve for potentiometric titration. The content in acidic groups is obtained from the following equation:

$$c(\mu eq\ /\ g) = \frac{(V_{eq} - V'_{eq})\, C_{NaOH}}{m}$$

where m is the mass of o.d. fibres, V_{eq} is the NaOH volume required for neutralizing the acidic groups in the sample, V'_{eq} the volume required for neutralizing the acidic groups in the blank (Fras *et al.*, 2004).

Trials were made in triplicate and the difference between two obtained results did not excess 20%.

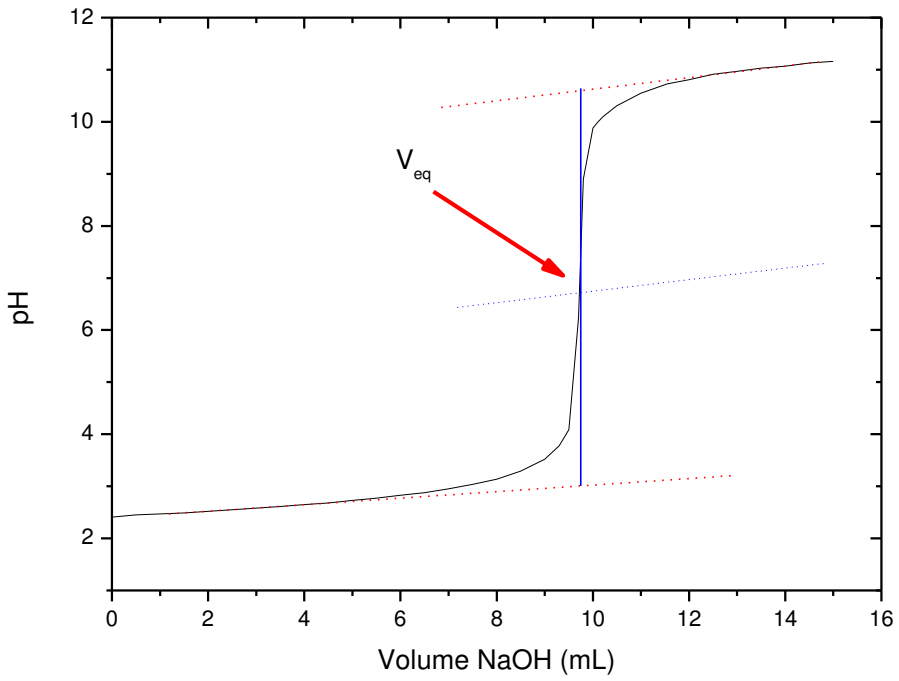

Fig. 2.2: Potentiometric titration curve and determination of the equivalent volume (V_{eq}) for Sodra blue pulp.

2.1.5.2. Determination of surface charge

Particles dispersed in an aqueous system will acquire a surface charge, mainly either by ionization of surface groups, or adsorption of charged species (Stanna-Kleinschek *et al.*, 2001; Castellan, 1986). These surface charges modify the distribution of the surrounding ions, resulting in an increased concentration of counter ions (ions of opposite charge to that of the particle), close to the surface. Thus, an electrical double layer exists all around each particle with:

(i.) an inner region (Stern layer), where the ions are strongly bound; and

(ii.) an outer region (diffuse layer), where they are less firmly associated (Castellan, 1986).

An important consequence of the existence of electrical charges on the surface of particles is that they interact with an applied electric field. These effects are collectively defined as electrokinetic effects. There are four distinct effects depending on the way in which the motion is induced: **(i.)** electrophoresis (the movement of a charged particle in a liquid under the influence of an applied electric field); **(ii.)** electroosmosis (the relative movement between a flowing liquid and a stationary charged surface under the influence of an electric field); **(iii.)** streaming potential (the electric field generated when a liquid is forced to flow through a stationary charged surface); and **(iv.)** sedimentation potential (the electric field generated when charged particles settle).

When a particle suspended in a liquid moves, under Brownian motion for example, the Stern layer and a part of the diffuse layer also move as parts of the particle. The ζ potential is the potential at the slipping plane. Figure 2.3 shows the double layer model according to Gouy-Chapman-Stern-Grahame (GCSG), for negatively charged surfaces in suspension.

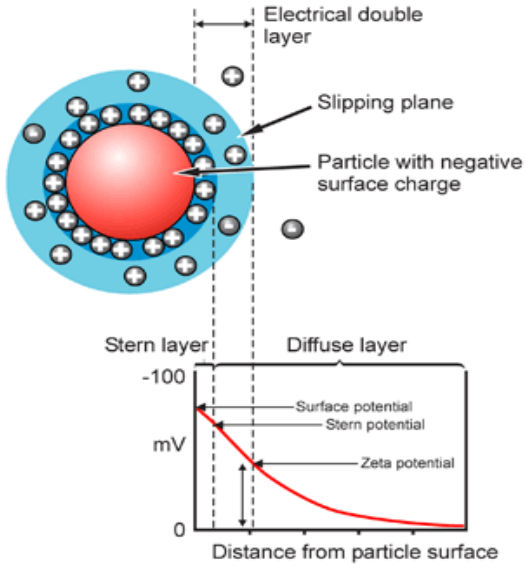

Fig. 2.3: Schematic representation of a particle in a suspension based on double layer model from Castellan (1986).

2.1.5.3. Polyelectrolyte titration using a particle charge detector (PCD-03)

Polyelectrolyte titrations were first performed using a particle charge detector from Mütek (PCD-03) and an automatic titrator (Mettler DL21). Pulp samples of c.a. 0.5 g were mixed with 100 g of 0.001 N polydadmac (polydiallyldimethylammonium chloride Sigma Aldrich M_w 400.000-500.000), and stirred for 2 h by a magnetic stirrer with Teflon rod. During this time, a certain quantity of cationic polyelectrolyte completely neutralizes the anionic charge on the surface of the fibres while the excess remains in solution. The sample was then filtered on a Nylon sieve (70 µm). 10 mL of the filtrate were introduced into the PCD-03 cell, and the polydadmac in excess was titrated with 0.001 N PES-Na (sodium polyethylene sulfonate - Novi Profibre) to the endpoint (streaming potential of 0 mV). The titrant addition was controlled at 0.1 mL/min. Determination of the blank curve was carried out by titrating 10 mL of polydadmac solution with 0.001 N PES-Na. Figure 2.4 presents the curve obtained for polyelectrolyte titration using PCD-03 apparatus and the determination of the equivalent volume.

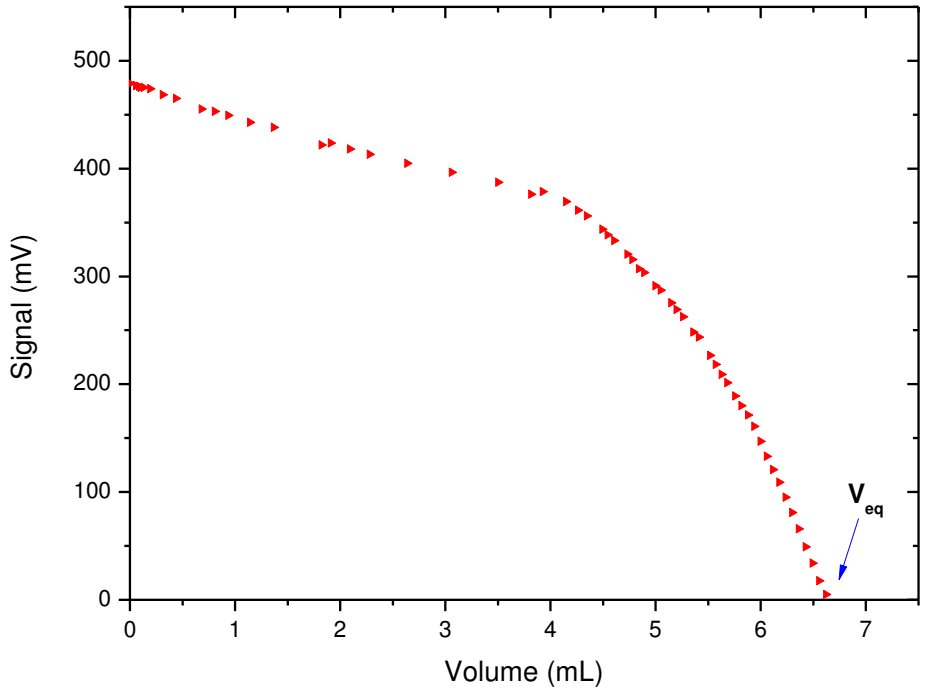

Fig. 2.4: Polyelectrolyte titration curve obtained for Sodra Blue pulp using a particle charge detector (PCD03 from Mütek).

2.1.5.4. Polyelectrolyte titrations using Zeta potential measurements (ζ): electrophoretic mobility and streaming potential methods

Surface charge of the fibres was also determined by colloidal titration measuring the ζ potential of the pulp suspensions treated with polyelectrolytes by two methods: electrophoretic mobility and streaming potential. For this purpose, 500 mL of pulp having 10 g/L consistency, a pH in the range of 7.5 to 8 and a conductivity of 700 to 800 µS/cm were mixed with increasing amounts of polydadmac (Sigma Aldrich M_w 400.000-500.000) varying from 0 to 0.4% (w/w with respect to o.d. pulp) and PAE (Eka WS 505) varying from 0 to 0.9%, for 5 min, under gentle magnetic stirring. The suspension was then left to repose for 2 h. The equivalent point was determined as the volume of polymer solution needed to change the negative ζ potential of the fines and fibres to ζ = 0 V. At this point we consider that the neutralization of all charges located

on the surface of the fines and/or fibres by the polyelectrolytes was completed. This polymer volume is used to determine the surface charge by mass unit of the fibres.

Electrophoretic mobility of the suspensions was measured using a Zetasizer 2000 (Malvern). As required for this technique, a filtration of the fibre suspensions was performed on Nylon sieves (70 μm), before injecting the samples. When an electric field is applied across an electrolyte, charged particles suspended in the electrolyte are attracted towards the electrode of opposite charge. Viscous forces acting on the particles tend to oppose this movement. Nevertheless, when an equilibrium is reached between these two opposing forces, the particles moves with constant velocity which is dependent on the strength of the dielectric field or voltage gradient (*Ka*), the dielectric constant (ε), the viscosity of the medium (η) and the ζ potential (ζ). The velocity of a particle in a unit electric field is referred as its electrophoretic mobility. ζ potential is related to the electrophoretic mobility by the Henry equation (Equation 2.1):

$$U_E = \frac{2\varepsilon\zeta}{3\eta} . f \ Ka \qquad \textbf{(Eq. 2.1)}$$

Electrophoretic determinations of the ζ potential are most commonly made in aqueous media and moderate electrolyte concentration. *f (Ka)* in this case is 1.5 and this is the value used in the Smoluchowski approximation. Therefore, calculation of ζ potential from the mobility is straightforward for systems that fit the Smoluchowski model, i.e. particles larger than about 0.2 microns dispersed in electrolytes containing more than 10^{-3} mol/L salt. For small particles in low dielectric constant media, the f (ka) becomes 1.0 and allows an equally simple calculation. This is the Hückel approximation.

On the other hand, the streaming potential of the suspensions was measured using a Magendans SZP 04 from Mütek. The method is based on an electric field generated when a liquid is forced to flow through a stationary charged surface (Onabe, 1979). For this technique, the samples were introduced without filtration and the apparatus detects the surface charge of fibres and fines. The centerpiece of the SZP is a plastic measuring cell with embedded patented platinum electrodes. A fibre suspension is drawn into the cell by

applying a vacuum. At the screen electrode a fibre plug is formed. A pulsating vacuum causes the aqueous phase to flow down and up through the plug, thus shearing off the counter ions and generating a streaming potential. The ζ potential is calculated by using the measured streaming potential, conductivity and the pressure differential.

Figure 2.5 presents the polyelectrolyte titration curve obtained for Sodra Blue by measuring ζ potential using electrophoretic mobility method.

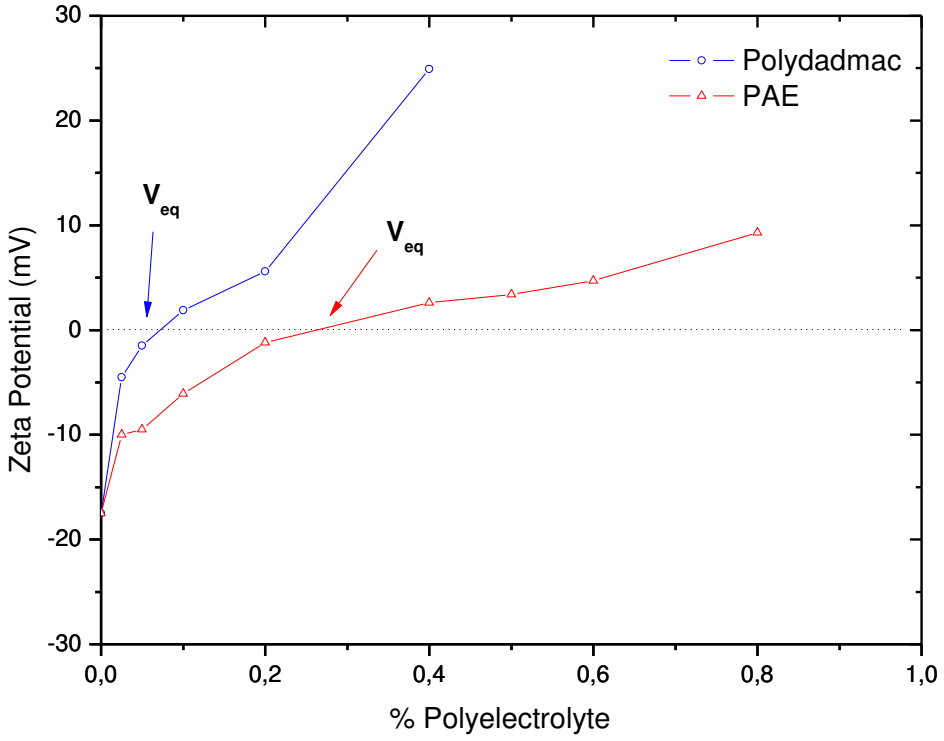

Fig. 2.5: Polyelectrolyte titration curve obtained for Sodra Blue pulp by ζ potential measurements using electrophoretic mobility method.

2.1.6. Study of the adsorption of PAE resins by Eucalyptus pulp suspension

PAE adsorption by fibres was indirectly followed by zeta potential (ζ) measurements using electrophoretic mobility and streaming potential methods. For this purpose, *Eucalyptus* (Suzano) pulp suspension was refined to 30°SR (*Schopper-Riegler*), as already described**.** The pH of the pulp suspension was adjusted between 7.5

and 8 with NaOH and the conductivity between 700 and 800 µS/cm with NaCl. Three concentrations of PAE resin (EKA) based on dry weight of the pulp were added to the *Eucalyptus* pulp suspension: 0.1% ($\zeta < 0$), 0.6% (ζ c.a. 0) and 1% ($\zeta > 0$). A study of the variation of ζ potential values of the suspension after addition of the PAE resin was performed as a function of mixing time (1, 3 and 5 min), and standing time (5, 15, 30, 60 and 120 min).

A mechanical agitation was carried out using the apparatus described in Materials and Methods (see Part II: Chapter III). ζ potential measurements of the pulp suspension using electrophoretic mobility method were carried out in a Zetasizer 2000 (Malvern) after filtration of the samples on Nylon sieves (70 µm). ζ potential measurements of the pulp suspension using streaming potential method were performed in a SZP-04 (Mütek).

2.2. RESULTS AND DISCUSSION

2.2.1. Characterization of pulp suspensions

The two pulps used in this study were analyzed by optical microscopy. Table II.1 shows the species constituents of Sodra Blue and Suzano pulps determined from optical examination.

Tab. II.1: Characteristics of the pulps determined by optical microscopy.

Pulp	***Grade***	***Species***
Sodra Blue	bleached softwood (SW)	Spruces, Scots pine
Suzano	bleached hardwood (HW)	*Eucalyptus*

These pulps were refined separately on a Valley beater until a Shopper-Riegler degree of 30 was reached. A blend composed of 40% of SW (Sodra Blue) and 60% of HW (Suzano) was also tested. Figure 2.6 shows the refining kinetics for the three pulp suspensions.

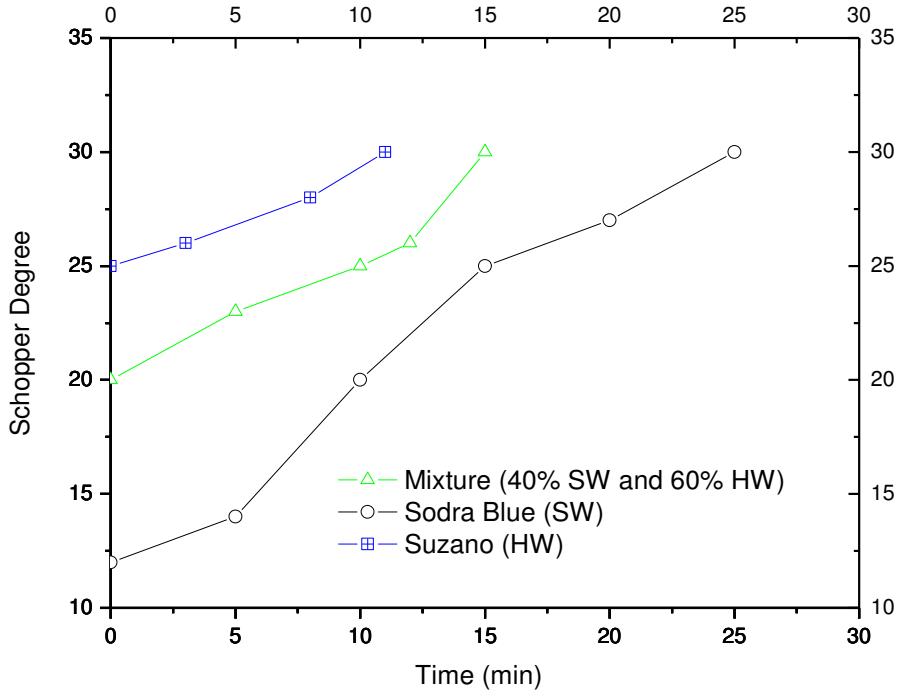

Fig. 2.6: Refining kinetics of pulp suspensions measured by the Schopper-Riegler values (30^{o} SR).

As expected, the time necessary to reach a Schopper Riegler degree of 30 is shorter for the HW suspension when compared to the SW one: c.a. 10 and 25 min for HW (Suzano) and SW (Sodra Blue) fibres, respectively. The mixture of HW (60%) and SW (40%) fibres needs a refining time of c.a. 15 min, which is intermediate between the refining time of the HW and that of SW pulp.

Morphological characteristics of the fibres, before and after refining, were assessed by MORFI analysis. Table II.2 and II.3 show the obtained results for Sodra Blue and Suzano pulps, respectively.

Tab. II.2: Morphological characterization of Sodra Blue pulp suspension (SW), before and after refining, determined from MORFI analysis.

	Unrefined Sodra Blue (sampled after brushing)	***Refined Sodra Blue (30^o SR)***
Arithmetic length (mm)	1.31	1.03
Weighed length (mm)	2.12	1.70
Width (µm)	31.7	33.5
Coarseness (mg/m)	0.146	0.162
Macrofibrills (%)	0.31	0.66
Fines (% length)	15.9	27.0

Tab. II.3: Morphological characterization of Suzano pulp suspension (HW), before and after refining, determined from MORFI analysis.

	Unrefined Suzano (sampled after brushing)	***Refined Suzano (30^o SR)***
Arithmetic length (mm)	0.680	0.660
Weighed length (mm)	0.781	0.764
Width (µm)	20.8	21.25
Coarseness (mg/m)	0.0850	0.0730
Macrofibrills (%)	0.490	0.580
Fines (% length)	21.2	23.6

Refining modifies the fibre morphological properties in different ways. As expected, refining induces a decrease of the fibre length, but this decrease is very limited for *Eucalyptus* fibres (2.5%) when compared to softwood fibres (24.5%) when considering the arithmetic length, for instance. As a consequence of the fibre swelling during refining, the fibre width increases of 5.7 and 0.24% for softwood and *Eucalyptus* fibres, respectively. As fibre surfaces are peeled off during refining, increasing amounts of fines and macrofibrils are formed. An increase of 69 and 11% of the fine content and an increase of 113 and 18% of macrofibrills were thus observed for softwood and *Eucalyptus* fibres, respectively. Here again, the effect of refining on the morphological properties of the fibres is stronger for the softwood fibres.

Fillers and fines disturb coarseness measurements, because fibre analysers do not recognize such small particles in the same way. When the small fibres and fines are not all recognized, the coarseness values may be overestimated. The fines that pass through a 200-mesh screen are so small that analysers may not detect a part of them (Turunen *et al.*, 2005). Thus, we can postulate that the small variation observed on coarseness values at the refining degree used (30° SR) in this study is considered to be negligible.

The results related to the total charge measurements determined by potentiometric and NaOH and $NaHCO_3$ conductimetric titrations are reported in Table II.4.

Tab. II.4: Total charge of pulps obtained from conductimetric and potentiometric titrations.

Total charge (µeq/g)		***Sodra Blue***	***Suzano***
Potentiometric	***NaOH***	25.5 ± 4.8	44.0 ± 7.6
Conductometric	***NaOH***	30.2 ± 1.2	39.8 ± 1.7
	$NaHCO_3$	10.2 ± 1.8	14.9 ± 2.7

Suzano fibres (HW) show a higher amount of acidic groups when compared to that of Sodra Blue (SW) fibres. As discussed before, SW and HW fibres differ in terms of amount and chemical structure of hemicelluloses that they contain. HW and SW fibres show hemicelluloses content in the range of 25 to 35% and 25 to 29%, respectively. SW fibres have a high proportion of mannose units and more galactose units than HW, whilst HW fibres have a high proportion of xylose units and more acetyl

groups than SW. The carboxylic acid groups born by the hemicelluloses being the main functional groups that give rise to the generation of charged sites on the fibres, the difference in chemical composition justifies the highest total charge of HW when compared to SW fibres for the two total charge determination methods.

Conductimetric titration values differ somewhat from those of potentiometric titrations, as also observed by other authors (Bhardwaj *et al.*, 2004; Fras *et al.*, 2004). The stabilization of the measuring cell and the reproducibility was easier for conductimetric than for potentiometric titration which can partly explain this difference.

NaOH conductimetric titrations give higher pulp charge values compared to $NaHCO_3$ titration for the two pulps analyzed. With NaOH, it is assumed that the total quantity of the carboxylic groups are titrated (which is not the case with $NaHCO_3$). Moreover, some other acid functions may also become ionized at high pH (between 9.0 and 10.0 at the end of the titrations), such as lactone or some phenolic hydroxyl groups associated to the residual lignin. The presence of phenolic groups is nevertheless less probable for the tested pulps (bleached chemical pulps). Fardim *et al.* (2002) and Bhardwaj *et al.* (2004) also observed differences between the results obtained from NaOH and $NaHCO_3$ titration, when comparing methods for determining the total charge of pulp fibres. The observed differences depending on the type of pulp being titrated.

To conclude, it seems reasonable to consider that the values obtained from the NaOH conductimetric titrations are the most representative of the content in acidic groups and more precisely in carboxylic groups associated to the fibres. Table II.5 shows some titration values from literature for total and surface charge. The values for Suzano and Sodra blue fibres are close to those reported in the literature.

Tab. II.5: Total and surface charge of some pulps from literature.

(mmol/Kg)	*Total charge*			*Surface charge*	
	Potent.	***Conduct.***	***Low MW Polyelect.***	***High MW Polyelect.***	
Cotton	52.3*	43.2*	25	18.5	**Fras *et al.*, 2004**
Viscose	40.6*	48.6*	24	4.7	
Modal	26.1*	27.2*	16	3.5	
Lyocell	18.4*	20.6*	15	3.5	
Kraft pulp kappa 26	-	73.7*/48.5**	57	-	**Lloyd *et al.*, 1993**
Kraft pulp Kappa 110	-	146.4*/89.4**	102	-	
Radiata pine BK	-	30.1*/24.0**	35	-	
Stone groundwood pulp	-	98.1*/59.2**	c.a. 50	-	
Pressurized refined mechanical pulp	-	81.6*/44.0**	c.a. 50	-	
TMP	-	88.8*/56.6**	c.a. 50	-	
TMP 4% H_2O_2	-	252.8*/109.3**	145	-	
Wood (sulfonated for 12.5 min at pH 7)	199*	211*	-	-	**Katz *et al.*, 1984**
Wood (sulfonated for 110 min at pH 7)	341*	352*	-	-	
CMP from chips sulfonated at pH 7	351*	360*	-	-	
Higher yield bisulfite	271*	295*	-	-	
Low yield bisulfite	68*	71*	-	-	
Low yield acid bisulfite	28*	30*	-	-	
Unbleached kraft	-	201*	-	-	

*NaOH titration; **$NaHCO_3$ titration

Regarding now the surface charge determination, a polyelectrolyte titration using a particle charge detector (PCD) was used. The amount of adsorbed polymer on the fibres was determined by titrating the excess (not adsorbed) of polymer with a polyanion (PES-Na). The obtained values are reported in Table II.6. The results showed that HW pulp (Suzano) has the highest surface charge**.** The surface charge represents 30 and 34% of the total charge for SW and Eucalyptus fibres, respectively.

Tab. II.6: Surface charge measurements obtained by polyelectrolyte titration with a particle charge detector PCD apparatus.

Surface charge (µeq/g)	*Titrant*	*Sodra Blue*	*Suzano*
Streaming current (PCD-03)	*PES-Na*	**8.9**	**13.7**

Titrations with polydadmac give the surface charge of pulp because acidic groups located in the fibre wall are not easily accessible when polymers with high molecular mass weight are used. However, a basic assumption of this method is that there is a 1 to 1 stoichiometric relationship between the number of cationic groups born by the polydadamac bound to the fibre surface, and the number of anionic groups on the cellulosic surface. This assumption is considered to be valid if the adsorbed polymer lies in a flat conformation, which will be the case for polymer with high charge density. Although polydadmac exhibits a high charge density, deviations from a 1 to 1 stoichiometric reaction have already been discussed in the literature. Indeed, the experimental procedure itself may lead to an overestimation of the surface charge as an excess of polydadmac was added into the pulp suspension during these experiments. Other adsorption conformations of the polyelectrolyte on the fibre surface, as will be discussed in the Chapter I (Part II), may also to be considered in order to explain this discrepancy.

In order to get a more reliable estimation of the surface charge, colloidal titrations were performed by adding increasing amounts of polydadamac to the pulp suspension and simultaneously measuring the resulting change in zeta potential of the fibres or fines. The zeta potential (ζ) of the charged surfaces was measured using microelectrophoresis and streaming potential methods. For comparison purposes, the same procedure was applied by adding PAE solutions to the suspension. The surface charge is determined from the curves ζ versus added amount of polyelectrolyte (see Figure 2.5) by interpolating the titrant dosage for $\zeta = 0$ V. The results are reported in Table II.6.

Tab. II.7: Surface charge measurements obtained by determining ζ potential.

Surface charge (µeq/g)	*Titrant*	*Sodra Blue*	*Suzano*
Streaming potential	***Polydadmac***	**7.52**	**11.7**
	PAE	**11.0**	**13.7**
Electrophoretic mobility	***Polydadmac***	**4.42**	**4.94**
	PAE	**6.23**	**8.40**

In all cases, the results show that the polyelectrolyte titration using PAE resin leads to highest values of the surface charge when compared to titrations with polydadmac. Four explanations can be postulated acting or not together:

(i.) the lowest charge density of PAE resin when compared to polydadmac;

(ii.) the stability of the charge of PAE resin is pH and ionic strength dependent which makes this titration less accurate;

(iii.) the penetration of PAE resin in the pores of the pulp fibres, because PAE resins has lower molecular weight; and

(iv.) the reaction between PAE macromolecules after neutralization of the charge of the fibre surface.

From these considerations, it clearly appears that the determination of the surface charge from polydadmac titrations is more appropriate.

Regarding now the measuring techniques, we observe that the surface charge determined from the streaming potential technique is greater than compared to that determined from the electrophoretic mobility technique. This difference is particularly high for the Suzano pulp whose surface charge determined with polydadmac and microelectrophoresis is surprisingly low. Two explanations can be postulated, namely:

(i.) the different measuring principles between the two techniques; and

(ii.) the sample preparation. For the streaming potential technique, the whole pulp suspension (fibres + fines) was used, whereas for electrophoretic mobility, only the fines < 70 µm were measured.

Strazdins (1989) reviewed the merits of these methods and concluded that the microelectrophoresis procedure provides the most reliable data, which correlates with the papermaking qualities of the fibre furnishes and the performance of the wet end additives. In our case, it is difficult to conclude, but we can assume that the surface charge of the Sodra Blue is close to 5-6 µeg/g and that of Suzano is probably slightly higher about 7-8 µeg/g (if we consider the two techniques used). These values are probably more representative of the "true" surface charge than those determined in the presence of an excess of polydadmac (which are actually greater). Considering the total charge, we can then postulate that between 15 and 20% of the electrical charges are located at the surface of the fibres for both pulps.

2.2.2. Study of the adsorption of PAE resins by Eucalyptus pulp suspension

In order to better understand the phenomena related to the adsorption of PAE by lignocellulosic fibres, trials were carry out on the Suzano pulp (*Eucalyptus* fibres). PAE was added at different dosages (0.1, 0.6 and 1%) into the pulp suspension, and adsorption was indirectly followed by measuring the zeta potential for different mixing and standing times. As previously, both techniques of microelectrophoresis and streaming potential were used.

Figure 2.7 shows the ζ potential values obtained for *Eucalyptus* pulp suspension, as a function of PAE addition levels, and mixing time. The adsorption of PAE can be considered as a result of the collision process between PAE and fibres in suspension during mixing and derived from electrostatic interactions between two opposite charges, fibres (-) and polyelectrolyte (+). As observed, the adsorption process seems to be very fast for the used conditions. There is only a small variation of the ζ potential up to 5 min of mixing for all concentrations and for the two electrokinetic methods.

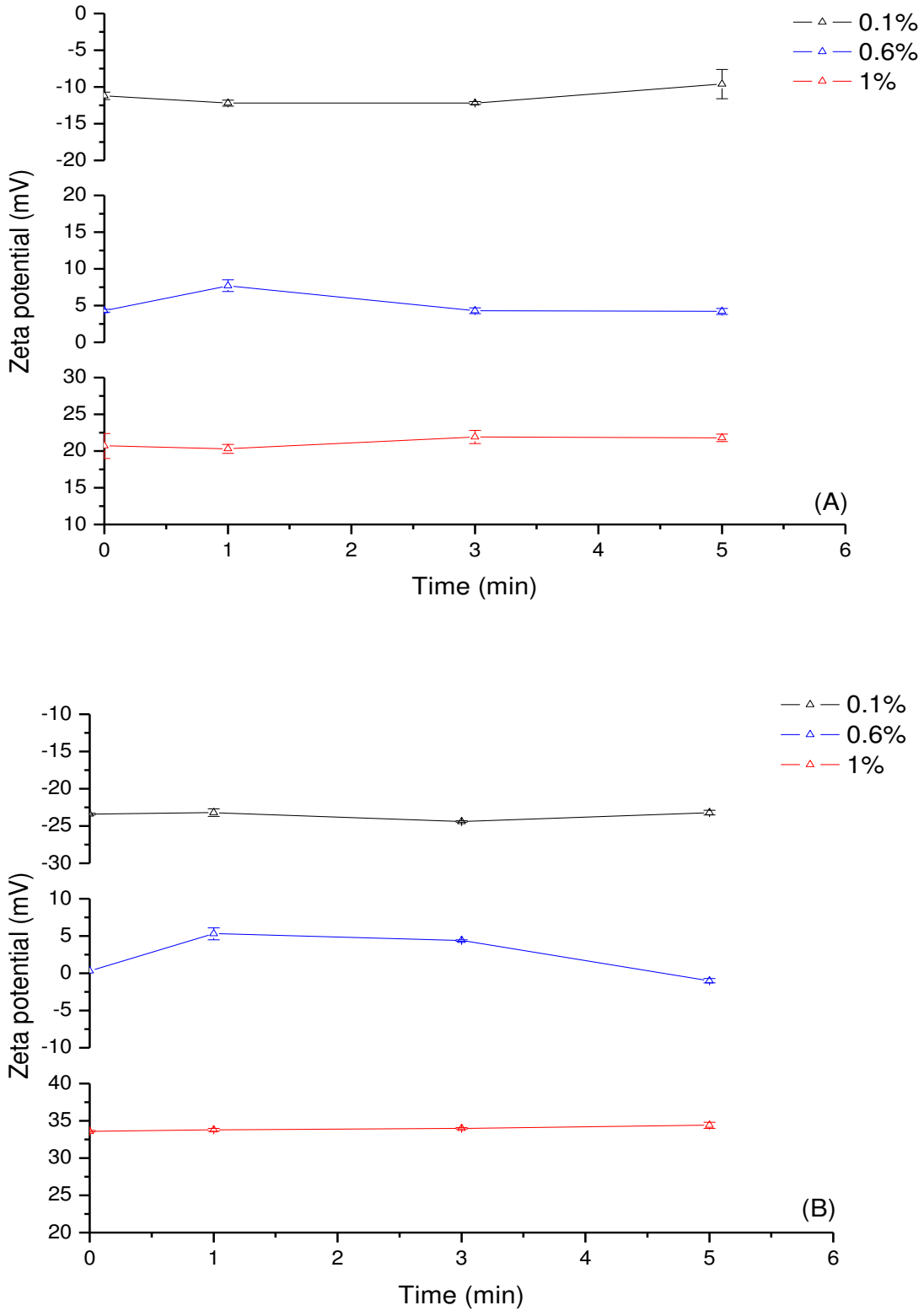

Fig. 2.7: Zeta potential measurements for *Eucalyptus* pulp using **(A)** electrophoretic mobility and **(B)** streaming potential methods, as a function of the PAE concentration and the mixing time.

Figure 2.8 shows the ζ potential measurements obtained for *Eucalyptus* pulp suspension as a function of the PAE addition levels, and standing time (up to 120 min). From this curve, it can be postulated that the PAE adsorption process is divided into a minimum of two stages occurring or not simultaneously: the first, fast stage can be viewed as an electrostatic favored situation, while the second can be related to polymer reconformation. The highest PAE dosage produced the highest initial ζ potential.

The results indicate that the adsorption, reconformation and/or penetration reach an apparent equilibrium for the three concentrations used at c.a. 10 min for electrophoretic mobility and streaming potential method. Nevertheless, as we did not measure the concentration of remaining PAE in solution, it is not possible to ascertain that the adsorption is completed.

Yoon (2007) also studied the adsorption kinetics of a commercial PAE in a fibrous suspension made of SW and HW bleached chemical fibres. The addition levels were in the same range that those used in our work. The adsorption was determined by measuring the PAE concentration in solution and the zeta potential of the fibres (streaming potential) as a function of time. The results obtained by this author show that adsorption of PAE induces extremely great variations of zeta potentials of the fibres when compared to our results. These variations are difficult to explain because they are generally not observed with this intensity when cationic polyelectrolytes are added to a pulp suspension. Moreover, significant changes of ζ still occur after 30 min of contact time even after adsorption. This phenomenon could be partly explained by a difference in the MW of the two PAE.

Considering our results, a contact time of 30 min will be chosen for the further experiments.

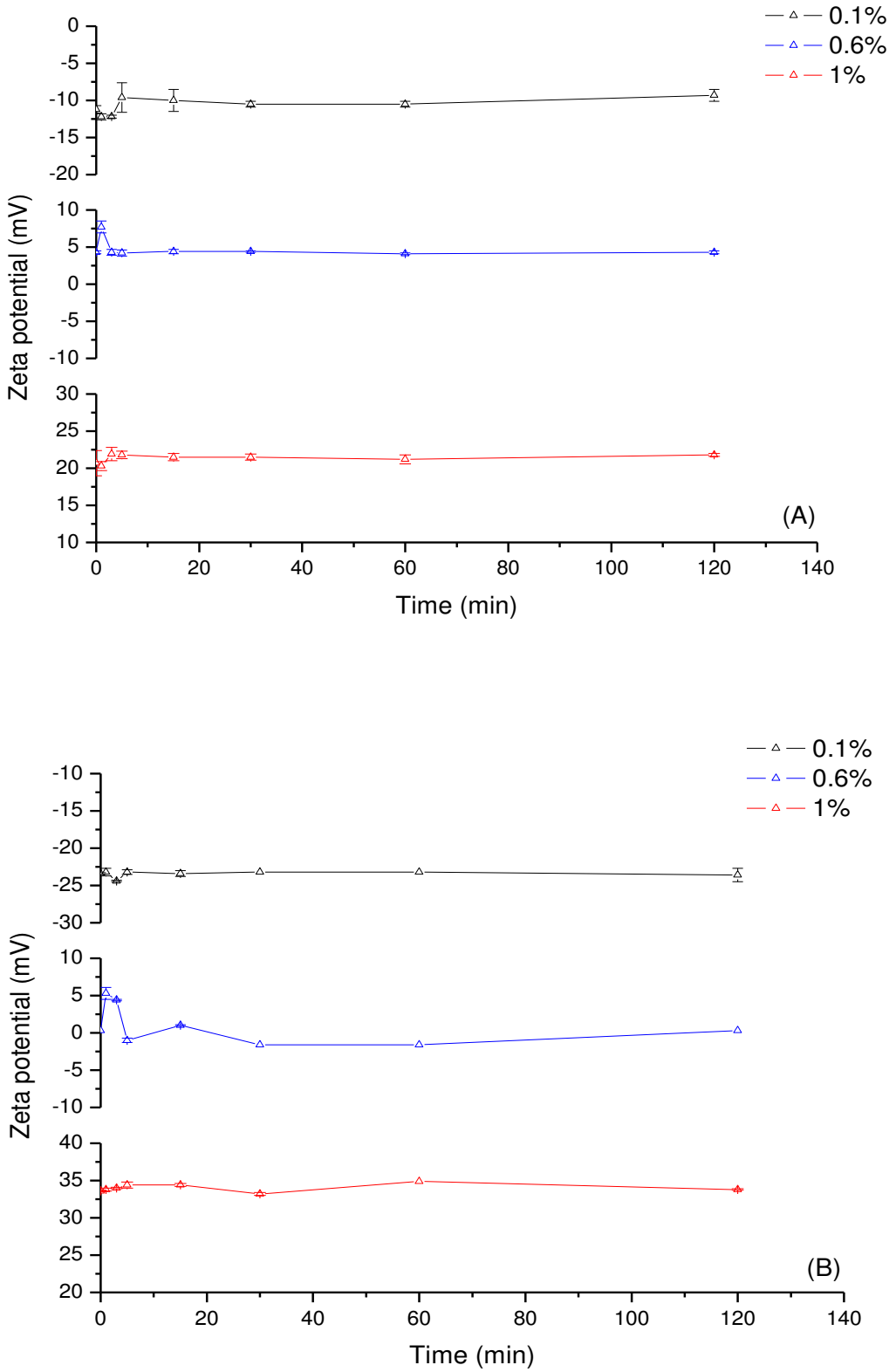

Fig. 2.8: Zeta potential measurements of *Eucalyptus* pulp using **(A)** electrophoretic mobility and **(B)** streaming potential techniques as a function of PAE concentration and standing time.

CHAPTER III: STUDY OF PAE-BASED WET STRENGTHENED PAPERS

3.1. MATERIALS AND METHODS

3.1.1. Degradation of PAE films

Degradation of thermally treated (in an oven at 105°C for 24 h) PAE films were studied in the absence of fibres. Figure 3.1 shows the stirring system used for these experiments.

Speed: 14 rps

D / d = cte = 3

h / d = cte = 1

H / D = cte = 1

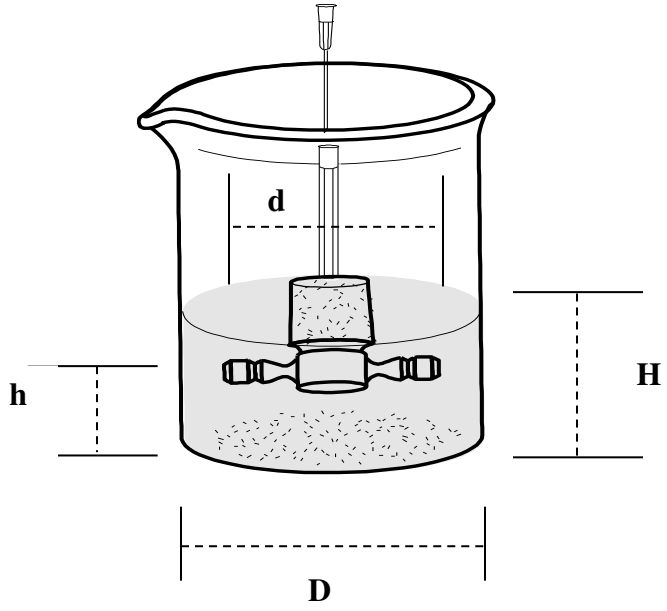

Fig. 3.1: Experimental device used for the study of the degradation of cross-linked PAE films.

The concentration of the repulping agents, the pH of the mixture, the temperature and the stirring time were varied with the aim of increasing the degradation rate of PAE films. A silicon oil bath and a thermometer were used to control the temperature. The pH values were measured continuously and adjusted when necessary. After stirring, the mixture was filtered through a Nylon sieve (1 μm). The gel fraction was washed with distilled water, dried at 105°C for 48 h and weighed. The percentage

of degradation was evaluated as the weight difference between dry PAE films before and after degradation.

3.1.2. Preparation of PAE-based wet strengthened papers

A bleached HW kraft pulp (Suzano), furnished in dry sheet form, was used in this study. The pulp was disintegrated in a laboratory pulper in deionized water at about 25 g/L consistency for 20 min. The pulp concentration was then adjusted to 20 g/L and it was beaten in a Valley beater up to 30°SR after a brushing step of 20 min. Finally, the pulp suspension was diluted and stored at 10 g/L consistency. The pH value of the pulp slurry was adjusted between 7.5 and 8, and the conductivity between 700 and 800 μS/cm with NaOH and NaCl solutions, respectively. In order to study the effects of the ionic strength of the pulp suspension on the properties of PAE-based papers prepared thereof, the conductivity of the pulp suspension was adjusted at three values: 100, 1500 and 3000 μS/cm with NaCl solution.

Handsheets were prepared in a sheet former according to ISO standards (ISO 5269-2). Samples of 2 L of the pulp slurry at 10 g/L consistency were diluted with distilled water (the pH and the conductivity of the distilled water was also previously adjusted between 7.5 and 8, and between 700 and 800 μS/cm, respectively), up to 10 L (0.2% consistency). Ten handsheets were prepared at around 2 g each one.

For preparing PAE-based handsheets, two different concentrations of PAE resin (0.4 and 1%), based on dry weight of the pulp, were added into 2 L of the pulp slurry under moderated stirring for 5 min. In this case, a mixer similar to that discussed in the previous section was used (Figure 3.1). The PAE treated pulp suspension was then left to rest 30 min. Finally, it was diluted with deionized water at 0.2% consistency, and as described above, ten PAE treated handsheets were prepared.

The effects of aging and thermal post-treatment on wet and dry strength of papers were studied. For this purpose, two sets of PAE treated papers were prepared: without and with a heat curing at 130°C for 10 min in a felted dryer. The aging studies

were carried out up to six months and the handsheets were stored during this period under controlled conditions (23°C and 50% RH).

3.1.3. Paper characterization

Before testing, papers (handsheets or industrial papers) were conditioned under controlled conditions (23°C and 50% RH) for 24 h, thus following ISO 187 standard. The thickness of handsheets was measured: 30 measurements were performed for each set of handsheets with a precision micrometer (Adamel Lhomargy M 120) according to ISO 534. The basis weight (ISO 536) was determined as the ratio of the weight of a sample by its surface area (balance Mettler H 35 AR Toledo). The average basis weight was then determined from ten measurements.

For the dry and wet tensile tests, strips were cut with a width of 15 mm. Before wet tensile tests, the strips were put in deionized water for 10 min at 23°C. The excess water was removed by putting the strip between two pieces of blotting papers and pressing it. Then, the strip was carefully placed in a tensile testing machine (L & W tensile tester), and tensile tests were performed following ISO 1924 standard, respectively. A minimum of ten samples were measured for each series. Tensile force, stretch (elongation), Young modulus and energy are the parameters determined from a tensile test. In some cases, we will use the breaking length, which is defined as the length beyond which a paper strip, with uniform width and suspended by one end, would break under its own weight. It is then determined from the tensile force and allows comparing papers having slightly different basis weights.

A scanning electron microscope (Quanta 200) was used to examine, after tensile tests, the cross-section of strips.

Finally, the amount of adsorbed PAE in handsheets was estimated from their nitrogen contents (Thermo Finnigan EA 1112). The adsorption (expressed as the ratio of the adsorbed to the added amount) was then calculated.

3.1.4. Degradation of industrial PAE-based papers

In this preliminary study, two types of industrial PAE-based papers, produced in neutral conditions, were tested: an uncoated and a coated paper. The coating colour is basically constituted of kaolin, calcium carbonate and latex. The thickness and basis weight of the two papers are reported in Table III.1.

Tab. III.1: Thickness and basis weight mean values of industrial PAE-based papers.

	Thickness (µm)	**Basis weight (g/m^2)**
NC (neutral and coated)	51.0 ± 0.7	65.9 ± 0.5
NU (neutral and uncoated)	51.0 ± 1.2	47.8 ± 1.0

Degrading studies of industrial PAE-based papers were carried out at a consistency of 10%. 20 g of papers strips (width 15 mm) were put into a plastic bag with an aqueous solution of the degrading reagent (1.5% NaOH, 1% H_2O_2, 2.75% $K_2S_2O_8$ or 1.5% H_2SO_4). Before heating, the pH of the solution was measured and the plastic bag closed. The temperature (80°C) was controlled by a thermostatic bath. After a certain time (40 or 60 min), the pH was measured again and the paper samples immediately washed with distilled water in order to eliminate the reagent in excess. Tensile tests were carried out immediately after pressing the strip between two blotting papers. Table III.2 shows the initial pH of the degrading solutions and the amount of degrading reagent used.

Tab. III.2: Amount of reagent used for the degradation study and initial pH values of degrading solutions.

Reagent	***mmol***	***initial pH***
NaOH (1.5%)	7.50	12
H_2O_2 (2.75%)	18.4	5
NaOH (1.5%) + H_2O_2 (2.75%)	7.50 + 18.4	11
$K_2S_2O_8$ (2.75%)	2.03	4
NaOH (1.5%) + $K_2S_2O_8$ (2.75%)	7.50 + 2.03	12.5
H_2SO_4 (1.5%)	3.00	3

3.2. RESULTS AND DISCUSSION

3.2.1. Preparation and characterization of PAE-based wet-strengthened papers

Even with a reasonable number of publications in the literature concerning PAE-based wet strengthened papers, there are still efforts to be made in order to understand the relationships existing between the conditions of production of the PAE-based papers and their properties. Thus, from the data available and industrial interests, we decided to investigate some particular issues, namely:

(i.) the influence of the PAE addition level into an *Eucalyptus* pulp suspension on the wet and dry tensile strengths of PAE-based papers. After studying PAE adsorption by *Eucalyptus* fibres in the Chapter II, two concentrations of PAE resins based on dry weight of the pulp were used: 0.4% (leading to a negative value of the zeta potential of the fibres or fines and thus corresponding to a partial neutralization of their surface charges) and 1% (leading to a positive value of the zeta potential of the fibres or fines and thus corresponding to the adsorption of an excess of PAE). PAE adsorption level was determined from the N content of the handsheets;

(ii.) the influence of the ionic strength of the medium on the wet and dry tensile strengths of the handsheets prepared thereof. Three conductivity values of the pulp were used: 100, 1500 and 3000 μS/cm;

(iii.) the effects of a thermal post-treatment (130°C for 10 min) and storage time (up to 6 months) on the wet and dry tensile strengths of PAE-based papers; and

(iv.) the failure mechanisms after tensile tests of PAE-based papers in wet and dry conditions, using SEM analysis of the cross-section of broken strips.

3.2.1.1. Effect of the PAE dosage on the adsorption

For determining the amount of PAE resin adsorbed onto *Eucalyptus* pulp fibres, the nitrogen content of the prepared handsheets was determined. Two sets of analysis were performed. Table III.3 reports the nitrogen content of the PAE aqueous solution,

Eucalyptus handsheets (without PAE addition) and PAE-based wet strengthened papers (0.4 and 1% PAE addition based on dry weight of the pulp).

Tab. III.3: Nitrogen content of PAE solution, *Eucalyptus* handsheets and 0.4 and 1% PAE-based wet strengthened papers.

	Number of samples analyzed	***N (%)***
PAE solution	4	12.18 ± 0.04
***Eucalyptus* paper**	8	0.14 ± 0.02
0.4% PAE-based paper	16	0.17 ± 0.02
1.0% PAE-based paper	16	0.21 ± 0.01

The N content determined for PAE solution is in agreement with theoretical calculations based on the PAE chemical structure. *Eucalyptus* paper without PAE addition (reference papers) presents a surprisingly high amount of nitrogen, which was confirmed by a second set of experiments. The content in nitrogen resulting from the addition of PAE can be obtained by subtracting the nitrogen amount in PAE-based papers from that measured in reference papers. Thus, the resulting N content is 0.03 and 0.07 %, which corresponds to PAE adsorption ratio of 62 and 58% in 0.4 and 1% PAE-based papers, respectively. Taking into account the standard deviations associated to the results as well as the precision limit of this technique (about 0.2%), it seems to be difficult to get reliable values of the adsorption of PAE by this technique. Moreover, even though a second set of measurement showed close values of N content for PAE solution and *Eucalyptus* paper, it presented remarkable differences of N content value for 0.4 and 1% PAE-based papers. Consequently, colloidal titration of the pulp filtrate followed by centrifugation under controlled conditions probably remains the best technique for assessing PAE adsorption. Nevertheless, we know that the obtained experimental values are somewhat overestimated as lignocellulosic fines are not totally

removed during the centrifugation step: adsorbed PAE on these fine elements may be titrated. Colloidal titrations were then performed on fibrous suspensions for the 0.4% dosage only. After the addition of the PAE followed by a filtration step on a Nylon sieve (1 µm) and a centrifugation step (3000 g for 20 min), a titrant solution (PES-Na) was used to determine the amount of PAE in the supernatant. The obtained results show that, at this addition level adsorption is complete, thus confirming that nitrogen dosage was not in our case a reliable technique.

3.2.1.2. Effect of the conductivity of the pulp suspension on the wet and dry strength of handsheets

In order to determine the influences of the ionic strength on the dry and wet strength of PAE-based papers, three conductivity values were used for preparing handsheets: 100, 1500 and 3000 µS/cm. This study was carried out because we did not find in the literature any publication reporting a quantitative evaluation of the effect of the conductivity on the wet strength of PAE-based papers. Table III.4 shows the thickness and basis weight mean values of the handsheets. On Figures 3.2 and 3.3, the dry and wet breaking lengths obtained for 0.4 and 1% PAE-based papers are plotted as a function of the conductivity of the pulp suspension and storage time of the handsheets prepared thereof (up to 3 months). The curves for other parameters assessed from tensile tests as energy and stretch (elongation) also showed the same tracings.

Tab. III.4: Thickness and basis weight mean values for PAE-based papers.

Conductivity (µS/cm)	***% PAE***	***Thickness (µm)***	***Basis weight (g/m^2)***
100	0.4	114 ± 0.3	66.2 ± 0.3
	1.0	114 ± 0.2	66.7 ± 0.2
1500	0.4	110 ± 0.8	64.9 ± 0.9
	1.0	111 ± 0.2	66.9 ± 0.2
3000	0.4	109 ± 0.6	66.5 ± 0.6
	1.0	110 ± 0.2	66.7 ± 0.3

Considering the obtained results for the dry strength, it clearly appears that this property is not significantly affected by the conductivity level of the pulp suspension. Under the tested experimental conditions (stirring time: 5 min; contact time: 30 min; pH comprised between 7 and 8; thermal post-treatment at 130°C for 10 min), the dry breaking lengths of 0.4 and 1% PAE-based papers are constant for conductivity varying between 100 and 3000 µS/cm and over time (from 1 to 90 days of paper storage under controlled conditions: 23°C and 50% RH). When the PAE dosage increases from 0.4 to 1%, the dry breaking length rises from 5.4 to 5.8 km, approximately.

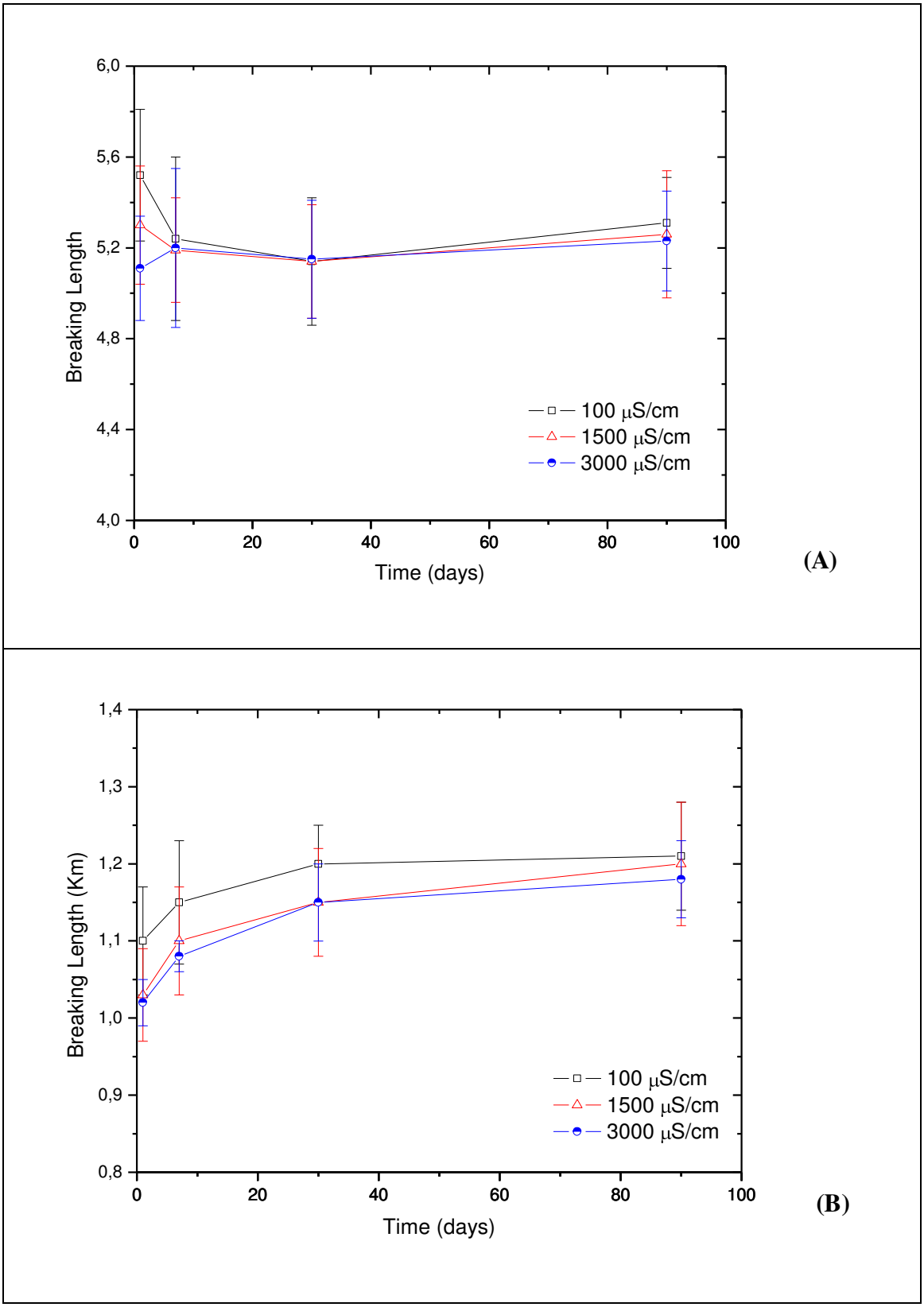

Fig. 3.2: Breaking length of heated 0.4% PAE-based wet strengthened papers obtained in **(A)** dry and in **(B)** wet conditions as a function of the conductivity of the pulp suspension and storage time of the handsheets.

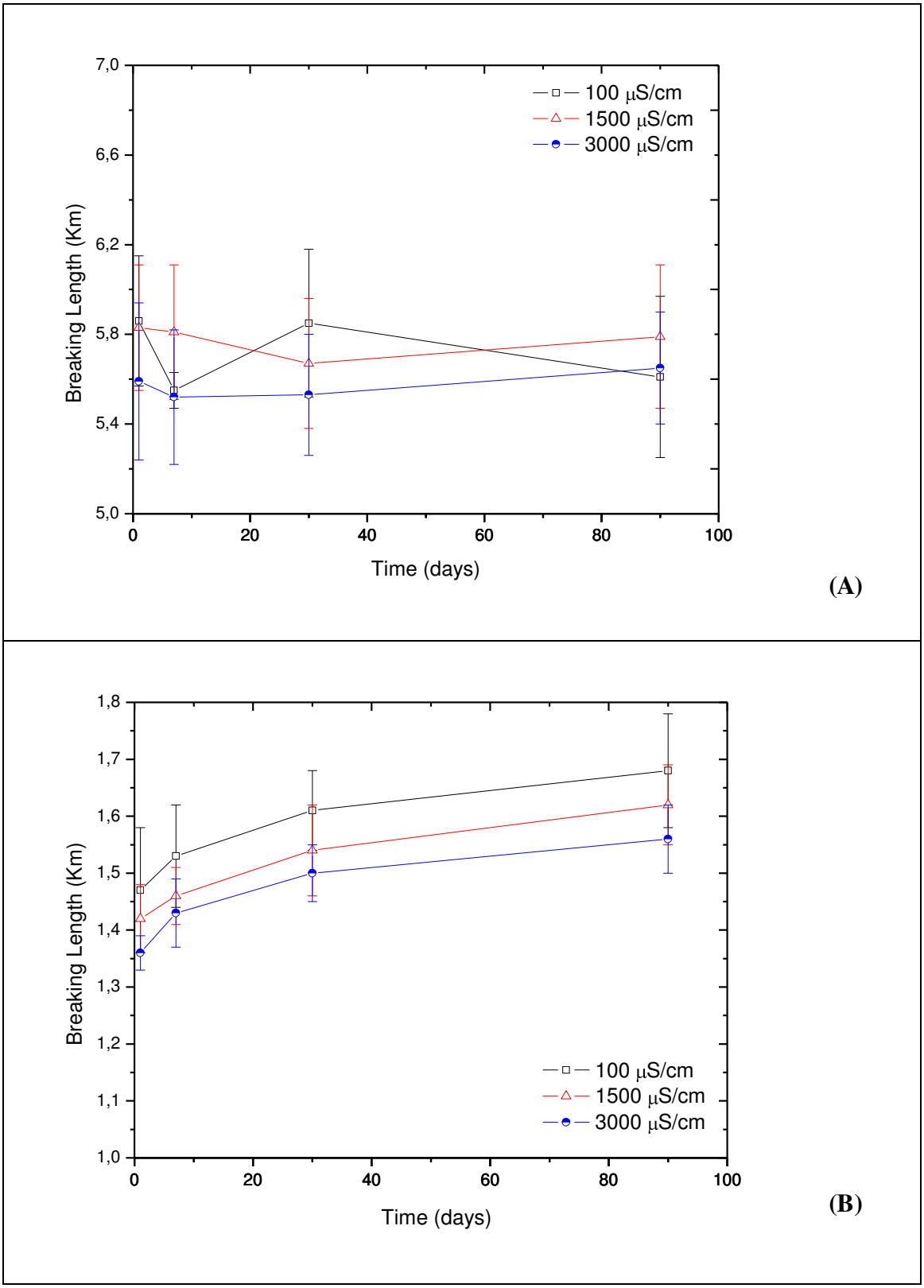

Fig. 3.3: Breaking length of 1% heated PAE-based wet strengthened papers obtained in **(A)** dry and in **(B)** wet conditions as a function of the conductivity of the pulp suspension and storage time of the handsheets.

Regarding now the wet breaking length, we observe that the obtained values are about 1.2 and 1.6 km for 0.4 and 1% PAE-based papers, respectively. As expected, these values correspond approximately to a ratio of wet to dry breaking lengths of about 25%. A more detailed analysis shows that the wet breaking length slightly increase with time whatever the conductivity level. This phenomenon can be explained by the fact that the cross-linking of the PAE polymers in the paper structure is a time dependent reaction. This increase is not visible when considering the evolution of the dry breaking length, as previously discussed, probably because it is very limited. Finally, the wet breaking length seems to be modified when the conductivity varies, especially for the 1% PAE-based papers and the values obtained at 100 µS/cm are always higher than those obtained at 3000 µS/cm. Of course, if we consider the standard deviations, the significance of this difference can be questioned. Nevertheless, as it exists whatever the storage time, we conclude that the conductivity has a detrimental impact on the wet strength of the papers and this effect seems to be enhanced when the PAE is added at 1%. One possible explanation is related to the salt screening effects of the attractive electrostatic interactions existing between cationic PAE and anionic fibres. For the highest dosage (1%), the zeta potential of the lignocellulosic surfaces is positive indicating that the PAE is adsorbed in excess, as already mentioned. Thus, we can suppose that when the zeta potential of the fibres switches from a negative value to a positive one, the interactions between the cationic PAE and the fibres become weaker. In this particular case, these interactions are probably more sensitive to the presence of salts because there are very few remaining anionic sites on the fibres. Moreover, it is worth noting that the polymer conformation changes when the ionic strength increases. This behaviour is well known and it may also lead to changes in the conformation of the adsorbed polymers. It is generally accepted that until a certain level of ionic strength, the increase of the salt concentration promotes the adsorption of the polymer as the new conformation (random coil) facilitates the polymer diffusion into the wall of the fibres. If the conductivity continues increasing, the adsorption decreases rapidly due to the screening effects. Finally, the conformation of the adsorbed polymer may also impacts the cross-linking of the PAE and then the wet strength of the treated papers. However, as it was not possible to determine the adsorbed amount of PAE as a function of the conductivity of the pulp by using nitrogen analysis, it was not possible to conclude. From these results, it appears that controlling the conductivity is fundamental to get

reliable data. Consequently, we decided to use a conductivity of the pulp suspension comprised between 700 and 800 µS/cm for further experiments.

3.2.1.3. Effect of a thermal post-treatment of PAE-based handsheets and their storage time on the wet and dry strength

The tensile strength of PAE-based papers was measured as a function of the storage time, in wet and dry conditions, for two PAE dosages (0.4 and 1%) and with a conductivity of the pulp adjusted between 700 and 800 µS/cm. Ageing studies of the handsheets were carried out with and without a thermal post-treatment at 130°C for 10 min and for storage times varying between one and 90 days. Table III.5 shows the thickness and basis weight mean values of these handsheets. Figure 3.4 and 3.5 show the breaking length obtained in wet and in dry conditions.

Tab. III.5: Thickness and basis weight mean values of the prepared handsheets with and without a thermal post-treatment.

Conductivity (µS/cm)	***% PAE***	***Thickness (µm)***	***Basis weight (g/m^2)***
Heated	0.4	104 ± 1.2	63.0 ± 1.3
	1.0	106 ± 0.3	64.1 ± 1.0
Unheated	0.4	112 ± 0.8	67.6 ± 0.4
	1.0	115 ± 0.6	66.8 ± 0.5

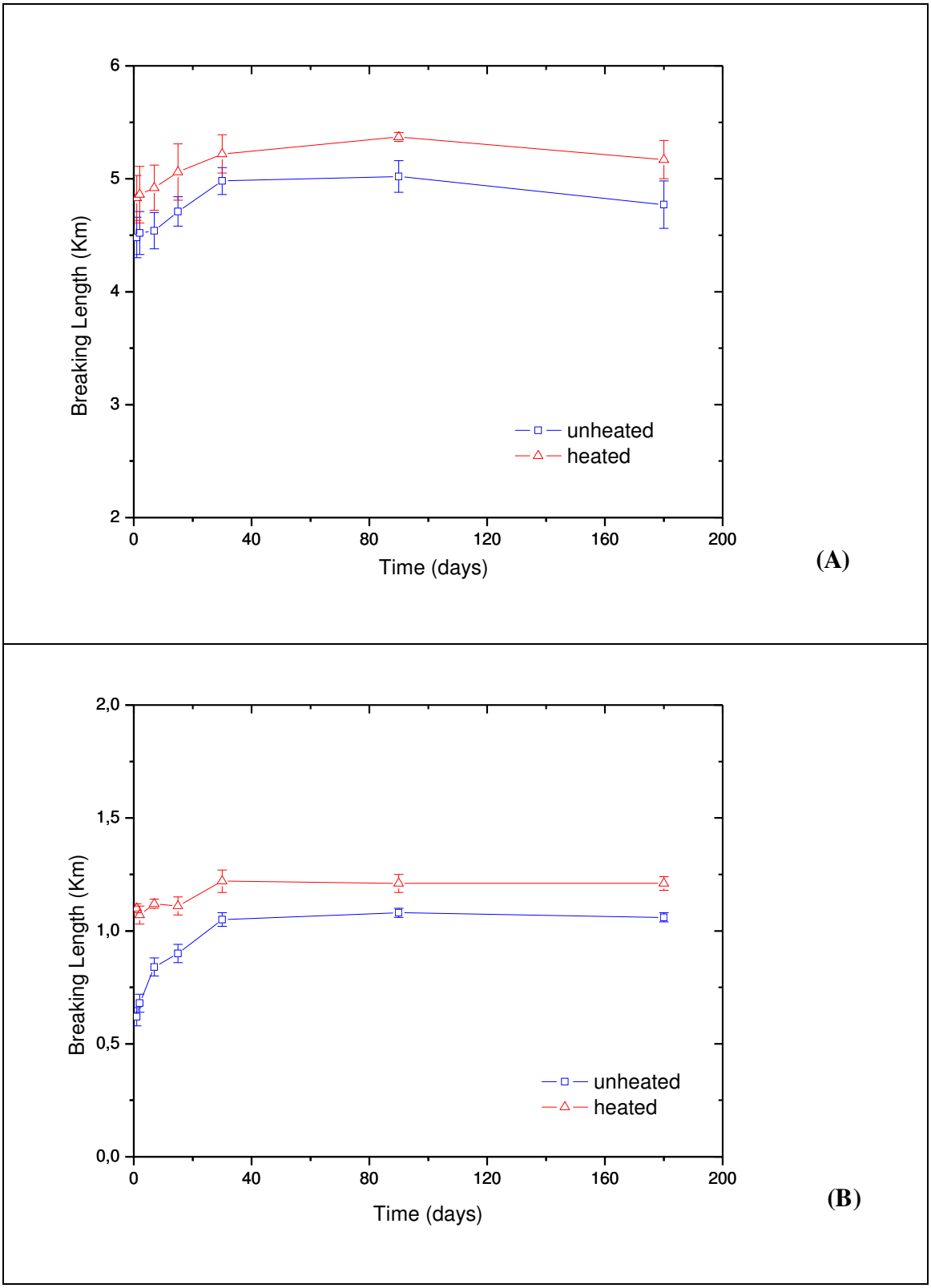

Fig. 3.4: Breaking length of heated and unheated 0.4% PAE-based papers in **(A)** dry and in **(B)** wet conditions as a function of storage time of handsheets.

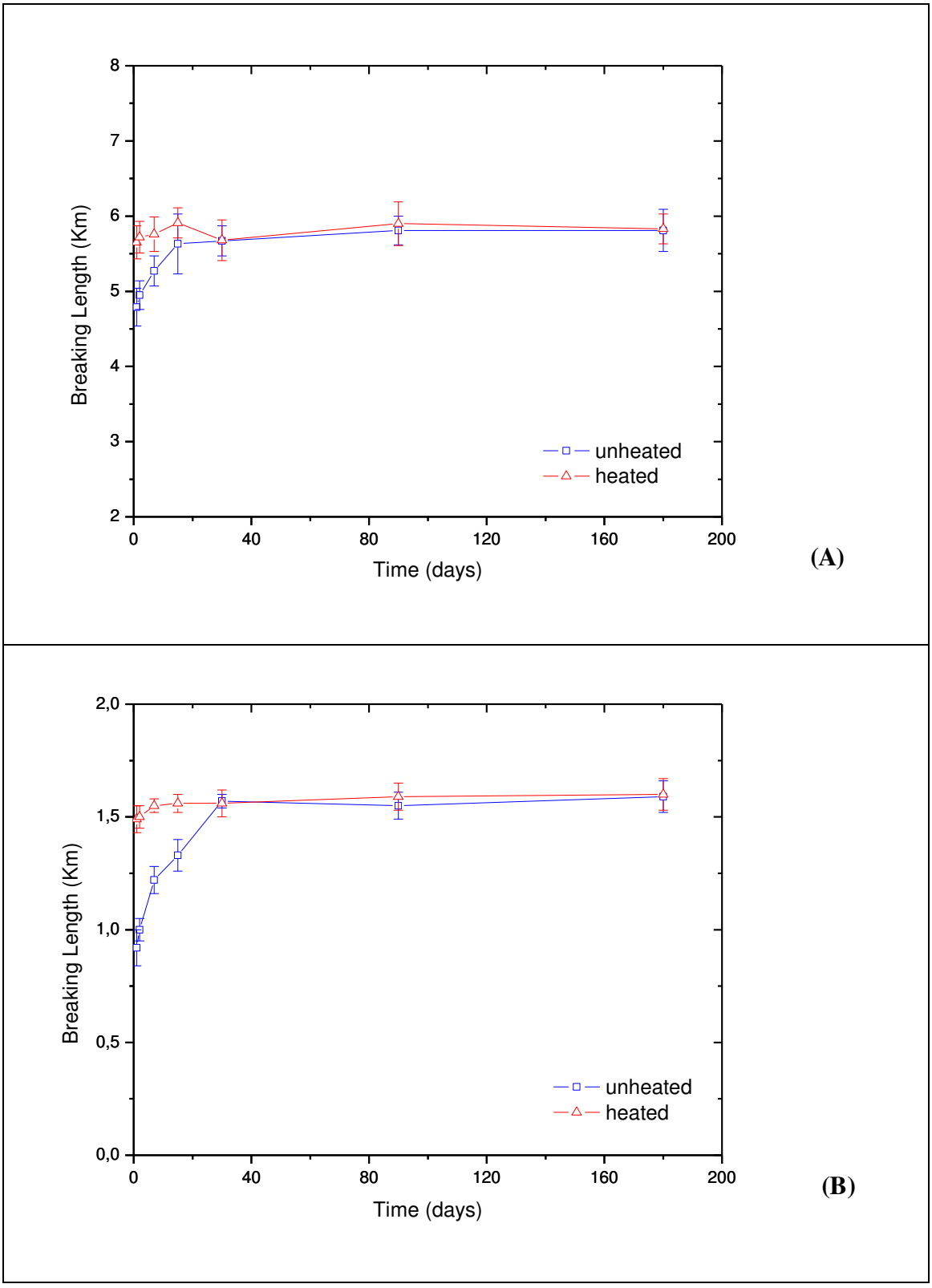

Fig. 3.5: Breaking length of heated and unheated 1% PAE-based papers in **(A)** dry and in **(B)** wet conditions as a function of storage time of handsheets.

An increase of about 40 and 59% of the breaking length is observed for 0.4 and 1% PAE-based papers, respectively, in dry conditions and at 40 days of storage when compared to that of handsheets without PAE addition (3.71 ± 0.22 Km). The W / D ratio for 0.4 and 1% PAE-based papers are approximately 23 and 28%, respectively, for the same storage period.

Whatever the storage time, unheated and heated 0.4% PAE-based papers show differences in terms of breaking length. In Table III.6, breaking length values are reported for two storage times (2 and 40 days). After a storage time of 2 days, the thermal post-treatment induces an increase of 57% (0.39 km) of the wet breaking length. This increase is reduced to 16% (0.17 km) after 40 days. It is remarkable that the differences observed in the wet state also exist in the dry state. Here again, the thermal post-treatment allows an increase of 8% (0.34 km) after 2 days and of 5% (0.24 km) after 40 days.

Tab. III.6: Breaking length obtained by tensile tests of heated and unheated 0.4 and 1% PAE-based papers up to 40 days of ageing.

Km	**0.4%**				**1%**			
	Dry		**wet**		**Dry**		**Wet**	
days	**H**	**UH**	**H**	**UH**	**H**	**UH**	**H**	**UH**
2	**4.86 ± 0.25**	**4.52 ± 0.19**	**1.07 ± 0.04**	**0.68 ± 0.04**	**5.72 ± 0.21**	**4.95 ± 0.19**	**1.50 ± 0.05**	**1.00 ± 0.05**
40	**5.22 ± 0.17**	**4.98 ± 0.12**	**1.22 ± 0.05**	**1.05 ± 0.03**	**5.90 ± 0.30**	**5.67 ± 0.20**	**1.56 ± 0.06**	**1.57 ± 0.03**

H: heated UH: unheated

Oppositely, 1% PAE-based papers with and without thermal post-treatment exhibit similar values of the breaking length (wet or dry) from 40 days of storage. Thus, for this series, the results show that it is possible to reach the same "equilibrium" state by storing unheated handsheets for a given period and under controlled conditions (23°C and 50% RH) or boosting the PAE cross-linking with a thermal post-treatment (130°C for 10 min) just after the drying of the handsheets. Before 40 days, the breaking length of the 1% PAE-based handsheets is significantly improved by the thermal post-treatment.

The observed difference between the behaviours of the 0.4 and 1% PAE-based papers is surprising. At low dosage (0.4%), the curing period does not allow the dry or wet PAE-based papers recovering the strength of the heated samples even after 6 months of storage. At high dosage (1%), the PAE cross-linking seems to occur at a sufficient extent during the curing period to reach the same strength values than those obtained for the heated samples. In both cases, a plateau value is obtained from 40 days i.e. after 40 days under controlled conditions, the dry and wet properties are stabilized and the cross-linking reaction of the PAE is considered to be over even if its extent is less important in the particular case of the unheatead 0.4% PAE-based handsheets.

Finally, these results do not allow proving that a thermal induced reaction between PAE (AZR) resin and cellulosic fibres (carboxylic groups) occurs resulting in the formation of ester bonds. Indeed, even if these bonds are formed, their contribution to the dry strength of the handsheets seems to be negligible. Thus, for the 1% PAE-based papers, there is no difference in terms of dry breaking length between heated and unheated samples. For the 0.4% dosage, there is a difference between the dry strengths of the heated and unheated samples. But, as this difference also exists for the wet breaking length, it seems disputable to affect it to the reinforcing effect of these ester bonds which are hydrolysable. Moreover, as discussed in Part I, these thermally induced bonds may also be partially hydrolysed in not anhydrous conditions.

Other parameters of the tensile test (elongation, Young modulus, specific energy) present close behaviours and their evolution as a function of the storage time leads to the same conclusions. All these data are shown in Annex.

In order to better understand how the breaking occurs during a tensile test in the PAE-based handsheets, SEM observations of the breaking zone have been made. Figure 3.6 shows micrographs of *Eucalyptus* handsheets after tensile tests in dry conditions. As observed (Figure 3.6-A, B), there is a pull-out of the fibers in the paper strips in the direction of the stress. During a tensile test of strips, the fibres seem to slide without damaging the wall in a great extent (Figure 3.6-D). Only very few broken fibres are observed (Figure 3.6-C).

.

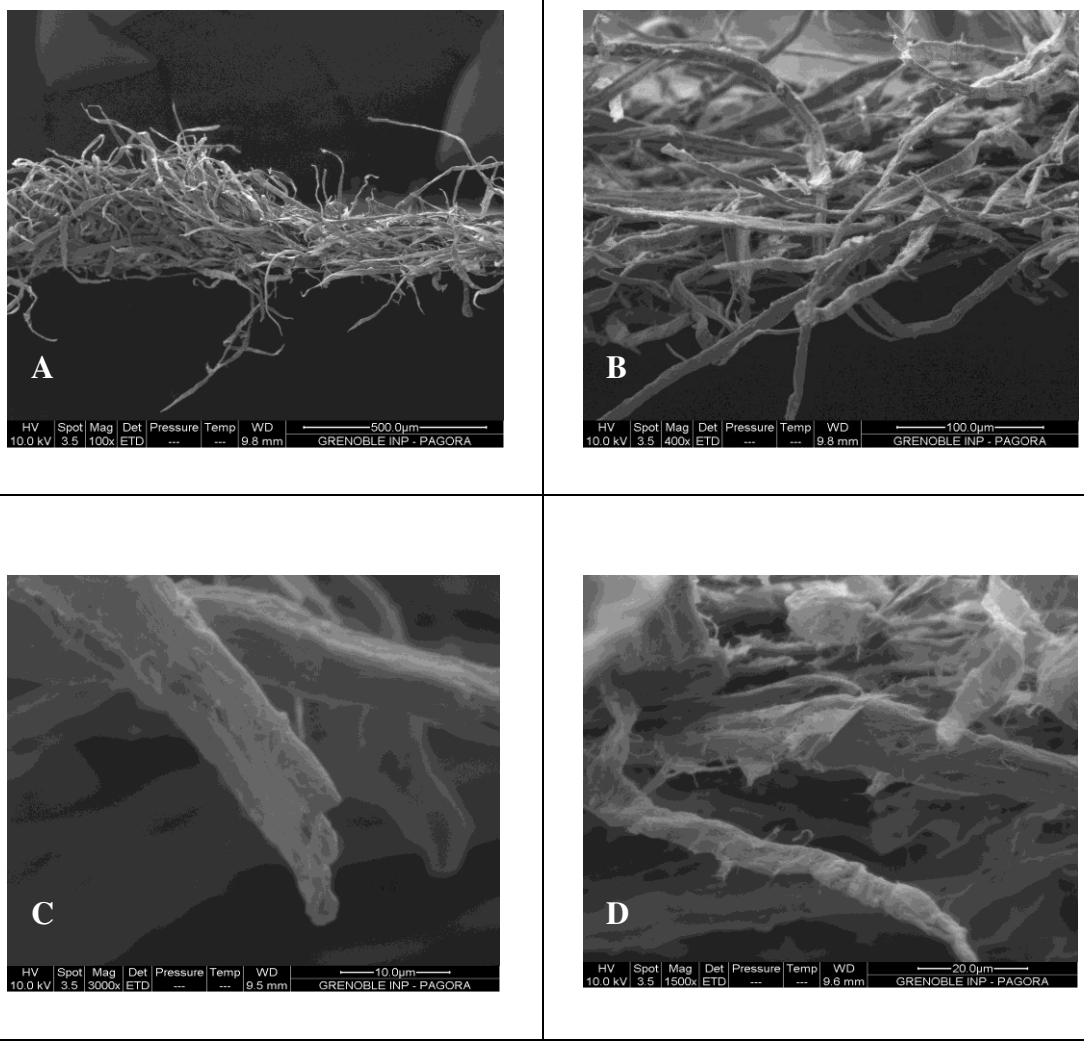

Fig. 3.6: Micrographs obtained by SEM of *Eucalyptus* handsheets after tensile tests on dry conditions.

Figures 3.7 and 3.8 show heated 1% PAE-based papers after tensile tests in dry and wet conditions, respectively. In dry conditions, the breaking zone is different (Figure 3.7-A) and the failure seems to occur in the fibre walls (Figure 3.7-B, C, D). We can observe a peeling off of the external layers of the fibre wall probably due to the adhesive properties of the PAE resin adsorbed on fibre surface.

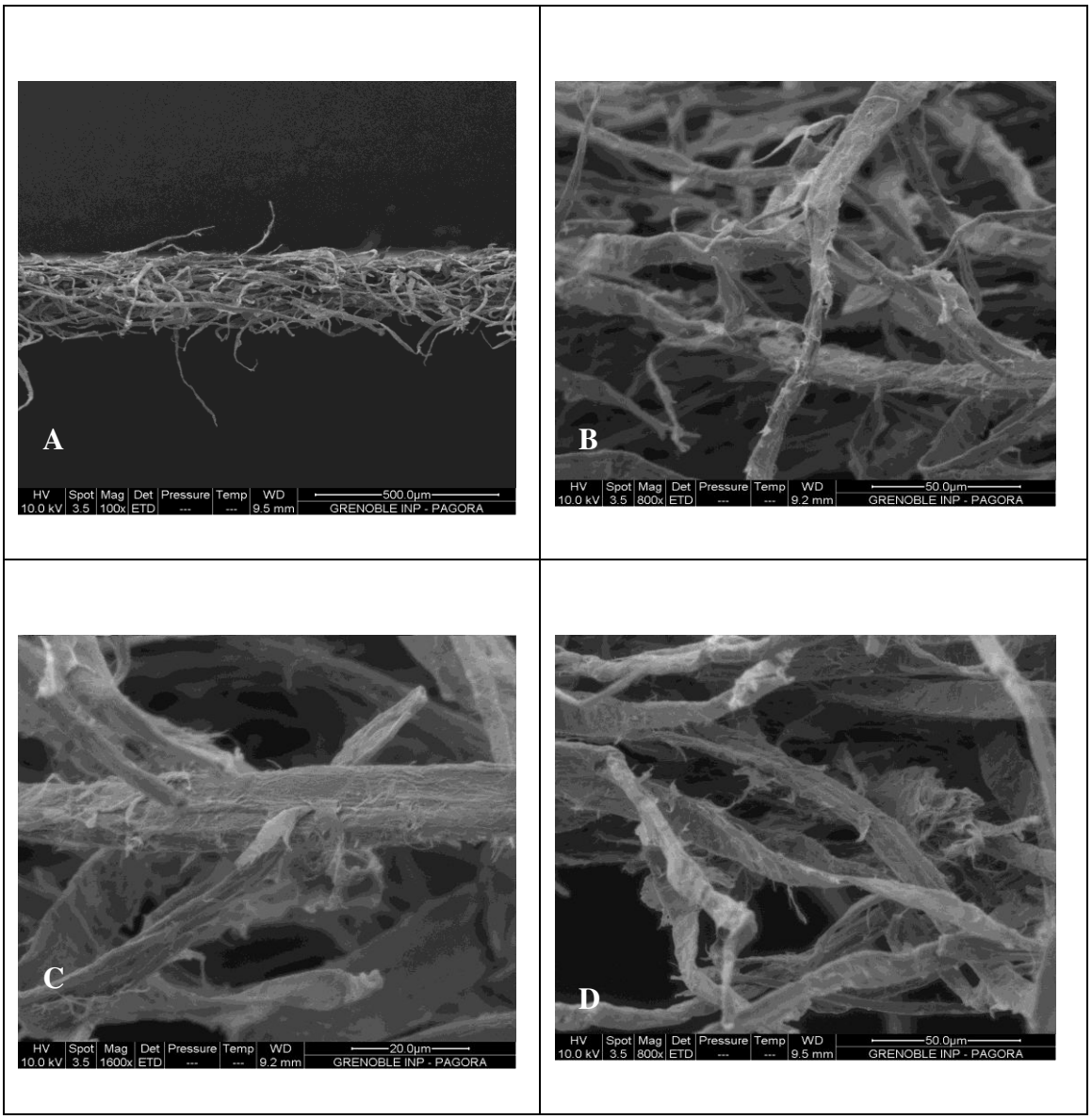

Fig. 3.7: Micrographs obtained by SEM of heated 1% PAE-based papers after tensile tests in dry conditions.

In wet conditions, we again observe a pull-out of the fibres from the strips (Figure 3.8-C). In this case, the surface of the fibres remains intact (Figure 3.8-B, D). Apparently, the absorbed water induces a swelling of the paper structure and the fibres and it may contribute to the slipping of the fibres without a severe delamination of the fibre walls. However, it is still difficult to conclude because dried strips were observed and the appearance of the fibres could have been modified by the drying of the strips after the tensile test.

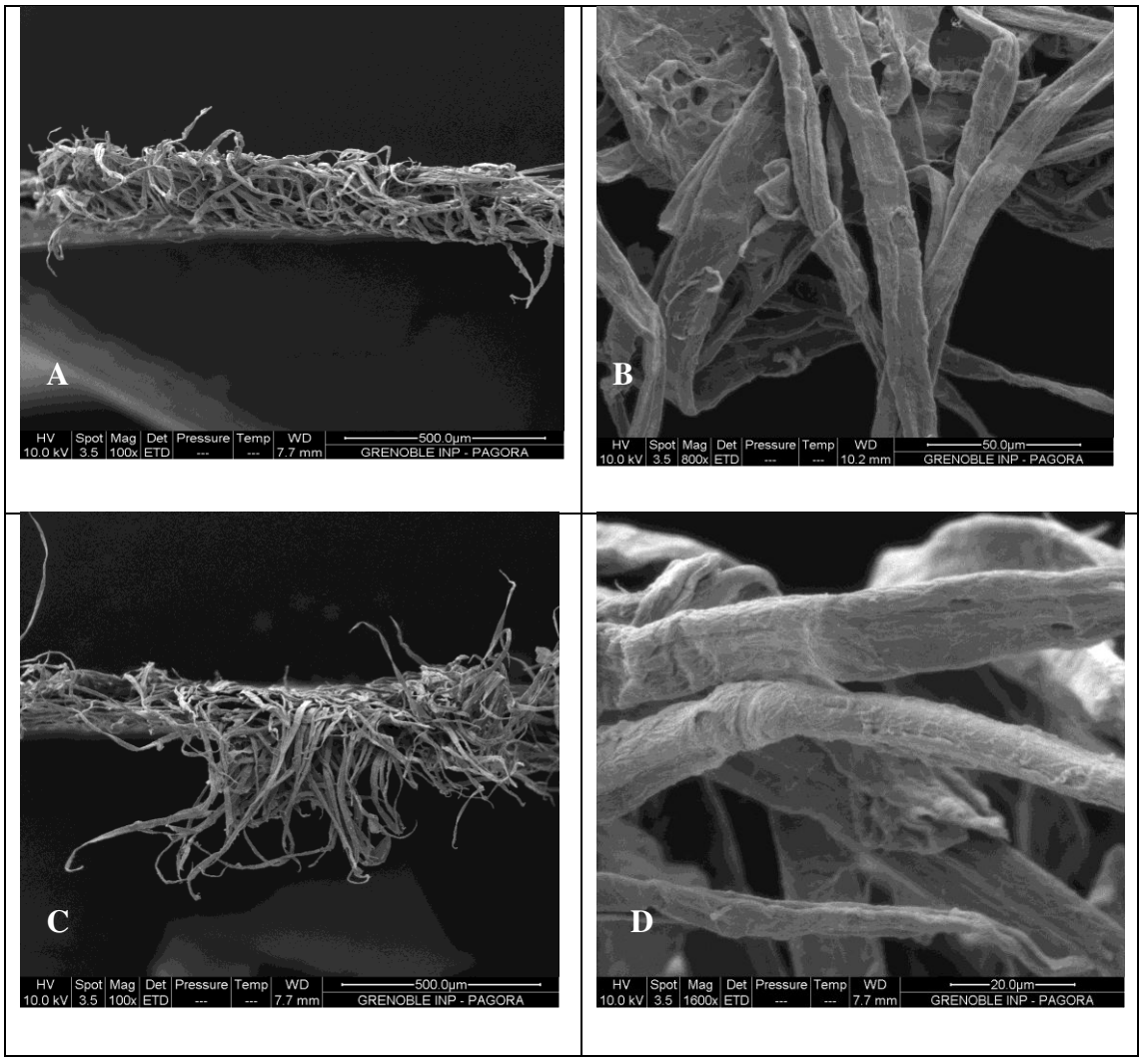

Fig. 3.8: Micrographs obtained by SEM of heated 1% PAE-based papers after tensile tests in wet conditions.

To conclude, the increase on wet strength is probably a result of combined effects, namely: **(i.)** cross-linking of PAE in the fibre walls resulting in a significant reduction of the fibre swelling; **(ii.)** cross-linking of PAE at fibre-fibre contacts; and **(iii.)** formation of covalent ester bonds between PAE resin and cellulosic fibres as a secondary contribution.

3.2.2. Repulping of PAE-based papers

3.2.2.1. Degradation of PAE films

As previously discussed, PAE-based papers are difficult to repulp. Intensive treatments coupling the use of chemical reagents and mechanical actions are then necessary. In this study, we focused on the effect of reagents on degradation of cross-linked PAE films (in the absence of fibres) in order to gain a better understanding of the involved phenomena.

Table III.7 shows the results obtained after the treatment of PAE films in water, and in sodium hydroxide (NaOH), sulphuric acid (H_2SO_4), hydrogen peroxide (H_2O_2) and potassium persulfate ($K_2S_2O_8$) aqueous solutions, at 40°C for 40 min. Δm represents the relative weight difference between the initial (m_i) and final mass (m_f) of the PAE film samples:

$$\% \Delta m = (m_f - m_i) / m_i$$

Tab. III.7: Study of the degradation of heated PAE films at 40°C for 40 min.

	(mmol)	pH_i	*Conductivity* $(\mu S/cm)_i$	pH_f	*Conductivity* $(\mu S/cm)_f$	Δm *(%)*
H_2O	**100mL**	**5.8**	**2.87**	**3.4**	**6970**	**7.95**
NaOH	**2.50**	**10.7**	**170**	**4.4**	**16060**	**8.57**
H_2SO_4	**1.02**	**1.9**	**656**	**2.5**	**4680**	**8.27**
$K_2S_2O_8$	**0.866**	**3.9**	**1817**	**3.5**	**4880**	**9.40**
H_2O_2	**1**	**5.4**	**6.38**	**3.2**	**2714**	**9.71**

i: initial (before the introduction of the PAE films); f: final (after 40 min)

In these experimental conditions, there is only a small degradation of the PAE films, amounting around 10%, whatever the chemicals used. A decrease of the initial pH value from 10.7 to 4.4 during the NaOH degradation is due to the neutralization of the acids added into the PAE solutions immediately after the PAE synthesis and neutralization of protonated nitrogen atoms in the structure of the starting PAE resin. The high final conductivity of the solution with NaOH treatment could be explained by:

(i.) the relatively high amount of NaOH used in this experiment in order to reach alkaline conditions; and

(ii.) the limiting ion conductivity in water of Na^+ ions (5.011 mS m^2mol^{-1}) at 298 K (Atkins *et al.*, 2006).

In water, there is a decrease of the pH value and an increase of the conductivity due to the dissolution of species from PAE film. This dissolution is probably less important for experiments carried out with H_2SO_4 and $K_2S_2O_8$ which could explain the lower value of the final conductivity. All these results represent one set of measurements.

Table III.8 shows results obtained with the same chemicals, but at higher temperature and reaction time. With NaOH treatment, a ten folds concentration was needed to maintain an alkaline pH during all the time when compared with the experiment at 40°C for 40 min, where the alkaline condition was only initially adjusted. Increasing the temperature to 80°C and the reaction time to 180 min gives rise to an increase of the % degradation of PAE, when using NaOH, $K_2S_2O_8$ and H_2O_2, as degrading chemical reagents.

Tab. III.8: Degradation of heated PAE films at 80°C for 180 min.

	(mmol)	pH_i	***Conductivity*** $(\mu S/cm)_f$	pH_f	***Conductivity*** $(\mu S/cm)_f$	Δm ***(%)***
H_2O	100mL	5.9	1.64	3.2	12980	7.48
NaOH	20	11	7800	10	44400	17.4
H_2SO_4	1.04	2.8	921	3	13200	7.31
$K_2S_2O_8$	1.04	3.9	2162	3	8160	17.8
H_2O_2	1	5.4	6.4	2.6	5990	20.7
H_2O_2 + ***NaOH***	1 + 30	12	7564	11.5	16450	22.3

i: initial (before the introduction of the PAE films); f: final (after 180 min)

From these results, it appears that:

(i.) PAE degradation is not efficient neither in water nor in H_2SO_4 solution, even with an increase of the treatment time (from 40 to 180 min), and of the temperature (from 40 to 80°C);

(ii.) PAE degradation with NaOH solution is considerable. However, due to the acidification of the PAE solution after synthesis, a very high amount of NaOH is needed to maintain the alkalinity of the medium during experiment; and

(iii.) PAE degradation with persulfate and hydrogen peroxide is significantly increased by an increase of the temperature and/or the time.

Fischer (1997) repulped PAE-based paper samples using the following treatment sequence:

(i.) heating with an oxidizing agent at pH ≤ 7 for 30 min;

(ii.) then raising the pH to 11; and

(iii.) heating for additional 30 min.

By this way, he obtained significantly higher amounts of repulped paper. Based on these results, a double pH degradation study of cross-linked PAE films was performed at 80°C. First, the degradation was carried out in acidic conditions (H_2SO_4 or $K_2S_2O_8$) for 90 min, followed by an alkaline treatment (NaOH) for 90 min. Table III.9 reports the obtained results.

Tab. III.9: Degradation of cross-linked PAE films at 80°C for 180 min using a double pH method (90 min in acidic conditions and 90 min in alkaline conditions).

	(mmol)	***pH_i***	***Conductivity $(\mu S/cm)_f$***	***pH_f***	***Conductivity $(\mu S/cm)_f$***	***Δm (%)***
H_2SO_4 + NaOH	1.04	2.0	5970	2.4	4610	18.7
	20	11	9680	9.8	31800	
$K_2S_2O_8$ + NaOH	1.04	4.0	2320	2.7	6910	23.5
	20	11.5	33400	8.6	28900	

Performing a double pH treatment in the presence of H_2SO_4 + NaOH does not significantly improve the degradation of the PAE film when compared to a one-step treatment with NaOH only. An increase from 17 to 23% was observed when using persulfate + NaOH double pH treatment, when compared to the same treatment but only with persulfate in acidic conditions. From these results, we decided to study only the persulfate effects on the degradation of cross-linked PAE films. Three drastic conditions were used at 80°C. Table III.10 shows the obtained results for the following sequences:

(i.) Sample 1 (S_1): 60 min of stirring in a $K_2S_2O_8$ solution at acid pH (pH < 7) + 120 min of stirring at alkaline pH (pH ≤ 9);

(ii.) Sample 2 (S_2): 180 min of stirring in a $K_2S_2O_8$ solution at pH value of 11;

(iii.) Sample 3 (S_3): 60 min of stirring in a $K_2S_2O_8$ solution at acid pH (pH < 7) + 120 min of stirring at alkaline pH (pH = 11).

Tab. III.10: PAE degradation with potassium persulfate in drastic conditions.

	(mmol)	***pH_i***	***Conductivity $(\mu S/cm)_f$***	***pH_f***	***Conductivity $(\mu S/cm)_f$***	***Δm (%)***
(S_1) $K_2S_2O_8$ + NaOH	1.04 20	3.4	580	9.0	32700	26
(S_2) $K_2S_2O_8$ + NaOH	1.85 30	11	5690	11	50700	28
(S_3) $K_2S_2O_8$ + NaOH	3.67 30	3.3	7650	11	45300	33.7

From the obtained results, we can postulate that:

(i.) PAE degradation in a persulfate solution at alkaline medium (28%) was more effective when compared to the degradation yield reached under acidic conditions (17.8%) and at a double pH treatment (23%). Here again, a high amount of NaOH is needed to maintain the alkaline condition of the medium during the experiment;

(ii.) the drastic conditions for S_3 permitted to reach the highest degraded amount of PAE.

PAE contains primary, secondary (molecules not modified by epichlorohydrin), and tertiary amines and N-substituted amides that are susceptible to oxidation. Figure 3.9 shows a schematic representation of cross-linked PAE degradation.

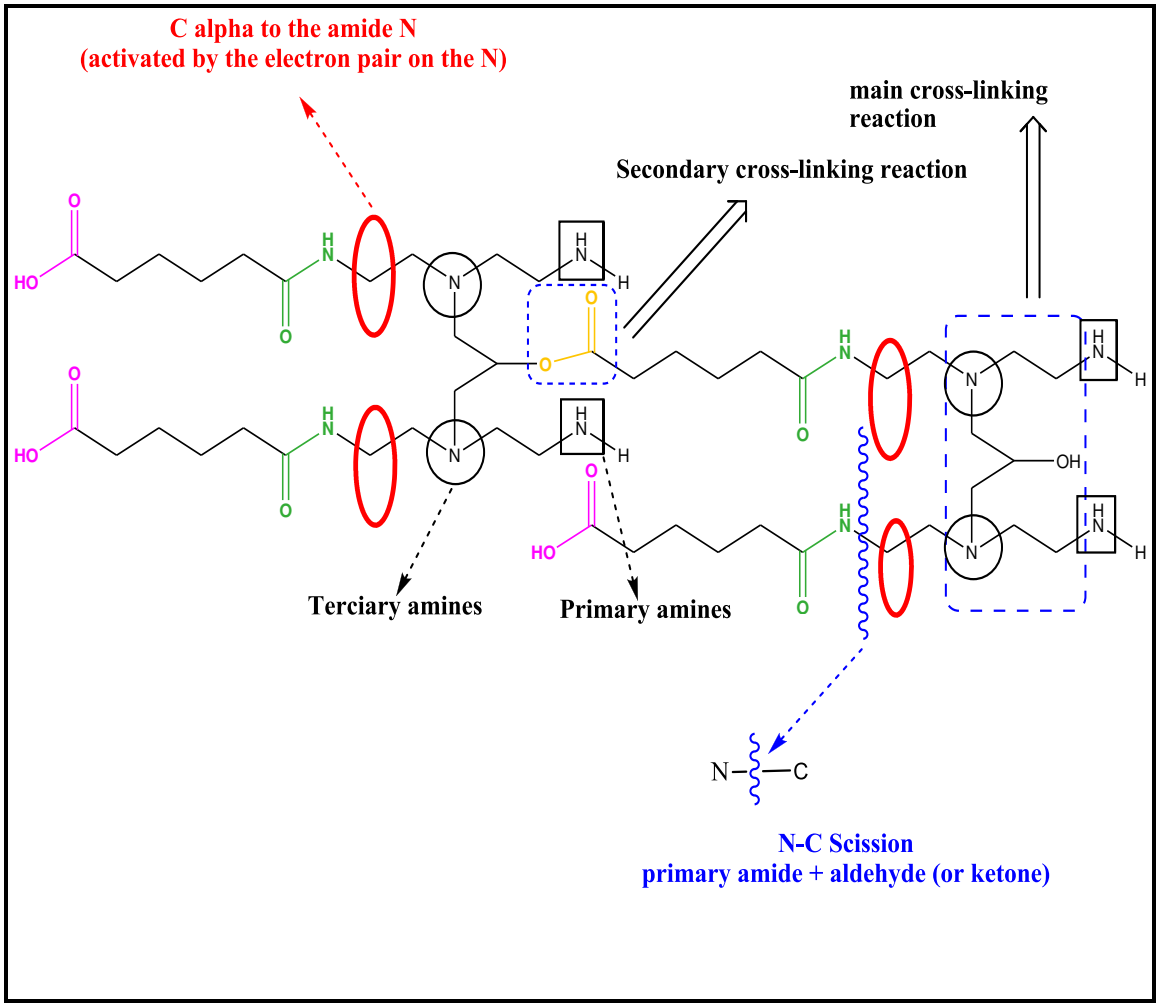

Fig. 3.9: Schematic representation of persulfate degradation of cross-linked PAE films.

Oxidation of N-substituted primary amides (i.e. amides on the backbone of the PAE resin) may proceed by a free radical attack on the α-carbon (with respect to the amide nitrogen), which is activated by the electron pair on the nitrogen atom. For example with one mol of potassium persulfate salt, three free radicals are formed during the initiation step, i.e.: $2\ SO_4^{\ominus}\bullet$ and $\bullet OH$. This is followed by the resin decomposition reaction (N-C scission), yielding an unsubstituted primary amide and an aldehyde moiety by dealkylation (Fischer, 1997; Espy and Geist, 1993; Needles and Whitfield, 1964; Mare, 1960; Kennedy and Albert, 1960; Levitt, 1955). In order to confirm this mechanism, Fischer (1997) has reacted an aqueous solution of commercial PAE resin with a hydrogen peroxide-iron redox couple (Fenton's reagent), at a pH value of 4 and at 50°C. An aldehyde by-product and chemical shifts in the amide structure were observed in ^{13}C NMR spectra of the treated PAE solution, suggesting that the oxidation by a free radical mechanism is plausible.

Other possible degrading mechanisms are: nucleophilic or electrophilic addition of persulfate anions and cations, followed by the hydrolysis of the structure under acidic and alkaline conditions. Thus, this resin has oxidizable secondary and tertiary amine groups and a possible path of oxidation is a nucleophilic attack of the amines in the resin (i.e., by free radicals), thus forming amine oxides. The cleavage follows and produces alkenes and hydroxylamines (the Cope Elimination Reaction). However, from thermodynamical considerations, these mechanisms are considered secondary for the PAE degradation, when compared to the direct oxidation by a free radical attack.

As perspective, other efforts can be made for optimizing the conditions used in this section (temperature, time, concentration of reagents, consistency of the medium, stirring, catalysts, and etc). Nevertheless, as postulated at the beginning of this section, this is only a preliminary study.

3.2.2.2. Degradation of industrial PAE-based papers

Following the study of the degradation of PAE films, industrial papers were tested with the same reagents in order to ascertain if the tendencies observed for degradation of PAE films could be transposed to PAE-based papers. Moreover, as uncoated and coated papers were available, the effect of the coating was also investigated. For these experiments, the effectiveness of the reagents was evaluated by measuring the tensile force in wet conditions immediately after the chemical treatments as described in "Materials and Methods".

The mean values of the dry and wet breaking force, stretch, specific energy and Young modulus of the industrial PAE-based papers are reported in Table III.11.

Tab. III.11: Wet and dry tensile strengths of industrial PAE-based papers.

	Force (N)	**Breaking length (Km)**	**Stretch (mm)**	**Specific energy (mJ/g)**	**Young modulus (GPa)**
NC dry	61.7 ± 2.9	6.42 ± 0.32	1.51 ± 0.11	592 ± 63	8.90 ± 0.32
NU dry	46.3 ± 3.5	6.51 ± 0.53	1.72 ± 0.12	724 ± 9	6.11 ± 0.41
NC wet	19.6 ± 1.3	2.02 ± 0.13	3.38 ± 0.20	424 ± 64	0.444 ± 0.385
NU wet	13.0 ± 1.8	1.84 ± 0.25	3.78 ± 1.58	397 ± 77	1.06 ± 0.35

Table III.12 presents the results obtained from the wet tensile tests of NU paper after the chemical treatments. Some degrading experiments were performed on duplicate to check the reproducibility of the results. Persulfate treatment was the more efficient and the tensile force of persulfate degraded paper samples was not measurable. Then, treatments with NaOH or NaOH+H_2O_2 give raise to close tensile force suggesting

that hydrogen peroxyde does not significantly improve the degradation. Finally, H_2SO_4 is the less efficient reagent thus confirming the results obtained with the cross-linked PAE films alone. An increase of the degrading time from 40 to 60 min does not modify the efficiency of the degrading treatments in the conditions used.

Tab. III.12: Tensile tests of neutral uncoated (NU) paper after degrading treatments**.**

40 min					
	pH_f	**Force (N)**	**Stretch (mm)**	**TEA index (mJ/g)**	**Young modulus (GPa)**
NaOH	12	7.00 ± 0.32	2.36 ± 0.15	42.8 ± 4.9	0.200 ± 0.007
H_2O_2	6.4	6.80 ± 0.63	1.80 ± 0.23	100 ± 23	0.69 ± 0.07
	6.4	7.20 ± 0.27	1.81 ± 0.09	111.3 ± 8.7	0.91 ± 0.09
H_2O_2 + NaOH	11.3	4.40 ± 0.23	1.50 ± 0.09	56.4 ± 6.4	0.61 ± 0.04
	11.5	4.60 ± 0.20	1.59 ± 0.13	62.8 ± 9.3	0.63 ± 0.05
$K_2S_2O_8$	2.7	nm*	nm*	nm*	nm*
$K_2S_2O_8$ + NaOH	11.4	nm*	nm*	nm*	nm*
H_2SO_4	7.1	9.90 ± 0.63	2.56 ± 0.10	63.9 ± 5.0	0.26 ± 0.02

*nm: not measurable

Table III.13 shows the obtained results for tensile tests of NC paper. In this case, we can consider that all treatments were inefficient in the used conditions, even with a decrease of force, TEA index and Young modulus values of degraded samples when compared with undegraded samples (see Table III.11). Probably, the main cause of the inefficiency of persulfate treatment of NC when compared with NU paper samples is the constitution of the coating. Side reactions of free radicals with these constituents make inefficient persulfate treatment of coated paper.

Tab. III.13: Tensile tests of neutral coated (NC) paper after degrading treatments.

	pH_f	**Force (N)**	**Stretch (mm)**	**TEA index (mJ/g)**	**Young modulus (GPa)**
NaOH	12	11.4 ± 0.5	2.70 ± 0.20	59.6 ± 7.0	0.298 ± 0.010
H_2O_2	6.4	12.3 ± 0.6	2.52 ± 0.12	198 ± 17	1.17 ± 0.09
	6.4	12.0 ± 0.5	2.52 ± 0.21	186 ± 21	0.950 ± 0.130
NaOH + H_2O_2	11.3	7.40 ± 0.78	1.84 ± 0.25	88.9 ± 22.4	0.92 ± 0.11
	11.2	7.60 ± 0.21	1.95 ± 0.13	93.7 ± 10.2	0.83 ± 0.08
$K_2S_2O_8$	2.4	6.00 ± 0.11	1.78 ± 0.19	74.2 ± 9.9	0.97 ± 0.08
$K_2S_2O_8$ + NaOH	11.6	7.60 ± 0.40	1.90 ± 0.11	90.7 ± 11.3	0.88 ± 0.09
H_2SO_4	7.0	14.2 ± 2.6	2.59 ± 0.81	73.3 ± 26.6	0.383 ± 0.01

Based on the obtained results of tensile tests after degrading treatments of industrial PAE-based papers, we can postulate that:

(i.) the more efficient degrading treatment was with persulfate salt. Side reactions between free radicals and constituents of the coating are the main responsible of the inefficiency of persulfate treatment with coated papers;

(ii.) even with a decrease of the wet tensile force of coated and uncoated papers with NaOH and H_2SO_4, these degrading treatments can be considered inefficient in the used conditions; and

(iii.) increase of degrading time does not affect the efficiency of the degradation of these industrial PAE-based papers in the used conditions.

3.3. CONCLUSIONS

In this study, an *Eucalyptus* (Suzano) pulp suspension refined at 30°SR was used mainly due to industrial interests. The charge content of the fibres was determined. The total charge was assessed by conductimetric (NaOH and $NaHCO_3$) and potentiometric (NaOH) titrations. The surface charge was studied by polyelectrolyte adsorption using a particle charge detector and zeta potential measurements: electrophoretic mobility and streaming potential methods.

In order to better understand the phenomena related to the adsorption of PAE by lignocellulosic fibres, PAE was added at different dosages (0.1, 0.6 and 1%) into the *Eucalyptus* pulp suspension. The adsorption was indirectly followed by measuring the zeta potential (microelectrophoresis and streaming potential methods) for different mixing and standing times. Results of ζ potential measurements obtained as a function of the PAE addition levels and standing time (up to 120 min) indicate that the adsorption, reconformation and/or penetration phenomena reach an apparent equilibrium for the tested concentrations at c.a. 10 min for electrophoretic mobility and streaming potential method.

Attempts to determine the amount of PAE adsorbed on handsheets were carried out by analysis of their N content. However, it seems difficult to get reliable values of the PAE adsorption by this technique due to its poor reproducibility. Even if colloidal titration presents some experimental limitations, it was then performed on fibrous suspensions for the 0.4% dosage. The obtained results showed that, at this addition level adsorption was complete.

In order to investigate the influence of the ionic strength on the dry and wet strength of PAE-based papers, three conductivity values were used for preparing handsheets: 100, 1500 and 3000 µS/cm. The dry strength was not significantly affected by the conductivity level of the pulp suspension whatever the storage time (from 1 to 90 days of paper storage under controlled conditions: 23°C and 50% RH). For the wet breaking length, we observed that the obtained values were about 1.2 and 1.6 km for 0.4 and 1% PAE-based papers, respectively, which corresponds approximately to a ratio of wet to dry breaking lengths of 25%. Oppositely, the conductivity has an impact on the wet strength of the papers and this effect seems to be enhanced when the PAE is added at 1%. Some explanations could be postulated like: salt screening effects of the

attractive electrostatic interactions between cationic PAE and anionic fibres, changes of polymer conformation with the increases of ionic strength and influences of the conformation of the adsorbed polymer on the PAE cross-linking reaction. However, as it was not possible to determine the adsorbed amount of PAE using N content technique, it was not possible to conclude if the results were directly related to the amount of adsorbed PAE. A more detailed analysis showed that the wet breaking length slightly increased with time whatever the conductivity level. This phenomenon could be explained by the fact that the cross-linking of the PAE polymers in the paper structure is a time dependent reaction.

For PAE-based papers prepared under controlled conditions (pH between 7 and 8 and conductivity between 700 and 800 µS/cm), an increase of 40 and 59% of the breaking length was observed for 0.4 and 1% PAE-based papers, respectively, in dry conditions and at 40 days of storage when compared to that of handsheets without PAE addition. The W / D ratio for 0.4 and 1% PAE-based papers were 23 and 28%, respectively, for the same storage period. Whatever the storage time, unheated and heated 0.4% PAE-based papers showed differences in terms of breaking length. Oppositely, 1% PAE-based papers with and without thermal post-treatment exhibited similar values of the breaking length (wet or dry) from 40 days of storage. Thus, for this series, the results showed that it is possible to reach the same "equilibrium" state by storing unheated handsheets for a given period under controlled conditions or by boosting the PAE cross-linking with a thermal post-treatment (for example at 130°C for 10 min) just after the drying of the handsheets.

SEM observations of the breaking zone after tensile tests were made. A pull-out of the fibers in the paper strips in the direction of the stress was observed for handsheets without PAE addition and the fibre walls were not damaged in a great extent as if the fibres have slid during the tensile test. For 1% PAE-based papers in dry conditions, the failure seemed to occur in the fibre walls. A peeling off of the external layers of the fibre wall was observed probably due to the adhesive properties of the PAE resin adsorbed on fibre surface. In wet conditions, we again observed a pull-out of the fibres from the strips and apparently in this case the surface of the fibres remains intact. The absorbed water could induce a swelling of the paper structure and the fibres and contributed to the slipping of the fibres without a severe delamination of the fibre walls.

However, it was difficult to conclude because dried strips were observed and the appearance of the fibres could have been modified by their drying after the tensile test.

Preliminary degrading studies of cross-linked PAE films were performed without fibres and parameters as degrading time, temperature and reagent were varied in order to obtain the highest amount of degraded film samples. PAE degradation was not efficient neither in water nor in H_2SO_4 solution, even with an increase of the treatment time (from 40 to 180 min), and of the temperature (from 40 to 80°C). PAE degradation with NaOH is considerable, but a very high amount of NaOH is needed to maintain the alkalinity of the medium during experiment. PAE degradation with persulfate and hydrogen peroxide was significantly increased by an increase of the temperature and/or the time. PAE degradation in a persulfate solution at alkaline medium (28%) was more effective when compared to the degradation yield reached under acidic conditions (17.8%), but a high amount of NaOH is needed to maintain the alkaline condition of the medium. The condition that permitted to reach the highest degraded amount of PAE was: 60 min of stirring in a $K_2S_2O_8$ solution at acid pH (pH < 7) + 120 min of stirring at alkaline pH (pH = 11).

On the same time, a preliminary study of industrial PAE-based papers (coated and uncoated papers) was also performed. The efficiency was determined with tensile tests of the degraded strips just after treatment. For uncoated paper, as observed for cross-linked PAE films, persulfate treatment was the most efficient and the tensile force of persulfate degraded paper samples was not measurable. Treatments with NaOH or NaOH+H_2O_2 gave raise to close tensile force suggesting that hydrogen peroxyde does not significantly improve the degradation. H_2SO_4 was the less efficient reagent. For coated papers, all treatments were inefficient in the used conditions, although a decrease of the tensile force of degraded samples was observed when compared with undegraded samples. The main responsible of the inefficiency of persulfate treatment of coated papers when compared with uncoated papers samples was probably related to the composition of the coating. Side reactions of free radicals with these constituents could make the persulfate treatment inefficient.

GENERAL CONCLUSION

PAE resins are the most used wet strength chemicals from 1960 (when they were synthesized) due to their good performance and relatively low costs. However, there is still yet a lack of data concerning this chemical in the literature. PAE resins present some drawbacks and the bad re-pulpability of PAE-based papers is probably the most important. Then, the main objectives of this thesis were:

(i.) a characterization of PAE resin and of the cross-linking mechanisms;

(ii.) effect of certain operating conditions of the preparation of PAE-based handsheets on the paper wet strength, and

(iii.) the recycling of PAE-based wet strengthened papers.

In the Part I 'Characterization of PAE resin: toward a better understanding of cross-linking mechanisms', NMR analyses allowed elucidating the PAE structure from various experiments (for example DEPT, COSY, HMQC and HMBC). Experimental evidences of the cross-linking reactions were achieved using spectroscopic methods (FTIR and NMR) during thermal and ageing studies. Other indirect evidences were also obtained from thermal and mechanical analysis (DSC and DMA, respectively).

A study of CMC salts, which is a chemical normally used in combination with PAE resin to prepare PAE-based papers, was performed. Even if this was not the main aim of this thesis, some unknown properties were observed: they are related to the influences of by-products from synthesis on CMC films preparation and thermal transitions of CMC structure. These studies provide some new insights in thermal properties of carbohydrates derivatives.

An innovative study aiming to elucidate the mechanism related to PAE resin when used to prepare PAE-based wet strengthened papers was also carried out. Considering CMC as a model compound for cellulosic fibres and CMC-PAE interactions as a model for fibres-PAE interactions, we found evidences of the reaction mechanism of PAE in wet strengthened papers. Films of polyelectrolyte complexes were thus prepared using different CMC/PAE mass ratios and analyzed from spectroscopic and thermal analyses. Based on obtained results, the protection of fibre-fibre contacts by a network of cross-linked resin molecules (protection mechanism) was considered the main mechanism for wet strength development of PAE-based papers. Even if the formation of resin-fibres chemical bonds (reinforcement mechanism) can

occur during preparation of PAE-based papers their contribution for wet strength is considered secondary. SEM micrographs of unheated CMC/PAE films showed formation of interesting like crystals structures. Apparently, they are polyelectrolytes complexes salts formed during preparation of CMC/PAE films.

Besides considering the mechanisms of wet strength development, the recycling of the PAE treated papers and broke presents problems. The re-pulping is normally realized at high temperature, concentration of additives and consistency. Here again, the involved reactions are not well known and the effectiveness of these treatments is low. The Part II 'Use of PAE resin in papermaking: improvement of the preparation and repulping of PAE-based papers' was dedicated to the preparation and characterization of *Eucalyptus* pulp suspension and PAE-based papers and their recycling. In order to better understand the phenomena related to the adsorption of PAE by lignocellulosic fibres, PAE was added at different dosages into the *Eucalyptus* pulp suspension and the adsorption was indirectly followed by electrokinetics methods.

The dry strength of handsheets was not significantly affected by a variation of the conductivity of the pulp suspension. On the other hand, this variation has an impact on the wet strength of the papers. As it was not possible to determine the adsorbed amount of PAE in handsheets, it was not also possible to conclude if the results were directly related to the amount of adsorbed PAE. Analyses showed that the wet breaking length of handsheets slightly increase with time due to the fact that the cross-linking of the PAE polymers in the paper structure is a time dependent reaction. However, for high PAE dosages (c.a. 1%), the results showed that it is possible to reach the same "equilibrium" state by storing unheated handsheets for a given period under controlled conditions or by boosting the PAE cross-linking with a thermal post-treatment after the drying of the handsheets.

Preliminary degrading studies of cross-linked PAE films were performed without fibres and parameters as such degrading time, temperature and reagent were varied. PAE degradation in a persulfate solution at alkaline medium was the more effective. On the same time, a preliminary study of industrial PAE-based papers was also carried out. The efficiency was quantitatively determined with wet tensile tests of the degraded strips just after treatment. For uncoated papers, as observed for cross-linked PAE films, persulfate treatment was the most efficient and the tensile force of

persulfate degraded paper samples was not measurable. For coated papers, all treatments were inefficient in the used conditions, although a decrease of the tensile force of degraded samples was observed when compared with undegraded samples. Here again, persulfate treated paper samples led to lowest tensile force. Side reactions of free radicals with the constituents of the coating probably are the main responsible for a lower efficiency of persulfate treatment of coated when compared to uncoated paper. As postulated in this thesis, these were only preliminary studies and a high number of variables (time, temperature, consistency of the medium, reactant concentration, disintegrator apparatus, rewetters, etc) can be still varied in future studies in order to optimizing the recycling step.

ANNEXE

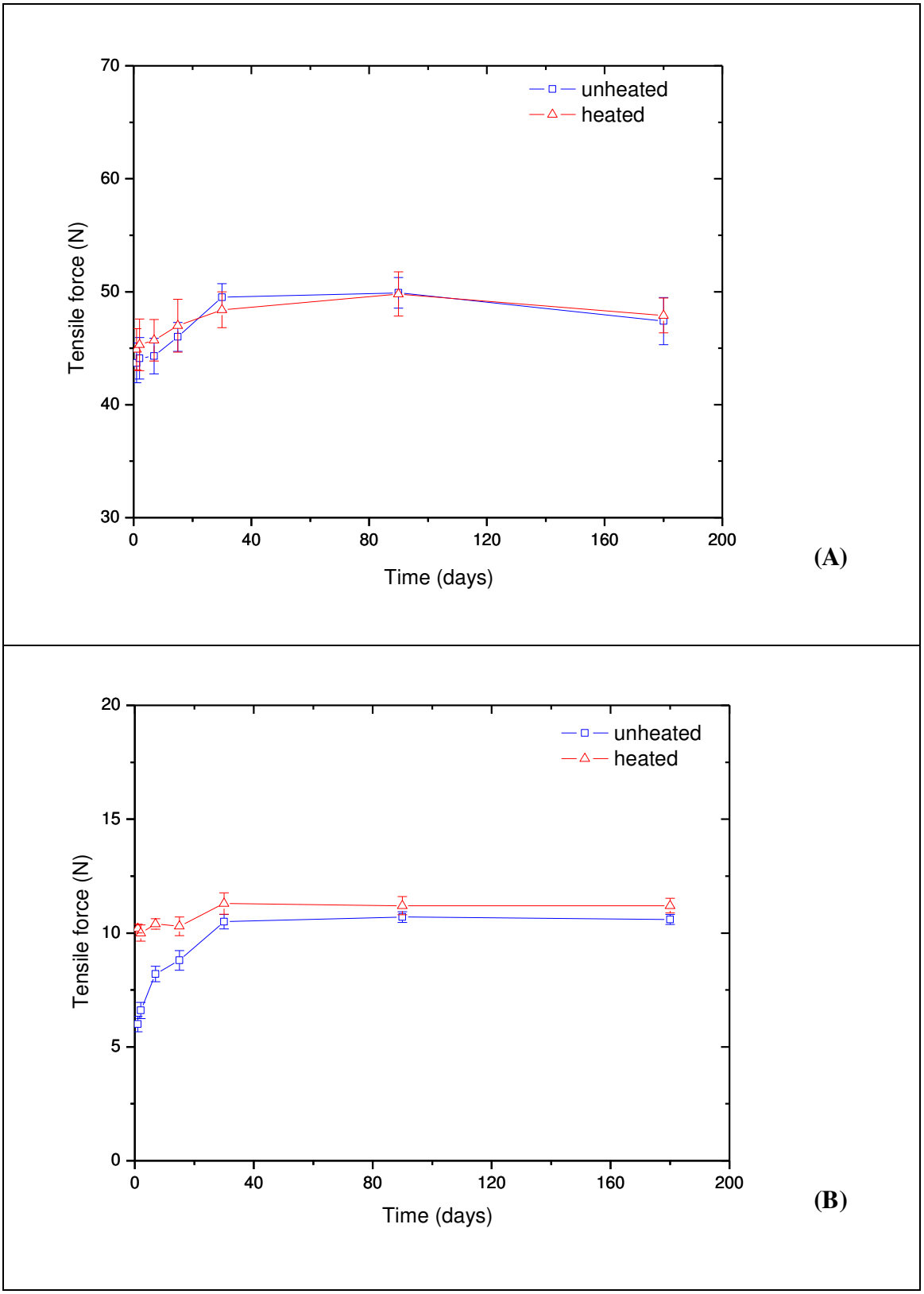

Fig. A: Tensile force of heated and unheated 0.4% PAE-based paper in **(A)** dry and in **(B)** wet conditions as a function of storage time of handsheets.

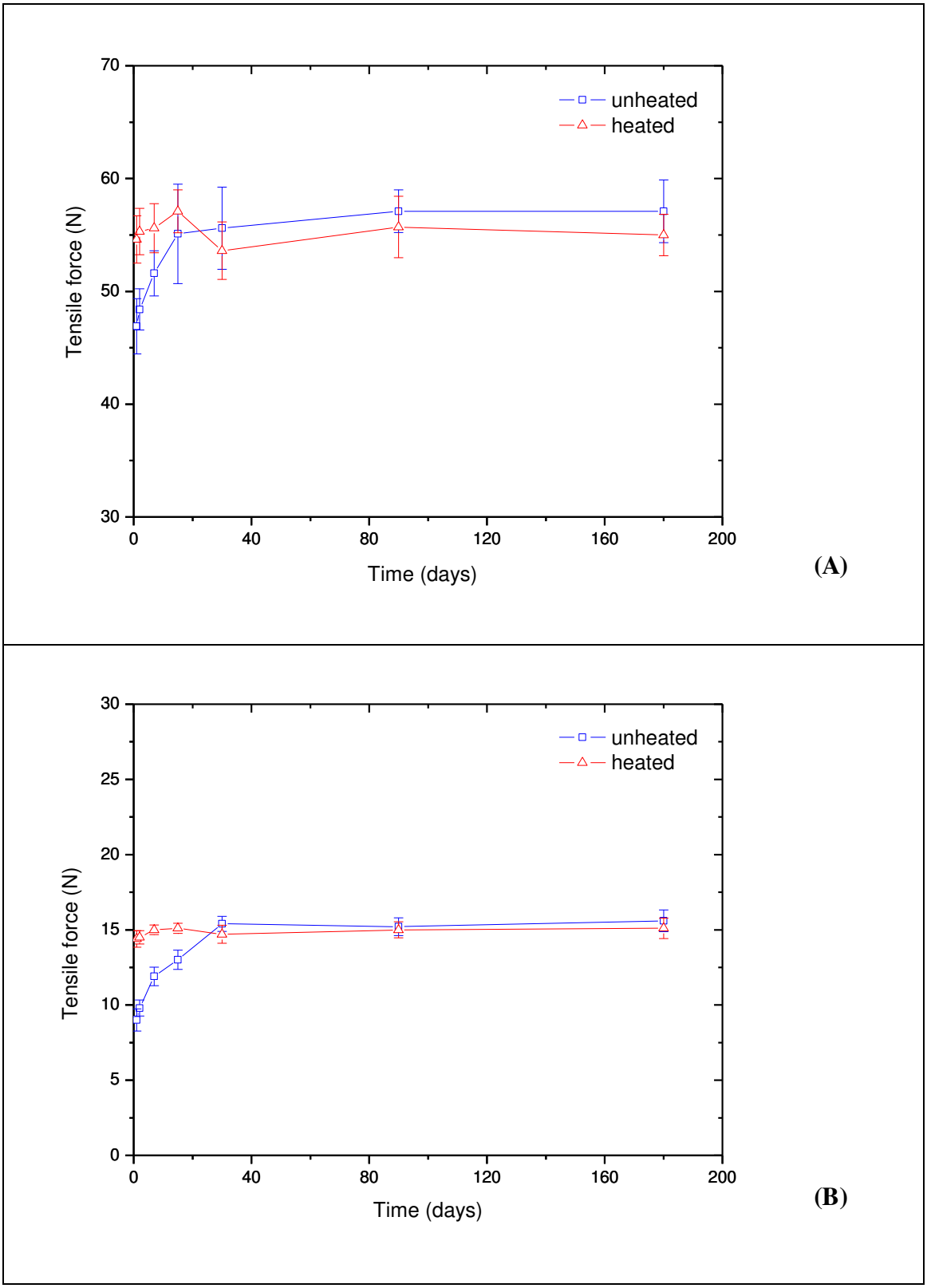

Fig. B: Tensile force of heated and unheated 1% PAE-based paper in **(A)** dry and in **(B)** wet conditions as a function of storage time of handsheets.

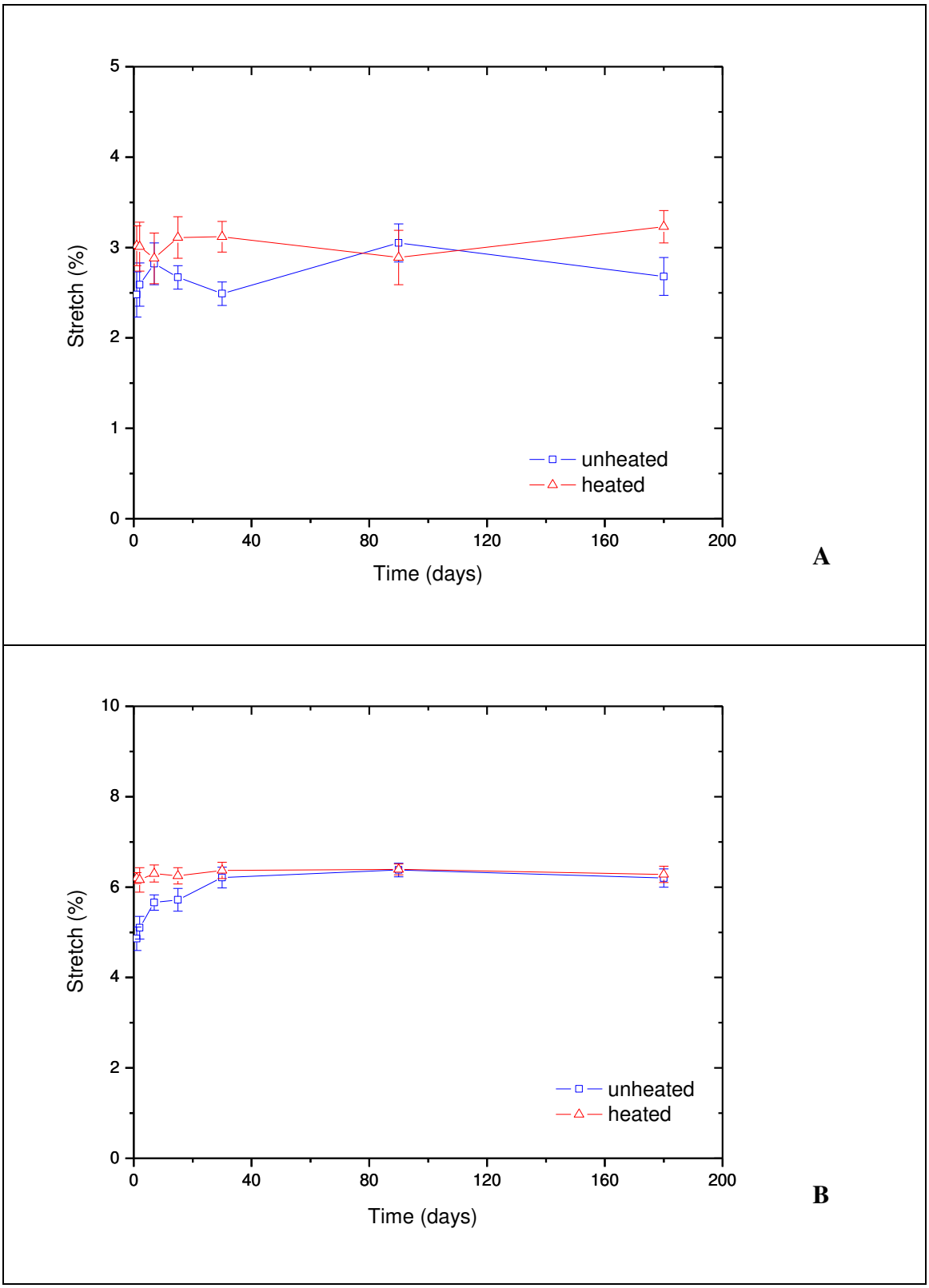

Fig. C: Stretch of heated and unheated 0.4% PAE-based paper in (A) dry and in (B) wet conditions as a function of storage time of handsheets.

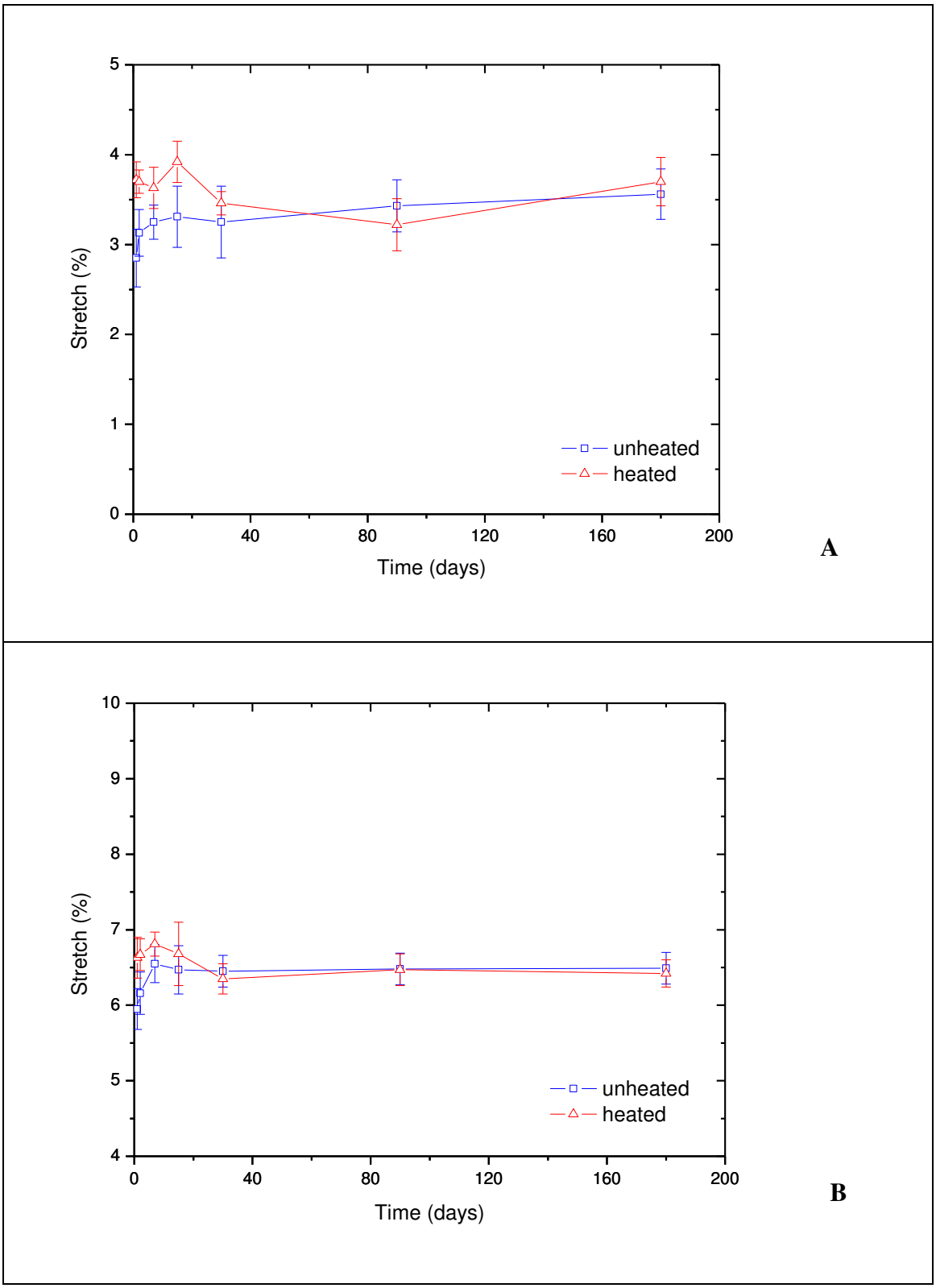

Fig. D: Stretch of heated and unheated 1% PAE-based paper in (A) dry and in (B) wet conditions as a function of storage time of handsheets.

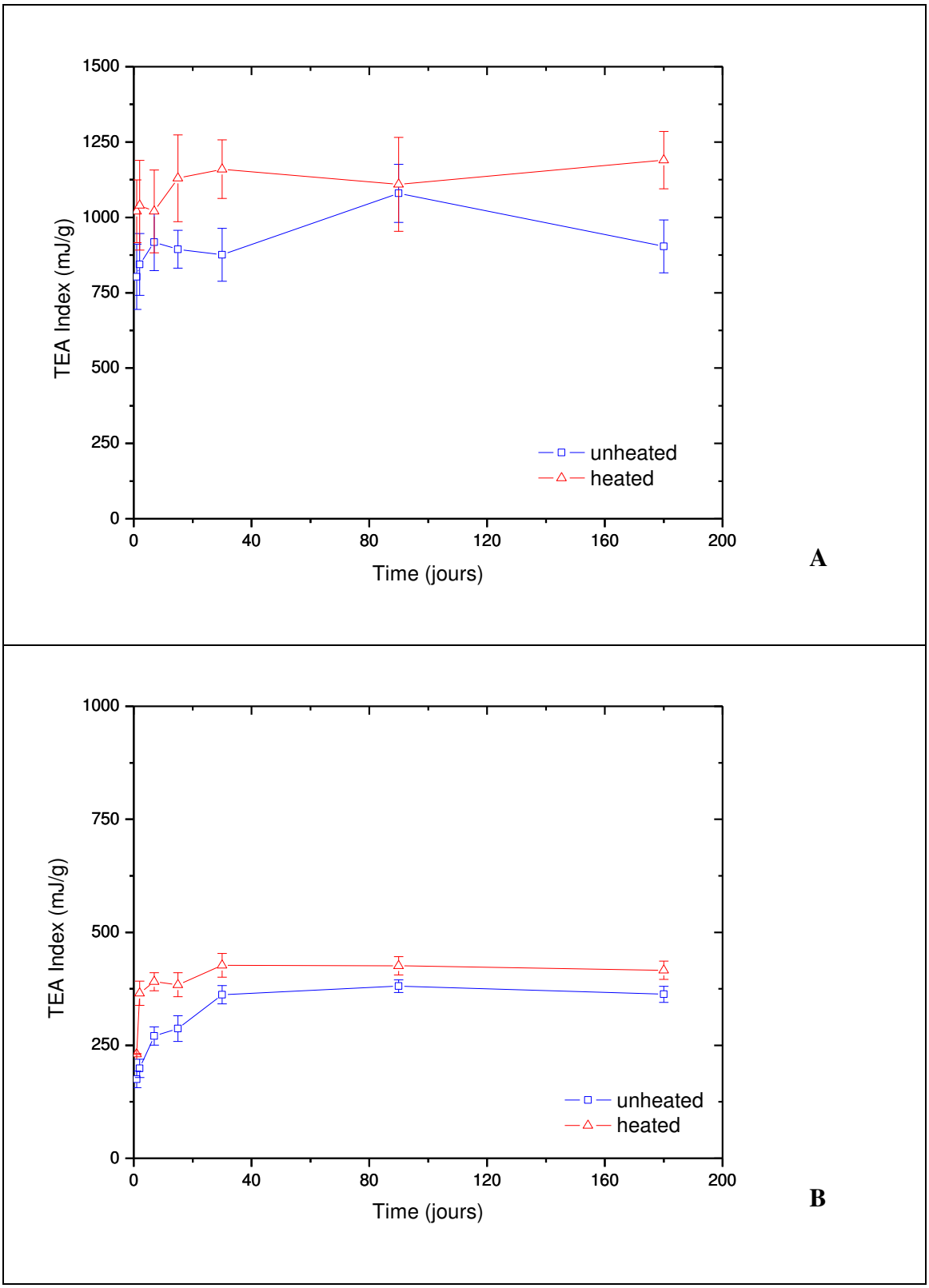

Fig. E: TEA index of heated and unheated 0.4% PAE-based paper in (A) dry and in (B) wet conditions as a function of storage time of handsheets.

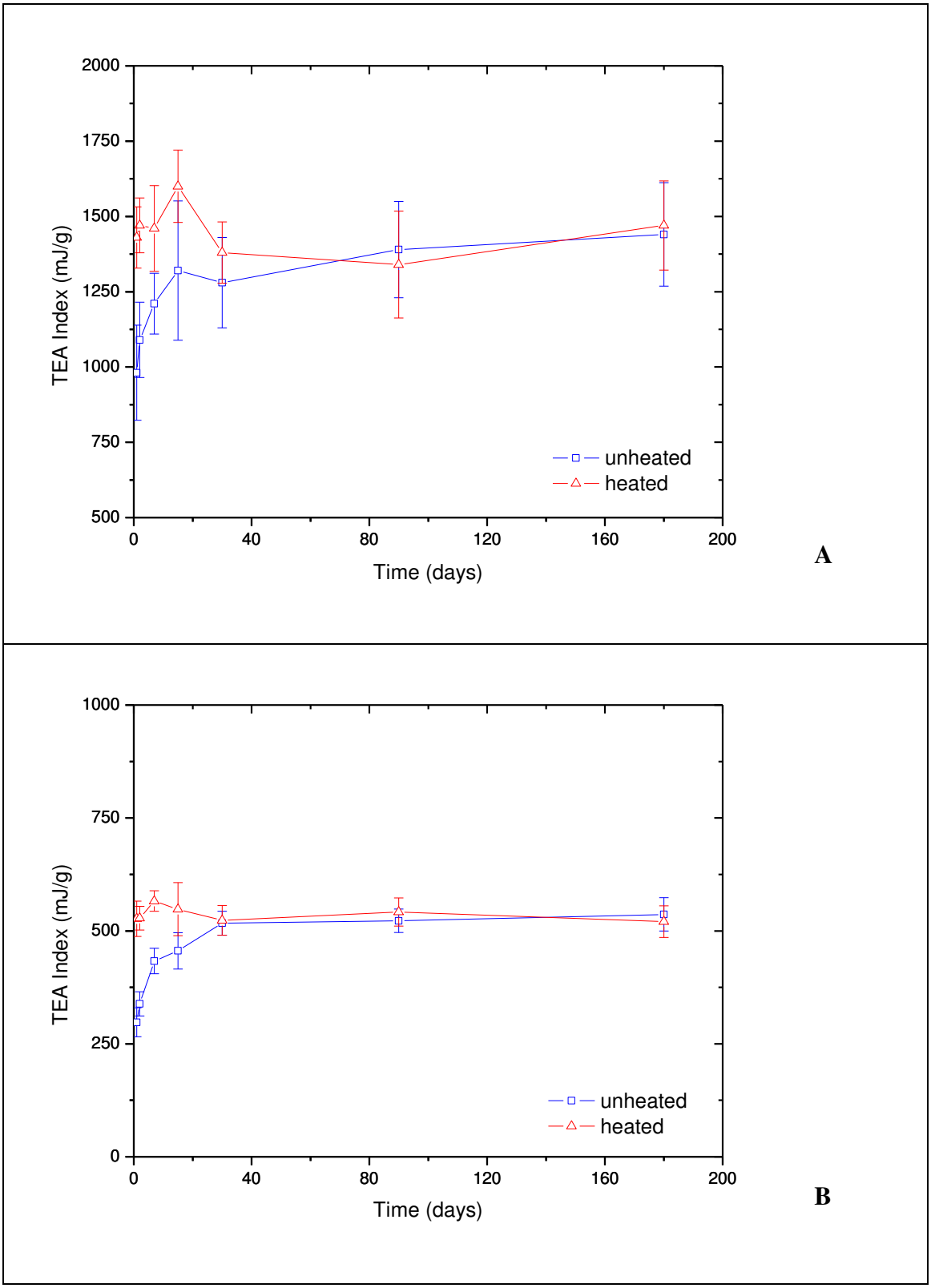

Fig. F: TEA index of heated and unheated 1% PAE-based paper in (A) dry and in (B) wet conditions as a function of storage time of handsheets.

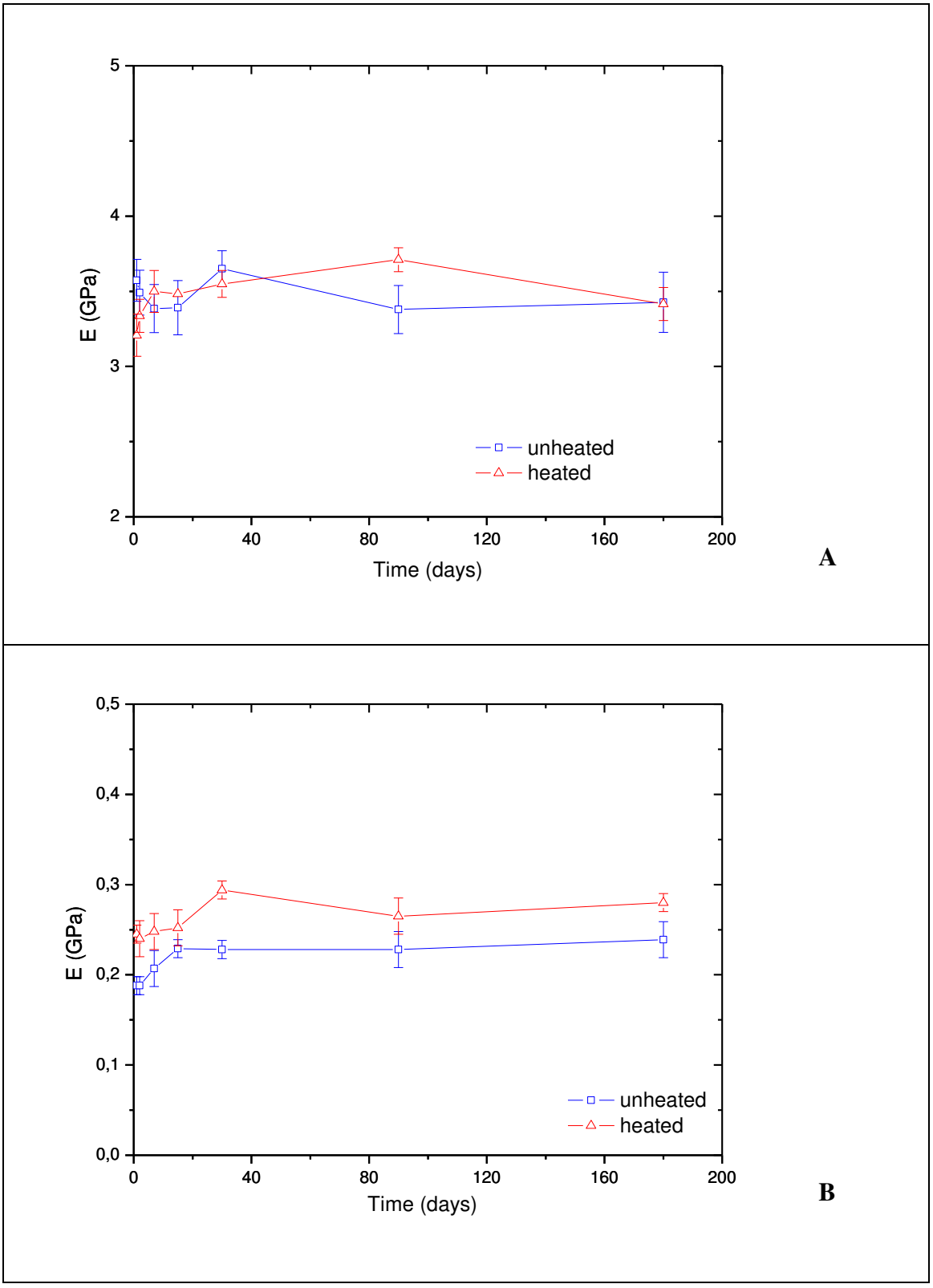

Fig. G: Storage modulus of heated and unheated 0.4% PAE-based paper in (A) dry and in (B) wet conditions as a function of storage time of handsheets.

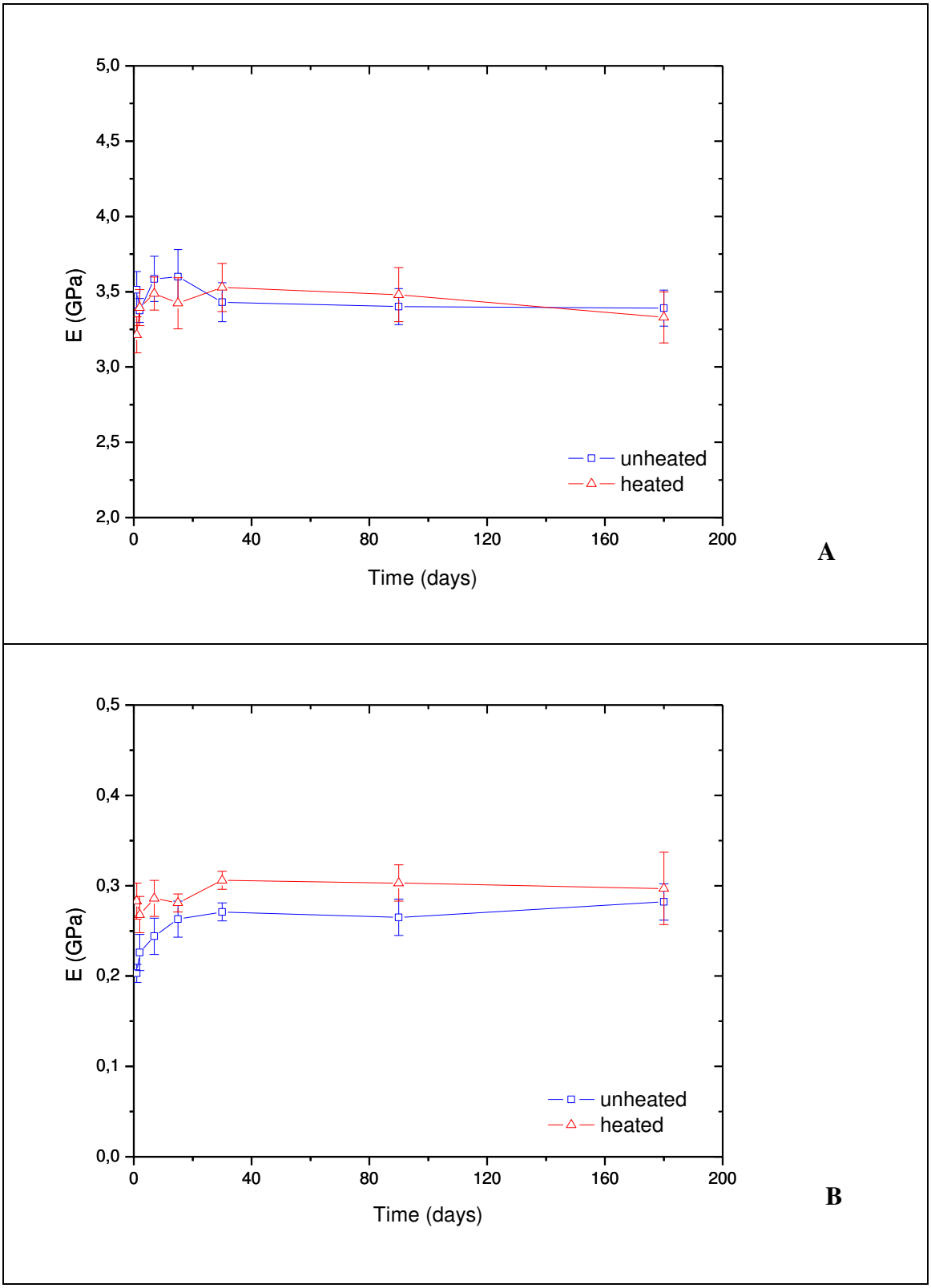

Fig. H: Storage modulus of heated and unheated 1% PAE-based paper in (A) dry and in (B) wet conditions as a function of storage time of handsheets.

Tab. A: Tensile force obtained by tensile tests of heated and unheated 0.4 and 1% PAE-based papers up to 40 days of ageing.

N	0.4%				1%			
	dry		wet		dry		wet	
days	H	UH	H	UH	H	UH	H	UH
2	44.1 ± 1.8	45.3 ± 2.3	10.0 ± 0.4	6.6 ± 0.4	53.6 ± 2.1	48.4 ± 1.8	14.5 ± 0.4	9.8 ± 0.5
40	49.5 ± 1.2	48.4 ± 1.6	11.3 ± 0.5	10.5 ± 0.3	55.3 ± 2.6	55.6 ± 3.7	15.4 ± 0.5	14.7 ± 0.5

H: heated UH: unheated

Tab. B: % stretch obtained by tensile tests of heated and unheated 0.4 and 1% PAE-based wet strengthened papers up to 40 days of ageing of handsheets.

%	0.4%				1%			
	dry		wet		Dry		wet	
days	H	UH	H	UH	H	UH	H	UH
2	3.01 ± 0.27	2.49 ± 0.13	6.16 ± 0.27	5.10 ± 0.25	3.46 ± 0.13	3.13 ± 0.26	6.67 ± 0.21	6.16 ± 0.28
40	3.12 ± 0.17	2.59 ± 0.24	6.37 ± 0.18	6.25 ± 0.23	3.7 ± 0.13	3.25 ± 0.40	6.35 ± 0.20	6.45 ± 0.21

H: heated UH: unheated

Tab. C: TEA index obtained by tensile strength tests of 0.4 and 1% heated and unheated PAE-based wet strengthened papers up to 40 days of ageing.

mJ/g	0.4%				1%			
	dry		wet		Dry		wet	
days	H	UH	H	UH	H	UH	H	UH
2	1040 ± 148	844 ± 102	365 ± 27	199 ± 20	1380 ± 91	1090 ± 124	523 ± 26	338 ± 27
40	1160 ± 97	876 ± 88	427 ± 26	362 ± 20	1470 ± 101	1280 ± 150	528 ± 33	517 ± 26

H: heated UH: unheated

Tab. D: Storage modulus obtained by tensile strength tests of 0.4 and 1% heated and unheated PAE-based wet strengthened papers up to 40 days of ageing.

GPa	0.4%				1%			
	dry		wet		Dry		wet	
days	H	UH	H	UH	H	UH	H	UH
2	3.34 ± 0.11	3.49 ± 0.15	0.24 ± 0.02	0.19 ± 0.01	3.40 ± 0.12	3.38 ± 0.08	0.27 ± 0.02	0.23 ± 0.02
40	3.55 ± 0.90	3.65 ± 0.12	0.30 ± 0.01	0.23 ± 0.01	3.53 ± 0.16	3.43 ± 0.13	0.31 ± 0.01	0.27 ± 0.01

H: heated UH: unheated

REFERENCES

ALLAN G.G., REIF W.M. Fibre surface modification Part 6. The Jack in the box effetc: a new mechanism for the retention of polyethyleneimine and other polyelectrolytes by pulp fibres, Svensk Papperstidn, 1971, 74 (2), p. 25.

ALINCE B., VANEREK A., OLIVEIRA M. H. de, VAN DE VEN T.G.M. The effect of polyelectrolytes on the wet-web strength of paper, Nordic and Pulp Paper Research Journal, 2006, 21 (5), p. 653.

ARMSTRONG R.W., STRAUSS U. P. Polyelectrolytes, 2002, EPST, 1 ed., Vol. 10, p. 781.

ANDO W., KAKO M., AKASAKA T. Direct observation of an azetidinium imide intermediate in [$\pi^2 + \sigma^2$] addition of 1,2,4 – triazoline – 3,5 – dione to disilirane, Journal of American Chemical Society, 1991, 113 (16), p. 6286.

ANDRENASSON B., FORSSTROM J., WÄGBERG L. Determination of fibre pore structure: influence of salt, pH and conventional wet strength resins, Cellulose, 2005, 12, p. 253.

ANKERFORS C., LINGSTRÖM R., WÄGBERG L., ÖDBERG L. A comparison of polyelectrolyte complexes and multilayers: their adsorption behaviour and use for enhancing tensile strength of paper, Nordic Pulp and Paper Research Journal, 2009, 24 (1), p. 77.

ATKINS P., OVERTON T., ROURKE J., WELLER M., ARMSTONG F. Inorganic chemistry, 2006, Oxford, 4 ed.

BATES N.A. Polyamide-epichlorohydrin wet-strength resin II: A study of the mechanism of wet-strength development in paper, Tappi, 1969, 52 (6), p. 1162.

BATES N.A. Evidence for the reaction of cellulose with melamine-formaldehyde resin, Tappi, 1966, 49 (4), p. 184.

BANSAL N., SZCZEPANIAK D., TERNULLO D., FLECKENSTEIN J.L., MALLOY C.R. Effect of exercise on ^{23}Na NMR and relaxation characteristics of the human calf muscle, Journal of Magnetic Ressonance, 2000, 11, p. 532.

BHARDWAJ N.K., RAJAN V. Wet-strength paper repulping: effect of process variables, Appita Journal, 2004, 57 (4), p. 305.

BHARDWAJ N.K., DUONG T.D., NGUYEN K.L. Pulp charge determination by different methods: effect of beating/refining, Colloids and Surfaces A, 2004, 236 (1-3), p. 39.

BIDDLESTONE F., KEMISH D.J., HAY J.N., MILLS P.J., WETTON R.E., ROWE A.M. The application of the minimal to plastic fracture: a review, Polymer Testing, 1986, 6 (3), p. 163.

BOATENG J.S., STEVENS H.N.E., ECCLESTON G.M., AUFFRET A.D., HUMPHREY M. J., MATTHEWS K.H. Development and mechanical characterization of solvent cast-polymeric films as potential drug delivery systems to mucosal surfaces, Drug Development and Industrial Pharmacy, 2009, 35 (8), p. 986.

BOBALEK J.F., CHATURVEDI M. The effects of recycling on the physical properties of handsheets with respect to specific wood species, Tappi Journal, 1989, 72 (6), p. 123.

BORCHERT P.J., MIRZA J. Cationic dispersion of dialdehyde starch I: theory and preparation, Tappi, 1964, 47 (9), p. 525.

BLEDZKI A.K., GASSAN J. Composites reinforced with cellulose based fibres, Prog. Polym. Sci, 1999, 24 (2), p. 117.

BRITT K.W. Wet Strength in Pulp and Paper Chemistry and Chemical Technology, Casey JP Wiley Interscience, 1981, 3 ed., vol. 3, p. 1609.

BROIULLETTE F., DANEAULT C., DORRIS G. M. Effect of initial repulping pH on the deflaking rate of recovered papers, Pulp and Paper Canada, 2003, 104 (7), p. 35.

BRUCE P.G. Structure and electrochemistry of polymer electrolytes, Electrochemica Acte, 1955, 40, p. 2077.

BUCHHAMMER H.M., KRAMER G., LUNKWITZ K. Interaction of colloidal dispersions of non-stoichiomectric polyelectrolyte complexes and silica particles, Colloid and Surfaces A, 1994, 95, p. 299.

CAPITANI D., PORRO F., SEGRE A.L. High field NMR analysis of the degree of substitution in carboxymethylcellulose sodium salt, Carbohydrate Polymers, 2000, 42, p. 283.

CARR M.E., DOANNE W.M., HAMERSTRAND G.E., HOFREITER B.T. Interpolymer from starch xanthate and polyamide-polyamine-epichlorohydrin resin. Structure and papermaking application, Journal Applied Polymer Science, 1973, 17 (3), p. 721.

CASTELLAN G.W. Physical Chemistry, Addison Wesley Publishing Company, 1986, 3 ed.

CHAN L.L. Wet strength resins and their application, Tappi Press, 1994, Atlanta.

CHAN L.L., Lau P.W.K. Repulping of wet-strength paperboard, Pulp and Paper Canada, 1988, 89 (8), p. 57.

CHENG L.H., KARIM A.A., NORZIAH M.H., SEOW C.C. Modification of the microstructural and physical properties of konjac glucomannan-based films by alkali and sodium carboxymethylcellulose, Food Research International, 2002, 35, p. 829.

CLAESSON P.M., DEDINAITE A., ROJAS O.J. Polyelectrolytes as adhesion modifiers, Advances in Colloid and Interface Science, 2003, 104, p. 53.

COOPER S.J., COOGAN M., EVERALL N., PRIESTNALL I. A polarized μ-FTIR study on a model system for nylon 6.6: implications for the nylon Brill structure, Polymer, 2001, 42, p. 10119.

COSTA S.C.G., GONÇALVES M.C., FELISBERTI M. I. Blends of polyamide 6 and epichlorohydrin elastomers I. graft copolymerization in the melt blending, Journal of Applied Polymer Science, 1999, 72, p. 1827. (a)

COSTA S.C.G., FELISBERTI M.I. Blends of polyamide 6 and epichlorohydrin elastomers II. Thermal, dynamic mechanical and mechanical properties, Journal of Applied Polymer Science, 1999, 72, p. 1835. (b)

COUTY F., DAVID O., DROUILLAT B. Opening of azetidinium ions with C-nucleophiles, Tetrahedron Letters, 2007, 48, p. 9180.

DANIEL J.R. Cellulose structure and properties. In Encyclopedia of polymer Science and engineering Kroschwitz, J.I., Ed. Wiley-Interscience Publication John Wiley & Sons: New York, 1985, 3, p.86.

DANG Z., ELDER T., RAGAUSKAS A.J. Influence of kraft pulping on carboxylate content of softwood kraft pulps, Ind. Eng. Chem. Res., 2006, 45, p. 4509.

DANKELMAN W., DAEMEN J.M.H., de BREET A.J.J. Angew. Makromol. Chem., 1986, 54, p. 187.

DAUTZENBERG H., JAHGER W., KÖTZ J., PHILLIP B., SEIDEL C., STSCHERBINA D. *Polyelectrolytes: Formation, Characterization and Application*, Hanser Publishers, 1994, New York.

DAVISON, R. W. Electrokinetic effects in papermaking processes, Tappi, 1974, 57 (12), p. 85.

DEVORE D.I., FISCHER S.A. Wet-strength mechanism of polyaminoamide epichlorohydrin resins, Tappi Journal, 1993, 76 (8), p. 121.

DUNLOP-JONES, N. (1991) in 'Paper Chemistry' edited by ROBERTS J.C., Chapman and Hall, 1991, p. 77.

DYER J.R. Applications of absorption spectroscopy of organic compounds, Prentice-Hall, 1965.

EDWARDS O.E., FODOR G., MARION L. Investigation of the structure of 1,5-methylene-quinolizidinium ion, Canadian Journal of Chemistry, 1966, 44, p. 13.

EL-ARNAOUTY M.B., EID M., ATIA K.S., DESSOUKI A.M., Characterization and application of grafted polypropylene and polystyrene treated with epichorohydrin coupled with cellulose or starch for immobilization processes, Journal of Applied Polymer Science, 2009, 112, p. 629.

ENARSSON L.E., WÄGBERG L. Kinetics of sequential adsorption of polyelectrolyte multi-layers on pulp fibres and their effect on paper strength, Nordic Pulp and Paper Research Journal, 2007, 22 (2), p. 258.

ERIKSSON M., NOTLEY S.M., WÄGBERG L. The influence on paper strength properties when building multilayers of weak polyelectrolytes onto wood fibres, Journal of Colloid and Interface Science, 2005, 292, p. 38.

ESPY H.H., RAVE T.W. The mechanism of wet-strength development by alkaline curing amino polymer-epichlorohydrin resins, Tappi Journal, 1998, may, p. 133.

ESPY H.H. The mechanism of wet strength development in paper: a review, Tappi Journal, 1995, 78 (4), p. 90.

ESPY H.H., GEIST G.W. Persulfate as repulping reagents for neutral/alkaline wet-strength broke, Tappi Journal, 1993, 76 (2), p.139.

ESPY H.H., GEIST G.W. Using neutral/alkaline-curing resins to produce wet-strength grades from recycled pulp, 1992, 75 (7), p. 192.

ESPY H.H. The effects of pulp refining on wet strength resin, Tappi Journal, 1987, 70 (7), p. 129.

FAOSTAT 2012 [en ligne]: Food and Agriculture Organization of the United Nations. [ref. mar 2012]. http://faostat.fao.org/

FISCHER S.A. Repulping wet-strenght paper, Tappi Journal, 1997, 80 (11), p. 141.

FISCHER S.A. Structure and wet strength activity of polyamidoamine epichlorohydrin resin having azetidinium functionality, Tappi Journal, 1996, 79 (11), p. 179.

FRAS L., LAINE J., STENIUS P., STANA-KLEINSCHEK K., RIBITSCH V., DOLECEK V. Determination of dissociable groups in natural and regenerated cellulose fibers by different titration methods, Journal of Applied Polymer Science, 2004, 92, p. 3186.

FREDHOLM B., SAMUELSSON B., WESTFELD L. The chemistry of paper wet-strength VII: effects of model polymers on wet-strength, water absorbency and dry strength, Cellulose Chemistry and Technology, 1983, 17 (3), p. 279.

FUKUDA S., ISOGAI A., KITAOKA T., SUMIKAWA N. Water and oil penetration resistances of handsheets prepared by internal addition of diperfluoroalkylethyl phosphate: influence of cationic polymers co-added, Nordic Pulp and Paper Research Journal, 2005, 20 (4), p. 496.

GANDIDINI A., BELGACEM M.N. Monomers, Polymers and Composites from renewable resources, Great Britain, 2008, 1 ed.

GÄRDLUND L., NORGREN M. The use of polyelectrolyte complexes (PEC) as strength additives for different pulps used for production of fine paper, Nordic Pulp and Paper Research Journal, 2007, 22 (2), p. 210.

GÄRDLUND L., WÄGBERG L., GERNANDT R. Polyelectrolyte complexes for surface modification of wood fibres II. Influence of complexes on wet and dry strength of paper, Colloids and Surfaces A, 2003, 218, p. 137.

GERNANDT R., WÄGBERG L., GÄRDLUND L., DAUTZEMBERG H. Polyelectrolyte complexes for surface modification of wood fibres I. Preparation and characterization of complexes for dry and wet strength improvement of paper, Colloids and Surfaces A, 2003, 213, p. 15.

GRADIN P.A., Bäklund J. Fatigue debonding in fibrous composites, International Journal of adhesion and adhesives, 1989, 1 (3), p. 154.

HAERI S., HASHEMABADI S.H. Experimental study of gravity-driven film flow of non-Newtonian fluids, Chem. Eng. Comm., 2009, 196, p. 519.

HÄGGKVIST M., SOLBERG D., WÄGBERG L. The influence of two wet strength agents on pore size and swelling of pulp fibres and on tensile strength properties, Nordic Pulp and Paper Research Journal, 1998, 13 (4), p. 292.

HARA M. Polyelectrolytes: Science and Technology, Marcel Dekker, 1993, New York.

HAMERSTRAND G.E., HOFREITER B.T., KAY D.J., RIST C.E., Dialdehyde starch hydrazones –cationic agents for wet strength paper, Tappi Journal, 1963, 46 (7), p. 400.

HASEGAWA M., ISOGAI A., ONABE F. Alkaline sizing with alkylketene dimers in the presence of chitosan salts, Journal of Pulp and Paper Science, 1997, 23 (11), p. 528.

HILL C.G.J., HEDREN A.M., MYERS G.E. Raman spectroscopy of urea-formaldehyde resins and model compounds, Journal of Applied Polymer Science, 1984, 29 (9), p. 2749.

HEINZE T., KOSCHELA A. Carboxymethyl ethers of cellulose and starch: a review, Macromolecules Symposium, 2005, 223, p. 13.

HEINZE T., Pfeiffer K. Studies on the synthesis and characterization of carboxymethylcellulose, Angewandte Makromolekulare Chemie, 1999, 266, p. 37.

HUANG H., HE P., HU N., ZENG Y. Electrochemical and electrocatalytic properties of myoglobin and hemoglobin incorporated in carboxymethyl cellulose films, Bioelectrochemistry, 2003, 61, p. 29.

HUBBLE M.A., VENDITTI R.A., ROJAS O.J. What happens to cellulosic fibers during papermaking and recycling? A review, BioResources, 2007, 2 (4), p. 739.

HUBBE M. A., MOORE S.M., Lee S.Y. Effects of charge ratios and cationic polymer nature on polyelectrolyte complex deposition onto cellulose, Ind. Eng. Chem. Res., 2005, 44, p. 3068.

ISE N., TSUNEO O. Thermodynamics and kinetic properties of polyelectrolyte solutions. A unified interpretation in terms of Manning's theory 1, Macromolecules, 1978, 11, p. 3.

ISOGAI A. Mechanism of paper sizing by cationic emulsion of fatty acid anhydrides, Journal of Pulp and Paper Science Journal of Pulp and Paper Science, 1999, 25 (6), p. 211.

ISOGAI A. Effect of cationic polymer addition on retention of alkylketene dimer, Journal of Pulp and Paper Science, 1997, 23 (6), p. 276.

JURECIC I.A., LINDH T., CHURCH S.E., STANNETT V. Mechanism of wet strength development, TAPPI, 1958, 41, p. 465.

JURECIC A., HOU C.M., SARKANEN K., DONOFRIO C.P., STANNETT V. The mechanism of wet strength development II, TAPPI, 1960, 43, p. 861.

KATZ S., BEATSON R.P., SCALLAN A.M. The determination of strong and weak acidic groups in sulphite pulps, Svensk Papperstidning, 1984, p. 6.

KENNEDY R.J., ALBERT M.S. The oxidation of organic substances by potassium peroxymonosulfate, Journal of Organic Chemistry, 1960, 25, p. 1901.

KIM B., ISOGAI A. Alkyl ketene dimer sizing of mechanical pulp, Appita Journal, 2001, 54 (2), p. 116.

KINDLES W.A., SWANSON J.W. Journal of Polymer Science A- 29, 1971, p. 853.

KITAOKA T., ISOGAI A., ONABE F. Sizing mechanism of rosin size-alum system Part 4. Surface sizing by rosin emulsion size on alum-treated base paper, Nordic Pulp and Paper Research Journal, 2001, 16 (2), p. 96.

KITAOKA T., ISOGAI A., ONABE F. Chemical modification of pulp fibers by tempo-mediated oxidation, Nordic Pulp and Paper Research Journal, 1999, 14 (4), p. 279.

KLUNGNESS J.H. Recycled fibers properties as affected by contaminants and removal processes, Tappi Journal, 1974, 57 (11), p. 71.

KONING J.W., GODSHALL W. D. Repeated recycling of corrugated containers and its effect on strength properties, Tappi Journal, 1975, 58 (9), p. 146.

KRAMMER G., BUCHAMMER H.M., LUNKWITZ K. Surface modification by polyelectrolyte complexes components and substrates, Colloids and Surfaces A, 1997, 122, p. 1.

KRICHELDORF H. R. ^{15}NMR spectroscopy 32. Synthesis and characterization of polyelectrolytes based on polyaminamides, Journal Polymer Science Chemistry, 1981, 19 (9), p. 2195.

LAINE J., LINDSTRÖM G.N., RISINGER G. Studies on topochemical modification of cellulose fibres. Part II: The effect of carboxymethylcellulos attachment on fibre swelling, Nordic and Pulp Paper Research Journal, 2002, 17 (1), p. 50.

LAINE J., LINDSTRÖM G.N., RISINGER G. Studies on topochemical modification of cellulose fibres. Part V: Comparison of the effects of surface and bulk chemical modification and beating on pulp and paper properties, Nordic and Pulp Paper Research Journal, 2003, 18 (3), p. 325.

LAINE J., LINDSTRÖM G.N., RISINGER G. Studies on topochemical modification of cellulose fibres. Part I: Chemical conditions for the attachment of carboxymethylcellulose onto fibres, Nordic and Pulp Paper Research Journal, 2000, 15 (5), p. 520.

LEVITT L.S. The common basis of organic oxidations in acidic solution, Journal Organic Chemistry, 1955, 20, p. 1297.

LI W., SUN B., WU P. Study on hydrogen bonds of carboxymethyl cellulose film with two-dimensional correlation infrared spectroscopy, Carbohydrate Polymers, 2009, 78, p. 454.

LII C., TOMASIK P., ZALESKA H., LIAW S., LAI V. Carboxymethyl cellulose gelatin complexes, Carbohydrates Polymers, 2002, 50, p. 19.

LINDGREN J., ÖHMAN L. Characterization of acid/base properties for bleached softwood fibres as influenced by ionic salt medium, Nordic Pulp and Paper Research Journal, 2000, 15 (1), p. 18.

LINDSTRÖM T., WÄGBERG L., LARSSON T. On the nature of joint strength in paper, 13th Fundamental Research Symposium, 2005.

LINDQVIST H., SALMINEN J., KATAJA-AHO J., SUNDBERG B.H., RETULAINEN E. Effects of electrolytes, pH and surface tension on dewatering, dry and wet web properties, Journal of Pulp and Paper Science, 2009, 35 (3-4), p. 148.

LLOYD J.A., HORNE C.W. The determination of fibre charge and acidic groups of radiate pine pulps, Nordic and Pulp Paper Research Journal, 1993, 8 (1), p. 48.

MANDEL M. Physical Properties of Polyelectrolyte Solutions: An Introduction, 1999, Pacini Editore, Pisa, Italy.

MARE H.E. Reaction of some aliphatic amines with tert-butyl hydroperoxide. The fate of the amine, 1960, 25, p. 2114.

Marton, J.; Marton, T. Some new principles to optmize rosin size, Tappi Journal, 65 (11), 1982, p. 105.

MEGAN C.F., MOORE S.M., HUBBE M.A., LEE S.Y. Deposition of polyelectrolyte complexes as a mechanism for developing paper dry strength, Tappi Journal, 2005, 4 (9), p. 3.

MERRET K. J. Repulping at high consistencies, Appita, 1987, 40 (3), p. 185.

MIAO C., PELTON R., CHEN X., LEDUC M. Microgels versus linear polymers for paper wet strength – size does matter, Appita, 2007, 60 (6), p. 465.

MICHELMANN J.S., CAPPELA D.M. Repulpability of coated corrugated paperboard, Tappi Journal, 1991, 74 (10), p. 79.

MIHARA I., YAMAUCHI T. Dynamic mechanical properties of paper containing a polyacrylamide dry-strength resin additive and its distribution within a fiber wall: effect of the application method, Journal of Applied Polymer Science, 2008, 110, p. 3836.

MINATO T., SATOH M. Counterion binding in Na poly(acrylate) gel. An ^{23}Na-NMR study, Journal of Polymer Science: Part B, 2004, 42, p. 4412.

MORA A.J., BRUNELLI M., FITCH A.N., WRIGHT J., BÁEZ M.E., CARRASQUERO F.L. Structures of (S)-(_)-4-oxo-2-azetidinecarboxylic acid and 3-azetidinecarboxylic acid from powder synchrotron diffraction data, Acta Crystallographica Section B, 2006, B62, p. 602.

MUTALIK V., MANJESHWAR L.S., WALI A., SAIRAM M., SRREDHAR B., RAJU K.V.S.N., AMINABHAVI T.M. Aqueous-solution and solid-film properties of poly(vinyl alcohol), poly(vinyl pyrrolidone), gelatin, starch, and carboxymethylcellulose polymers, Journal of Applied Polymer Science, 2007, 106, p. 765.

NEEDLES H.L., WHITFIELD R.E. Free-radical chemistry of peptide bonds. I. Dealkylation of substituted amides, Journal of Organic Chemistry, 1964, 29, p. 3632.

NEOGI A.H., JENSEN J.R. Wet strength improvement via fibre surface modification, Tappi, 1980, 63 (8), p. 86.

OBOKATA T., ISOGAI A. Wet-strength development of cellulose sheets prepared with polyamideamine-epichlorohydrin (PAE) resin by physical interactions, Nordic Pulp and Paper Research Journal, 2009, 24 (2), p. 135.

OBOKATA T., ISOGAI A. The mechanism of wet strength development of cellulose sheets prepared with polyamideamine epichlorohydrin (PAE) resin, Colloids and Surfaces A, 2007, 302, p. 525.

OBOKATA T., YANAGISAWA M., ISOGAI A. Characterization of polyamideamine-epichlorohydrin (PAE) resin : roles of azetidinium groups and molecular mass of PAE in wet strength development of paper prepared with PAE, Journal of Applied Polymer Science, 2005, 97, p. 2249.

OBOKATA T., ISOGAI A. Deterioration of polyamideamine-epichlorohydrin (PAE) in aqueous solutions during storage: structural changes of PAE, Journal of Polymer and Environment, 2005, 13 (1), p. 1.

OBOKATA T., ISOGAI A. Effects of polyamideamine-epichlorohydrin (PAE) resin deterioration on PAE retention and wet strength performance in handsheet making, Appita Journal, 2004, 57 (5), p. 411. (a)

OBOKATA T., ISOGAI A. ^{1}H- and ^{13}C-NMR analyses of aqueous polyamideamine epichlorohydrin resin solutions, Journal of Applied Polymer Science, 2004, 92, p. 1847. (b)

PUSHPAMALAR V., LANGFORD S.J., AHMAD M., LIM Y.Y. Optimization of reaction conditions for preparing carboxymethylcellulose from sago waste, Carbohydrate Polymers, 2006, 64, p. 312.

ROBERTS, J.C. Paper Chemistry, Chapman and Hall, 1991.

REMBAUM A., SELEGNY E. Polyelectrolytes and Their Applications, 1975, D. Reidel Publishing, Boston.

REN D., LI K. Development of wet strength additives from wheaten gluten, Holzforschung, 2005, 59, p. 598.

REYNOLDS W.F., WASSER R.B. Dry strength resins in Pulp and Paper Chemistry and Chemical Technology, J. P. Casey Willey Interscience, 1980, 3 ed., vol. 3, p. 1447.

RUSSEL T.P., PIERMARINNI G. J., MILLER P. J. Pressure/Temperature and reaction phase diagram for dinitro azetidinium dinitramide, Journal Physical Chemistry B, 1997, 101(18), p. 1997.

SANG Y., QIAN L., HE B., XIAO H. The adsorption of cationic PVA on cellulose fibres and its effect with polyelectrolyte complex on paper strength, Appita Journal, 2010, 63 (4), p. 294.

SARKANEN K.V., DINKLER F., STANNET V. The effects of polyethylenimine on some properties of pulp and paper, Tappi, 1966, 49 (1), p.4.

SANDSTROM, E. R. First pass fines retention critical to efficiency of wet strength resin, Paper Trade J., 1979, 163 (2), p. 47.

SCHMALZMANN A.C. Handling of polyamide-type wet strength broke, Tappi Journal, 1961, 44 (4), p. 275.

SCHMITZ K. S. Macroions in Solution and Colloidal Suspension, 1993, VCH Publishers, New York.

SCOTT W.E., ABBOT C.J. Properties of paper: an introduction, Tappi Press, 1995.

SHANG J., SHAO Z., CHEN X. Electrical behavior of a natural polyelectrolyte hydrogel : chitosan / carboxymethylcellulose hydrogel, Biomacromolecules, 2008, 9, p. 1208.

SILVERSTEIN R.M., WEBSTER F.X., KIEMLE D.J. Identification of organic compounds, 2005, Jonh Wiley & Sons, 7 ed, State University of New York – College of environmental Science and Forestry.

SIXTA H. Handbook of pulp, Willey-VCH, 2006.

SJÖSTROM E., Wood Chemistry Fundamentals and Applications, Academic Press, 1981, New York.

SJÖSTROM E., ENTRÖN B. A method for the separate determination of sulpho and carboxyl groups in sulphite pulps, Svensk Papperstidining, 1966, p. 3.

SOLAREK D., TESSLER M.M., JOBE P. STFI/SPCI, Paper chemistry simposium, 1988, Stockolm, Sweden, p. 1.

SOLOMONS G. Organic Chemistry, 2007, Willey, 10 ed.

STANNA-KLEINSCHEK K., KREZE T., RIBITSH V., STRNAD S. Reactivity and electrokinetical properties of different types of regenerated cellulose fibres, Colloids and Surfaces A, 2001, 195, p. 275.

STANNETT V. Mechanisms of wet strength development in paper in Surfaces and Coatings related to paper and wood, Marchessault RH and Skaar C. Syracuse University Press, 1967, Syracuse, USA.

STEEG H.G.M., STUART M.A.C., KEIZER A. BIJSTERBOCH B.H. Polyelectrolyte adsorption: a subtle balance of forces, Langmuir, 1992, 8 (10), p. 2538.

STRAZDINS, E. Surface chemical aspects of polymer retention, Tappi, 1974, 57 (12), p. 76.

STTRATON R.A. Dependence of sheet properties on the location of adsorbed polymer, Nordic Pulp and Paper Research Journal, 1989, 2, p. 104.

SWERING A., WÄGBERG L. Size exclusion chromatography for characterization of cationic polyelectrolytes used in papermaking, Nordic Pulp and Paper Research Journal, 1994, 1, p. 18.

SU J., HUANG Z., YUAN X., WANG X., LI M. Structure and properties of carboxymethyl cellulose / soy protein isolate blend edible films crosslinked by Maillard reactions, Carbohydrate Polymers, 2010, 79, p. 145.

TAYLOR D.L. Mechanism of wet tensile failure, Tappi, 1968, 51 (9), p. 410.

TERAYAMA H. Method of colloid titration (a new titration between polymer ions), Journal of Polymer Science, 1951, 8 (2), p. 243.

TOMITA B., ONO H. Melamine formaldehyde resins: constitutional characterization by Fourier transform ^{13}C NMR spectroscopy, Journal of Polymer Science, 1979, 17 (10), p. 3205.

TONG Q., XIAO Q., LIM L. Preparation and properties of pullulan-alginate-carboxymethylcellulose blend films, Food Research International, 2008, 41, p. 1007.

TVARDOVSKI A., TONDEUR D., FAVRE E. Description of multicomponent adsorption and absorption phenomena from a single viewpoint, Journal of Colloid and Interface Science, 2003, 265, p. 239.

VAINIO A., PAULAPURO H., KOLJONEN K., LAINE J. The effect of drying stress and polyelectrolyte complexes on the strength properties of paper, Journal of Pulp and Paper Science, 2006, 32 (1), p. 9.

VAN DE STEEG H.G.M., STUART M.A.C.M., KEIZER A., BIJSTERBOSCH B.H. Polyelectrolyte adsorption: a subtle balance of forces, Langmuir, 1992, 8, p. 2538.

WÄGBERG L., HÄGGLUND R. Kinetics of polyelectrolyte adsorption on cellulosic fibers, Langmuir, 2001, 17 (4), p. 1096.

WÄGBERG L., ANNERGREN G. Physico-chemical characterization of paper making fibres. Fundamentals of papermaking materials, 11th Fund Res Symp., 1997, (1), p.1.

WÄGBERG L., ÖDBERG L., LINDSTRÖM T., AKSBERG R. Kinetics of adsorption and ion-exchange reactions during adsorption of cationic polyelectrolytes onto cellulosic fibers, Journal of Colloid and Interface Science, 1988, 123 (1), p. 287.

WÄGBERG L., BJÖRKLUND M. On the mechanism behind wet strength development in papers containing wet strength resins, Nordic Pulp and Paper Research, 1993, 1, p. 53.

WALKER C.A., KIRKY J.T., DENTEL S.K. The streaming current detector: a quantitative model, Journal of Colloid and Interface Science, 1996, 182, p. 71.

WANG J., SOMASUNDARAM P. Adsorption and conformation of carboxymethyl cellulose at solid-liquid interfaces using spectroscopic, AFM and allied techniques, Journal of Colloid and Interface Science, 2005, 291, p. 75.

WANG L.K., SHUSTER W.W. Polyelectrolyte determination at low concentration, Ind. Eng. Chem. Prod. Res. Dev., 1975, 14 (4), p. 312.

WATANABE M., GONDO T., KITAO O. Advanced wet-end system with carboxymethyl-cellulose, Tappi Journal, 2004, 3 (5), p. 15.

WESTFELDT L. Chemistry of paper wet strength I. A survey of mechanisms of wet strength development, Cellulose Chemical Technology, 1979, 13, p. 813.

WUNDERLICH B. The heat capacity of polymers, Thermochemica Acta, 1997, 300 (1-2), p. 43.

XU G.G., YANG C.Q., DENG Y. Combination of bifunctional aldehydes and poly(vinyl alcohol) as the crosslinking systems to improve paper wet strength, Journal of Applied Polymer Science, 2004, 93, p. 1673.

XU Y., CHEN C.M., YANG C.Q. Application of polymeric multifunctional carboxylic acids to improve wet strength, Tappi Journal, 1998, 81 (11), p. 159.

YOON S.H. Analysis on adsorption equilibrium of polyamide-epichlorohydrin in aqueous suspension fibrous suspension by colloid titration, J. Ind. Eng. Chem., 2007, 13 (3), p. 345.

ZACARIA S. Development of wet-strength paper with dianhydride and diacid, Materials Chemistry and Physics, 2004, 88, p. 239.

ZAUSCHER S., KLINGENBERG D.J. Normal forces between cellulose surfaces measured with colloidal probe microscopy, Journal of Colloid and Interface Science, 2000, 229, p. 497.

ZHAO Q., QIAN J., AN Q., DU B. Speedy fabrication of free-standing layer-by-layer multilayer films by using polyelectrolyte complex particles as building blocks, Journal of Material Chemistry, 2009, 19, p. 8448.

ZHANG J., JIANG N., DANG Z., ELDER T., RAGAUSKAS A.J. Oxidation and sulfonation of cellulosics, Cellulose, 2008, 15, p. 489.